
# Targeting DNA damage repair pathways in breast and ovarian cancers

Youvica Singh

Thesis presented to

The University of Nottingham

## Acknowledgements

I would like to express my gratitude to my supervisor Prof. Srinivasan Madhusudan for his advice and guidance throughout this research. He has provided me invaluable encouragement and support in various ways. I am very thankful to him.

I am also very grateful to Dr Reem Ali. I have learnt a lot from her while performing experiments in laboratory. She has generously given me her invaluable time for training and advice.

I also want to express my sincere gratitude to Prof. Emad Rakha for his support as he never closes his door for any student who seeks advice.

My gratitude to those great scientists not only they support me for this research work but also I learnt from them research ethics, incredible enthusiasm and a lot of other things that enlightened my path.

I would also like to thank the Breast Pathology Group members, Dr Eslam Miligy, Dr Michael Toss for the fruitful collaborations and collecting cohort data.

I want to thank my colleagues in the Translational DNA Repair Group for their friendship and support.

Finally, I wish to express my deep gratitude to my parents for their care and support during this research journey. I thank God for showering his blessings throughout the studies.

## Abstract

### Background

DNA damage could be due to many endogenous and exogenous agents producing DNA lesions which in turn block the transcription process affecting the gene expression, cell growth and survival. The DNA damage response network detects the damage and any flaw in network including defects in DNA repair systems can lead to cancer. Thus, drugs targeting DNA repair systems relying on this concept are under development with various drugs monotherapy or combination therapies. Targeting DNA repair genes of nucleotide excision repair system (XAB2) and fanconi anemia repair system (FANCD2 and FANCA) for synthetic lethality is a novel strategy for treating breast and ovarian cancers. Hence, synthetic lethality concept is an exciting area for future research.

### Methods

In this study, XAB2 expression in breast cancer cohort was investigated. Cisplatin and olaparib sensitivity was evaluated in a panel of gene XAB2, FANCD2, FANCA deficient and proficient breast and ovarian cancer cell lines. In the ovarian cancer cohort, XAB2 expression and the clinicopathological outcomes were investigated. The gene knockdown and cisplatin sensitivity were tested in platinum sensitive and platinum resistant in ovarian and breast cancer cell lines. Functional studies for wild and knockdown genes such as PI FACS-cell cycle and Annexin V-apoptosis assay were performed.

### Results

In breast cancer cases, results showed that a low XAB2 nuclear expression was associated with a high tumour grade and poor breast cancer-specific survival

(BCSS) in patients. In invasive breast cancer, low XAB2 expression had clinicopathological associations with aggressive forms of breast cancer.
In gene knockdown, cisplatin and olaparib were synthetically lethal in gene deficient breast cancer cell lines. In ovarian cancers, XAB2 was significantly overexpressed in serous adenocarcinoma. The low XAB2 expression was significantly linked to good overall survival. The cisplatin was selectively toxic in gene deficient platinum-sensitive ovarian cancer cell lines. The drug cytotoxicity was associated with double strand breaks (DSBs) formation, cell cycle arrest and apoptosis in gene deficient cells. The gene expression was a predictor of platinum sensitivity in ovarian cancer patients. The gene knockdown not only increased platinum sensitivity but also reduced invasion and migration in breast and ovarian cancer cell lines. The cisplatin drug was selectively toxic in gene deficient breast and ovarian cancer cells.

**Conclusion**

Targeting DNA repair genes was an attractive synthetic lethality strategy and the chemoprevention in gene deficient breast cancers. In ovarian cancers, gene deficiency was a biomarker for drug inhibitor sensitivity. It provided alternative synthetic lethality approaches for inhibitors in clinics. The gene depletion can re-sensitize ovarian cancer patients to platinum. Therefore, studying the expression of DNA repair proteins assisted in new drug therapies development and opened alternative treatment options.

**Certificates**

1. Research Poster Presentation – 2019.
2. Postgraduate Research Impact Forum – 2020.
3. Cancer Research Nottingham (CRN) symposium hosted by the University of Nottingham- Abstract submission and Research oral presentation – 2020.
4. Certificate of attendance- Commercializing your research – 2020.
5. Nottingham Breast Cancer Research Centre (NBCR) - Research Day – 2022, University Of Nottingham.
6. Certificate of attendance- Breast Cancer and alternatives to HRT- Dovetail Medical & Healthcare Events (UK) – 2022.
7. Certificate of attendance and participation in workshop- Innovations in Health Education Conference – 2022.
8. Certificate of attendance- Breast Cancer - Presented by London Bridge Hospital GP Webinar – 2022.
9. Certificate of attendance- 6th Symposium on Primary Breast Cancer in Older women at East Midlands Conference Centre, University Of Nottingham – 2022

## Abbreviations

| Abbreviation | Definition |
|---|---|
| AJCC | American Joint Committee on Cancer |
| AML | Acute Myeloid Leukemia |
| ATCC | American Type Culture Collection |
| BCSS | Breast cancer-specific survival |
| BER | Base Excision Repair |
| CENPE | Centrosome-associated protein E |
| Cis | Cisplatin |
| CS | Cockayne syndrome |
| CTD | C-Terminal Domain |
| DAB | Diaminobenzidine tetrahydrochloride |
| DBR | Double Strand Breakage Repair |
| DCIS | Ductal carcinoma in situ |
| DDR | DNA Damage Response |
| DDS | DNA Damage Signalling |
| DFS | Disease free-survival |
| DMSO | Dimethyl sulphoxide |
| DSBR | Double-strand breakage repair |
| EGA | European Genome-phenome Archive |
| EOC | Epithelial Ovarian Cancer |
| ER | Estrogen Receptor |
| FA | Fanconi Anemia |
| FACS | Fluorescence-Activated Cell Sorting |
| FDA | Food and Drug Administration |
| FFPE | Formalin-Fixed Paraffin-Embedded |

| | |
|---|---|
| GEO | Gene Expression Omnibus |
| GEP | Global Gene Expression Profiling |
| GGR | Global Genome Repair |
| H-score | Histochemical score |
| HER2 | Human Epidermal growth factor receptor 2 |
| HGSC | High-Grade Serous Carcinoma |
| HIF | Hypoxia-Inducible Factors |
| HR | Homologous Recombination |
| HRD | Homologous Recombination Deficient |
| HRP | Horseradish peroxidase |
| HRR | Homologous Recombination Restoration |
| HRT | Hormone Replacement Therapy |
| HTS | High Throughput Screening |
| ICL | Interstrand Cross-Link |
| IHC | Immunohistochemistry |
| LCIS | Lobular carcinoma in situ |
| LOH | Loss of Heterozygosity |
| LVI | Lymphovascular invasion |
| MGMT | Methylguanine DNA methyl transferase |
| MMR | Mismatch Repair |
| NER | Nucleotide Excision Repair |
| NHEJ | Non-homologous End Joining |
| OC | Ovarian Cancer |
| OS | Overall Survival |
| PARG | Poly ADP-ribose glycohydrolase |
| PARP | Poly (ADP-ribose) polymerase |
| PARPi | PARP inhibitor |

| | |
|---|---|
| PBS | Phosphate-buffered saline |
| PCNA | Proliferating Cell Nuclear Antigen |
| PFI | Platinum-free interval |
| PFS | Progression-free survival |
| PR | Progesterone Receptor |
| PS | Phosphatidylserine |
| PVDF | Polyvinylidene fluoride |
| ROS | Reactive Oxygen Species |
| RNAi | RNA interference |
| SA | Strand annealing |
| SAC | Spindle assembly checkpoint |
| sDNA | Single stranded DNA |
| SDH | Succinate dehydrogenase |
| SDS | Sodium dodecyl sulfate |
| SE | Strand Exchange |
| SNPs | Single Nucleotide Polymorphisms |
| TBS | Tris Buffered Saline |
| TCGA | The Cancer Genome Atlas |
| TCR | Transcription coupled repair |
| TLS | Translesion synthesis |
| TMA | Tissue microarray |
| TNBC | Triple-Negative Breast Cancer |
| TNM | Tumor-Node-Metastasis |
| TTD | Trichothiodystrophy |
| TTDM | Time To Distant Metastasis |
| UV-DDB | UV DNA Damage Binding |
| XP | Xeroderma Pigmentosum |

**Table of contents**

**List of Figures**

**List of tables**

# 1 Introduction

## 1.1 Breast cancer

### 1.1.1 General information

The most frequent cancer diagnosed in women is breast cancer. Due to this cancer, women death rate is high in the world leading to the second most common cause of death from cancer. There are some ways of diagnosing breast cancer in women including tissue biopsy, physical examination, mammography and imaging. Early diagnosis of breast cancer is crucial to improve the survival rate in patients. When breast cancer spreads to the adjacent tissues through the lymphatic system and blood circulatory system, it leads to distant metastasis and poor survival (Menon G, 2024).

### 1.1.2 Major categories for risk factors of breast cancer

With aging of a person, the risk of developing breast cancer increases and most cancer cases are noticed when a person is 50 years or older. Sixty-three years is the median age when breast cancer appears. When a woman has breast cancer history in one breast then the possibility of this cancer increases in the other breast tissues as well (Feng Y, 2018). Men with breast cancer cases accounts for less than 1%. 67 years is the average age of men at the time of diagnosis of this disease. Radiation exposure, older age, klinefelter syndrome, family history of breast cancer, increased oestrogen levels and BRCA1/BRCA2 mutations are the prime factors that increase the risk of breast cancer. Generally, white non-hispanic women have the highest rate of the breast cancer incidence. However, black women affected with this malignancy have high mortality (Lukasiewicz S, 2021).

Under personal history of ovarian cancer**,** the risk of developing ovarian and breast cancers rises with mutations in BRCA1 and BRCA2 genes. Therefore, the chances of breast cancer increase when a person is diagnosed with hereditary ovarian cancer carrying BRCA gene mutations. There is a risk of developing both ovarian and breast cancer if the genetic mutations are also found in other genes including RAD51D, PALB2 and RAD51C. The risk of breast cancer can also increase with other genetic mutations or hereditary conditions such as Lynch syndrome (MLH1*,* MSH2, MSH6, PMS2 genes), Cowden syndrome (PTEN), Li-fraumeni syndrome (TP53 gene), Peutz-jeghers syndrome (STK11*)*, Ataxia telangiectasia (ATM), hereditary diffuse gastric cancer (CDH1 gene) and other susceptible genes including PALB2 and CHEK2 gene (Petrucelli N, 2023). The early menstruation and late menopause affect the rate of this carcinogenesis. It is found that if the menstruation cycle of a person begins before twelve years old and menopause after fifty-five years then the probability of breast cancer increases due to the longer exposer of **o**estrogen and progesterone hormones in the breast cells. The characteristics like breast development and pregnancy are controlled by oestrogen and progesterone hormones. There is excessive decline of oestrogen and progesterone production around menopause. The prospect of breast cancer grows with longer exposure of these hormones (Travis RC, 2003).

One of the major factors significantly related to breast cancer risk is a family history of a patient. It is found that around 13-19% of patients have first-degree relatives with breast cancer background. In addition, more the first-degree relatives affected; the risk of developing breast cancer increases particularly when the relatives are below fifty years old. The breast cancer is prevalent in patients with a family history regardless of age. This link is

managed by epigenetic changes and environmental factors which appear as possible triggers. A greater risk of breast cancer is observed in patients with a family history of ovarian cancer (BRCA1 and BRCA2 mutations) (Lukasiewicz S, 2021). The patients with first-degree relatives suffered by breast cancer have 1.75 fold more cancer risk in comparison to patients who do not have affected first-degree relatives and this particular is demonstrated in a cohort study of over 113,000 women in UK (Sun YS, 2017).

It is reported that breast cancer risk is increased with several genetic mutations in cells. BRCA1 and BRCA2 are two major genes marked by a high inducibility. These are mostly connected to a high possibility of breast carcinogenesis. TP53, CDH1, PTEN and STK11 are other breast cancer genes accountable for the disease. The mutations in the carrier genes are also susceptible to ovarian cancer. Other genes for instance CHEK2, ATM, BRIP1 or PALB2 interact with DNA repair BRCA genes are capable of inducing breast carcinogenesis with low penetrance. As per the recent studies, when one of the DNA repair genes XRCC2 undergoes genetic mutation, it leads to increased risk of breast cancer. The risks of secondary malignancies are frequently observed in patients after radiotherapy treatment. However, this tumour formation is related to an individual's age; a greater risk of breast cancer is marked in patients (under the age of 30) with radiation therapy (Lukasiewicz S, 2021).

The risk of developing breast cancer is affected by both endogenous and exogenous oestrogens. The reproductive organ ovary in premenopausal women produces the endogenous oestrogen. Therefore, the chance of breast cancer is decreased with ovariectomy. The hormone replacement therapy (HRT) and oral contraceptives are key sources of exogenous oestrogen. The

probability of breast cancer increases with intake of dietary fat and excessive alcohol consumption in today's modern lifestyles. The level of oestrogen-related hormones can be elevated with alcohol consumption which results in triggering the oestrogen receptor pathways (Sun YS, 2017).

### 1.1.3 Pathophysiology and histopathology of breast cancer

Breast cancer develops due to DNA damage and genetic mutations that can be influenced by exposure to oestrogen. Mutations in genes like BRCA1 and BRCA2 can be inherited. According to the connection of breast cancer to the basement membrane, it can be broadly categorized into invasive and non-invasive cancer. There are two major types of non-invasive neoplasms of the breast including lobular carcinoma in situ (LCIS) and ductal carcinoma in situ (DCIS).

LCIS is considered a risk factor for the development of breast cancer. The outline of the normal lobule with expanded and filled acini confirms the location of LCIS. DCIS is recognized as discrete spaces filled with malignant cells and a basal cell layer composed of normal myoepithelial cells. DCIS is more morphologically heterogeneous than LCIS. There are four categories of DCIS papillary, comedo, cribriform, and solid. The solid and comedo types of DCIS are generally higher-grade lesions. DCIS, if not treated, usually transforms into invasive cancer.

There are several features on which the classifications of ductal carcinoma in situ (DCIS) depend like architecture, presence of necrosis and cytological appearance. According to the Van Nuys classification system, it includes three categories namely group 1, 2 and 3. In group 1, low grade tumours without necrosis are present, group 2 involves low grade with necrosis (low debris with

five pyknotic nuclei) and group 3 incorporates high grade tumours with or without necrosis condition.

The high nuclear grade DCIS comprises with multiple nucleoli, pleomorphic state, asymmetrical nuclear outline and irregularly spaced nuclei. It includes high frequency of mitoses and the size of the nuclei is 5-fold the diameter of lymphocyte nuclei. In intermediate nuclear grade DCIS, pleomorphic lesions vary from mild to moderate condition, non-uniform low nuclear grade lesions and the largest nuclei has 4-fold the diameter of lymphocyte nuclei. Low grade DCIS has small, uniform and rounded nuclei. The largest nuclei has 3-fold the diameter of lymphocyte nuclei (Douglas-Jones AG, 2000).

There are diverse characteristics for the stratification of pure comedo DCIS in the traditional sub-type and 'Nottingham' DCIS grade classification. It includes high-grade DCIS with solid architectural pattern in more than 50% of the connected duct spaces and central confluent necrosis (Pinder SE, 2010).

The architectural properties of the lesions were traditionally used by the pathologists for the classification of DCIS. However, it is remarked that DCIS lesions often show architectural heterogeneity which indicate the limited clinical value of this categorization. Currently, all DCIS stratification strategies counting nuclear grade based grouping are inadequate to truly differentiate between DCIS and fully progressed invasive tumour.

There are no molecular biomarkers identified for local recurrence following surgery in patients and establishing difference between benign and aggressive DCIS. According to the studies of whole-genome expression data using hierarchical clustering, type I and type II subgroups of high-grade DCIS lesions are recognised. Type I shows an exclusive gene expression profile contrary to type II DCIS (Muggerud AA, 2010).

DCIS has also been sorted on account of architectural marking of the proliferation. It comprises solid or mixed, micropapillary, cribriform and comedo subtypes. This classification approach imparts knowledge on extent of disease like multiquadrant (71%) state is more acknowledged in micropapillary DCIS in comparison to comedo-type disease (8%). However, the reproducibility of this classification depending on single factor of growth pattern is an anomalous situation. Moreover, an isolated duct space has potential to indicate an architectural pattern which makes it challenging to classify (Pinder SE, 2010).

Mostly, DCIS are grouped on the basis of ultrasound findings including architectural deformation, calcification, masses and ductal aberrations. As specified by recent studies, DCIS also covers non-mass abnormalities.

A conceptual classification system was introduced for proposing instructions based on breast ultrasound findings by the Japan Association of Breast and Thyroid Sonology (JABTS) in 2003. It integrates the conventional concept of masses and non-mass abnormalities for making DCIS detection possible to a large extent. The subtypes of non-mass abnormalities incorporate architectural deformity, hypo-echoic areas in the mammary gland and ducts aberrations. This explains the alterations in ultrasound images of DCIS along with masses (Watanabe T, 2017).

Invasive breast cancers lack an overall architecture; cells are unsystematically arranged into a variable amount of stroma or sheets of monotonous cells affecting the structure and function of a glandular organ. Pathologists broadly divide invasive breast cancer into ductal and lobular histologic types. Out of these categories, invasive ductal cancer grows as a cohesive mass often appears as a discrete lump in the breast and it is smaller than lobular cancers. Invasive lobular carcinoma accounts for 10% of breast cancers while mixed

ductal and lobular cancers have been increasingly recognized and described in pathology reports. Tubular and mucinous tumours are usually low-grade (grade I) lesions; these tumours account for approximately 2% to 3% of invasive breast carcinomas. Medullary cancer is characterized by invasive cells with high-grade nuclear features, many mitoses and a lack of an in situ component (Menon G, 2024).

### 1.1.4 Breast cancer subtypes

Breast cancer is the most common cancer in women and it is a complex disease characterized by multiple molecular alterations. The current clinical management of breast cancer requires clinicopathological, individual molecular prognostic and predictive factors to support decision-making. However, to reflect the genetic heterogeneity of breast tumours; the varied behaviour and response to therapy within the clinically and morphological similar classes indicate that the traditional prognostic factors need to be upgraded. Immunohistochemistry on formalin-fixed paraffin-embedded (FFPE) is a laboratory technology as an alternative approach to use patient tumour samples with a set of proteins that shows biological and clinical relevance in breast cancer. The minimum number required for the classification of breast tumours into the six classes is reduced from 25 biomarkers to 10. These biomarkers include ER, EGFR, HER2, c-erbB3 (HER3) progesterone receptor, p53, cytokeratin (CK) 5/6, cytokeratin 7/8, c-erbB4 (HER4) and Mucin 1 (Green AR, 2013).

The gene expression microarray studies analyse thousands of genes in a single experiment and mark molecular tumour classes based on the simultaneous expression. The unsupervised clustering includes samples and genes that are

aggregated based on similarity to each other. The two main branches are clinically described as ER-positive and ER-negative; these are distributed under subset cluster analysis. The tumours in the ER-positive group are termed as the luminal group, characterized by the relatively high expression of many genes present in breast luminal cells (ER-responsive genes, luminal cytokeratins and other luminal-associated markers). Luminal-like breast cancer is sub-classified into three subclasses namely luminal-A, luminal-B and luminal-C. Luminal-A subgroup of ER-positive tumours is being identified with the best outcome. The new molecular classification system in breast cancer evolves with gene expression profiling and microarray analysis studies. In recent years, a new approach called mutational profiling explains the biological mechanism of carcinogenesis and tumour progression. To improve knowledge of breast cancer biology and understanding complex process of metastasis, certain technological advances such as array comparative genomic hybridization (array-CGH), single nucleotide polymorphism (SNP) and high throughput screening (HTS) are applied for *in vitro* and *in vivo* research studies (Yersal O, 2014).

The molecular classification of breast cancer is necessary to establish benefit from targeted therapies like anti- HER2 therapy and endocrine therapy. Newly discovered prognostic biomarkers and therapeutic targets for individual breast cancer subtypes are required. In recent studies, RASDF7 for luminal A group, DCTPP1 for luminal B group, ABDHD14A, ADSSL1 for TNBC group and DHRS11, KLC3, NAG3, TMEM98 for HER2 group are described as differentially expressed genes, RNA binding proteins and long non-coding RNAs. There are four prime breast cancer subtypes including luminal A, luminal B, HER2-positive and TNBC sets. The features of luminal cancers show low molecular weight cytokeratins

(CK7, CK8, CK18 and others) and three class luminal A, luminal B, HER2 are considered from the IHC perspective.

In luminal A tumours, ER and PR are present, lacking HER2 and cell proliferation marker Ki-67 (less than 20%) has low expression. Clinically, this subtype is marked with high survival rate, slow tumour growth, low grade condition and good prognosis with low relapse rate. These are highly responsive to hormone therapy such as aromatase inhibitors, selective oestrogen receptor degraders or tamoxifen and limited benefit to chemotherapy. With these objectives, genetic principles are mentioned to set up patient benefits from adjuvant chemotherapy treatment depends on the possibility of tumour relapse and survival rate under the guidelines of European Society for Medical Oncology (ESMO) and National Comprehensive Cancer Network (NCCN) from USA.

The luminal B tumours are characterised with higher grade and poor prognosis condition in contrast to luminal A subtypes. It shows Ki67 high expression, ER positive and possible PR negative. The histologic grades are intermediate/high in general. The patients may take advantage from chemotherapy and hormonal therapy. The rate of tumours growth is higher than luminal A subtypes. Approximately 10-20% of luminal tumours are luminal B cases. It has high expression of cell cycle, proliferation genes and low expression of oestrogen receptors. It demonstrates the worst prognosis among the luminal tumours subtypes. The patients get much benefit from chemotherapy and hormonal therapy.

The HER2-positive group comprises around 10–15% of breast carcinomas and it shows high expression of HER2. The ER and PR receptors are absent. These tumours are fast growing and the HER2-targeted therapies can improve survival. This subgroup shows fast-growing and aggressive tumours. It can be

further subdivided into two types HER2-enriched (HER2+ve, PR-ve, E-ve, Ki-67>30%) and luminal HER2 (HER2+ve, PR+ve, E+ve and Ki-67:15–30%). It requires targeted drugs directed against the HER2/neu protein which includes tyrosine kinase inhibitors (lapatinib, tucatinib, neratinib), trastuzumab, trastuzumab combined with emtansin (Kadcyla, T-DM1) trastuzumab combined with durectecan (Enhertu, T-DXd), pertuzumab along with chemotherapy treatment and surgery. The patients are highly responsive to these chemotherapy strategies.

In triple-negative breast cancer, HER2-negative, PR-negative and ER-negative condition is present. Approximately 20% of all breast carcinomas are triple-negative breast cancers. These are differentiated into luminal androgen receptor (LAR), basal-like (BL1 and BL2), immunomodulatory (IM) and claudin-low mesenchymal (MES) tumours. All these subdivisions show distinctive clinical results, pharmacological sensitivities and phenotypes. The risk factors of this breast malignancy include parity, breastfeeding patterns, genetics, age, race and obesity. It indicates early relapse rate, potential to proceed in advanced stages and aggressive tumour nature. DNA repair genes mutations, high proliferation and genomic instability state are noticed. Under the criteria of histology, these are poorly differentiated, heterogeneous neoplasm and very proliferative types. In immunohistochemical (IHC) settings, these are more differentiated into basal and non-basal TNBC types. The basal TNBC are specified with the presence of human epidermal growth factor receptor type 1 (EGFR1) and cytokeratins (CK) 5/6 expressions. Further, the CK5/6 cytokeratins expressions are absent in the non-basal TNBC type (Orrantia-Borunda E, 2022).

According to the histological stratification, invasive breast cancers (IBC) are characterised on the basis of morphology, behavioural pattern and clinical

instances. At least 18 histological breast cancer varieties are defined by the World Health Organization (WHO). The most frequent class (40–80%) is invasive breast cancer of no special type (NST) also called invasive ductal carcinoma. The invasive lobular carcinoma, mucinous A, mucinous B, tubular and neuroendocrine are acknowledged as specific subdivision (25%) due to the exclusive cytological aspects and growth patterns of invasive breast cancers.

In accordance with mRNA gene expression levels, invasive breast cancer can be grouped into molecular subtypes. As reported by Perou CM (2000) using microarray gene expression details, four molecular subtypes luminal, HER2-enriched, basal-like and normal breast-like are recognised. The four prime breast cancer intrinsic subtypes are distinguished into luminal A, luminal B, HER2-enriched, and basal-like. Furthermore, a combined analysis of murine and human mammary tumours in 2007 revealed a new fifth intrinsic subtype called claudin-low breast cancer. Invasive breast carcinoma (IBC) of no special subtype is further differentiated into invasive micropapillary, invasive cribriform, invasive lobular, tubular and mucinous carcinomas (Lukasiewicz S, 2021).

Gene expression profiling studies conclude the derivation of TNBCs into six subdivisions including basal-like (BL1 and BL2), unspecified group (UNS), mesenchymal (M), immunomodulatory (IM) and mesenchymal stem-like (MSL) tumours. However, the clinical relevance of above differentiation needs more research and approval. Intensive studies can assist in determining its influence on TNBC treatment options.

In Claudin-low (CL) breast cancers, PR-negative, ER-negative and HER2-negative condition is mostly prevailed. Approximately 7–14% of all invasive breast cancers are claudin-low breast cancers. These are poor prognosis tumours. It includes low gene expressions of claudins 3, 4, 7, occludin and E-cadherin

participating in cell-cell adhesion mechanisms. Apart from this, it demonstrates high expression of stem cell-like gene expression and epithelial-mesenchymal transition (EMT) genes patterns.

In surrogate markers classification, the subdivisions are spotted on the basis of immunohistochemical (IHC) markers and pathological morphology. The applications of these categories are to get guidance and recommendations on adjuvant therapy and risk stratification. For clinical decisions depending on IHC- grounds surrogate subtype ranking was proposed in the guidelines of St. Gallen (2013).

The Elston-Ellis modification of Scarff-Bloom-Richardson grading system is extensively noted histologic grading system of breast cancer and it is also named as the Nottingham grading system. The morphologic features of a tumour play important roles in establishing the tumour grades. It includes mitotic count, formation of tubules, variability, shape and size of cellular nuclei (Lukasiewicz S, 2021).

### 1.1.5 Breast cancer staging

In 2017, the American Joint Committee on Cancer (AJCC) announced the 8th edition of its cancer staging system. There is the incorporation of biomarkers for breast cancer into the anatomic staging to obtain prognostic stages and it is considered the most significant change in the staging system. According to the characteristics like tumour grade, hormone receptor (oestrogen and progesterone) status and HER2 status, different prognostic stages are specified for tumours with the same anatomic stages. Since 1959, the American Joint Committee on Cancer has published seven editions of the tumour-node-metastasis (TNM) system for cancer staging. In this 8th edition, the revisions

are made based on newly acquired clinical and pathological data. It creates a fundamental change in breast cancer marking in which a group of diseases with different molecular characteristics like prognosis, patterns of recurrence, metastasis and sensitivities to available therapies are included. As per the new staging system, biomarkers (histologic grade, hormone receptor, HER2 expression and multigene panels) are incorporated into the traditional anatomic TNM staging. The prognostic staging protocol is created by the AJCC committee under the 8th edition of the staging system. Along with the pathologic stages, the different biomarkers that are integrated with the TNM staging system could affect survival. The biomarkers indicate tumour grade, hormone receptor status and HER2. In limited sub-groups of the staging system, multigene panel status of breast cancer is also incorporated. The clinical and pathological prognostic stages are determined in the discussion of a staging system that combines anatomic staging with tumour grade, hormone receptor status and HER2 status (Koh J, 2019).

## 1.2 Ovarian Cancer

### 1.2.1 General information

Ovarian cancer is one of the most common gynaecologic cancers ranking third after cervical and uterine cancer. It has a poor prognosis and the mortality rate is also very high. Although breast cancer is highly prevalent in comparison to ovarian cancer, the mortality rate of ovarian cancer will increase significantly by the year 2040 and it is three times more lethal than breast cancer. Mostly ovarian cancer is diagnosed at the advanced stages and the mortality rate is high. There are several factors behind late diagnosis like asymptomatic growth of the tumour, delayed onset of symptoms and lack of proper screening. The

epidemiological diversity of ovarian cancer in different regions can be attributed to the risk factors that account for the occurrence of ovarian cancer. Ovarian cancer is highly prevalent in non-Hispanic white women (12.0 per 100,000) followed by Hispanic (10.3 per 100,000), non-Hispanic black (9.4 per 100,000) and Asian/Pacific Islander women (9.2 per100, 000). However, the mortality of ovarian cancer has a different pattern due to limited access to diagnostic and therapeutic services and African populations show the highest mortality rate (Momenimovahed Z, 2019). The major categories for risk factors of ovarian cancer are summarised in Table 1-1.

### 1.2.2 Major categories for risk factors of ovarian cancer

**Table 1-1:** Factors related to ovarian cancer risk. (Original table)

| | **Factors** |
|---|---|
| **Demographic** | Age |
| **Reproductive** | Menstrual-related factors, age of menarche and menopause, parity, pregnancy characteristics |
| **Gynecologic** | Pelvic inflammatory disease |
| **Hormonal** | Contraceptive methods, Hormone Replacement Therapy (HRT) |
| **Genetic** | Family history, BRCA mutations |
| **Lifestyle** | Nutrition and diet, obesity and physical activity, alcohol, caffeine, cigarettes |
| **Other** | Lactation |

### 1.2.3 Ovarian cancer subtypes

In several studies, ovarian cancer is divided into different subtypes. Approximately 90% of all ovarian cancer has an epithelial origin and the remaining ovarian cancer (OC) has a non-epithelial origin. Among epithelial ovarian cancer, 3% are mucinous and others are non-mucinous. Non-mucinous is further dissected to serous (70% non-mucinous), endometrioid (10%), clear cell (10%) and unspecified subtypes (5%). High-grade and low-grade carcinomas are two subtypes under serous carcinomas. Epithelial cancers are more invasive than non-epithelial cancers (Momenimovahed Z, 2019).

Ovarian cancer is a heterogeneous disease and it contains several histological subtypes. Epithelial ovarian cancer (EOC) can be classified into distinct morphologic categories including serous, mucinous, clear cell, endometrioid, transitional cell, mixed and undifferentiated types. The classification of epithelial ovarian cancer and its histological subtypes are based on clinical, pathologic and molecular evidence. At the junction of the fallopian tube and the peritoneum, mucinous and malignant Brenner tumours could arise.

The majority of ovarian cancers are derived from epithelial cell origins. Tumours under the category sex cord-stromal account for 5-6% and 2-3% derived from germ cell origin. Ovarian cancer is a heterogeneous group of diseases with many histological subtypes hence it is not a single neoplasm. According to recent studies high and low-grade serous carcinomas derive from the fallopian tubes (Reid BM, 2017) while clear cell and endometrioid carcinomas are originated from endometriotic cysts.

Mesothelium cell junctions can give rise to mucinous carcinomas (Ricci F, 2018). A revised version of the dualistic model by Shih and Kurman (2016) is proposed to classify epithelial ovarian cancers. Type I tumours of EOC are

further differentiated into mucinous, low-grade serous, endometrioid and clear cell carcinomas. Three subtypes of Type I tumours include a) endometriosis subgroup- endometrioid, clear cell and mullerian neoplasms b) fallopian tube-related tumours c) germ cell and transitional cell-related neoplasms. The classification of ovarian cancer is illustrated in Figure 1-1.

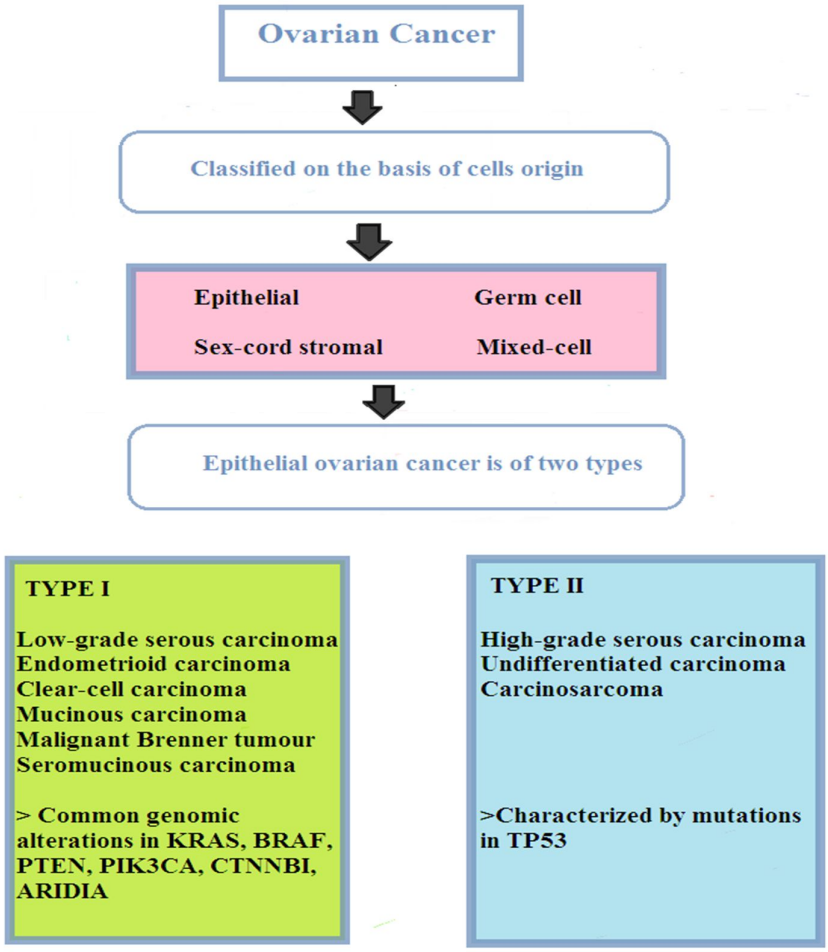


**Figure 1-1**: Classification of ovarian cancer. (Original figure)

### 1.2.4 Ovarian cancer staging

According to the International Federation of Gynaecology and Obstetrics (FIGO) staging system, ovarian malignancies are surgically staged as outlined in Table 1-2. A thorough inspection of the organ is required for staging laparotomy a) peritoneal cavity, pelvis and domes of the diaphragm b) bilateral salpingo-oophorectomy (BSO) and total abdominal hysterectomy (TAH) c) lymph node sampling washings d) liver palpation and biopsy e) omentectomy and peritoneal. For the treatment of ovarian cancer patients, the degree of surgical debulking, size, location and extent of residual disease should be traced. The least commonly diagnosed stage of ovarian cancer is stage II disease because there is no anatomic boundary between the pelvis and upper abdomen. It is more likely to spread to the upper abdomen if the disease has advanced outside of the ovary to pelvic structures. As reported in Gynaecologic Oncology Group (GOG), the category of early ovarian cancer combines stages I and II however, advanced ovarian cancer integrates stages III and IV. Ovarian cancer stage II disease shows a high recurrence rate and it is now classified under advanced disease for trial purposes (Gaitskell K, 2018).

**Table 1-2:** FIGO staging and prognosis of ovarian cancer

| FIGO | CHARACTERISTIC | Stage | Survival rate |
|---|---|---|---|
| **I** | Disease confined to the ovaries | 20% | 73% |
| **IA** | One ovary, capsule intact, no ascites | | |

| | | | |
|---|---|---|---|
| **IB** | Both ovaries, capsule intact, no ascites | | |
| **IC** | Stage IA or IB plus ascites, capsule ruptures, tumour on ovarian surface | | |
| **II** | Disease spread confined to the pelvis | 5% | 45% |
| **III** | Abdominal cavity, surface of the liver; pelvic, para-aortic lymph nodes; bowel | 58% | 21% |
| **IIIA** | Negative lymph nodes, plus microscopic seeding of peritoneal surface | | |
| **IIIB** | Negative lymph nodes, peritoneal implants <2 cm | | |
| **IIIC** | Positive lymph nodes, abdominal implants >2 cm | | |
| **IV** | Spread to liver parenchyma, lung, pleura, or other extra-abdominal sites | 17% | <5% |

### 1.2.5 Molecular profile of ovarian cancer

The treatment recommendations for ovarian carcinoma rely on the extent of surgical debulking and the stages of the disease. Among different stages of ovarian cancer, FIGO stage I includes disease confined to one or both ovaries in approximately 25% of women and enfold to the pelvis called FIGO stage II. FIGO stage III or IV ovarian carcinoma is present in approximately 75% of women. The extent of residual disease after primary debulking surgery accommodates prognosis of the ovarian carcinoma. Approximately 25% long-term overall survival (OS) rate is found in women with optimally

debulked stage III disease, treated with surgery followed by platinum-based chemotherapy. Optimally debulked disease in women have good prognosis than residual disease larger than 1 cm after initial debulking surgery. Nevertheless, a small proportion of the women with residual disease will have long-term disease free-survival (DFS). The survival in women is extended by the chemotherapy treatment with stage III disease (optimally or sub-optimally debulked) and possibly in stage IV disease (Jelovac D, 2011).

The first platinum-based drug approved by the US Food and Drug Administration (FDA) is cisplatin (cis) for cancers including ovarian cancer, cervical cancer, bladder cancer and testicular cancer in adults and against germ cell tumours, hepatoblastoma, osteosarcoma medulloblastoma and neuroblastoma in children. Cisplatin has antitumor activity however; its clinical efficacy is limited owing to resistance and severe side effects. The mechanisms of cisplatin resistance include lowered accumulation of platinum in the cells caused by upregulated efflux and downregulated influx drugs and increased levels of thiol-containing compounds. With a decrease in the mismatch repair process along with an increase in translesion DNA synthesis and NER pathway, such conditions improve tolerance to DNA damages induced by platinum compounds. For effective ovarian cancer cisplatin-based therapies, there is a need to address the problems associated with its adverse effects and resistance. Cisplatin increases intracellular reactive oxygen species (ROS) levels in cancer cells thus inducing oxidative stress. Redox regulation machinery can counter oxidative stress induced by platinum based chemotherapy and contribute to resistance (Mittal D, 2021). Adjuvant chemotherapy options for epithelial ovarian cancer are summarised in Table 1-3.

**Table 1-3:** Primary adjuvant chemotherapy for epithelial ovarian cancer.

| | |
|---|---|
| **Intravenous regimens** | Paclitaxel followed by carboplatin |
| | Docetaxel followed by carboplatin |
| | Dose-dense paclitaxel and carboplatin |
| **Intraperitoneal regimens** | Paclitaxel, cisplatin and paclitaxel |

After initial cytoreductive surgery and combination chemotherapy, the patients achieve a good clinical result although attaining a complete response for advanced ovarian cancer is uncommon. The objectives of therapies against recurrent ovarian cancer are to prolong survival, controlling disease-related symptoms, delaying time to progression, minimizing treatment-related symptoms and improving quality of life. Duration of remission after the completion of initial platinum based chemotherapy determines options for future therapy. Patients who progress during initial chemotherapy (platinum-refractory) or within 6 months of completing primary platinum-based chemotherapy are considered platinum resistant. Cytoreductive surgery may also be considered the disease recurs depending on the site and extent of recurrence. The standard treatment for patients recurring after 6 months of initial therapy is platinum-based combination therapy (Luvero D, 2014). The treatment recommendations for patients with platinum-sensitive ovarian cancer are summarised in Table 1-4.

**Table 1-4**: Treatment recommendations for patients with platinum-sensitive ovarian cancer. (Original table)

| |
|---|
| Consider secondary cytoreductive surgery for appropriate patients |
| Platinum retreatment is the standard of care |
| Platinum-based combinations improve PFS and in some cases, overall survival compared with platinum alone |
| Prior and persistent toxicities should be considered when choosing therapy |

### 1.3 DNA Damage

Deoxyribonucleic acid (DNA) is the hereditary molecule crucial for storing genetic information and passing it from one generation to the next to sustain life on earth (Alberts B, 2003).

Each species has its unique genetic characteristics due to the genetic information stored in the genes which progress from one generation to the next through a series of biological processes like replication, transcription and translation. These processes are collectively known as gene expression (Minchin S, 2019). The human genome is comprised of nearly ~20,000-25,000 genes that encode the genetic information into a large variety of proteins. In the cellular system, the octameric histone proteins are wrapped around by these genes to constitute a chromosome. DNA contains these octameric histone proteins in a cellular body called nucleosomes and many such nucleosomes are joined together by linker DNA to form chromatin. The histone proteins compact DNA and these play an essential part in protecting the DNA

from internal and external damages (Figure 1-2) hence it regulate the gene expression in cells (Alberts B, 2002).

Several factors are accountable for DNA damage in all cellular organisms. DNA damage can be subdivided into two types: (1) endogenous damage caused by internal elements like reactive oxygen species (ROS) mainly derived from metabolic byproducts and (2) exogenous damage caused by external agents like radiation (UV rays, X-rays and gamma), viruses, plant toxins, and viruses (Chatterjee N, 2017).

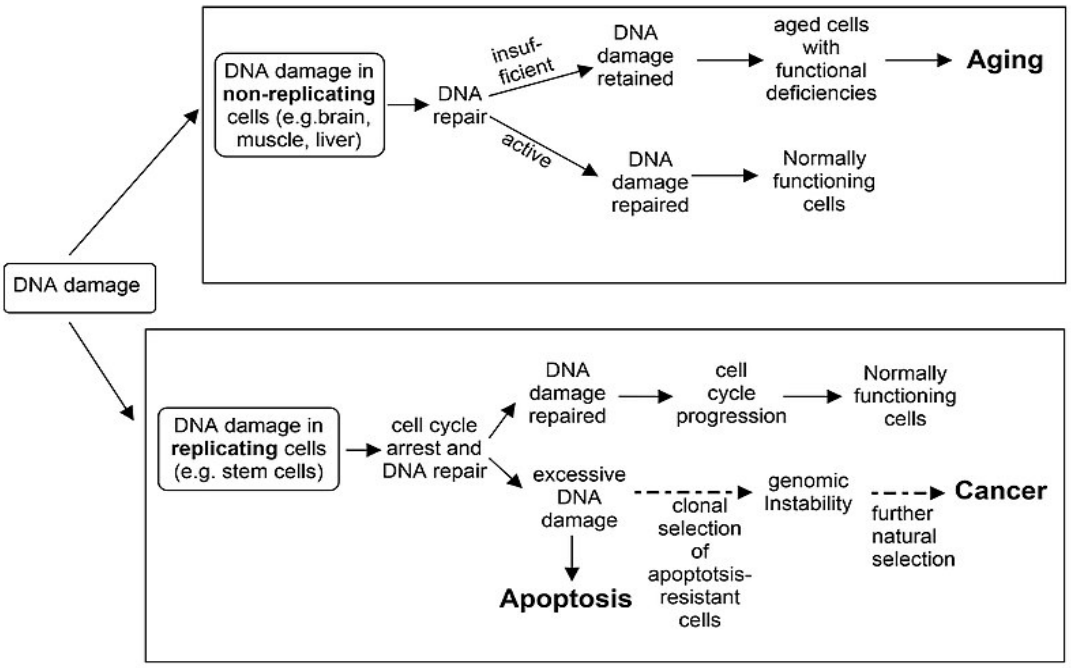


**Figure 1-2.** The role of DNA repairs in replicating and non-replicating cells. In non-replicating cells, DNA damage load can lead to aging. In replicating cells, DNA damage if not repaired promotes either apoptosis or cancer. Adapted from Nowsheen S, 2012.

### 1.3.1 DNA Damage Response

DNA damage and the resultant genomic instability can affect important processes in the cells such as replication, transcription and translation. DNA damages are recognized and removed through a network of enzymes and a highly synchronized cascade of molecular events (Figure 1-3). DNA damage response (DDR) is comprised of a web of proteins that coordinate the repair machinery. DDR senses the damage, activates the alarm and participates in damage removal and repair. Furthermore, DNA damage responses (DDR) activate apoptosis, cell-cycle arrest and damage specific DNA repair pathways. Ataxia telangiectasia, fanconi anaemia and xeroderma pigmentosum disorders emerge due to the flaws in these repair pathways that affect the neurological system and promote cancer susceptibility (Giglia-Mari G, 2011). DNA repair pathways, transcriptional regulation and apoptotic mechanisms activation are the consequences of the global DNA damage response. DNA damage sensor proteins detect the damage caused by endogenous and exogenous agents. DNA double-strand breaks are detected by ataxia telangiectasia mutated (ATM), a cell cycle checkpoint-specific sensor; UV-induced DNA damage is marked by ataxia telangiectasia, Rad 3 related (ATR) and multiple damage types are located by RAD17- replication factor C (RFC complex) in conjunction with the RAD9-HUS1 complex. BRCA1, MDC1 (mediator and DNA damage checkpoint 1), 53 BP1 and claspin are requisite for downstream activation of Chk1 (activated downstream from ATM signalling) and these are the mediator proteins that function in conjunction with DNA damage sensor proteins.

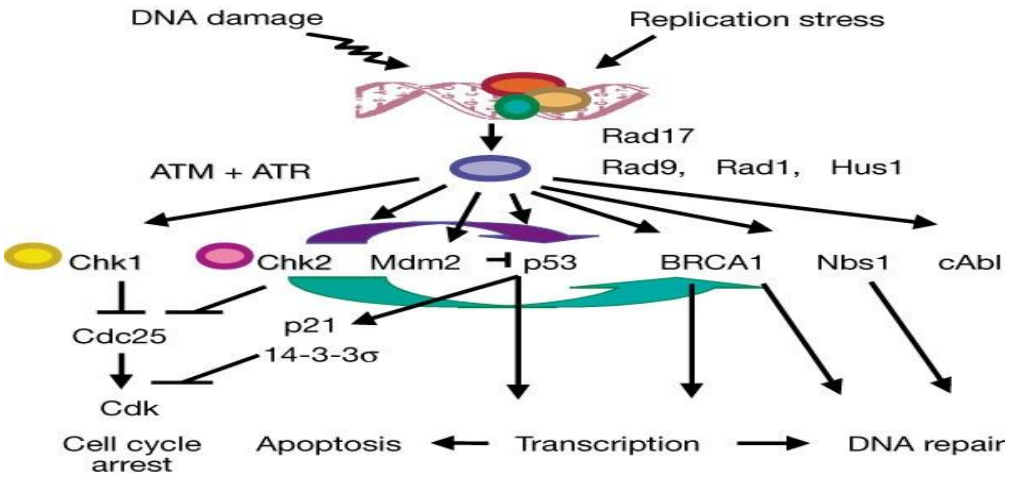


**Figure 1-3** DNA damage response signalling.

Adapted from Zhou BB, 2000.

The DNA replication fork can be blocked by DNA lesions including bulky adducts, crosslinks, helix distortions and intercalations. In response to DNA damage, DNA damage tolerance mechanism can allow the replication machinery to bypass these lesions thereby allowing the cell to continue to replicate but at the cost of acquiring mutations. Template switching is a sub-pathway of the HR pathway and plays a part in bypassing DNA lesions during the replication process (Abbotts R, 2014). The simplified representation of the DNA damage response pathway is illustrated in Figure 1-4.

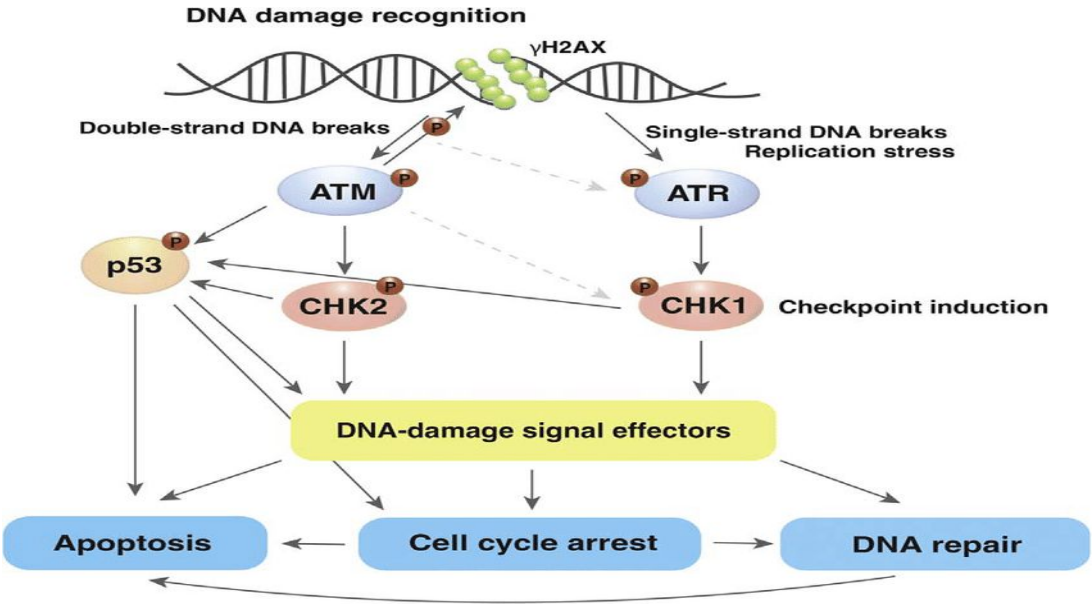


**Figure 1-4**. Simplified representation of the DNA damage response pathway. Adapted from Tsuiko O, 2018.

Single-strand and double-strand DNA breaks that are generated by DNA damage and as repair intermediates during DNA repair activate ATR and ATM kinases pathways respectively. In DDR, ATR and ATM are important signal transducers. Cell-cycle regulators CHK1 and CHK2 are activated by phosphorylation which in turn regulates the downstream signals leading to cell cycle arrest, activating DNA damage repair or tolerance mechanisms. The DNA damage signal is amplified by the phosphorylated form of histone protein H2AX and this protein modification is performed by ATM. Furthermore, tumour suppressor gene p53 is a critical sensor of DNA damage in DDR.

### 1.3.2 DNA Repair

DNA repair processes play major roles in sustaining the genetic information of all organisms. The endogenous metabolic processes e.g. reactive oxygen species and environmental agents threaten the stability of the genome in cells

and produce errors during cellular processes. Genetic mutations are caused by the modifications of DNA, altering the coding sequences of DNA which can risk the development of cancer. Organisms have evolved various DNA repair mechanisms to counteract DNA damage (Figure 1-5). The genome is protected against a large number of different chemical and structural alterations by these systems to ensure the stability of DNA and accurate transmission of genetic information (Milanowska K, 2011). A group of specific proteins recognizes and repair damaged DNA. It is crucial to study the molecular basis of protein-mediated DNA damage repair to comprehend the evolution of various genetic diseases (Giglia-Mari G, 2011). Response to chemotherapy and radiotherapy may be influenced in cancer cells by impaired DNA repair capacity (Figure 1-6). According to recent studies, the overexpression of DNA repair factors may predict chemotherapy or radiotherapy resistance and adversely impact on prognosis. For improving cancer cell killing strategy, DNA repair inhibitors can be used in combination with chemotherapy or radiotherapy (Abbotts R, 2014). The task of repairing DNA is vital to prevent mutation *via* oxidative DNA damage that is frequently found within the tumour microenvironment (Nowsheen S, 2012). During the DNA damage repairing process, tumour cells respond in distinct ways such as removal of damaged DNA parts, reconstruction of DNA strands, activation of cell cycle checkpoints and apoptosis (Huang R, 2021). There are many DNA repairing systems present in a cell including base excision repair (BER), mismatch repair (MMR), nucleotide excision repair (NER) and the function of O-methylguanine DNA methyl transferase (MGMT) (Chatterjee N, 2017).

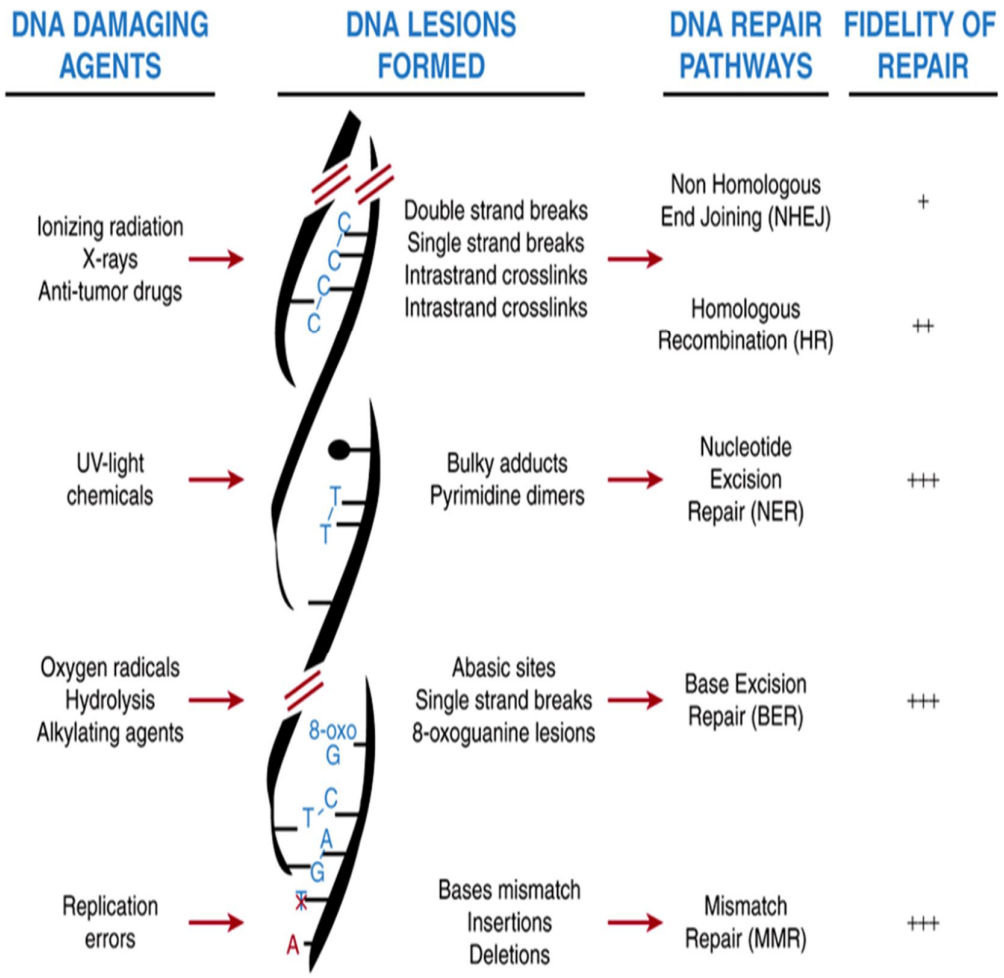


**Figure 1-5**. Multiple DNA repair pathways. DNA damage is repaired by multiple DNA repair pathways in mammals. There are some recognised DNA damaging agents, the significant DNA repair pathways for repairing the distinct lesions and the relative accuracy of these pathways. Adapted from Blanpain C, 2012.

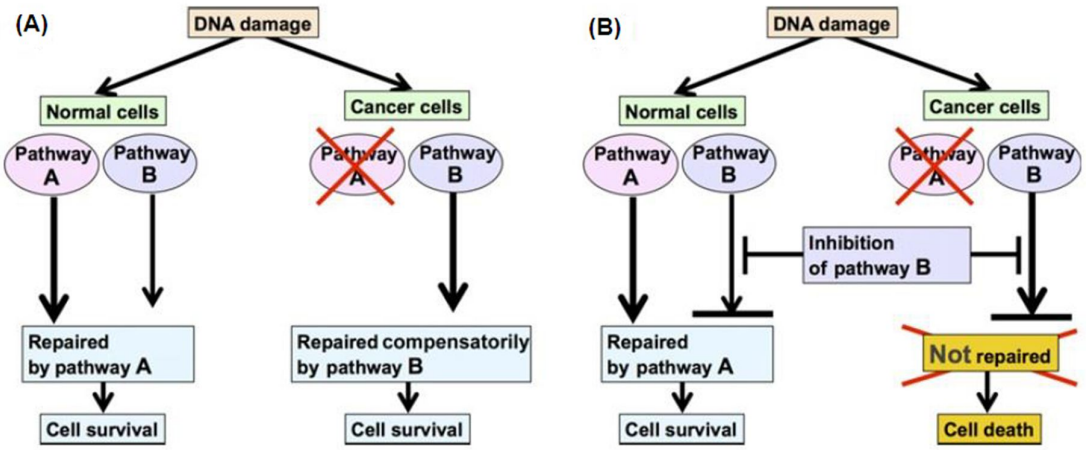


**Figure 1-6**. DNA repair mechanisms are involved in restoring DNA lesion. In normal cells, A and B pathways are active but cancer cells have non-functional A pathway. A) Since the inhibitor for pathway B is not used, it could be an alternative pathway in cancer cells when pathway A is defective. B) The use of pathway B inhibitors will cause cancer cell death whereas the normal cells are not affected. Adapted from Hosoya N, 2014.

### 1.3.3 DNA Damage Repair pathways

Different repairing mechanisms are evolved and interconnected to cope with excess DNA damage in a cell. DNA damage response includes activation of DNA repair pathways (Figure 1-7) such as nucleotide excision repair (NER), inter-strand cross-link repair, base excision repair (BER), a direct reversal of damage, mismatch repair (MMR), double-strand breakage repair (DSBR), non-homologous end-joining (NHEJ) and homologous recombination (HR) (Boiteux S, 2013).

DNA repair system, DNA damage signalling (DDS) and damage tolerance pathways can be categorized as:

•DDS: this signalling is induced in response to the DNA damage in a cell caused by some internal and environmental factors.

•Direct reversal repair (DDR): directly re-establish the original nucleotide residue by removing the chemical modification.

•Base-excision repair (BER): involves the excision or removal of modified base from the damaged part. This pathway is divided into two sub-pathways relaying on the length of DNA resynthesis: short-path (SP-BER) or long-path (LP-BER).

•Nucleotide excision repair (NER): removes bulky damage from the polynucleotide chains of DNA. It includes transcription coupled repair (TCR) NER, eliminating the damage part from the active strand of transcribed genes and global genome repair (GGR) NER removes impaired DNA while screening the whole genome.

•Mismatch repair (MMR): insertions and deletions of nucleotides cause errors during replication and this post-replicational DNA repair keeps checking the inaccurate nucleotide sequences.

•Homologous recombination repair (HRR): the homologous DNA strand is used as a template for repairing double-strand breaks. There are two primary models for HR pathway mechanism, the double-strand break repair (DSBR) pathway and the synthesis-dependent strand annealing pathway.

•Non-homologous end joining repair (NHEJ): no homologous template is required for repairing DNA double strand breaks and break ends are ligated directly. It includes micro homologous DNA sequences with error-prone end joining mechanism.

•Translesion synthesis (TLS): it is a damage-tolerance pathway that synthesis DNA *via* polymerases bypassing DNA lesions for promoting error free replication process.

It is significant to note that different DNA repair pathways are interconnected and share some steps or proteins involved in the repairing mechanism. As a result, DNA repair proteins infrequently function in isolation and activity of proteins may also dependent on the components of other DNA repair systems (Milanowska K, 2011).

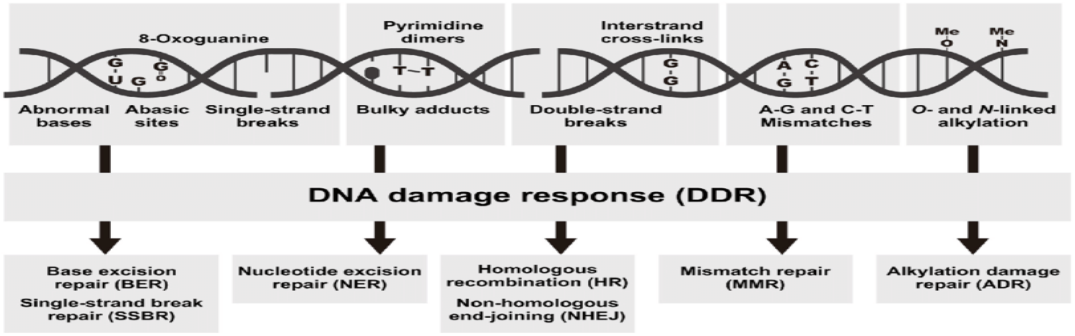


**Figure 1-7:** Types of DNA damages and the repair pathways. There are varieties of DNA repairing pathways mending DNA lesions. Examples of DNA lesions, activation of the DNA damage response and the most appropriate repairing pathways controlling the removal of the lesions. Adapted from Tasaki E, 2018.

### 1.3.4 Nucleotide Excision Repair (NER)

The environmental mutagens, UV-induced DNA lesions and chemotherapeutic adducts are removed by the nucleotide excision repair pathway (NER) which removes bulky DNA adducts. Xeroderma pigmentosum is a skin cancer-prone hereditary disorder which arises due to deficiencies in the NER system (Scharer

OD., 2013). The representation of Nucleotide Excision Repair (NER) is illustrated in Figure 1-8.

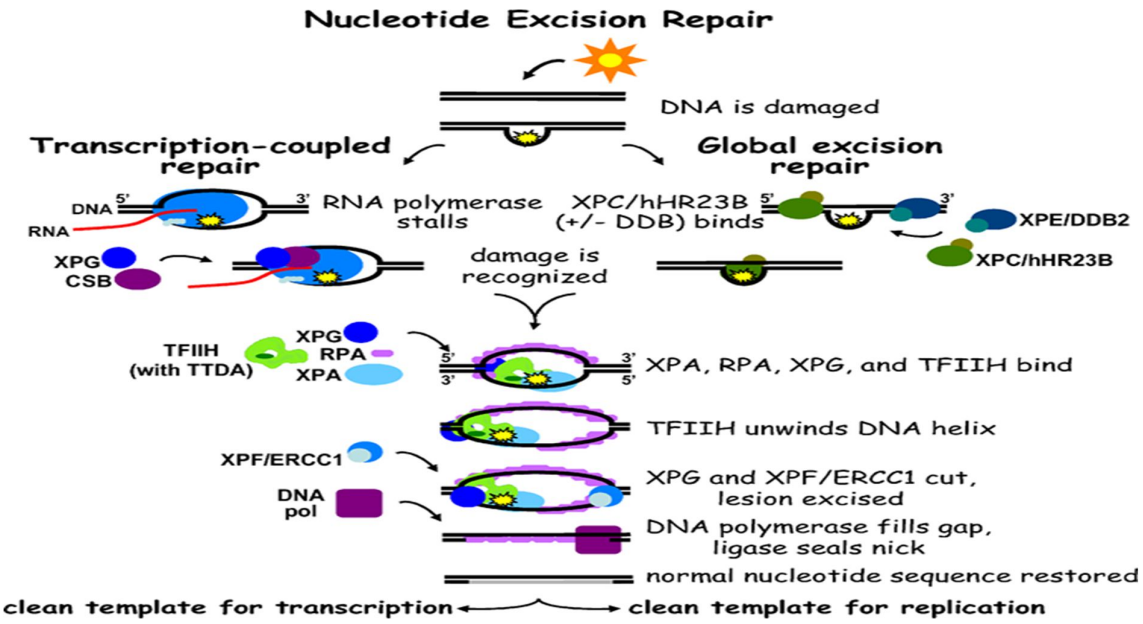


**Figure 1-8**: Representation of Nucleotide Excision Repair. Sunlight can damage the DNA and activates the NER pathway; determined by the state of DNA transcriptionally active (transcription-coupled repair) or not (global excision repair). The initial step of DNA damage recognition is different in these two sub-pathways however; the damage is repaired in a similar manner resulting in the restoration of the correct nucleotide sequences. Adapted from Fuss JO, 2006.

**Global genome NER (GG-NER)**

This type of NER is proficient in sensing and repairing DNA lesions throughout the genome. The DNA helix distortions with structural changes to nucleotides present in the entire genome are examined by global genome NER (Figure 1-9).

1) DNA helical deformations are examined by prime damage sensor protein XPC/RAD4, UV damage sensor protein Rad23B and centrin 2. 2) XPC-RAD23 is guided to the site of UV damage particularly CPDs by UV-DNA damage binding protein (UV-DDB). 3) RAD23B is dissociated upon the binding of XPC-RAD23 to DDB protein.

Transcription initiation and repair factor TFIIH with ten protein subunits connect at the damage site after binding of XPC to lesions. DNA configuration around the lesion is opened by two DNA helicases, two TFIIH basal transcription factor complex helicase subunits XPB and XPD (encoded by ERCC3 and ERCC2 respectively). Transcription initiation requires the trimeric CDK-activating kinase subcomplex of TFIIH. The CAK subcomplex dissociates from the lesion when TFIIH binds to DNA-bound XPC.

Dual incision and gap filling- the structure-specific endonucleases XPF-ERCC1 and XPG (encoded by ERCC5) excise the damaged strand at short distances of 5’ and 3’ from the lesion respectively. DNA-damage-signalling response is triggered by a single-strand gap of 22-30 nucleotides that remained after the excision process. The group of XPA, XPG and replication protein A (RPA) at the site of the lesions are marked by XPC and TFIIH verifies the correct coordination of incision. There are two main functions of RPA (single-strand binding protein) including to protect the non-damaged DNA part from endonucleases enzyme and another purpose is to check XPF-ERCC1 and XPG are properly oriented to specifically incise only the damaged strand. The large ssDNA gaps that induce DNA-damage signalling are prevented by the synchronization of lesion excision along with gap-filling DNA synthesis and this process is coordinated by RPA and XPG. The replication proteins proliferating cell nuclear antigen (PCNA), DNA Pol δ, replication factor C (RFC), DNA Pol-E or

DNA Pol k and DNA ligase 1 or XRCC1-DNA ligase 3 execute the final DNA gap-filling synthesis and ligation (Sugasawa K., 2016).

**Transcription-coupled NER**

This pathway maintains the transcription process, gene expression and repairs the transcription-blocking lesions. It is initiated by the enzyme RNA polymerase II at the lesion site and it recruits the TC-NER-specific protein CSA (ERCC8). The core NER factors and TC-NER specific proteins like UV-stimulated scaffold protein A (UVSSA), ubiquitin-specific-processing protease 7 (USP7), XPA-binding protein 2 (XAB2), high mobility group nucleosome-binding domain-containing protein 1 (HMGN1) essentially require CSA and CSB. The DNA lesions are recognised by RNA Pol-II which triggers other important downstream signalling proteins in TC-NER (Figure 1-9).

1) RNA Pol II in the transcription elongation process interacts with other significant proteins such as UV-stimulated scaffold protein A (UVSSA), ubiquitin-specific-processing protease 7 (USP7) and cockayne syndrome protein (CSB). 2) The interruption of RNA polymerase II activity at the damaged site results in the increase of CSB affinity for RNA Pol II thus forming the CSA-CSB complex. 3) The monitoring of RNA Pol II facilitates the repair of a DNA lesion. 4) After damage recognition, the TFIIH complex plays a role at the damaged site in both TC-NER and GG-NER. The structure-specific endonucleases XPF and XPG bind to the NER complex either individually or accompanying TFIIH. After the cohesion of nucleases, CDK-activating kinase (CAK) sub-complex separates from the TFIIH main complex. The helicase enzymes elongate the length of a bubble at the damage site and ATPase activity of the XPD factor verifies the presence of lesions. XPA and XPB are the

single-strand binding proteins that stabilize the strands of the elongated bubble. XPA further recruits XPF-ERCC1; its endonuclease activity cut DNA lesions. XPG then removes 22-30 nucleotide long damaged strand. Proliferating cell nuclear antigen (PCNA) with trimeric subunits binds towards the 50 incisions of the bubble and attracts proteins like DNA Pol k DNA Polδ or DNA Polε for filling the gap with correct nucleotides. The DNA ligation process is completed by DNA ligase-1 or DNA ligase-3 in the NER pathway (Scharer OD., 2013).

Cells are protected from cancer and premature ageing by retaining the balance between TCR and GG-NER pathways. In case of imbalance with TCR deficiency, DNA damage load cause the cells to die from transcriptional stress leading to the increased possibility of ageing and cancer.

DNA lesion recognition steps are distinct in TC-NER and GG-NER. The detection of DNA helix distortions in global genome NER is performed by UV-DDB and XPC/RAD23B whereas TC-NER specific factors assemble at the DNA lesion site following RNAPII. After identifying DNA damages, the same protein components are utilized for the assembly of the repair complex in both NER sub-pathways resulting in the excision of a damaged DNA fragment. The undamaged strand is used as a template for filling the remaining gap by DNA repair patch synthesis. The defects in the NER system cause the rare autosomal inherited diseases including xeroderma pigmentosum (XP), Cockayne syndrome (CS) and trichothiodystrophy (TTD). Mutation in the seven complementation groups (XP-A to XP-G) can result in defective GG-NER (Lagerwerf S, 2011). The functions of nucleotide excision repair (NER) proteins are summarised in Table 1-5.

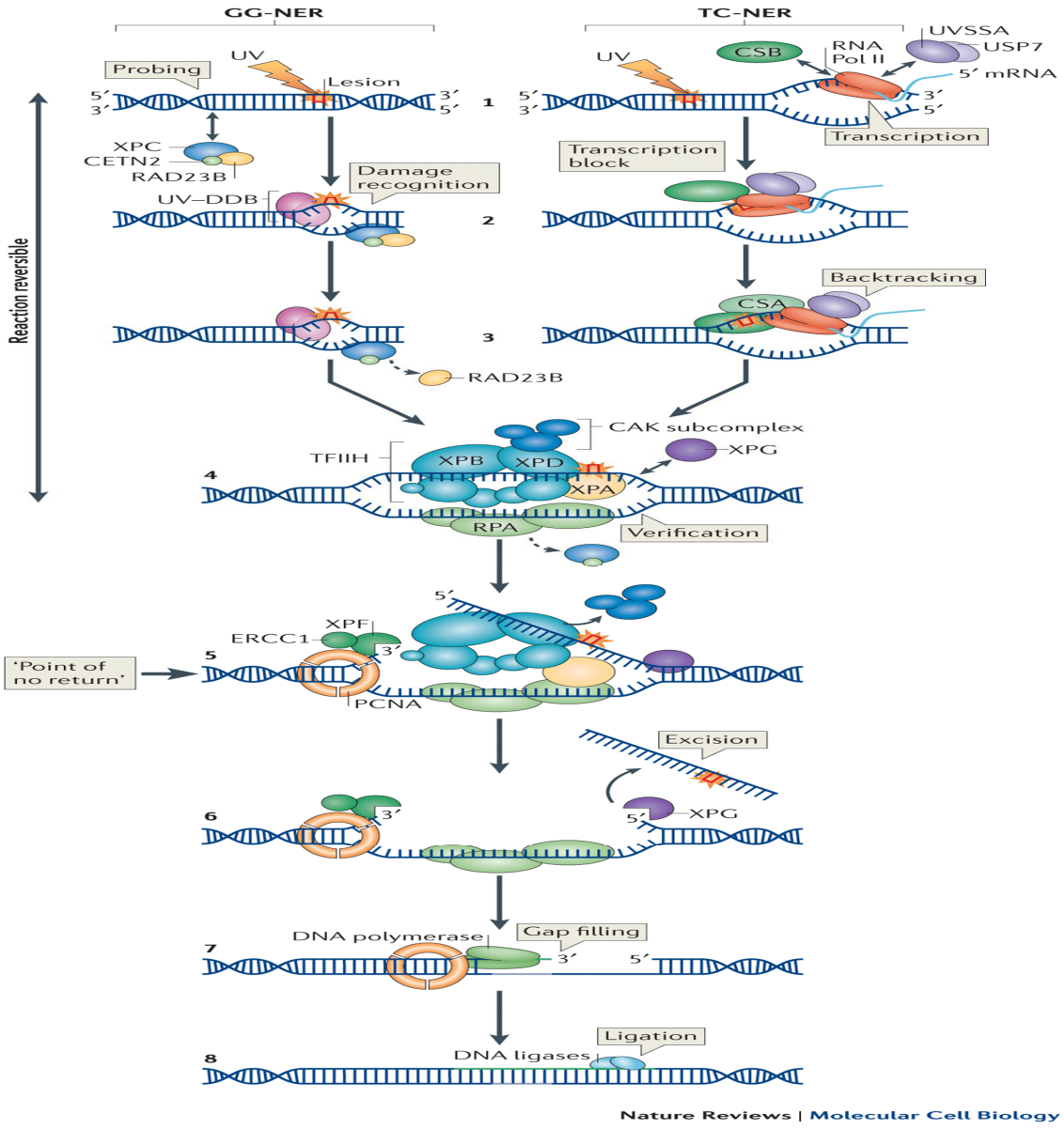


**Figure 1-9**: Types of Nucleotide excision repair (NER) pathway. In GG-NER, the DNA damage sensor proteins XPC and CETN2 examine the DNA for helix-distortion and UV-DDB protein assist in recognising the lesions. RAD23B dissociates from the previous protein complex formed once XPC binds to the damage. In TC-NER, the stalled RNA polymerase II enzyme recognises the damage during transcription elongation step. RNA Pol II gets interaction with CSB, UVSSA and USP7. Once the DNA damage is recognised, the TFIIH complex is engaged in both GG-NER and TC-NER. Adapted from Marteijn JA, 2014.

**Table 1-5**: Functions of nucleotide excision repair proteins

Adapted from Marteijn JA, 2014.

| Mammalian complex or protein | Subunits | HUGO nomenclature | Main function or functions outside nucleotide excision repair |
|---|---|---|---|
| XPF–ERCC1 (excision repair cross-complementation group 1) | ERCC1 | *ERCC1* | Interstrand crosslink repair (ICLR), single-strand annealing (SSA) and gene conversion |
| | XPF | *ERCC4* | ICLR, SSA and gene conversion |
| XPG | None | *ERCC5* | Base excision repair (BER) and resolving of stalled replication |
| Cockayne syndrome protein CSB | None | *ERCC6* | BER |
| Cockayne syndrome WD repeat protein CSA | DNA damage-binding protein 1 (DDB1)–cullin4A (CUL4A)–regulator of cullins 1 (ROC1) | *DDB1–CUL4A–RBX1* (RING-box 1, E3 ubiquitin protein ligase) | Ubiquitylation of many different targets |
| | CSA | *ERCC8* | Unknown |
| DNA ligase 1 | None | *LIG1* | DNA replication |
| Proliferating cell nuclear antigen (PCNA) | None | *PCNA* | DNA replication; translesion synthesis (TLS) (by ubiquitylated PCNA) |
| DNA Polymerase δ (DNA Pol δ) | DNA Pol δ subunit (POLD1–4) | *POLD1–4* | DNA replication |
| DNA Pol ε | DNA polymerase ε subunit (POLE1–3) | *POLE1–3* | DNA replication |
| DNA Pol κ | None | *POLK* (polymerase (DNA directed) κ) | TLS and somatic hypermutation |
| Replication factor C (RFC) | RFC1–5 | *RFC1–5* | DNA replication |
| Replication protein A (RPA) | RPA1–3 | *RPA1–3* | DNA replication and homologous recombination |
| TFIIH (transcription initiation factor IIH) core complex | TFIIH subunit 1 (GTF2H1)–4 | *GTF2H1–4* | Transcription |
| | TFIIH basal transcription factor complex TTDA subunit | *GTF2H5* | Transcription and repair of oxidative lesions |
| | TFIIH basal transcription factor complex XPB subunit | *ERCC3* | Transcription |
| | TFIIH basal transcription factor complex XPD subunit | *ERCC2* | Transcription and chromosome segregation |
| TFIIH CAK (CDK activating kinase) subcomplex | Cyclin H (CCNH) | *CCNH* | Transcription and cell cycle control |
| | Cyclin-dependent kinase 7 (CDK7) | *CDK7* | Transcription and cell cycle control |
| | MNAT1 | *MNAT1* | Transcription and cell cycle control |
| UV–DDB | DDB1–CUL4A–ROC1 | *DDB1–CUL4A–RBX1* | Ubiquitylation of different targets |
| | DDB2 | *DDB2* | Unknown |
| UV-stimulated scaffold protein A (UVSSA) | None | *UVSSA* | Unknown |
| XPA | None | *XPA* | Unknown |
| XPC | XPC | *XPC* | Repair of oxidative lesions |
| | UV excision repair protein RAD23 homologue B (RAD23B) | *RAD23B* | Ubiquitin proteasome system |
| | Centrin 2 (CETN2) | *CETN2* | Centrosome component |
| DNA repair protein XRCC1 and DNA ligase 3 | XRCC1 | *XRCC1* | BER |
| | DNA ligase 3 | *LIG3* | BER |

*Proteins identified in nucleotide excision repair (NER) deficiency disorders or that are structurally required for NER are listed.

## 1.4 DNA Repair Genes

More than 130 DNA repair genes are identified in humans (Wood RD, 2001) and single nucleotide polymorphisms (SNPs) have been reported in these genes (Deng N, 2017). The DNA repair process may be impaired if the DNA repairing genes encoding proteins are defective and lead to human disorders.

Endogenous and exogenous mutagens or carcinogens have the potential to damage DNA. DNA damage induced mutations can lead to either activation of oncogenes or inactivation of tumour suppressor genes leading to genomic instability. Due to the DNA lesions, oncogenes are activated, tumour suppressor genes get inactivated leading to genomic instability and carcinogenesis (Hanahan D, 2011).

### 1.4.1 XPA binding protein 2 (XAB2)

XPA binding protein 2 (XAB2) gene encodes a protein in humans which is a pre-mRNA splicing factor, SYF1. This splicing factor interacts with XPA and ERCC8. XAB2 or HGNC is located at chromosome 19 and has 855 amino acids with a molecular mass of 100010 Da (Nakatsu Y, 2000).

There are many functions of XAB2 protein including a role in transcription, pre-mRNA splicing, transcription-coupled DNA repair, mRNA export and homologous recombination. Mitotic arrest and cell death could be induced with XAB2 knockdown.

Yeast two-hybrid system was used to identify the protein XAB2; it interacts with XPA and recognizes it as a highly conserved gene. There are many repeated motifs in XAB2 protein including 15 tetratricopeptides that facilitate protein-protein interactions.

XAB2 protein plays role in the transcription elongation step and transcription-coupled DNA repair process. It is confirmed with the downregulation of XAB2 using an anti-XAB2 antibody which inhibits RNA synthesis and recovers after UV irradiations. Hence, it is reported that the XAB2 complex is associated with RNA and its knockdown affects Bcl-x pre-mRNA splicing.

The XAB2 expression has been observed in ovarian cancer, primary gastric cancer, rhabdoid tumour and triple-negative breast cancer. XAB2 plays a part in ageing where its level is found to be reduced in aged hematopoietic stem cells.

XAB2 has a role in mRNA export as its disruption leads to the retention of intron less mRNAs in the nucleus. The expression of cell cycle and mitotic genes are modulated by XAB2 (Hou S, 2016).

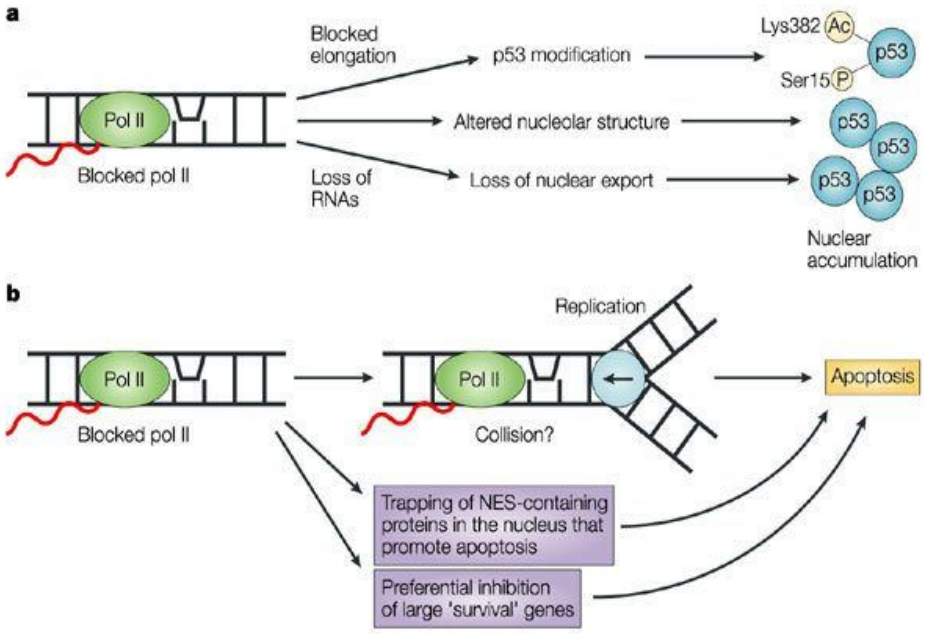


**Figure 1-10**. Cellular consequences of blocked transcription.

Adapted from Ljungman.M, 2004.

XP patients hypersensitive to sunlight also exhibit neurological and developmental abnormalities. XAB2 interconnects with CSA, CSB and RNA polymerase (TCR-specific factors). Microarray analysis studies show that the expression of genes working in the mitotic cell cycle is regulated by XAB2 knockdown (Kuraoka I, 2008).

XAB2 complex unit (hAquarius, Prp19, XAB2, hISY1, PPIE and CCDC16) binds to RNA. It interacts with RNA polymerase II and regulates the transcription elongation process. Genome instability or aneuploidy arises due to mitosis dysregulation causing a mitotic catastrophe, cell death and cancers associated diseases (Figure 1-10) (Hou S, 2016).

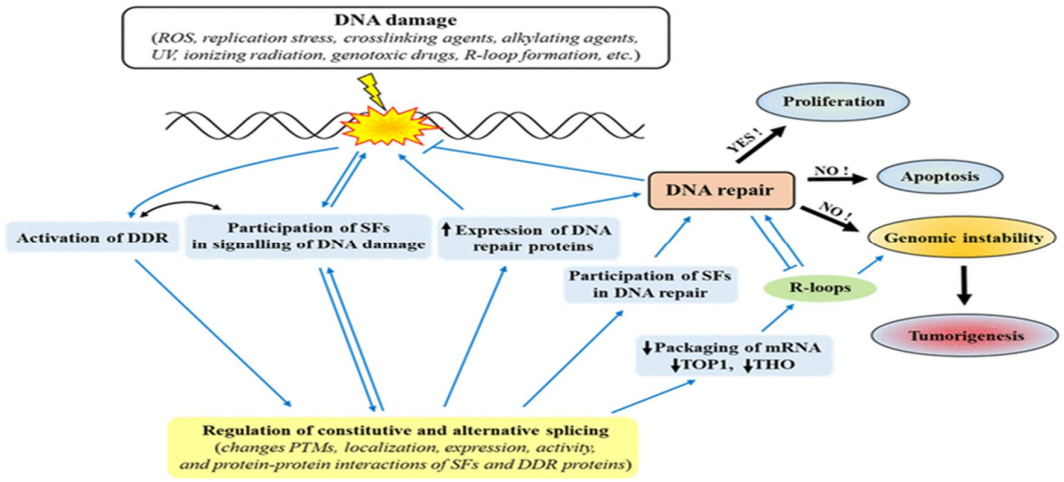


**Figure 1-11**. The interconnections between the DNA damage response and RNA-processing pathways. The role of DNA repairs in determining the fate of cells. Adapted from Mikolaskova B, 2018.

The emergence and progression of numerous diseases like cancer occur with the mutations in DNA repairing and binding proteins. The gene amplification, point mutations, epigenetic modifications and deletions result in the alteration of proteins activities. Due to the insufficient high-throughput screening

techniques previously, it has been difficult to develop drugs targeting cancer related proteins for cancer therapy. New therapeutics targeting cancer related proteins are developed with the advancement in technologies; it enables the identification and selective inhibition of DNA repairing and binding proteins. There are various DNA binding proteins that play crucial role in the regulation of gene expression like transcription factors. Hence, these proteins provide promising approaches for the development of anticancer agents selectively inhibiting the activity of non-regulated proteins. The oncogenic signalling pathways are activated due to the chromosomal abnormalities and gene alternations that affect transcriptional activity and tumour malignancy (Figure 1-11). In recent studies, small molecule inhibitors against cancer-related proteins are developed with protein knockdown methods and high-throughput screening systems (Shiroma Y, 2020).

Cancer metastasis causes troubles with cancer-related death globally despite boost in cancer research and treatment methods. Due to the lack of latest clinical diagnostic tools, it is difficult to anticipate metastatic progression and to locate minimal residual disease affecting the patient outcomes (Ring A, 2023).

The fruit flies and yeast models are used for understanding the concept of synthetic lethality (SL) initially. This approach depends on the simultaneous error (gene mutation, inhibition or overexpression) in two or more genes causing cell death however; the cell viability is not affected when only one gene is mutated. The overexpressed and mutated genes form tumour cells. Therefore, inhibitor molecules targeting synthetic lethal participants of such genes in malignant cells can stop cancer growth without influencing normal cells survival.

Genetically targeted cancer therapies are noticed extensively in recent studies. Synthetic lethality arranges a favourable anticancer treatment possibility with enhanced research studies and implementations in the clinical settings. Based on the biological mechanisms of synthetic lethality, it is divided into gene level, organelle level, biological pathway level and conditional synthetic lethality. Several personalized or precise genotype-targeted cancer treatments exhibit optimistic solutions in cancer patients. For example, diverse studies on imatinib, a KIT inhibitor indicate an effective treatment option in patients with KIT-mutant gastrointestinal stromal tumours (50% response rates). The BCR-ABL fusion tyrosine kinase is also targeted by imatinib inhibitor in chronic myelogenous leukemia patients (Li S, 2020).

One of the promising characteristics of synthetic lethality is the representation of cancer metabolism. Normal cells are transformed into malignant cells and these modified cells maintain metabolism for tumour initiation and progression. The cancer pathophysiology and clinical applications can be attained with a grasp on cancer metabolism concepts.

The principles of glycolytic regulation in cancer cells reveal interrelated signalling and metabolic networks. The tricarboxylic acid (TCA) cycle produces intermediates that act as the precursors for the nucleotides, amino acids and lipids. These progenitors complement the metabolite molecules obtained from various biological pathways including glycolysis and it contribute cancer cell proliferation. The cancer cells need metabolic reserves for its functioning like acetate, fatty acids, lactate and amino acids (serine and glycine) (Vander Heiden MG, 2017).

The cell metabolism-based cancer therapy can be utilized with the understanding of cancer cell metabolism outlook. The genetic mutations in the prime metabolic enzymes result in the cell malignancy by reprogramming

metabolic activities. Cancer cells grow and show metastasis by using three important metabolic processes including mitochondrial oxidative phosphorylation, amino acid catabolism and glycolysis. The cancer-specific metabolic remodelling applies the concept of synthetic lethality with cellular metabolism.

The metabolic enzymes can be targeted with synthetic lethality screening techniques for anticancer therapy and overcoming drug resistance. For example, a possible target is glycogen phosphorylase liver shows enhanced expression after bevacizumab treatment in an *in vivo* xenograft model. Understanding the synthetic lethality gene combinations could result in exposing the biomarkers and drug combinations with clinical relevance (Ju SH, 2022).

The research work of Sydney Farber based on cancer metabolism targets used inhibitors of folate synthesis to kill leukaemia cells successfully. The antifolates are effectively used in combined therapies against increased nucleotides and DNA replication in tumour cells however, normal proliferative tissues toxicity is observed in bone marrow and intestinal epithelium. It leads to the development of antimetabolites (anticancer drugs) affecting nucleotide biosynthesis for cancer therapy.

Beyond conventional therapeutic drugs, synthetic lethality (SL) establishes therapeutic perspectives for targeting tumour cells specifically. The inhibitor molecules or high-throughput RNAi-based screening techniques are used for the systematic screening of synthetic lethality interactions in human cells. These screens assist in locating synthetic lethality signalling pathways in cancer cells. In recent studies, synthetic lethality partners of MYC gene show that high expression genes among functional categories are cell cycle and DNA-repair genes. The newly emerged synthetic lethality linked MYC genes are cyclin-

dependent kinase 12 (CDK12), AAA domain containing 2 (ATAD2), ATPase family, BRCA1-associated RING domain protein 1 (BARD1) and cat eye syndrome chromosome region candidate 2 (CECR2).

The cellular metabolism also utilizes the idea of synthetic lethality. For instance, the functional mammalian target of rapamycin (mTOR) pathway presents the synthetic lethality connection between the oncogenic MYC and AMPK-related kinase 5 (ARK5). It maintains the therapeutic advantage of the synthetic lethal interactions. The personalised metabolic profiles of breast and lung cancer patients are organised which concludes the outcomes effectively (Zecchini V, 2017). The synthetic lethality link between PARP inhibitors and BRCA1-DNA repair pathway deficient system is represented in Figure 1-12.

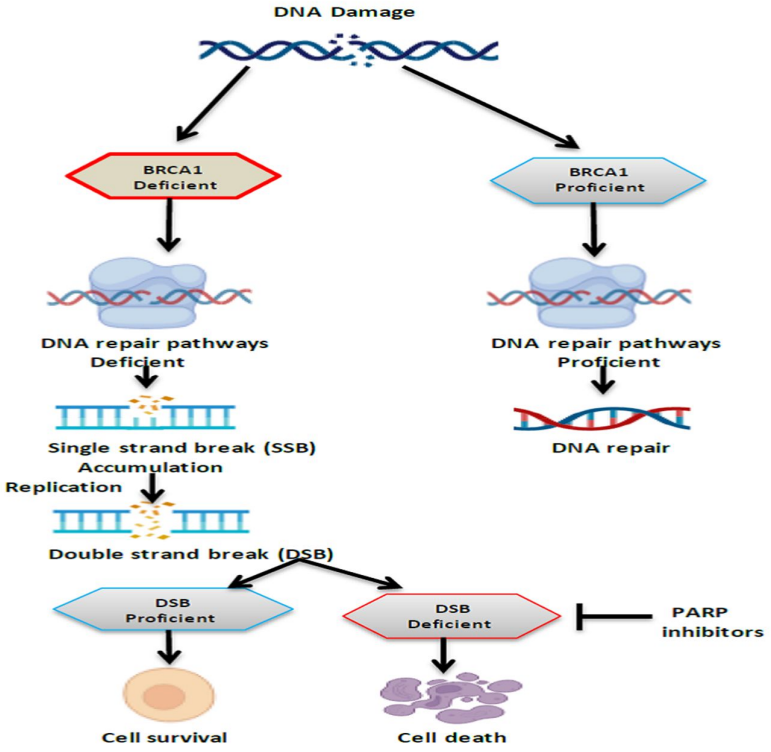


**Figure 1-12**: Representation of synthetic lethality between PARP inhibitors and BRCA1-DNA repair pathway deficient system. (Original figure)

### 1.4.2 NER gene polymorphisms in ovarian cancer

Single nucleotide polymorphisms (SNPs) in drug transport, drug metabolism, drug target and DNA repair have been described including in NER patients. Most of the genes are polymorphic in the nucleotide excision repairing (NER) system. The efficiency of DNA repair is affected as these SNPs could alter the function of these proteins. However, the significance of SNPs in this context is largely unknown. An impaired NER system in individuals will remove minimum carcinogen-induced adducts hence it increases cancer risk. Chemotherapy drug efficacy and clinical outcome are improved in patients carrying inefficient NER genotypes as chemotherapy-induced DNA adducts are removed at a lower rate (Saldivar JS, 2007).

### 1.4.3 Alterations in DNA repair in ovarian cancer and their prognostic/predictive value

For the repair of platinum-induced intra-strand crosslinks and the elimination of inter-strand crosslinks; the nucleotide excision repair (NER) pathway functions along with the HR pathway and FA repairing system is required. Approximately 8% of epithelial ovarian cancer (EOC) genes show splice mutations and homozygous deletions of NER genes. Overall survival (OS) and progression-free survival (PFS) improve in patients with NER alterations compared to those without NER alteration conditions. Similar to BRCA1/2-mutated tumours inactive NER pathways could promote platinum sensitivity in EOC. ERCC1 is the most studied NER protein as a possible predictive biomarker of platinum response in EOC. The platinum-induced adducts are eliminated with 5'cleavage of the DNA strands by a complex unit of ERCC1 protein and XPF. Other NER genes studied at the mRNA level and gene polymorphisms are

XPB, XPA, XPD and XPF but these do not show any correlation with cisplatin resistance in the ovarian cancer cells (Damia G, 2019).

### 1.5 Fanconi anemia pathway

Fanconi anemia (FA) is a complex genetic disorder marked by ineffective repairing of DNA interstrand cross-links (ICLs) leading to congenital defects, bone marrow failure (BMF) and cancer risk. FA is characterized by massive cell death of the hematopoietic stem and progenitor cells (HSPC) causing bone marrow failure (BMF) and uncontrolled cell proliferation generating FA malignant cells. FA proteins are known to interact with various DNA repair proteins to remove clastogenic (chromosome-breaking) effects of DNA ICLs.

The biallelic homozygous germline mutations in 22 FANC genes cause Fanconi anemia (FA). Monoallelic heterozygous germline mutations in FA can also increase cancer susceptibility compared to general population (Niraj J, 2019). The classification of Fanconi anemia genes and their molecular functions are summarised in Table 1-6.

**Table 1-6**: Classification of Fanconi anemia genes and their molecular functions

| | | Gene | Alias | Patient frequency (%) | Molecular functions |
|---|---|---|---|---|---|
| Genes mutated in FA patients | FA core complex | *FANCA* | | 64 | Subcomplex with FANCG and FAAP20[a] |
| | | *FANCB* | | 2 | FA core complex; subcomplex with FAAP100 and FANCL |
| | | *FANCC* | | 12 | FA core complex; forms a ternary complex with FANCE, FANCF, and FANCD2 |
| | | *FANCE* | | 1 | FA core complex |
| | | *FANCF* | | 2 | FA core complex; required for interactions among FANCA, FANCC, and FANCE |
| | | *FANCG* | *XRCC9* | 8 | FA core complex; subcomplex with FANCA and FAAP20; complex with BRCA2, XRCC3, and FANCD2 |
| | | *FANCL* | | 0.4 | RING domain containing E3 ubiquitin ligase within FA core complex |
| | | *FANCM* | | 0.1 | ATR-mediated checkpoint activation; recruitment of FA core complex and BLM |
| | | *FANCT* | *UBE2T* | 0.1 | FA core complex; E2 ubiquitin-conjugating enzyme |
| | ID2 | *FANCP* | *SLX4* | 0.5 | Master scaffold and regulator of ERCC1-XPF, MUS81-EME1/2, and SLX1 nucleases to excise ICLs |
| | | *FANCD2* | | 4 | ID2 complex; functions in the ICL excision and bypass step, multiple downstream functions |
| | | *FANCI* | | 1 | ID2 complex; multiple functions in the ICL repair and replication stress response |
| | FA/HR | *FANCD1* | *BRCA2* | 2 | HR; stimulates RAD51 recombinase; fork stabilization |
| | | *FANCJ* | *BRIP1* | 2 | Interaction with BRCA1 promotes HR and inhibits TLS; DNA-dependent ATPase and 5′-3′-helicase |
| | | *FANCN* | *PALB2* | 0.7 | HR; stimulates RAD51 recombinase; fork stabilization; links BRCA1 and BRCA2 |
| | | *FANCO* | *RAD51C* | 0.1 | HR |
| | | *FANCR* | *RAD51* | Rare | HR; fork stabilization |
| | | *FANCS* | *BRCA1* | 0.1 | HR; eviction of CMG (CDC45-MCM-GINS) complex at ICL-induced stalled forks |
| | | *FANCU* | *XRCC2* | 0.1 | HR |
| | Recent | *FANCV* | *REV7/MAD2L2* | One patient | Negatively regulates DNA end resection; promotes end joining; modulates PARPi response |
| | | *FANCW* | *RFWD3* | One patient | E3 ubiquitin ligase for regulating turnover of RPA and RAD51 during HR and ICL repair |
| | | *FANCQ* | *ERCC4, XPF* | 0.1 | DNA incision and NER |
| FA-associated genes | | *FAAP10* | *STRA13/CENPX/MHF2* | | FA core complex; histone fold–containing protein; constitutive chromatin localization of FANCM |
| | | *FAAP16* | *APITD1/CENPS/MHF1* | | FA core complex; histone fold–containing protein; constitutive chromatin localization of FANCM |
| | | *FAAP20* | *C1orf86* | | FANCA stability; binds ubiquitinated TLS polymerase REV1 |
| | | *FAAP24* | *C19orf40* | | FA core complex; interacts with FANCM |
| | | *FAAP100* | *C17orf70* | | FA core complex |
| | | *FAN1* | | | Nuclease; restart of stalled replication forks |
| | | *UAF1* | | | ID2 deubiquitination |
| | | *UHRF1* | | | Lesion recognition |
| | | *USP1* | | | ID2 deubiquitination |

### 1.5.1 Molecular details of the FA pathway

There are 22 identified complementation groups (FANCA–FANCW) known as FA genes. Fanconi anemia (FA) is an autosomal biallelic germline disorder caused by the inactivation of FA genes excluding X-chromosomal-FANCB. FA pathway repairs ICLs where FA proteins interact with FA-associated proteins

(FAAP) in a common cellular pathway. In eukaryotes, the FA pathway accommodates nucleotide excision repair (NER) and homologous recombination (HR) for the recognition and elimination of ICLs damage. The biallelic mutations in the ovarian and breast cancer susceptibility genes BRCA1 (FANCS), PALB2 (FANCN) and BRCA2 (FANCD1) are recognized in FA patients hence the importance of the FA pathway to cancer. FA patients are inclined to various types of cancer. For instance, acute myeloid leukemia (AML) and embryonic tumour patients have mutations in FANCD1 and FANCN genes although other FA complementation groups mutated develop squamous cell carcinoma and AML (Niraj J, 2019).

### 1.5.2 The detection and removal of DNA interstrand cross-links by the FA pathway

The chemotherapeutic agents such as platinum compounds (cisplatin, carboplatin etc.), mitomycin C, nitrogen compounds and psoralen produce hypersensitivity in FA deficient cells. The endogenous sources of interstrand cross-links (ICLs) such as acetaldehyde and formaldehyde (biological intermediates) are generated by metabolic processes such as lipid peroxidation, alcohol metabolism and histone demethylation. ICLs are repaired by the components of transcription-coupled (TC) NER at actively transcribed regions in non-dividing cells. ICLs can be recognized by the mismatch or nucleotide excision-repair (NER) repair components throughout the cell cycle however, the repair is ineffective with incomplete removal of ICLs. The FA core complex is constructed with FA associated proteins and interconnected with other DNA repair proteins (Figure 1-13).

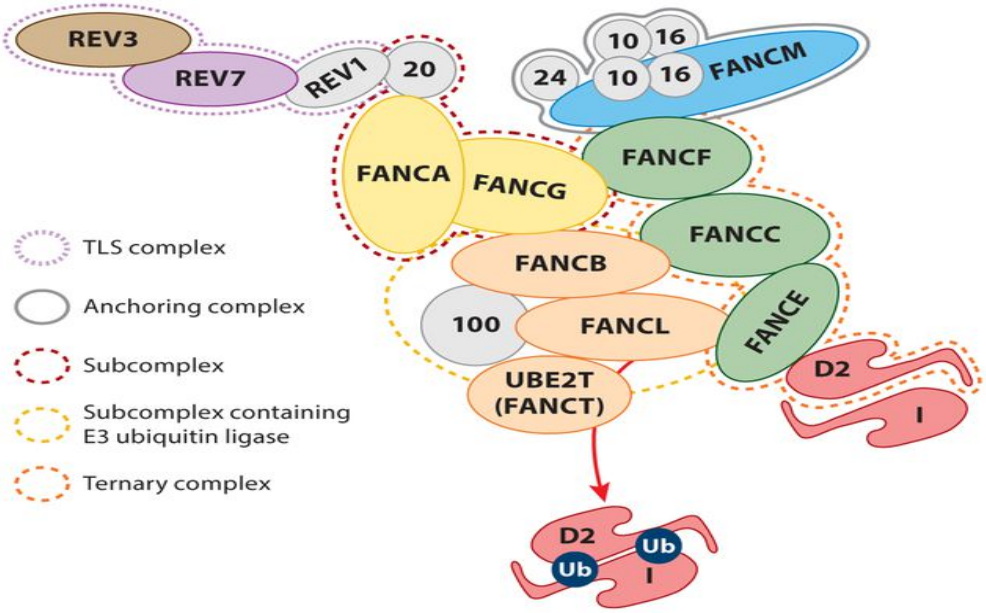


**Figure 1-13**: Fanconi anemia (FA) core complex is constructed with Fanconi anemia-associated proteins indicated by numbers. The link between the translesion synthesis mechanism and the FA pathway is the FAAP20-FANCG-FANCA subcomplex. Adapted from Niraj J, 2019.

### 1.5.3 FA deficient cancers are vulnerable to DSB repair and DNA damage response targeted therapies

Topoisomerase I and topoisomerase II inhibitors can induce DSBs in cells. In FA deficient cells, DSBs are not repaired leading to cell death. Poly ADP-ribose polymerase (PARP) inhibitors have synthetic lethality approaches to different DNA repair mechanisms including the HR pathway.

The concept of synthetic lethality promotes the killing of tumour cells (BRCA1/BRCA2 deficient) by Poly (ADP-ribose) polymerase (PARP) inhibitors effectively. In BRCA1/2 defective cells, PARP inhibitors form single-strand breaks (SSBs) of DNA eventually converting into double-strand breaks (DSBs) during replication (Helleday T., 2011).

Clinically, in ovarian and breast cancers a durable antitumor response is generated by the PARP inhibitor olaparib. These cancerous cells are more sensitive to PARP inhibitors and commonly carry mutations in BRCA1/2 or other FA genes. For the treatment of relapsed breast and ovarian cancers, the FDA-approved PARP inhibitors are rucaparib, niraparib and olaparib. DNA damage activates the DNA damage responses that coordinate with the cellular processes including transcriptional changes, DNA damage repair pathways and cell cycle checkpoints.

The agents in early-phase clinical trials are double-strand break (DSB) DNA damage response proteins, inhibitors of DNA-dependent protein kinase, ATR and ATM proteins. Similarly, inhibitors show promising antitumor activity in phase I and II trials of the cell cycle checkpoints CHK1, CHK2 and WEE1. Further, agents targeting deubiquitinating enzymes like USP1 and inhibitors of DNA polymerases (POLQ) have emerged as new promising preclinical therapeutic targets (Niraj J, 2019).

### 1.5.4 Mechanisms of resistance to DNA-damaging therapies

Cancer cells develop resistance to DNA-damaging therapies and it is a notable obstacle to improve patient outcomes. Tumours may modulate the tumour microenvironment, reducing the bioavailability of the compound is one of the mechanisms contributing to resistance to ICL-inducing agents (platinum). The future combination therapies for the patients expose the biomarkers and mechanisms of resistance in the cancer cells (Niraj J, 2019).

Cancers in advanced stages face a common obstacle of drug resistance. For improving cancer treatment efficacy, it is of paramount importance to control this trouble of drug resistance (Janysek DC, 2021).

The genomic stability and integrity are maintained by eliminating DNA damages using several pathways of DNA damage response (DDR). One of the DDR inhibitors (DDRis) are poly (ADP-ribose) polymerase inhibitors (PARPi) approved for the treatment of pancreatic, prostate, ovarian and breast cancer. In clinical settings, PARPi resistance is a major concern surrounding disease relapse and patients' outcome. There are several factors that participate in the mechanisms of DDRi resistance including drug efflux, stabilization of the replication fork, epigenetic modifications and reversion mutations (Jurkovicova D, 2022).

Targeting DNA damage repair proteins, synthetic lethality and combination with immunotherapy are strategies for acknowledging drug resistance. The promising drug targets like tumour metabolism and the microenvironment are considered for overcoming drug resistance. For effective cancer treatment, the understanding of metabolic changes and vulnerabilities of cancer play a crucial role (Tiek D, 2021).

### 1.6 FA Complementation Group D2 (FANCD2) structure and function

FA genes that have been cloned are ten in number (A, C, D1/BRCA2, D2, E, F, G, J, L, and M) and 12 FA complementation groups (A, B, C, D1, D2, E, F, G, I, J, L and M) have been described. The role of all the FA proteins is performed through a common pathway. For the activation/ monoubiquitination of the downstream FANCD2 (FA Complementation Group D2) protein, FA proteins (A, B, C, E, F, G, L and M) are assembled in a nuclear complex. FANCD2 is monoubiquitinated at Lys561 by the E3 ubiquitin ligase activity of FANCL. The

USP1 is the newly identified deubiquitinating enzyme of FANCD2. In response to DNA damage, there is monoubiquitination and foci formation of FANCD2 which require BRCA1 along with colocalization of FANCD2 with BRCA1 and BRCA2. Consequently, a common FA-BRCA pathway of DNA damage response functionally incorporates Fanconi anemia proteins, BRCA1 and BRCA2.

It has been reported that in response to infrared radiation (IR) or psoralen/UV-A, ATM or ATR kinase pathway mechanisms phosphorylate FANCD2. In response to IR, hydroxyurea or mitomycin C; FANCD2 requires ATR for its monoubiquitination. DNA cross-linking agents form chromosome aberrations (breaks and radials) in FA cells. For maintaining the chromosomal stability in cells, FANCD2 plays a crucial role. It repairs DNA double-strand breaks cooperating with the HR pathway, single-strand annealing and promotes pairing of homologous strands during meiosis. During cell division, it prevents breakage and loss of missegregation of chromatin (Wang Y, 2006).

The mitomycin C (MMC) or diepoxybutane (DEB) treatment results in the cytogenetic quantitation of chromosomal breakage which is used as the current diagnostic test for Fanconi anemia (FA). A study suggests a biochemical pathway for FA which includes the monoubiquitination of the FANCD2 protein. The patient monitoring and treatment decisions depend remarkably on an accurate, early diagnosis of FA disease in which the family members of the patients engage in the genetic counselling.

In recent studies, the explanation of FA signalling pathway provides a diagnostic and subtyping screen for FA. For the functioning of multiple FA genes, the FANCD2 monoubiquitination and the protein translocation to nuclear foci is required (Shimamura A, 2002). The structure of singly monoubiquitinated human FANCI–FANCD2 is illustrated in Figure 1-14.

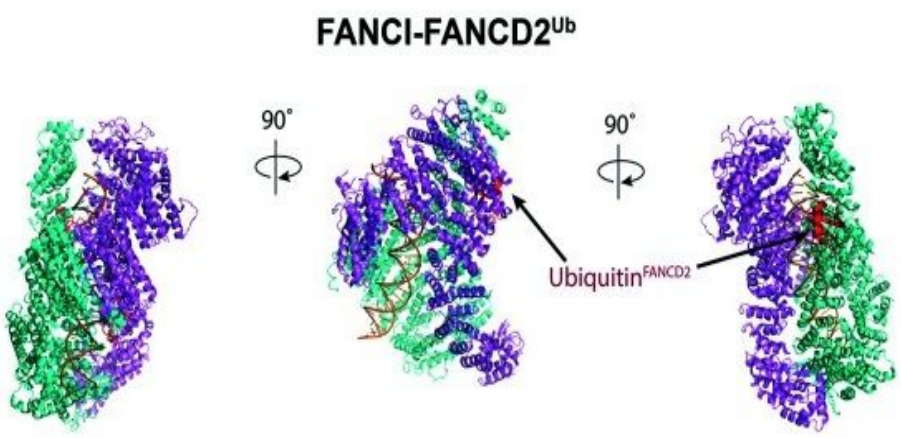


**Figure 1-14:** Structure of singly monoubiquitinated human FANCI–FANCD2. Adapted from Li L, 2020.

The DNA interstrand crosslinks repairing need mono-ubiquitination of FANCD2 and proteins interaction with FANCI on DNA strands. To protect DNA from stalled replication, the process called monoubiquitination results in the formation of the FANCD2: FANCI complex surrounding DNA in a filament-like array.

The interaction of the nuclease FAN1 enzyme on DNA requires a mono-ubiquitination process. The chromosomal abnormalities and DNA replication fork progression are restricted by FAN1 recruitment and its consequent activity. Deficiency in FANCD2 may increase the risk of acute myeloid leukemia (AML) and squamous cell carcinomas (head, neck and anogenital squamous cell carcinomas). The expression level of FANCD2 protein is high in lung squamous tumours (Lachaud C, 2016).

## 1.7 FA Complementation Group A (FANCA) structure and function

The most frequently affected complementation group in FA patients approximately ~64% of all mutations is FA Complementation Group A (FANCA), an element of the FA core complex (Figure 1-15). In FA repairing pathway, one of the FA proteins FANCA promotes DSB and ICL repair *via* FANCD2 monoubiquitination. In an *in vitro* system, the secondary function of FANCA is to support FANCD2 monoubiquitination although it plays a role in ICL repair. Furthermore, the FANCD2 monoubiquitination is found in FA disease developed due to FANCA mutants. FANCA may have roles besides the FA pathway and it is suggested after mitomycin C sensitivity testing. However, differential diagnosis of FA disease shows FANCA protein contributes to DNA double-strand break (DSB) repair by catalysing single-strand annealing and strand exchange processes. Hence, FANCA promotes the biochemical activities of strand exchange (SE) and single-strand annealing (SA). FANCA promotes DNA double-strand breaks repairing with RAD52 factor and the FA pathway in human cells. The SSA sub-pathway of DSB repair involves the FA core complex through the established FA pathway.

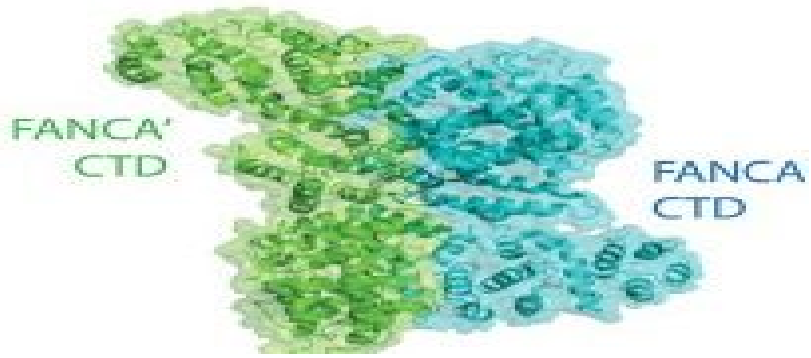


**Figure 1-15**: Structure of FANCA C-terminal domain (CTD) dimer.

Adapted from Li L, 2020.

FANCA has a high affinity for a single-strand DNA compared to dsDNA. It is suggested from the homodimeric structure of FANCA that it functions to bring two complimentary ssDNA adjacent forming dsDNA and it indicates its high affinity for ssDNA. FANCA conducts the formation of dsDNA since it has low dsDNA affinity, releasing the dsDNA product for commencing the next round of catalysis. It is a key point to note that a mutation in the FANCA gene even a change in single residue results in defective strand annealing but it is capable of DNA binding. This shows that FANCA DNA binding affinity is inadequate to anneal ssDNA and that a dynamic interaction between DNA and FANCA is required for FANCA-catalyzed strand annealing (Benitez A, 2018).

## 1.8 Hypothesis

In this study, it was aimed to investigate FA pathways for synthetic lethality (SL) application. The hypothesis stated that SL relationship may exist between DNA repair genes (XAB2, FANCD2 and FANCA) and PARP inhibitors. It was postulated that repair gene deficient breast and ovarian cancers could be targeted with DNA damaging agent (cisplatin) and repair inhibitor (olaparib). This new application will offer personalised therapies for new cohorts of patients with repair gene deficient tumours. In addition, it was hypothesised that targeting XAB2 could be a novel biomarker and strategy for personalization of cancer therapy. Expression of XAB2, FANCD2 and FANCA may have clinicopathological significance in breast and ovarian cancers. Low XAB2 expression was associated with good overall survival in ovarian cancer. It was postulated that cisplatin and olaparib could be a possible chemo preventative management for gene deficient cancer. In the context of dysregulation of nucleotide excision repair pathway, hypothesis dictated that low expression of XAB2 was associated with high tumour grade and platinum resistance in cancer patients. It was postulated that FANCD2 and FANCA inhibition can be a novel approach for platinum chemo sensitization in ovarian cancers and DNA repair inhibitors can induce synthetic lethality in gene deficient breast and ovarian cancers.

## 1.9 Objectives

The aims of this project are as follows:

1) To investigate the expression of XAB2 (at the transcriptomic and protein level) in large clinical cohorts of breast and ovarian cancers.

2) To profile a panel of breast and ovarian cancer cells for XAB2 expression, studying the effects of XAB2 gene depletion by siRNA and investigating chemosensitivity.

3) To profile a panel of breast and ovarian cancer cells for FANCD2 expression, studying the effects of FANCD2 gene depletion by siRNA and investigating chemosensitivity.

4) To profile a panel of breast and ovarian cancer cells for FANCA expression, studying the effects of FANCA gene depletion by siRNA and investigating chemosensitivity.

# 2 Materials and Methods

## 2.1 Materials:

### 2.1.1 Compounds

The cisplatin compound (catalogue no.-232120) was obtained as a solution (3.3mM) from the pharmacy of Nottingham University Hospitals and stored at room temperature.

AstraZeneca Pharmaceuticals provided the compound olaparib (catalogue no.-S1060) and stored at room temperature. This compound was suspended in 100% v/v dimethyl sulphoxide (DMSO) (Sigma, UK).

### 2.1.2 Cell lines and culture media

The cell lines used in the experiments were purchased from the American Type Culture Collection (ATCC) and these were cultured according to ATCC recommendations. The cell line authentication was performed with AuthentiFiler TM PCR Amplification Kit. All cells were tested for mycoplasma using a MycoProbe Mycoplasma Detection Kit (R&D systems) regularly. All cell lines were used for up to fifteen passages. RPMI-1640 medium (L-Glutamine 580mg/L, 4500 mg/L D-Glucose and 110mg/L Sodium Pyruvate) (Invitrogen, UK) was supplemented with 10% FBS and 1% penicillin/ streptomycin. All materials were obtained from (Sigma and Thermo Fischer Scientific, UK) unless otherwise stated. The cell lines and its culture conditions were summarised in Table 2-1.

**Table 2-1**: Cell lines and its culture conditions

| Cell Lines | Description | Culture Media |
|---|---|---|
| MCF7 | Human breast adenocarcinoma adherent cell line. Purchased from ATCC®. | RPMI 1640 + 1% penicillin/Streptomycin +10% FBS. |
| MDA-MB-231 | Human breast adenocarcinoma adherent cell line. Purchased from ATCC®. | RPMI+ 2 mM L-glutamine +10% FBS + 1% penicillin/streptomycin. |
| SKBR3 | Human breast adenocarcinoma adherent cell line. Her positive. Purchased from ATCC®. | Mc Coy's media + 2 mM L-glutamine +10% FBS + 1% penicillin/streptomycin. |
| DCIS | Human breast adenocarcinoma adherent cell line. | RPMI 1640 + 1% penicillin/Streptomycin +10% FBS. |
| PEO1 | Human ovarian cancer. Oestrogen receptor positive. Purchased from ATCC®. | RPMI -1640 + 10% FBS + 1% penicillin/streptomycin |
| PEO4 | Human ovarian cancer. Oestrogen receptor positive. Purchased from ATCC®. | RPMI -1640 + 10% FBS + 1% penicillin/streptomycin |
| A2780 | Human ovarian cancer. Sensitive to cisplatin. Purchased from ATCC®. | RPMI -1640 + 10% FBS + 1% penicillin/streptomycin |
| A2780-Cis | Human ovarian cancer. Resistance to cisplatin. Purchased from ATCC®. | RPMI -1640 + 10% FBS + 1% penicillin/streptomycin |
| OVCAR4 | Human ovarian cancer. Purchased from ATCC®. | RPMI -1640 + 10% FBS + 1% penicillin/streptomycin |
| SKOV3 | Human ovarian cancer. Purchased from ATCC®. | RPMI -1640 + 10% FBS + 1% penicillin/streptomycin |

## 2.2 Methods

### 2.2.1 Clinical studies

#### 2.2.1.1 Breast cancer study

The clinical study of XAB2 was conducted on a consecutive series of 1849 patients with invasive breast cancers. The primary tumour site was selected for tumour samples during surgery. The patients included in this study were diagnosed between 1986- 1999 and added into the Nottingham Tenovus Primary Breast Carcinoma series. The demographics of patients were summarised in Table 2-2. Patients received standard surgery (mastectomy or wide local excision) with radiotherapy. Prior to 1989, patients did not receive systemic adjuvant treatment (AT). After 1989, AT was scheduled based on prognostic and predictive factor status, including NPI, oestrogen receptor-α (ER-α) status, and menopausal status. Patients with NPI scores of <3.4 (low risk) did not receive AT. In pre-menopausal patients with NPI scores of ≥3.4 (high risk), classical Cyclophosphamide, Methotrexate, and 5-Flourouracil (CMF) chemotherapy was given; patients with ER-α positive tumours were also offered HT. Postmenopausal patients with NPI scores of ≥3.4 and ER-α positivity were offered HT, while ER-α negative patients received classical CMF chemotherapy. Median follow up was 111 months (range 1 to 233 months). Survival data, including breast cancer specific survival (BCSS) and the development of loco-regional and distant metastases (DM), was maintained on a prospective basis. Breast cancer specific survival (BCSS) was defined as the number of months from diagnosis to the occurrence of BC related-death. DM-free survival was defined as the number of months from diagnosis to the occurrence of DM relapse. Survival was censored if the patient was still alive at the time of analysis, lost to follow-up, or died from other causes.

The Reporting Recommendations for Tumour Marker Prognostic Studies (REMARK) criteria were recommended by McShane and associates (McShane LM, 2005) and it was followed throughout this study. The ethical approval for the study was granted by the Nottingham Research Ethics Committee following the Declaration of Helsinki and ethical approval (C202313). The written informed consent from patients was obtained where applicable. A total of 1849 cases of invasive breast cancer including ER+ and ER- were studied. The formalin-fixed paraffin-embedded (FFPE) blocks of these cases were retrieved (Queen's Medical Centre and Nottingham City Hospital) and TMA construction was obtained using an automated TMA Grand Master machine. The clinical-pathological data of cancer patients was collected from patent notes. The protein expression of the DNA repair factors had been assessed using immunohistochemistry (IHC). The clinicopathological characteristics of ER- cohort, ER+ cohort were summarised in Table 2-3 and Table 2-4 respectively.

**Table 2-2**: Clinicopathological characteristics of breast cancer patient's cohort

| **Clinicopathological Variables** | **Cases** | **(%)** n * 1849 |
|---|---|---|
| **Age at Diagnosis (years)** | 985 | (53.3%) |
| **Tumour Size (cm)** | 984 | (53.2%) |
| **Histological Tumour Grade** | 984 | (53.2%) |
| **Tubule Formation** | 973 | (52.6%) |
| **Pleomorphism** | 973 | (52.6%) |
| **Mitotic Count** | 971 | (52.5%) |
| **Histological Tumour Type** | 983 | (53.2%) |

| | | |
|---|---|---|
| **Nodal Stage** | 983 | (53.2%) |
| **NPI Prognostic Group** | 983 | (53.2%) |
| **LVI** | 983 | (53.2%) |
| **PR Status** | 984 | (53.2%) |
| **ER status** | 984 | (53.2%) |
| **HER2 Status** | 986 | (53.3%) |
| **Triple-Negative Status** | 986 | (53.3%) |
| **Reerral_method** | 756 | (40.9%) |
| **Menopausal status** | 756 | (40.9%) |
| **Bilateral** | 741 | (40.1%) |
| **Multifocality** | 555 | (30.0%) |
| **Type of operation** | 665 | (36.0%) |
| **Radiotherapy local** | 909 | (49.2%) |
| **Radiotherapy nodes** | 737 | (39.9%) |

**Table 2-3**: Clinicopathological characteristics of ER- cohort

| **Clinicopathological Variables** | **Cases** | **(%)** |
|---|---|---|
| **Age at Diagnosis (years)** | 194 | (54.8%) |
| **Tumour Size (cm)** | 194 | (54.8%) |
| **Histological Tumour Grade** | 194 | (54.8%) |
| **Tubule Formation** | 193 | (54.5%) |
| **Pleomorphism** | 193 | (54.5%) |

| | | |
|---|---|---|
| **Mitotic Count** | 193 | (54.5% ) |
| **Histological Tumour Type** | 193 | (54.5%) |
| **Nodal Stage** | 194 | (54.8%) |
| **NPI Prognostic Group** | 194 | (54.8%) |
| **LVI** | 194 | (54.8%) |
| **PR Status** | 193 | (54.5%) |
| **HER2 Status** | 194 | (54.8%) |
| **Triple-Negative Status** | 194 | (54.8%) |
| **Reerral_method** | 756 | (40.9%) |
| **Menopausal status** | 168 | (47.5%) |
| **Bilateral** | 166 | (46.9%) |
| **Multifocality** | 108 | (30.5%) |
| **Type of operation** | 138 | (39.0%) |
| **Radiotherapy local** | 186 | (52.5%) |
| **Radiotherapy nodes** | 169 | (47.7%) |

**Table 2-4**: Clinicopathological characteristics of ER+ cohort

| **Clinicopathological Variables** | **Cases** | **(%)** |
|---|---|---|
| **Age at Diagnosis (years)** | 789 | (53.3%) |
| **Tumour Size (cm)** | 788 | (53.2%) |
| **Histological Tumour Grade** | 788 | (53.2%) |
| **Tubule Formation** | 780 | (52.7%) |

| | | |
|---|---|---|
| **Pleomorphism** | 780 | (52.7%) |
| **Mitotic Count** | 778 | (52.6% ) |
| **Histological Tumour Type** | 788 | (53.2%) |
| **Nodal Stage** | 787 | (53.2%) |
| **NPI Prognostic Group** | 787 | (53.2%) |
| **LVI** | 787 | (53.2%) |
| **PR Status** | 789 | (53.3%) |
| **HER2 Status** | 790 | (53.4%) |
| **Triple-Negative Status** | 790 | (53.4% ) |
| **Menopausal status** | 587 | (39.7%) |
| **Bilateral** | 572 | (38.6%) |
| **Multifocality** | 447 | (30.2%) |
| **Type of operation** | 527 | (35.6%) |
| **Radiotherapy local** | 722 | (48.8%) |
| **Radiotherapy nodes** | 567 | (38.3%) |

### 2.2.1.2 Ovarian cancer study cohort

The investigation of XAB2 expression in epithelial ovarian cancers was carried out on tissue microarrays of 525 consecutive ovarian epithelial cancer cases treated at Nottingham University Hospitals (NUH). The classification of patient's staging was directed according to the International Federation of Obstetricians and Gynaecologists (FIGO) staging system for ovarian cancer. The

overall survival (OS) for patients was calculated from the operation date until the 1st of October 2016 when any remaining survivors were censored.

The investigation of XAB2 expression in epithelial ovarian cancers was carried out on tissue microarrays of 525 consecutive ovarian epithelial cancer cases treated at Nottingham University Hospitals (NUH) between 1997 and 2010. Tumour stage was determined according to the International Federation of Obstetricians and Gynaecologists (FIGO) Staging System for Ovarian Cancer. The clinicopathological data included the tumour histology type, International Federation of Obstetricians and Gynecologists (FIGO) stage, grade, and tumour surgical debulking and chemotherapy regimen used. All patients received platinum-based chemotherapy. Platinum resistance was defined as patients who developed progression during first-line platinum chemotherapy or relapse within 6 months after completing platinum treatment. Progression-free survival (PFS) was calculated from the date of the initial surgery to disease progression or from the date of the initial surgery to the last date known to be progression-free for those censored. Overall survival (OS) was calculated from the operation date until the time of death or the last date of follow-up, when any remaining survivors were censored.

The progression-free survival (PFS) is calculated from the date of the initial surgery to disease progression or from the date of the initial surgery to the last date known to be progression-free for those censored. The patient who had progression during first-line platinum chemotherapy or relapsed within 6 months after completion of chemotherapy was termed platinum resistance. The demographics of patients were summarized in Table 2-5.

**Table 2-5**: Clinicopathological characteristics of ovarian cancer patient's cohort

| **Clinicopathological Variables** | **Cases** | **(%)** n * 525 |
|---|---|---|
| **Death status** | 191 | (36.4%) |
| **Relapse status** | 187 | (35.6%) |
| **Menopausal Status** | 211 | (40.2%) |
| **Age at Surgery** | 213 | (40.6%) |
| **Type of Surgery**<br>**Biopsy Early debulking intervalde** | 210 | (40.0%) |
| **Surgical Pathology Type**<br>**Serous Mucinous Endometrial** | 213 | (40.6% ) |
| **Tumour Grade** | 185 | (35.2% ) |
| **Surgical Pathology Stage** | 207 | (39.4%) |
| **Surgical Result Optimal Debulking Not**<br>**optimally debulked** | 195 | (37.1%) |
| **Residual Tumour Following Surgery** | 194 | (37.0%) |
| **Measurable Disease Before Chemotherapy**<br>**Non Measurable** | 192 | (36.6%) |
| **Chemotherapy Treatment** | 188 | (35.8%) |
| **Platinum Sensitivity** | 183 | (34.9% ) |
| **Radiotherapy nodes** | 567 | (38.3%) |

### 2.2.2 Tissue microarray construction

In tissue microarray (TMA) construction, the formalin-fixed paraffin-embedded (FFPE) blocks with tumour load and ideal thickness for arraying was selected. The paraffin wax blocks carrying 2 replicates of 0.6mm cores were used for constructing TMAs. The centre and periphery parts of the tumours were selected for samples and other tissue sections for comprehensive evaluation of the tumour and surrounding stroma. The automated TMA array machine was used to load up to 60 donor blocks at a time on the recipient blocks. The orientation of the tissue cores was marked by using three normal kidney cores in the first row and two more tissue cores in the last row so that orientation could be preserved. To perform the IHC staining, the TMAs were constructed with sections (4μm thickness) on glass slides (Kononen J, 1998).

The TMA was constructed in the research laboratory prepared by Prof. Emad Rakha team. TMA was built from donor tumour tissue blocks including tumour samples, 0.6mm cores, the periphery of each invasive tumour was selected and arrayed using a tissue microarray (TMA) GrandMaster (3D Histech) (PMID: 28478613). Immunohistochemical staining was performed on 4μm TMA sections. Data from one core per tumour were considered for scoring as one version of the TMA blocks stained. Full face cases were selected randomly to represent large amount of tumour and normal tissue displayed the pattern of expression and suitability of TMA for depicting the tumours.

### 2.2.3 Immunohistochemical staining

The protocol for performing Immunohistochemistry (IHC) experiments was validated and published previously (Green AR, 2015). The Novolink Polymer

Detection System Kit (Leica Biosystems, RE7150-K) was used to stain TMAs on slides. The experiment was initiated by keeping the slides on a heating pan (60°C) for 10 minutes. The Leica autostainer machine was used for deparaffinization and rehydration of slides. The slides were automatically processed through immersion in two racks of xylene for 5 minutes each followed by washing three times (2 minutes each wash) with 100% industrial methylated spirit (IMS). The rehydration process was taken place in water racks and the slides were dipped three times for 5 minutes each.

#### 2.2.3.1 Antigen retrieval and staining

The antigen retrieval steps were performed for biomarkers .The slides were placed in 0.1M sodium citrate buffer (pH-6.0) using a microwave oven for 20 minutes. The running tap water was poured over the slides and primary antibodies were added at the indicated dilutions (Table 2-6).

The endogenous peroxidase activity was blocked by incubating the slides with 100 μl of the supplied peroxidase block solution (Novolink kit) for 5 minutes. The slides were then washed with tween phosphate buffer saline (TBS) three times for 5 minutes each. The post-primary block and Novolink polymer were added for 30 minutes followed by washing with TBS three times. The peroxidase reaction was visualised using the freshly prepared solution of 3-3' Diaminobenzidine tetrahydrochloride (DAB). The volume of 100 ml of diluted DAB chromogen was diluted at 1:20 dilution in the DAB substrate provided by the kit. Finally, the slides were counterstained with Novolink haematoxylin for 6 minutes and these were dehydrated in the Leica autostainer machine. The slides were then covered with coverslips and left in the fume cupboard to dry overnight.

The negative controls were included in each run without the primary antibody incubation step. The positive control tissues with known reactivity to stained antibodies were included for each antibody accordingly. Positive control was normal lymphoid (lymph node/spleen) tissue within the TMA. Negative control for IHC covered omission of the primary antibody and IgG-matched serum. The antibody staining conditions and cut-off points for analysis were summarised in Table 2-6.

**Table 2-6:** Antibodies for immunohistochemistry

| **Antibody** | **Supplier** | **Dilution** | **H-score cut-off** |
|---|---|---|---|
| Anti- XAB2 rabbit monoclonal antibody (Breast TMAs) | Abcam, catalogue number- ab180181 | 1:50. Incubation period for 60 minutes at room temperature. | XAB2_median_110 |
| Anti- XAB2 rabbit monoclonal antibody (Ovarian TMAs) | Abcam, catalogue number- ab180181 | 1:50. Incubation period for 60 minutes at room temperature. | XAB2_median_110 |

### 2.2.4 Optimisation of immunohistochemistry (IHC) conditions

The antibody supplier recommended the dilution range and the slides were incubated at three dilution factors of the antibody for the optimisation of the staining conditions. Furthermore, one hour of antibody incubation or overnight incubation and temperature were evaluated. For selecting the optimum conditions, the slides were reviewed by a pathologist. The nuclear, cytoplasmic

or membranous sub-cellular localisation of a protein was demonstrated. For staining the slides of the whole cohorts, the specific antibody dilution was chosen and the requirement was immunohistochemistry with minimal background. The studied biomarkers were evaluated previously in research group for homogeneity staining in full-face sections (Green AR 2015). The concordance between the expression in full face and the TMAs was high. Therefore, TMA staining was suitable for assessment of the biomarkers.

### 2.2.5 Evaluation of immunohistochemistry.

In tumour cases, the cores comprising two units were evaluated separately and the mean value of the two histochemical scores (H-scores) was calculated. The intensity and positivity of the immunohistochemistry were determined by H-score values. The negative, weak, moderate or strong intensity of the staining was assigned a score of 0, 1, 2 or 3 respectively. The percentage of the positive cells was exhibited on a scale of 0-100 %. The range of final score (0-300) was calculated by a formula and it was represented in the following manner, 3×percentage of strongly staining nuclei + 2×percentage of moderately staining nuclei + percentage of weakly staining nuclei. As the data had parametric distribution, median was taken as a cut-off.

### 2.2.6 Statistical analysis of immunohistochemical data

The SPSS software version 21 was used for the statistical analysis of the data. The distribution of data was marked based on the median using cut-off points for negative H-scores. The univariate correlation was established between the biomarker expression and each of the clinicopathological parameters using chi-

squared tests. For multivariate data, the Cox regression analysis was performed. The Kaplan-Meier method was used for survival curve analysis. The p-value of <0.05 was considered a significant result. Adjusted p-values were calculated using the Benjamini and Hochberg method (Benjamini Y, 2005). The newly constructed cohort was reviewed by colleagues in the Pathology group. X-tiles software was used to determine the best cut-off value that was associated with outcome. This cut-off can be used to dichotomise patient cohorts based on outcome. The statistical analysis of IHC by SPSS software was performed by Dr. Islam Miligy based at Prof. Emad Rakha (co-supervisor) Pathology group.

### 2.2.7 Sub-culturing of cancer cell lines

All cell lines were cultured at 37°C in a humidified incubator with 5% CO2 and 95% air. For subculturing, different cell lines had separate reagents and sterile conditions. The medium was discarded accordingly and cells were washed with phosphate-buffered saline (PBS) (without Ca2+ and Mg2+) two times. The cells were detached from the flask by adding 5 ml or less of 0.5mg/ml trypsin-EDTA (Sigma, UK) for 5 minutes in an incubator (37°C). The medium was added to deactivate the trypsin and the suspension was centrifuged at 1000rpm for 5 minutes to remove residual trypsin. The pellet was resuspended in medium, mixed well and split into a new tissue culture flask. All cell lines were routinely confirmed to be mycoplasma negative.

### 2.2.8 Cryopreservation of cell lines

The cells were cryopreserved at a low passage number for future use. Before the freezing method, the cells were trypsinized and counted using a haemocytometer. One million cells were resuspended in 1 ml of freezing medium and these were stored in cryovials at -80°C overnight. The vials were transferred to liquid nitrogen for long-term storage. The freezing medium was prepared by mixing fresh medium (cell line dependent) with 10% DMSO. The cells were recovered from liquid nitrogen by thawing rapidly in a water bath at 37°C. Next, the cells were resuspended in 9ml fully supplemented culture medium and centrifuged at 1000rpm (5 minutes) for removing traces of DMSO reagent. The supernatant was discarded and the pellet was resuspended in medium. The cell suspension was transferred to tissue culture flasks.

### 2.2.9 Transient transfection of cell lines by siRNA

The two siRNA constructs were used for XAB2, FANCD2 and FANCA knockdown. The silencer-select siRNA constructs and negative scrambled control construct were purchased from Thermo Fisher (UK). The constructs were resuspended in 50μl nuclease-free water to make a stock solution of 100μM and diluted to 10μM working dilution at the time of transfection as per manufacturer recommendations. The Lipofectamine 3000 transfection reagent (Thermo Fisher, UK) was used to deliver siRNA into the cells in Opti-Mem low serum media (Sigma, UK). The Lipofectamine proportions were used as recommended in the manufacturer's protocol. To transfect cells with siRNA, 1-1.5×$10^6$cells were seeded in T-25 flasks overnight to achieve a 60-70% confluence condition so that the experiment could be performed the following day. The volume of Lipofectamine 3000 (20.8ml) was diluted in a 0.75 ml Opti-

Mem medium. Next, 9.4ml of 10mM working siRNA solution or negative control (catalogue no.-4390843 Thermo Fischer, UK) was diluted in 0.75ml Opti-Mem for 2-3 minutes. The diluted lipofectamine was added to the diluted siRNA tube and incubated for 15 minutes. Meanwhile, cells were washed with Opti-Mem media before the addition of the transfection master mix. The transfected flasks were incubated at 37°C overnight. The next day, the transfection medium was relapsed with a fresh culture medium supplemented with 10% FBS. The transfection efficiency was checked by western blotting on day 3 and day 5. The siRNA constructs and their sequences were summarised in Table 2-7.

**Table 2-7:** siRNA constructs and their sequences

| **Construct** | **Sequences** |
|---|---|
| XAB2 siRNA (ID-s32465) | 5′CUCUGGUACCGAUACCUGAtt 3′- sense sequence<br>3′UCAGGUAUCGGUACCAGAGtt 5′- antisense sequence |
| FANCD2 siRNA (ID-s533670) | 5′CAUUGUCAGUCAACUAAAAtt 3′- sense sequence<br>3′UUUUAGUUGACUGACAAUGag 5′- antisense sequence |
| FANCA siRNA (ID-s164) | 5′GCACCGUAUUAAGUACAAtt 3′- sense sequence<br>3′UUGUACUUGAAUACGGUGCta 5′- antisense sequence |
| Negative scrambled siRNA (ID-s4611) | 5′CACAGGGUAAGGAACUCGUC 3′-sense sequence<br>3′UGAGAGACGAGUUCCUUACC 5′-antisense sequence |

## 2.2.10 Preparation of cell lysates

**Whole cell lysates**

To prepare whole cell lysate for western blotting experiments, the cells were collected by trypsinization as described. The cells were counted using a Neubauer chamber haemocytometer, one million cells were lysed by resuspending the pellets in 100ml of RIPA buffer (20mM Tris, 150mM NaCl, 0.5% sodium deoxycholate, 1mM EDTA, 0.1% SDS) purchased from Sigma (UK) supplemented with 1% protease inhibitor (Sigma, UK), 1% phosphatase inhibitor cocktails 2 and 3 (Sigma, UK). The cell lysate was incubated on ice for 3 minutes. The lysate samples were centrifuged at 13000 rpm for 20 minutes in a 4°C pre-setup microcentrifuge. The supernatant was stored at -20°C.

**Nuclear and cytoplasmic extracts**

In preparation of nuclear and cytoplasmic lysates for pre and post-cisplatin western blotting experiments, cells were collected by trypsinization as described. The cells were counted using a Neubauer chamber haemocytometer; one million cells were lysed by resuspending the pellets in 100ml of nuclear and cytoplasmic extraction reagents purchased from Thermo Fischer Scientific, UK (Catalogue no.-78833). The pellet was resuspended in 200ml ice-cold CERI buffer from the kit. It was incubated on ice for 10 minutes. Next, the volume of 11ml ice-cold CERII buffer was added to the above preparation. The eppendorf tube was microcentrifuge at 1500 rpm for 15 minutes. The cytoplasmic extract was removed from the pellet to a clean pre-chilled tube. The insoluble fraction (pellet) was suspended in 100µl ice-cold NER buffer. The mixture was vortexed periodically to re-suspend the pellet after every 10 minutes. The eppendorf tube with nuclear extract was microcentrifuged at 1500 rpm for 15 minutes. The nuclear extract

(supernatant) was transferred to a clean pre-chilled tube immediately. Both extracts were stored at -80°C.

### 2.2.11 BCA protein quantification assay

The Pierce TM BCA Protein Assay Kit was used to quantify proteins in the cell lysate. The volume of 8ml of diluted protein samples (diluted 1:5 in nuclease-free water) was pipetted in triplicates in a 96-well plate. Then, these were mixed with 200ml of the working solution of BCA reagent and incubated at 37°C for 30 minutes before reading on a FLUOstar OPTIMA, UK/ Infinite F50 (UK) microplate reader at a wavelength 570 nm.

### 2.2.12 Western blotting

Western blotting is a semi-quantitative technique and it is used in determining relative protein levels in cells or tissue lysates. It consists of two prime steps, separation of proteins based on electrophoretic mobility using sodium dodecyl sulfate (SDS) - polyacrylamide gel and the second step is a transfer of proteins on nitrocellulose or polyvinylidene difluoride PVDF membranes electrophoretically in which the appropriate antibodies are used to detect the protein of interest. In this protocol, the sample buffer SDS 4× is purchased from Thermo Fischer (UK). The SDS is an anionic detergent and it is capable of breaking the hydrogen bonds between molecules that result in protein unfolding. The reducing agent Dithiothreitol (DTT) 10× (Thermo Fischer, UK) is added to the sample for breaking disulphide linkages between cysteine molecules. The cell lysates (20μg) are diluted in reducing agents and sample buffer. The protein samples are denatured by heating at 100°C for 5 minutes.

The precast SDS 4-12% gels (Thermo Fisher, UK) are used for loading the samples in a propanesulfonic acid-sodium dodecyl sulfate (SDS) sample buffer at 150 V for 90 minutes.

There are five main steps for detecting the protein of interest including transfer of proteins, blocking membrane, primary antibody addition, secondary antibody incubation, protein detection and analysis. The antibodies used in western blotting technique were summarised in Table 2-8.

**Table 2-8:** Antibodies used in western blotting

| **Antibody** | **Supplier** | **Incubation** | **Molecular weight** |
|---|---|---|---|
| Anti- XAB2 rabbit monoclonal antibody | Abcam, catalogue number- ab180181 | 1:2000. Overnight incubation period at 4°C. | 100kDa |
| Anti- FANCD2 rabbit monoclonal antibody | Abcam, catalogue number- ab178705 | 1:2000. Overnight incubation period at 4°C. | 155kDa |
| Anti- FANCA rabbit monoclonal antibody | Abcam, catalogue number- ab201457 | 1:1000. Overnight incubation period at 4°C. | 161kDa |
| Anti- GAPDH rabbit polyclonal antibody | Abcam, catalogue number- | Incubation period for 60 minutes at room | 36kDa |

| | | | |
|---|---|---|---|
| | ab9485 | temperature. | |
| Anti- β-actin mouse monoclonal antibody | Abcam, catalogue number-ab8226 | Incubation period for 60 minutes at room temperature. | 42kDa |
| Anti- YY1 rabbit monoclonal antibody | Abcam, catalogue number-ab109228 | Incubation period for 60 minutes at room temperature. | 45kDa |

#### 2.2.12.1 Transfer

The proteins are transferred from gel to a nitrocellulose membrane (Whatman, GE Healthcare) in a transfer buffer containing 20% (v/v) methanol, 50mM Tris-HCl and 380mM glycine. The SDS-PAGE gel containing the proteins is blotted in an Xcell II Blot Module (Invitrogen) in a semi-dry transfer method and the gel-membrane-filter sandwich is prepared for running at 25 V for 90 minutes.

#### 2.2.12.2 Blocking

After transferring the proteins to the membrane, the remaining sites on the membrane are blocked for reducing non-specific binding with the given antibodies. The reagent 5% non-fat milk prepared in phosphate-buffered saline (PBS) solution and 0.05% Tween-20 is used to block the membrane and it is incubated for 1 hour at room temperature.

#### 2.2.12.3 Primary antibody incubation

The primary antibody against the target protein is incubated at 4°C overnight or 1 hour at room temperature. After the primary antibody incubation steps,

the membranes are washed with PBS and 0.05% Tween-20 solution three times for 5 minutes each to remove unbound primary antibodies. The membranes are then incubated with an antibody (housekeeper protein) for relative protein quantification and analysis. The housekeeping antibodies used in the experiment are the β-actin antibody (Sigma, UK) and GAPDH (abcam, UK). All primary antibodies are diluted in 1% BSA (bovine serum albumin). After one hour of membrane exposure to the housekeeping antibody, the same washing step is repeated.

#### 2.2.12.4 Secondary antibody incubation

The membranes are exposed to horseradish peroxidase (HRP) conjugated secondary antibodies to enable the detection of the primary antibodies. The secondary antibodies used are IRDye 680RD Donkey anti-mouse IgG (cat. no.-926-68072) and IRDye 800CW Donkey anti-Rabbit (926-32213) IgG. These antibodies are used at 1:10,000 dilutions in 1%BSA. The incubation period is one hour at room temperature and the membranes are washed with PBS/0.05% Tween three times for 5 minutes each before drying and scanning it.

#### 2.2.12.5 Detection and analysis

The LI-COR Odyssey Imaging System is used to detect the antibody-reacted bands on the membranes. The Image Studio Lite software (version 3.1) (Li-Cor, USA) is used for the quantification of the bands. The housekeeping readings are used for normalizing the data of protein of interest. The assay is performed in three independent experiments. The student t-test or one way-ANOVA test is used to calculate statistical significance between samples. The graphs are produced and statistical analysis is performed using GraphPad Prism version 8.2.0 (435) software.

### 2.2.13 Cell proliferation assay (MTS assay)

The MTS assay kit (Promega, UK) is used for screening different compounds to identify the effects of agents on cell proliferation and cell viability. The MTS reagent contains tetrazolium compound [3-(4, 5-dimethylthiazol-2-yl)-5-(3-carboxymethoxyphenyl)-2-(4-sulfophenyl)-2H-tetrazolium, inner salt; MTS] and an electron coupling reagent phenazine methosulfate (PMS). The cells can reduce MTS into a formazan product and it is soluble in tissue culture medium. The activity of the dehydrogenase enzyme produces formazan and this enzyme is present in metabolically active cells only (Riss TL, 2016). The MTS experiment was performed to evaluate the cytotoxicity of inhibitors and the protocol was obtained from the recommendation of the manufacturer. In a 96-well plate, 1000 cells in 100 µl of a medium were seeded. The cells were left to adhere to the surface for 24 hours followed by incubation with varying concentrations of inhibitors. The MTS assay was performed on day 6. On day 6, the MTS reagent (20 µl) was added to each well and the incubation period was 3-4 hours at 37°C in the dark. The formazan absorbance was measured at 490 nm using a plate reader (FLUOstar OPTIMA, UK/ Infinite® F50, UK). The percentage of the absorbance was determined by making a comparison with the control population of untreated cells. This assay was performed three times with triplicate samples. The graphs were produced by statistical analysis using GraphPad prism software version 8.2.0.

### 2.2.14 Clonogenic survival assay

#### 2.2.14.1 Assay principle

The clonogenic survival assay is based on identifying cell survival after exposing cells to cytotoxic agents. The colonies are produced by the viable cells (5-6 rounds of replication) and the assay determines the cell survival capacity after drug effects (Munshi A, 2005).

#### 2.2.14.2 Plating efficiency

The cell lines were plated in 6-well plates at varying densities. These plates were incubated for 12-14 days under normal incubator conditions then media was removed and cells were fixed with methanol and acetic acid solution in plates for 10 minutes. The six well plates were stained with crystal violet. The colonies produced by the cells were counted manually.

#### 2.2.14.3 Clonogenic assay

The cells were seeded in a 6-well plate and allowed to adhere for 24 hours. The tested drugs were added at different concentrations and a control sample was set up for each cell line without drug. The plates were left in the incubator for 14 days. After incubation, the media was discarded and cells were fixed (100% methanol and acetic acid). The cell colonies were stained with crystal violet (0.5% w/v) and later counted manually.

To evaluate cisplatin chemopotentiation, cells were seeded as described above and after 24 hours cells were exposed to cisplatin for the next 16 hours. The plates were washed with PBS twice, adding fresh media and keeping plates in

an incubator with or without inhibitors for 14 days. The cell colonies were fixed and stained as mentioned above. The experiment was performed in duplicate and it was repeated three times. The numbers of colonies (≥ 50 cells) were counted manually. The plating efficiency was calculated using (No. of colonies formed/No. of cells seeded) x 100 method. In this clonogenic study, the nonlinear regression analysis can be used to calculate the inhibitory concentration (IC50) of an inhibitor that results in the death of 50% of the cell population. The graphs were produced by statistical analysis performed using the GraphPad prism software version 8.0.2.

### 2.2.15 Cell cycle assay

#### 2.2.15.1 Assay principle

Using flow cytometry for studying the distribution of cell cycles is a widely accepted procedure. The fluorescent DNA binding dye is propidium iodide (PI), it is used for staining cells and the cellular DNA content is analysed. The cells are distributed in different phases of the cell cycle (G1, S and G2/M) and this information is reported in this method (Pozarowski P, 2004).

#### 2.2.15.2 Assay protocol

100,000 cells were plated in T25 flasks and allowed to adhere for 24 hours. The cells were treated with an inhibitory compound and these were collected after 48 hours of treatment by trypsinization. The samples were centrifuged at 1000 rpm for 5 minutes. 70% ethanol in PBS solution was used to fix cell pellets and incubated overnight at 4°C to allow fixation step and then stored under these conditions until performing FACS. Before FACS analysis, fixed cells were

centrifuged and the pellet was resuspended in 500 µl PBS containing propidium iodide (PI) (2 µg/ml) and DNAse-free RNase A (10 µg/ml). After this preparation, the samples were incubated at 37°C for 1 hour. To evaluate cisplatin chemopotentiation, the cells were seeded as above and cisplatin was added after 24 hours and then incubated for the next 16 hours. The plates were washed with PBS twice and it was followed by adding fresh media. These plates were kept in an incubator with or without inhibitors for 48 hours. Cell cycle analysis was carried out.

The samples were analysed on a Cytomics F500 flow cytometer (Beckman Coulter, USA) using a 488nm laser for excitation and a 620nm bandpass filter for the collection of data. The software FlowJo 7.6.1 (Tree Star, Ashland, USA) was used for data analysis. At least 50,000 cells from each cell suspension were analysed (Figure 2-1)

This assay was performed three times and the student t-test was used to calculate if there was a significant difference in sensitivity between mutant/knockdown cells before and after treatment with inhibitors. A p-value ≤0.05 was defined as a significant relationship. The graphs were produced by statistical analysis using GraphPad prism software version 8.2.0.

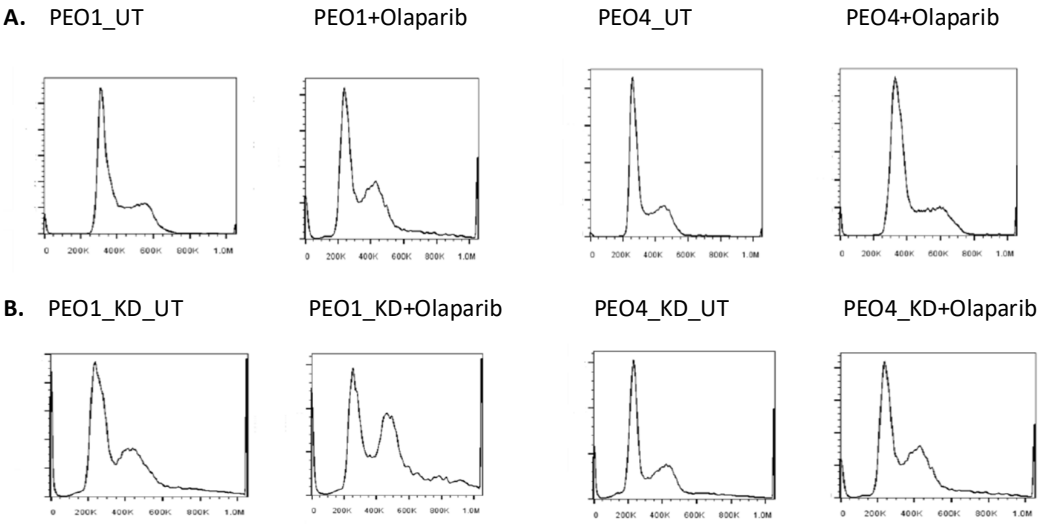


**Figure 2-1:** Representative figures of cell cycle analysis.

(A) Representative images of cell cycle analysis in PEO1 and PEO4 control cells, untreated and olaparib treated. Olaparib treated cells show G2/M cell cycle arrest. (B) Representative images of cell cycle analysis in PEO1 and PEO4 FANCD2_KD cells untreated and olaparib treated. Olaparib treated cells show substantial G2/M cell cycle arrest compared to control cells.

### 2.2.16 Apoptosis detection by Annexin V assay

#### 2.2.16.1 Assay principle

Apoptosis is the biological process of programmed cell death in eukaryotes, cells age under controlled signalling machinery. The most recognised characteristic of apoptosis is the translocation of phosphatidylserine (PS) from the inner side of the plasma membrane to the outer surface. The other features observed are chromatin condensation and alterations in cell volume. The phospholipid-binding protein called Annexin V (Ca2+-dependent) shows a high affinity for PS. The early and late apoptotic cells are identified by using Annexin V staining; it is conjugated with a second dye like propidium iodide

(PI). The viable cells with intact membranes are negative (cell surface reject) to PI whereas dead cells with damaged membranes are positive (permeable) to PI (Figure 2-2). Therefore, viable cells are both Annexin V and PI negative, early apoptotic cells are Annexin V positive and PI negative, late apoptotic cells are Annexin V and PI-positive finally, necrotic cells are Annexin V negative and PI positive (Figure 2-3) (Riccardi C, 2006).

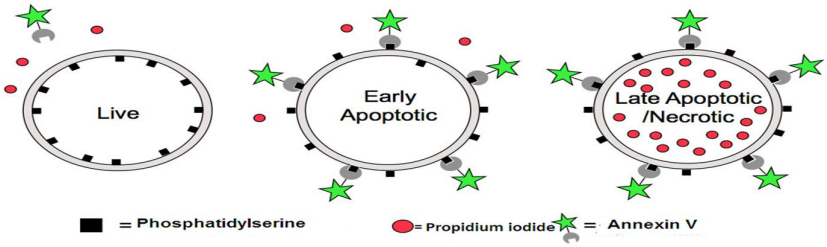


**Figure 2-2:** Annexin V flow cytometry mechanism (V-FITC).

In early apoptosis, phosphatidylserine (PS) initially located inside the plasma membrane moves to the cell's outer surface. Annexin V is a human vascular anticoagulant which represents a high affinity for PS. Annexin V-FITC/PI staining method is widely used for detecting apoptotic cells.
Adapted from (www.lifesci.dundee.ac.uk/flow-cytometry).

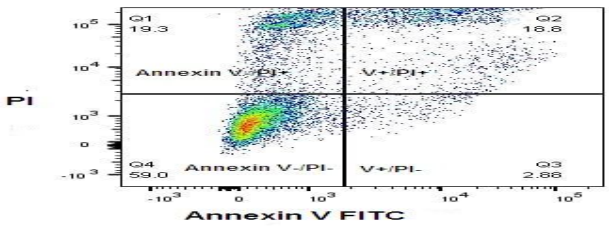


**Figure 2-3:** Annexin V and PI Staining.Viable cells are both Annexin V and PI negative, early apoptosis cells are Annexin V positive and PI negative, late apoptosis cells are Annexin V and PI positive, finally necrotic are Annexin V negative and PI positive. Adapted from biocompare.com.

### 2.2.16.2 Assay protocol

The cells were grown to sub-confluence (70-80 %) and harvested. 100,000 cells were plated in T25 flasks and allowed to adhere for 24 hours. The cells were exposed to inhibitory compounds and these were collected after 24 and 48 hours. The cells were collected by trypsinization step and centrifuged at 1000 rpm for 5 minutes. The cell pellets were washed twice with PBS (ice-cold) and then resuspended in Binding buffer (BioLegend, UK) at a concentration of one million cells/ml. 5 µl of FITC Annexin V (ImmunoTools, Germany) and 5 µl PI were added to 100 µl of the cell solution and incubated for 15 minutes at room temperature in the dark. The volume of prepared Binding buffer of 400 µl was added and the samples were analysed by FACS. To evaluate cisplatin chemopotentiation cells were seeded as above and cisplatin was added after 24 hours. The cells were exposed to cisplatin for 16 hours. The plates were then washed with PBS twice; fresh media was added and placed in an incubator with or without inhibitors for 24 and 48 hours. The cell cycle analysis was performed at the end of the experiment.

The samples were analysed on a Cytomics F500 flow cytometer (Beckman Coulter, USA) using a 488nm laser for excitation and a 575nm bandpass filter for the collection of data. The data was analysed using FlowJo 7.6.1 software (Tree Star, Ashland, USA). At least 20,000 cells from each cell suspension were analysed. This assay was performed three times and the student t-test was used to calculate if there was a significant difference in sensitivity between mutant/knockdown cells before and after treatment with inhibitors (Figure 2-4). The percentage of the absorbance was determined by comparing to a control population of untreated cells. A p- value ≤0.05 was defined as a

significant connection. The graphs were produced by statistical analysis using GraphPad Prism 8.2.0 software.

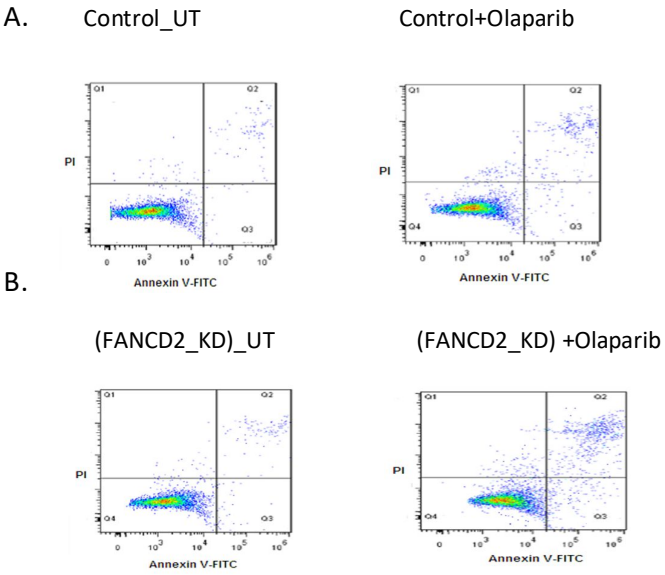


**Figure 2-4:** Representative images of Annexin V analysis (A) Annexin V apoptosis analysis in PEO1 and PEO4 control cells treated with olaparib (B) Annexin V apoptosis analysis in PEO1 and PEO4 FANCD2_KD cells untreated and treated with olaparib. The gene knockdown cells treated with olaparib show apoptotic cells accumulation.

# 3 XAB2 in invasive breast cancers

## 3.1 Introduction

The new therapeutic strategies selective to cancer cells are developed after understanding the tumour cell vulnerabilities. For cancer patient's survival, significant targets are identified in tumour cells. The minimal toxicity to normal cells is considered while targeting such proteins (Zecchini V., 2017).

The combination of mutations in two or more genes in the context of genetic interaction can induce cell death hence give rise to the concept of synthetic lethality. Synthetic lethal pairs can kill cancer cells selectively leaving normal cells unharmed with the synthetic lethal screens that lead to the drug development (Le Meur N, 2008).

Synthetic lethality is divided into synthetic dosage lethality and synthetic sickness lethality; this classification is based on the targeted therapies assigned around cancer genes. The DNA damage response pathway, tumour microenvironment, cell cycle control, epigenetic regulation and metabolic pathways have the potential to affect the mechanism of synthetic lethality.

The DNA double-strand breaks (DSBs) are accumulated when DNA damage response (DDR) inhibitors inhibit the corresponding proteins resulting in impaired DNA single-strand breaks (SSBs) which eventually lead to DSB accumulation during replication. This leads to the collapsed replication forks and the outcome is tumour cell apoptosis. During DDR, the cell cycle control checkpoints (CHK1/2) are regulated by ATM and ATR kinases since these are responsible for maintaining the DNA replication fork stability. The three general mechanisms of the potential resistance to DDR inhibitors are replication fork protection, cell cycle arrest and homologous recombination restoration (HRR).

The cells face various environmental and genetic challenges therefore, for mitigating the loss of cellular function; organisms maintain homeostasis by employing synthetic lethal genetic interaction mechanisms in the cells.

In the settings of loss-of-function mutants, synthetic lethality can be induced by the combinations of other factors for instance environmental change, overexpression of genes and the action of a chemical compound. In recent studies, synthetic lethality arranges new angles for therapies and it provides insight into the mechanism of drug sensitivity to cancer cells. The effects of drugs on cancer cells and its mechanism of action are considered for studying and analysing synthetic lethal interactions with DNA repair genes. The combination therapies can be designed and used for predicting drug sensitization or synergistic effect of drugs based on the knowledge of drug-gene synthetic lethal interactions. The synergistic drugs (lower concentrations) can be used to attain biological results carrying fewer side effects. The drug combinations with different cellular targets can restrict resistance in cancer and infectious disease treatment. The drugs that further disturb the cellular processes such as defective DNA repair, deregulated transcription and genomic instability reflect the hallmarks of cancer which could show specific toxicity in cancer cells (synthetic lethality). Drawing a chart of the synthetic lethal interactions between DNA damage-based cancer therapies and DNA repair pathways would provide crucial guidance on therapy choice. Hence, identifying new synthetic lethal interactions in distinct cancer types and individual tumours can play a key role in cancer treatment.

PARP (DNA repair enzyme) shows synthetic lethality with the BRCA genes hence the tumours with such mutations could be well treated using a PARP inhibitor with minimal side effects.

The synthetic lethal interactions in human cells can be identified selectively with the discovery of this technique RNA interference (RNAi) in the biological world (Nijman SM., 2011).

Cancer metabolism is a novel promising feature for studying synthetic lethality. The metabolic process targets (selective to cancer cells) have been identified with genomic studies of cancer metabolism (Zecchini V., 2017). The cancer cells sustain the first metabolic chemical reaction change in the upregulation of the glycolysis cytoplasmic pathway with increased glucose uptake (Dorr JR, 2013). This aspect is not only exclusive from normal cells but also results in remarkable cell cytotoxicity employing these glycolytic enzymes (McLornan DP, 2014). It also reveals an increase in amino acid production such as arginine, glycine, proline, glutamine and serine. Orlistat (fatty acid synthase inhibitor) and SB-204990 (inhibitor of ATP citrate lyase) are grouped under lipid metabolism that displayed some progress (Facchetti G, 2012). However, the current research study focuses on cancer metabolism for discovering synthetic lethality partners. An early sign of neoplasia is observed with the loss of heterozygosity in the succinate dehydrogenase (SDH) allele causing loss of its enzymatic tasks. A hypoxic-like situation in SDH deficient tumours is formed as it upregulates the expression of hypoxia-inducible factors (HIF) (Teicher BA, 2012). The prime factor lies in the secretion of more pyruvate carboxylase in SDH deficient cells as these fluctuate in pyruvate metabolism. Consequently, a synthetic lethal interaction of SDH enzyme inhibition with pyruvate carboxylase has been proved in recent studies (Hiller K., 2013). For improving the therapeutic options for breast cancer patients, research studies investigate the concept and applications of synthetic lethality.

PARP1 activates the signalling pathways and recruits DNA repair proteins at single-strand breaks describing a pivotal role of this protein in the base excision repair (BER) pathway. The concept of synthetic lethality concerns the use of PARP1 inhibitors as a therapeutic strategy in BRCA mutated tumours. In homologous recombination (HR) deficient cells, the use of PARP1 inhibitors will inhibit the action of PARP1 hence single strand breaks will not be repaired and results in the accumulation of double strand breaks (DSBs) (Murphy CG, 2010). In this study, it is hypothesised that drugs like cisplatin and olaparib can have a synthetic lethality in XPA Binding Protein 2 (XAB2) deficient breast cancer cell lines.

## 3.2 Methodology

Immunohistochemistry of XAB2 was performed on TMAs of 1650 patients with invasive breast cancers and a separate cohort of 281 ER-negative invasive breast cancers. Patient demographics were summarised in the methods chapter. The immunohistochemistry protocol and antibody details were described in the methods chapter. Evaluation of immunohistochemistry was performed by calculating H-scores (range 0-300). The statistical analysis and choosing cut-off value were performed by the pathologist group members.

Human cell lines used in this study were MCF-7, SKBR3, DCIS and MDA-MB-231. XAB2 knockdown was performed using XAB2 siRNA. Cell culture media was used to maintain all the cell lines, cell passaging and storage conditions were described in the materials and methods chapter. The assays performed in this study include BCA assay, western blotting, clonogenic survival assay, MTS assay, siRNA and flow cytometric analysis were mentioned in details in the methods section.

## 3.3 RESULTS

### 3.3.1 Clinical Data

#### 3.3.1.1 Breast cancer- Kaplan–Meier plotter (KM plotter) database for *XAB2* transcript survival analysis

The prognostic significance of *XAB2* transcripts was evaluated in the KM plotter online database. The KM plotter (publicly available) data base was generated by using gene expression datasets from The Cancer Genome Atlas (TCGA), Gene Expression Omnibus (GEO) and European Genome-phenome Archive (EGA). The Kaplan–Meier (KM) curve and log-rank test established the correlation between the mRNA expression levels of the target gene and the patient's survival outcomes including the overall survival (OS) rate, disease-free survival (DFS) rate, post-progression survival (PPS) and distant metastasis-free survival (DMFS) in breast cancer groups. The results were displayed as the Kaplan–Meier (KM) survival plots (Figure 3-1). The website tool calculated the hazard ratio (HR) and 95% confidence automatically. The mean standard deviation (± SD) values were represented for each group. Log-rank test used the p-value < 0.05 as statistically significant (Liu Y, 2021). The classification criteria for studying the gene expression analysis was summarised in Table 3-1.

**Table 3-1:** Classification criteria for studying the gene expression analysis

| **Classification criteria:** | |
|---|---|
| **Gene** | XAB2 |
| **Split patients** | Median |
| **Number of patients with available clinical data** | n |

| | |
|---|---|
| **Cut-off value used in analysis** | 145 |
| **Restrict analysis to subtypes** | ER, PR, HER2-status, grade and lymph node |
| **Systemic treatment** | Endocrine therapy and chemotherapy. |

**The survival graphs using KM plotter database.**

**A. OS (n= 1880)**

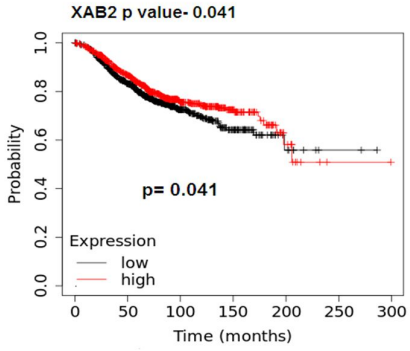


**B. PFS (n=458)**

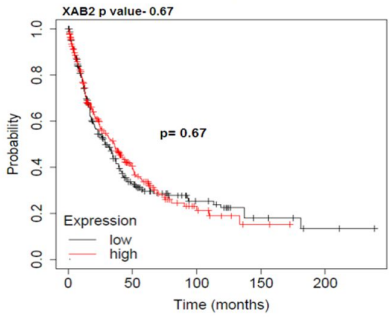


**C. DMFS (n=2767)**

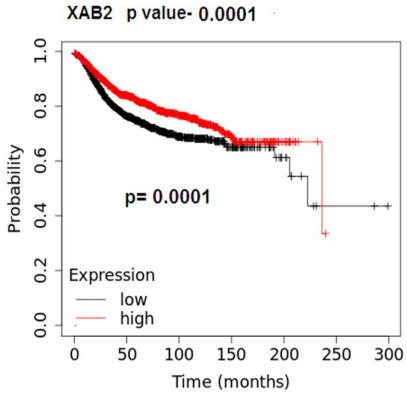


**D. RFS (n=4934)**

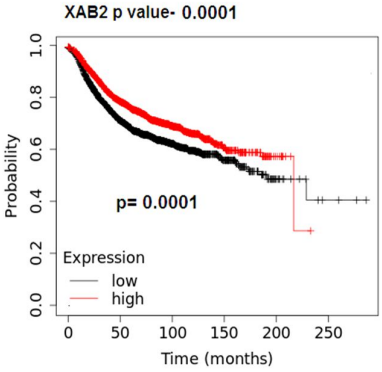


**Figure 3-1:** The survival graphs using KM plotter (A) Overall survival (B) Progression free survival (C) Distant metastasis free survival (D) Recurrence free survival in breast cancer patients using KM plotter analysis.

The patient survival graphs were obtained by using Kaplan–Meier (KM) plotter online database. The interconnection between XAB2 gene expression and the patient's survival outcomes inclusive of the overall survival, progression free survival, distant metastasis free survival and recurrence free survival in breast cancer groups was studied.

The data showed that low *XAB2* transcript was associated with poor OS and DMFS. It was proceeded to evaluate XAB2 protein expression by immunohistochemistry**.**

### 3.3.2 IHC

**Clinicopathological significance of XAB2 in breast cancer**

**Clinical data:**

Immunohistochemistry was used to detect the XAB2 expression (nucleus) from patients in a well-categorized breast cancer cohort [No.-1650]. Not all cores within the TMA were included for IHC analysis due to missing cores or absence of tumour cells.

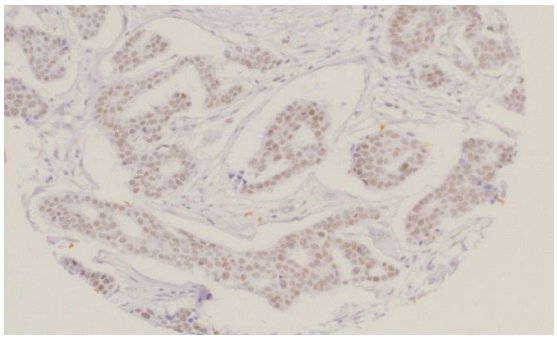

**a) 1:200 (weak)**

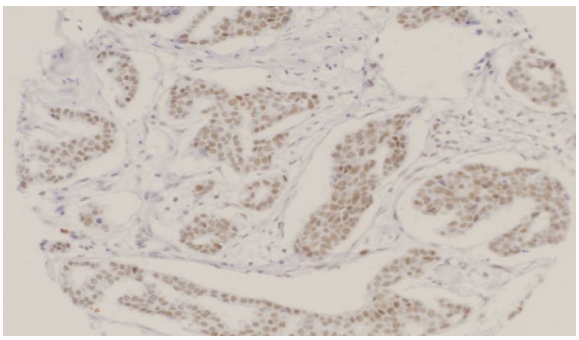

**b) 1:100 (moderate)**

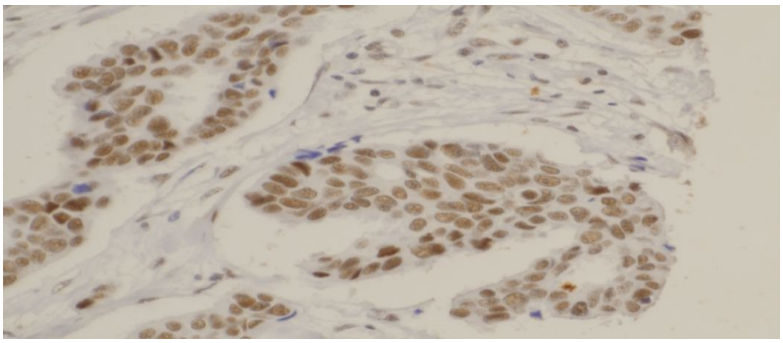

**c) 1:50 (strong)**

**Figure 3-2:** Representative photos of the immunoreactivity of XAB2 in breast cancer cells.

For optimization of the antibody, the immunoreactivity of XAB2 was checked at three different dilution factors 1:50, 1:100 and 1:200. The strong nuclear localization of XAB2 was obtained at 1:50 (Figure 3-2) and this dilution was

chosen for IHC staining of breast tissue microarray (TMA) cohorts. The statistical analysis and images acquisition were performed by Dr Islam Melligy in Prof. Emad Rakha (co-supervisor) pathology group.

Patient demographics was summarised in Table 3-2. The patient demographics of ER negative (ER-) cohort and ER positive (ER+) cohort were summarised in Table 3-3 and Table 3-4 respectively. The clinicopathological associations of XAB2 in breast cancers was summarised in Table 3-5.

**The KM survival curves using SPSS software.**

**A. IBC (whole cohort, no. =378)**

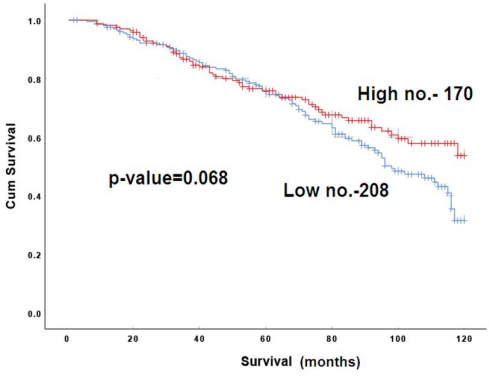


**B. TTRR (no. =401)**

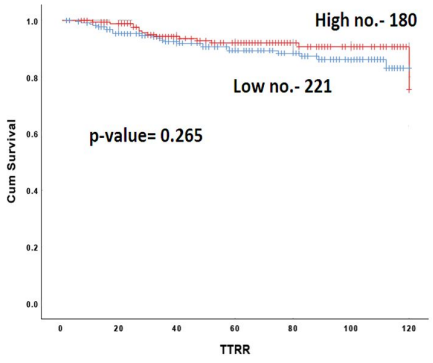


**Figure 3-3:** The KM survival curves using SPSS software. (A) Invasive breast cancer (whole cohort) (B) The mean time to recurrence (TTRR) survival in breast cancer patients.

The KM survival curves for invasive breast cancer (IBC) were studied under statistical analysis using SPSS software version 21 (Figure 3-3).

**Table 3-2**: Patient demographics.

| Clinicopathological Variables | Whole database (%) | |
|---|---|---|
| **Age at Diagnosis (years)** | | |
| <50 | 313 | (31.8%) |
| ≥50 | 672 | (68.2%) |
| **Tumour Size (cm)** | | |
| <2.0 | 607 | (61.7%) |
| ≥2.0 | 377 | (38.3%) |
| **Histological Tumour Grade** | | |
| 1 | 142 | (14.4%) |
| 2 | 394 | (40%) |
| 3 | 448 | (45.5%) |
| **Tubule Formation** | | |
| 1 (>75% of tumour) | 67 | (6.9%) |
| 2 (10%-75% of tumour) | 287 | (29.5%) |
| 3 (<10% of tumour) | 619 | (63.6%) |
| **Pleomorphism** | | |
| 1 (Small, regular uniform cells) | 9 | (0.9%) |
| 2 (Moderate increase and variability) | 264 | (27.1%) |
| 3 (Marked variation) | 700 | (71.9%) |
| **Mitotic Count** | | |
| 1 (0-5) | 457 | (47.1%) |
| 2 (6-10) | 194 | (20%) |
| 3 (>11) | 320 | (33%) |
| **Histological Tumour Type** | | |
| Mixed NST and Lobular | 105 | (10.7%) |
| Special type | 878 | (89.3%) |
| Tubular | | |
| **LVI_Cat** | | |

| | | |
|---|---|---|
| No/Probable | 700 | (71.2%) |
| Definite | 283 | (28.8%) |
| **Stage** | | |
| 1 | 609 | (62.0%) |
| 2 | 285 | (29.0%) |
| 3 | 89 | (9.1%) |
| **NPI Prognostic Group** | | |
| Good (2.4<NPI≤3.4) | 328 | (33.4%) |
| Moderate (3.4<NPI≤5.4) | 507 | (51.6%) |
| Poor (5.4<NPI) | 148 | (15.1%) |
| **ER Status** | | |
| Negative | 194 | (19.7%) |
| Positive | 790 | (80.3%) |
| **PR Status** | | |
| PR negative (PR-) | 392 | (39.8%) |
| PR positive (PR+) | 592 | (60.2%) |
| **HER2 Status** | | |
| HER2 negative (HER2-) | 860 | (87.2%) |
| HER2 positive (HER2+) | 126 | (12.8%) |
| **Triple-Negative Status** | | |
| No | 833 | (84.5%) |
| Yes | 153 | (15.5%) |
| **Menopausal status** | | |
| Pre | 259 | (34.3%) |
| Peri | 19 | (2.5%) |
| Post | 478 | (63.2%) |
| **Bilateral** | | |
| No | 729 | (98.4%) |
| Yes | 12 | (1.6%) |
| **Multifocality** | | |
| No | 426 | (76.8%) |

| | | |
|---|---|---|
| Yes | 129 | (23.2%) |
| **Type of operation** | | |
| WLE | 262 | (39.4%) |
| Mastectomy | 403 | (60.6%) |
| **Radiotherapy local** | | |
| No | 223 | (24.5%) |
| Yes | 686 | (75.5%) |
| **Radiotherapy nodes** | | |
| No | 553 | (75.0%) |
| Yes | 184 | (25.0%) |

**Table 3-3**: Patient demographics of ER negative (ER-) cohort.

| **Clinicopathological Variables** | **Whole database (%)** |
|---|---|
| **Age at Diagnosis (years)** | |
| <50 | 91 (46.9%) |
| ≥50 | 103 (53.1%) |
| **Tumour Size (cm)** | |
| <2.0 | 92 (47.4%) |
| ≥2.0 | 102 (52.6%) |
| **Histological Tumour Grade** | |
| 1 | 2 (1%) |
| 2 | 20 (10.3%) |
| 3 | 172 (88.7%) |
| **Tubule Formation** | |
| 1 (>75% of tumour) | 1 (0.5%) |
| 2 (10%-75% of tumour) | 24 (12.4%) |
| 3 (<10% of tumour) | 168 (87%) |
| **Pleomorphism** | |
| 1 (Small, regular uniform cells) | 1 (0.5%) |

| | |
|---|---|
| 2 (Moderate) | 4 (2.1%) |
| 3 (Marked variation) | 188 (97.4%) |
| **Mitotic Count** | |
| 1 (0-5) | 16 (8.3%) |
| 2 (6-10) | 33 (17.1%) |
| 3 (>11) | 144 (74.6%) |
| **Histological Tumour Type** | |
| Mixed NST | 179 (92.7%) |
| Special type | 14 (7.3%) |
| **Nodal Stage** | |
| 1 (No nodal involvement) | 122 (62.9%) |
| 2 (1-3 nodes involved) | 49 (25.3%) |
| 3 (>3 nodes involved) | 23 (11.9%) |
| **NPI Prognostic Group** | |
| Good (2.4<NPI≤3.4) | 12 (6.2%) |
| Moderate (3.4<NPI≤5.4) | 140 (72.2%) |
| Poor (5.4<NPI) | 42 (21.6%) |
| **PR Status** | |
| PR negative (PR-) | 193 (100%) |
| PR positive (PR+) | - |
| **HER2 Status** | |
| HER2 negative (HER2-) | 153 (78.9%) |
| HER2 positive (HER2+) | 41 (21.1%) |
| **Triple-Negative Status** | |
| No | 41 (21.1%) |
| Yes | 153 (78.9%) |
| **Menopausal status** | |
| Pre | 80 (47.6%) |
| Peri | 4 (2.4%) |
| Post | 84 (50%) |
| **Bilateral** | |

| | |
|---|---|
| No | 165 (99.4%) |
| Yes | 1 (0.6%) |
| **Multifocality** | |
| No | 95 (88%) |
| Yes | 13 (12%) |
| **Type of operation** | |
| WLE | 46 (33.3%) |
| Mastectomy | 92 (66.7%) |
| **Radiotherapy local** | |
| No | 47 (25.3%) |
| Yes | 139 (74.7%) |
| **Radiotherapy nodes** | |
| No | 130 (76.9%) |
| Yes | 39 (23.1%) |

**Table 3-4:** Patient demographics of ER positive (ER+) cohort.

| **Clinicopathological Variables** | **Whole database (%)** |
|---|---|
| **Age at Diagnosis (years)** | |
| <50 | 220 (27.9%) |
| ≥50 | 569 (72.1%) |
| **Tumour Size (cm)** | |
| <2.0 | 514 (65.2%) |
| ≥2.0 | 274 (34.8%) |
| **Histological Tumour Grade** | |
| 1 | 140 (17.8%) |
| 2 | 374 (47.5%) |
| 3 | 274 (34.8%) |
| **Tubule Formation** | |
| 1 (>75% of tumour) | 66 (8.5%) |

| | |
|---|---|
| 2 (10%-75% of tumour) | 263 (33.7%) |
| 3 (<10% of tumour) | 451 (57.8%) |
| **Pleomorphism** | |
| 1 (Small, regular uniform cells) | 8 (1%) |
| 2 (Moderate increase and variability) | 260 (33.3%) |
| 3 (Marked variation) | 512 (65.6%) |
| **Mitotic Count** | |
| 1 (0-5) | 441 (56.7%) |
| 2 (6-10) | 161 (20.7%) |
| 3 (>11) | 176 (22.6%) |
| **Histological Tumour Type** | |
| Mixed NST | 697 (88.5%) |
| Special type | 91 (11.5%) |
| **LVI_Cat** | |
| No/Probable | 559 (71%) |
| Definite | 228 (29%) |
| **Stage** | |
| 1 | 485 (61.6%) |
| 2 | 236 (30%) |
| 3 | 66 (8.4%) |
| **NPI Prognostic Group** | |
| Good (2.4<NPI≤3.4) | 316 (40.2%) |
| Moderate (3.4<NPI≤5.4) | 365 (46.4%) |
| Poor (5.4<NPI) | 106 (13.5%) |
| **PR Status** | |
| PR negative (PR-) | 198 (25.1%) |
| PR positive (PR+) | 591 (74.9%) |
| **HER2 Status** | |
| HER2 negative (HER2-) | 705 (89.2%) |
| HER2 positive (HER2+) | 85 (10.8%) |

| | |
|---|---|
| **Triple-Negative Status** | |
| No | 790 (100%) |
| Yes | - |
| **Menopausal status** | |
| Pre | 178 (30.3%) |
| Peri | 15 (2.6%) |
| Post | 394 (67.1%) |
| **Bilateral** | |
| No | 561 (98.1%) |
| Yes | 11 (1.9%) |
| **Multifocality** | |
| No | 331 (74%) |
| Yes | 116 (2.6%) |
| **Type of operation** | |
| WLE | 216 (41%) |
| Mastectomy | 311 (59%) |
| **Radiotherapy local** | |
| No | 176 (24.4%) |
| Yes | 546 (75.6%) |
| **Radiotherapy nodes** | |
| No | 422 (74.4%) |
| Yes | 145 (25.6%) |
| **LVI_2groups** | |
| 0 | 559 (71%) |
| 1 | 228 (29%) |

**Table 3-5:** Clinicopathological associations of XAB2 in breast cancers.

| Clinicopathological Parameters | XAB2 expression Low No. (%) | High No. (%) | χ 2 (p-value) |
|---|---|---|---|
| **Age (years)** | | | |
| <50 | 166 (53%) | 147 (47%) | 0.345 |
| ≥50 | 378 (56.2%) | 294 (43.8%) | |
| **Tumour Size (mm)** | | | |
| <20 | 344 (56.7%) | 263 (43.3%) | 0.267 |
| ≥20 | 200 (53.1%) | 177 (46.9%) | |
| **Tumour Grade** | | | |
| Low | 92 (64.8%) | 50 (35.2%) | |
| Moderate | 225 (57.1%) | 169 (42.9%) | **0.008** |
| High | 227 (50.7%) | 221 (49.3%) | |
| **Tumour Stage** | | | |
| 1 | 356 (58.5%) | 253 (41.5%) | **0.037** |
| 2 | 141 (49.5%) | 144 (50.5%) | |
| 3 | 47 (52.8%) | 42 (47.2%) | |
| **Nottingham Prognostic Index (NPI)** | | | |
| Good | 202 (61.6%) | 126 (38.4%) | **0.010** |
| Moderate | 271 (53.5%) | 236 (46.5%) | |
| Poor | 71 (48.0%) | 77 (52.0%) | |
| **LVI status** | | | |
| Negative (No/probable) | 400 (57.1%) | 300 (42.9%) | **0.059** |
| Positive( Definite) | 143 (50.5%) | 140 (49.5%) | |
| **Mitotic Index** | | | |
| M1 (low; mitoses < 10) | 281 (61.5%) | 176 (38.5%) | |
| M2(medium; mitoses 10-18) | 101 (52.1%) | 93 (47.9%) | **0.001** |
| M3(high; mitosis >18 | 156 (48.8%) | 164 (51.2%) | |

| | | | |
|---|---|---|---|
| **Tubule Formation** | | | |
| 1(>75% definite tubule) | 42 (62.7%) | 25 (37.3%) | |
| 2(10%-75% definite tubule) | 166 (57.8%) | 121 (42.2%) | 0.216 |
| 3(<10% definite tubule) | 331 (53.5%) | 288 (46.5%) | |
| **Pleomorphism** | | | |
| 1(small-regular uniform) | 5 (55.6%) | 4 (44.4%) | |
| 2(Moderate variation) | 159 (60.2%) | 105 (39.8%) | 0.179 |
| 3(Marked variation) | 375 (53.6%) | 325 (46.4%) | |
| **Oestrogen receptor** | | | |
| Negative | 110 (56.7%) | 84 (43.3%) | 0.681 |
| Positive | 435 (55.1%) | 355 (44.9%) | |
| **Progesterone receptor** | | | |
| Negative | 214 (54.6%) | 178 (45.4%) | 0.722 |
| Positive | 330 (55.7%) | 262 (44.3%) | |
| **HER2 status** | | | |
| Negative | 487 (56.6%) | 373 (43.4%) | **0.025** |
| Positive | 58 (46.0%) | 68 (54.0%) | |
| **Tumour type** | | | |
| NST | 475 (54.1%) | 403 (45.9%) | **0.038** |
| Special | 68 (64.8%) | 37 (35.2%) | |
| **Triple Negative** | | | |
| No | 456 (54.7%) | 377 (45.3%) | 0.433 |
| Yes | 89 (58.2%) | 64 (41.8%) | |
| **Multifocality** | | | |
| No | 260 (61.0%) | 166 (39.0%) | 0.066 |
| Yes | 67 (51.9%) | 62 (48.1%) | |
| **Menopausal_status** | | | |
| Pre | 149 (57.5%) | 110 (42.5%) | |
| Peri | 15 (78.9%) | 4 (21.1%) | 0.152 |
| Post | 270 (56.5%) | 208 (43.5%) | |
| **Radiotherapy_local** | | | |

| | | | |
|---|---|---|---|
| No<br>Yes | 139 (62.3%)<br>367 (53.5%) | 84 (37.7%)<br>319 (46.5%) | **0.021** |
| **Radiotherapy_nodes**<br>No<br>Yes | <br>325 (58.8%)<br>98 (53.3%) | <br>228 (41.2%)<br>86 (46.7%) | <br>0.190 |

**The KM survival curves using SPSS software**

**A. TTRR (n= 983)**

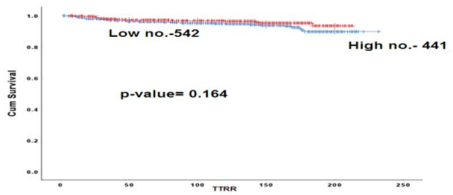


**B. Whole cohort (n= 983)**

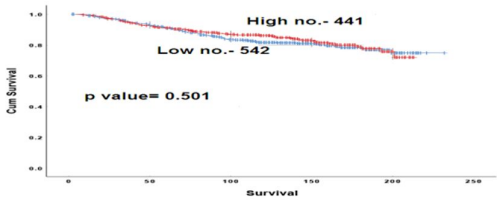


**C. TTRR ER- (n= 193)**

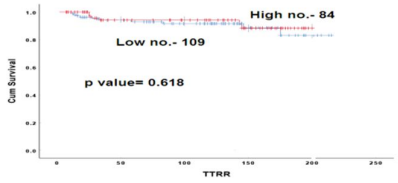


**D. TTRR ER+ (n=788)**

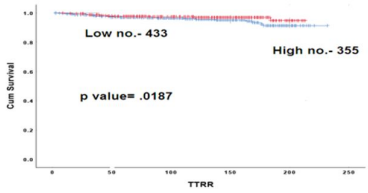


**E. Survival ER- (n=193)**

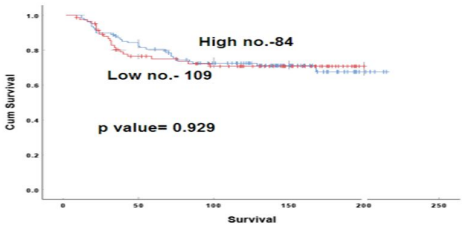


**F. Survival ER+ (n= 788)**

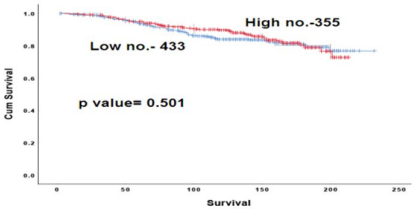


**Figure 3-4:** Kaplan-Meier curve for breast cancer-specific survival**.** (A) TTRR (B) Whole cohort (C) TTRR ER- (D) TTRR ER+ (E) Survival ER- (F) Survival ER+ in breast cancer patients by statistical analysis using SPSS software version 21.

In invasive breast cancer cohort, low nuclear expression of XAB2 was significantly associated with number of characteristics: high mitotic count (p

value-0.001), high tumour grade (p value-0.008), moderate NPI (p value-0.010), HER2- tumour (p value-0.025), tumour type-NST (p value-0.038), low tumour stage (p value-0.037), radiotherapy local (p value- 0.021) and no significance with ER, PR status.

Breast cancer-specific survival (BCSS) is the time period (months) a patient survived at the point of diagnosis to the breast cancer related death. The Kaplan-Meier (KM) curve for breast cancer-specific survival were acquired by statistical analysis using SPSS software version 21 (Figure 3-4).

In invasive breast cancer ER+ cohort, low nuclear expression of XAB2 was significantly associated with number of characteristics: high mitotic count (p value- 0.001), moderate tumour grade (p value-0.001), good NPI (p value-0.001), HER2- tumour (p value-0.024), tumour type-NST (p value-0.027), low tumour stage (p value-0.009) and radiotherapy local (p value-0.017). A low XAB2 nuclear expression was associated with moderate aggressive forms of breast cancer, low tumour stage and HER2- type of breast cancer.

### 3.3.3 XAB2 in breast cancer cell lines

For optimization, the primary antibody XAB2 (rabbit) was checked at three different dilution factors 1:750, 1:1000 and 1:2000. Several dilutions were checked for optimal antibody concentration. The specific band for the given antibody was obtained at 1:2000. The molecular weight of the primary antibody was 100kDa. The internal loading control used for the western blot was β -actin (mouse) with molecular weight 42kDa.

#### 3.3.3.1 Pre-clinical data:

A. XAB2 level in a panel of human breast cancer cell lines.

The expression level of XAB2 protein was examined in various breast cancer cell lines – DCIS, MCF7 and MDA-231. The relative protein level was compared with band quantification (Figure 3-5).

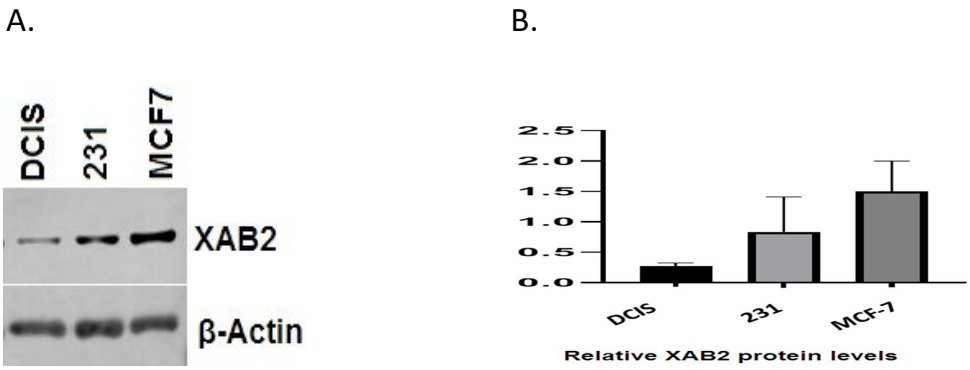


**Figure 3-5:** The western blot using breast cancer cell lines (A) Signal band intensity (protein expression) on the nitrocellulose membrane visualized under Licor Odyssey machine (B) Relative XAB2 protein expression level in different cell lines.

The protein expression of XAB2 was determined in breast cancer cell lines by western blotting. Briefly, cell lysates were prepared from 70-80% confluent cells and loaded onto polyacrylamide gels. Following electrophoresis, proteins

were transferred onto nitrocellulose and probed to target protein using specific antibody. Moreover, β-actin (mouse) with molecular weight 42kDa acted as the internal loading control in this western blot. Representative results were shown. The graph showed the XAB2 protein levels (ratio of protein/β-actin) quantitated using GraphPad Prism 8.2.0 software.

### 3.3.4 Pre and post cisplatin in breast cancer cell line

**A.**

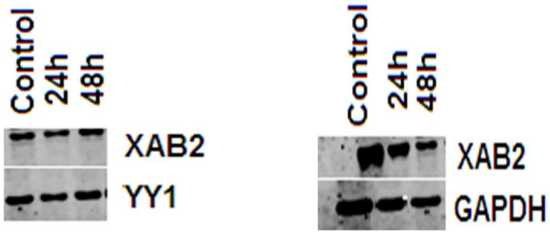


**B.**

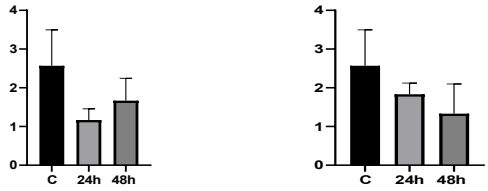


**Figure 3-6:** Nuclear and cytoplasmic extraction of MCF-7. (A) Western blot for XAB2 expression in nuclear and cytoplasmic extracts from MCF-7 breast cancer cell line untreated and treated with cisplatin for 24 and 48 hours. (B) Quantification of XAB2 protein expression by western blot. GAPDH was used as a loading control for cytoplasmic extracts and YY1 was used as the loading control for nuclear extracts.

The influence of XAB2 expression in the breast cancer cell line MCF-7 was investigated. The control cells showed XAB2 protein expression level. Upon cisplatin treatment, the significant change in the XAB2 expression was not

observed (Figure 3-6). The result of XAB2 expression varied after the use of platinum compound.

### 3.3.5 XAB2 siRNA knockdown in breast cancer cell line

MCF-7 (XAB2_KD) was generated by using siRNA transfection method for the purpose of cancer study. All the synthetic lethality experiments were conducted on MCF-7 (XAB2 proficient) and MCF-7 knockdown cells population. The observation depicted XAB2 protein knockdown on day 5 by using western blotting (Figure 3-7).

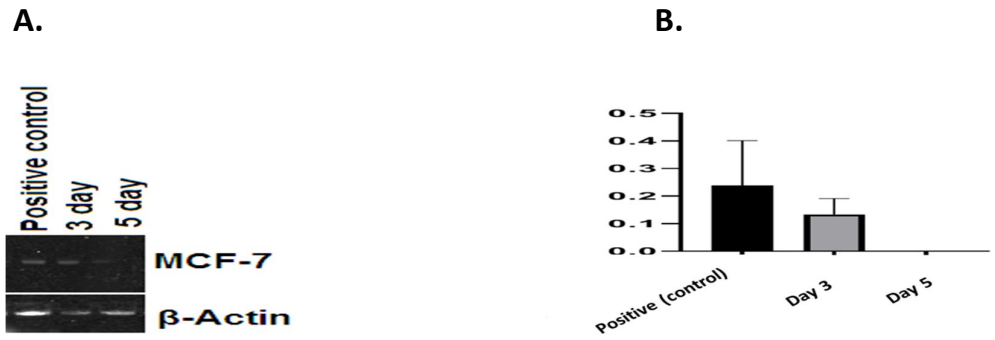


**Figure 3-7:** The siRNA knockdown of XAB2 in breast cancer cell line (A) Representative image for XAB2 levels by western blot in MCF-7 (B) Band quantification for XAB2 levels in MCF-7 control, day 3 and day 5 cell lysates.

The XAB2 mRNA was targeted for degradation by inducing sequence-specific gene silencing.

### 3.3.6 Selective drug toxicity in XAB2 deficient breast cancer cell line.

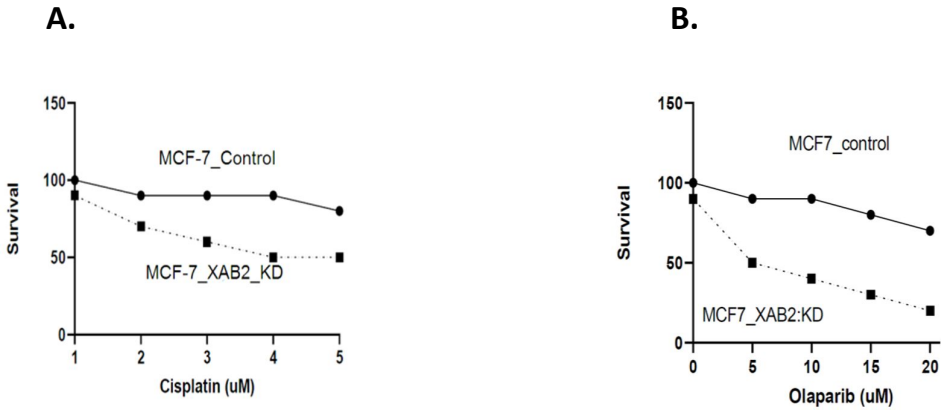


**Figure 3-8:** Drug sensitivity in XAB2 deficient cell line. Clonogenic survival assay (A) Cisplatin sensitivity in MCF-7 (XAB2_KD) breast cancer cell line (B) Olaparib sensitivity in MCF-7 (XAB2_KD) cell line.

The clonogenic cell survival and cell growth inhibition in response to cisplatin and olaparib drugs were studied. In this clonogenic survival assay, the breast cancer cells were treated at different doses of cisplatin and olaparib for MCF-7 control and MCF-7 (XAB2_KD) cells (Figure 3-8).

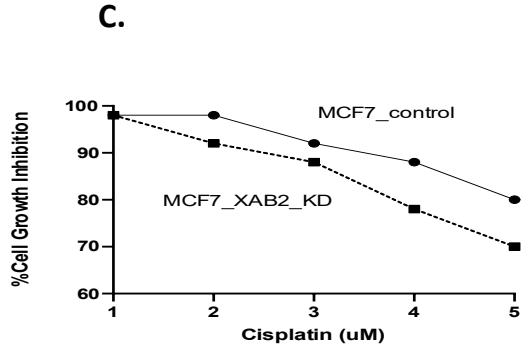


**Figure 3-9:** MTS cell growth inhibition assay of drug agent.

Cell line with XAB2 deficiency exhibited low cell growth after treatment with cisplatin at successive increased doses for 6 days compared to XAB2 proficient cell line. MCF7 control cells were compared to XAB2 gene knockdown cell line.

Data was shown as the mean and SD values for each concentration from three independent experiments (Figure 3-9).

### 3.3.7 Drug affects cell cycle progression in XAB2 deficient cell line.

The function of the PARP1 enzyme in cell cycle progression has been previously established (Jelinic P, 2014). The research studies indicate that olaparib influences cell cycle progression by regulating the expression levels of p21 and p53 (Han T, 2022). Therefore, the effect of olaparib treatment on cell cycle progression was investigated. MCF-7 control and MCF-7 XAB2_KD cells were treated with olaparib (10μM) for 24 hours. Then, cells were stained with propidium iodide for analysing DNA content. Observation depicted that olaparib-treated XAB2 knockdown cells underwent cell cycle arrest in the G2/M phase (Figure 3-10).

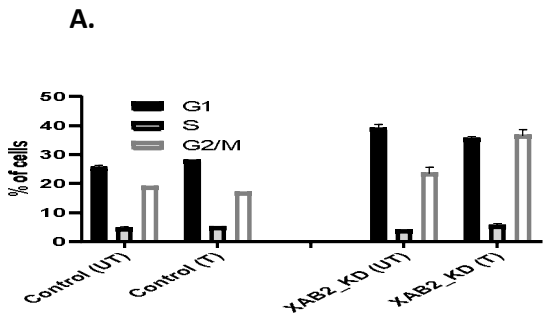


**Figure 3-10:** Functional studies of olaparib response in XAB2 knockdown cells.

In this cell cycle analysis by flow cytometry, MCF-7 control cells and XAB2 knockdown cells were treated with 10μM olaparib for 24 hours. On day 5, cells were collected and stained. MCF-7 control cells were compared to its XAB2 knockdown cells. Data were shown as the mean and SD values for each

concentration from three independent experiments. Graphs were produced and statistical analysis performed using GraphPad prism 8.2.0 software.

### 3.3.8 Accumulation of the apoptotic cells upon drug treatment.

To investigate the accumulation of apoptotic cells upon inhibition of PARP1 activity in XAB2 deficient cells, Annexin-V and PI staining was performed for the XAB2 proficient and deficient cell line treated with the drug. The result showed an accumulation of early and late apoptotic cells in XAB2 deficient cell line treated with the drug (Figure 3-11).

**A.**

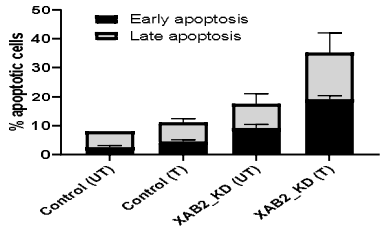


**Figure 3-11:** The percentage of apoptotic cells analysed by flow cytometry. Annexin V apoptosis assay was performed in MCF-7 cells treated (T) with olaparib (10μM), untreated (UT) control cells. XAB2_KD cells treated (T) with olaparib along with untreated (UT) knockdown cells for 24 hours.

The cell apoptosis process was studied by Annexin V-FITC flow cytometry after treatment with a drug inhibitor. The Annexin V was used in conjunction with a propidium iodide (PI) for recognising the apoptotic cells. The control cells and XAB2 knockdown cells were treated for 24 hours with 10μM olaparib. An increase in apoptosis after 24 hours in XAB2 deficient cells treated with 10μM olaparib compared to control cells was observed.

## 3.4 Discussion

One of the sub pathways in the nucleotide excision repair (NER) system is a transcription-coupled repair (TCR) pathway and this pathway is activated when the RNA polymerase II enzyme is blocked at the elongation step of the transcription process in response to the DNA damages. The XPA-binding protein 2 (XAB2) is a tetratricopeptide repeat that binds with xeroderma pigmentosum group A (XPA) protein. Additionally, XAB2 interconnects with other proteins for instance Cockayne syndrome group A (CSA), CSB, XPA and RNA polymerase which participate in transcription and TCR pathway.

The recovery of RNA synthesis after UV irradiation decreases with the knockdown of XAB2 using a technique called small interfering RNA in HeLa cells resulting in cell hypersensitivity. When cells are treated with DNA-damaging agents, it results in increased binding of XAB2 with XPA or RNA polymerase II suggesting the XAB2 complex has DNA damage-responsive activity (Kuraoka I, 2008).

XAB2 may take part in neoplasm development. In varieties of cancer including triple-negative breast cancer, rhabdoid tumour and primary gastric cancer, the expression of XAB2 is significantly downregulated in the cells. The gene expression of XAB2 has been explored however; the position of downstream signalling target genes and the subsequent physiological roles in human cells is not known yet. XAB2 regulates the expression of genes involved in cell cycle regulation and mitotic progression. The XAB2 knockdown results in chromosome misalignment causing mitotic arrest and cell death. XAB2 regulates the transcription of centrosome-associated protein E (CENPE) and the phenotype distinguished in XAB2 deficient cells is mediated by this motor protein (Hou S, 2016).

Furthermore, the breast tissue microarray (TMA) cohorts received was treated at the given optimization.

The clinical data presented here showed that in invasive breast cancer cohort, low nuclear expression of XAB2 was significantly associated with number of characteristics: high mitotic count (p value-0.001), high tumour grade (p value-0.008), moderate NPI (p value-0.010), HER2- tumour (p value-0.025), tumour type-NST (p value-0.038), low tumour stage (p value-0.037) and radiotherapy local (p value-0.021). Therefore, low XAB2 expression had clinicopathological associations with aggressive forms of breast cancer.

In invasive breast cancer ER+ cohort, low nuclear expression of XAB2 was significantly associated with number of characteristics: high mitotic count (p value- 0.001), moderate tumour grade (p value-0.001), good NPI (p value-0.001), HER2- tumour (p value-0.024), tumour type-NST (p value-0.027), low tumour stage (p value-0.009), radiotherapy local (p value-0.017). A low XAB2 nuclear expression was associated with moderate aggressive forms of breast cancer, low tumour stage and HER2- type of breast cancer.

In local radiotherapy cancer treatment, only a specific part of the body is affected. For instance, a lung cancer patient is treated at the chest area only and the whole body is not exposed to radiations. To discontinue the cancer cells growth, the DNA is damaged by using radiation therapy. Unlike chemotherapy treatment in which the whole body is affected, radiation therapy usually comes under the category of a local treatment. Only that part of the body is affected where the malignancy is located. It is found that improved breast cancer-specific survival is related with local radiotherapy (Formenti SC, 2008). External beam and internal radiations are two main types of radiation therapy. A specific part of the body is treated in external beam

radiation therapy (local treatment). When a radiation source (solid or liquid) is placed inside the body, a patient is treated with internal radiation therapy (Sadeghi M, 2010).

XAB2 deficient tumours could have promising clinical potential. BRCA1 and BRCA2 are the elements of a homologous recombination system. PARP1 inhibitors can target BRCA1 and BRCA2 associated cancers on synthetic lethality terms (Wang Y, 2016). Functional BRCA1 and BRCA2 genes are essential for repairing the damaged DNA after PARP1 inhibition (Farmer H, 2005). Addressing this perspective, it opens a large therapeutic scope for this PARP1 inhibitor olaparib and it is used for the treatment of advanced ovarian cancers with BRCA mutations after acquiring FDA approval in 2014. In 2018, olaparib was also approved for treating metastatic breast cancers with BRCA germline mutations. More PARP inhibitors for instance NSC-737664 & NSC-746045 (clinical trials.gov) are in different phases of clinical trials (Zimmer AS, 2018). In the current study, drug sensitivity screening was performed in XAB2 deficient and proficient breast cancer cell lines. A consistent sensitivity in the XAB2 deficient breast cancer cell lines was observed in the MTS and clonogenic survival assays. The accumulation of apoptotic cells after 24 hours of drug treatment in XAB2 deficient cells was evident. The drug's influence on cell cycle progression was investigated. The drug treatment induced cell cycle arrest which could be influenced by p53 genetic background. Furthermore, cell cycle analysis indicated that SSB lesions generated by PARP inhibition fail to be repaired and it was converted to more serious DSB DNA damage lesions. Interestingly, the investigation of breast cancer cell line confirmed that XAB2 deficient cell line was sensitive to PARP1 inhibitor and exhibited features of synthetic lethality.

Additionally, the mechanism of synthetic lethality encourages BRCA1/2 mutated tumours to show more sensitivity to PARP inhibitors (PARPi) and it has been evidenced by several studies addressing the DNA repair defect. However, the prolonged oral administration of PARP inhibitors causes PARPi resistance in cancer patients. Homologous recombination repair deficient (HRD) setting is essential for the mechanism of synthetic lethality to perform its role in killing tumour cells. As a consequence, the restoration or re-establishment of the HR DNA repairing system termed Homologous recombination restoration (HHR) is the primary reason for PARPi resistance. The recent studies are focused on developing strategies against drug resistance, preclinical and clinical data admit multiple mechanisms of resistance in the cells. Some possible strategies that could aid to overcome these mechanisms include targeting the cancer vulnerabilities associated with PARP inhibitors resistance, combinations chemotherapies or the objective of suppressing genomic instability (Li H, 2020). Thus, finding other targets that could achieve synthetic lethality with PARP inhibitors were an interesting approach at the core of this study.

Food and Drug Administration (FDA) approved many PARPi for the treatment of cancer patients including triple negative breast cancer (TNBC) in metastatic stage and oestrogen receptor negative (ER-)/HER2+ breast cancer carrying BRCA mutations. The BRCA-mutated HER2-negative breast cancer is treated with approved PARP inhibitors olaparib and talazoparib. However, many newly developed PARPi are not applied in clinical settings (Keung MY, 2020). PARP-1 regulates the gene expression settings in cancer-related pathways including $ER^+$ breast carcinomas. PARP-1 participates in modulating the hormonal binding of ERα and FoxA1 which consequently regulate the proliferation of $ER^+$ breast cancers. In ER+ breast cancers, antiestrogen therapies are

employed. Whether there is a role for PARP inhibitors in ER+ is not established although. PARP-1 participates in oestrogen-dependent transcription (Gadad SS, 2021).

The investigations of targeting XAB2 deficient ER+ breast cancer cell line with PARP1 inhibitors provide preliminary evidence for selective targeting in ER+ breast cancers. However, detailed functional studies of ER+ breast cancer cell lines and in vivo model will have to be performed to confirm this hypothesis.

The detailed functional studies of the drug showed that cell cycle arrest at the G2/M phase of the cell cycle was induced in XAB2 deficient cells upon PARP inhibitor treatment which was associated with increased apoptosis.

This data provides preliminary evidence that PARP blockade in XAB2 deficient breast cancer could be a strategy. Further detailed pre-clinical studies in several cell line models as well in vivo studies will be required to confirm this preliminary observation.

# 4 XAB2 in ovarian cancers

## 4.1Introduction

Among the cancer-related death in women, ovarian cancer (OC) is the fifth most common cause of cancer in the world (Luvero D, 2014). Patients with epithelial ovarian cancer (EOC) are diagnosed at an advanced stage and it is reported as the most fatal gynaecological malignancy. Every year approximately 7,400 ovarian cancer cases are diagnosed in the United Kingdom (UK) and it is the sixth most common cancer among various tumour groups (Van Zyl B, 2018). The platinum-based chemotherapy (carboplatin and paclitaxel) and surgery are the standard treatment for the ovarian cancer. Despite a good response to first line chemotherapy, most patients show recurrence. The period between the completion of the last platinum treatment and the point of relapse detection is called the platinum-free interval (PFI). It is a prime predictor of response to consecutive chemotherapy offered after observing recurrence in patients. Ovarian cancer patients are classified into two groups under PFI, platinum-sensitive patients have a PFI of at least 6 months and platinum-resistant with a PFI of less than 6 months (Luvero D, 2014). To define tumour recurrence**,** another specific biomarker cancer antigen 125 (CA125) is identified by the Gynaecological Cancer Inter Group. After first-line chemotherapy, the increased expression of this biomarker CA125 suggests recurrence (Gupta D, 2009).

Over the last two decades, despite platinum based chemotherapy surgery, most patients recur. Therefore, a large number of clinical studies have been conducted targeting novel targets to improve outcomes for patient (Gaitskell K, 2011). For example, targeting angiogenesis through VEGF blockade (bevacizumab) as a maintenance therapy has been a recent advance with the potential to improve progression free survival (PFS). In BRCA mutant ovarian

cancer patients PARP inhibitors have significantly improved PFS (Luvero D, 2014). For the treatment of ovarian cancer, three approved PARP inhibitors are currently available (Musella A, 2018).

In certain conditions such as platinum sensitivity, BRCA1/2 germline mutation and relapsing after a complete or partial response (CR/PR) to platinum-based chemotherapy; one of the PARP inhibitors olaparib has been standardised as a maintenance treatment for these conditions in Europe. Olaparib is accepted as a fourth-line treatment for advanced ovarian cancer (mutated BRCA1/2 genes) in the United States (US). In both US and Europe, another maintenance treatment of ovarian cancer in platinum-sensitive relapsed cases after a PR/CR to platinum-based chemotherapy is niraparib, a new PARP inhibitor. Likewise, a third-line treatment in platinum-sensitive, BRCA1/2 mutated and relapsed high-grade ovarian cancer is another PARP inhibitor, rucaparib approved in both Europe and the US (Jiang X, 2019).

However, only 17% of ovarian cancer patients have BRCA1/2 germline mutations (Van Zyl B, 2018). Homologous recombination deficiency (HRD) is much more common and seen in about 50% of EOC. Olaparib, rucaparib and niraparib are three approved PARP inhibitors for managing ovarian cancer disease in the US. There are significant benefits of Poly (ADP-ribose) polymerase inhibitors (PARPi) for the treatment of ovarian cancer patients. For predicting the PARP inhibitors response in ovarian tumours, platinum sensitivity and homologous recombination deficiency (HRD) are considered as potential biomarkers (Konstantinopoulos PA, 2010).

The three biomarkers are considered in HRD assay including large-scale state transitions (LSTs), telomeric allelic imbalance (TAI) and loss of heterozygosity (LOH). This assay works on the tumour scoring system (0-100) and a cut-off 42.

The tumours with defective homologous recombination (HR) pathway have a score range $\geq 42$ on the other hand a score covering $< 42$ range displays a functional HR DNA repairing system (Jiang X, 2019).

Although patients with BRCA germline mutations, HRD or platinum sensitive condition benefits from PARP inhibitors, most patients will eventually progress on treatment. Therefore, the identification of novel targets remains a priority.

Given the essential role of XAB2 in DNA repair pathway, the hypothesis is XAB2 expression may show platinum sensitivity and XAB2 deficient tumours can be PARP inhibitors sensitive.

## 4.2 Methodology

The immunohistochemistry protocol and antibody details were described in the methods chapter. The evaluation of immunohistochemistry was performed by calculating the H-score (range 0-300). The statistical analysis and choosing cut-off value were performed by the pathologist group members.

The transient knock-down of XAB2 by siRNA transfection method was performed as per the described protocol in the methods section. The clonogenic survival assay of drug sensitivity in ovarian cell lines was detailed in the methods section. The functional studies including cell cycle staining with propidium iodide and apoptosis detection by Annexin were analysed by the flow cytometric method. Detailed analysis and staining protocols were provided in the methods section. The significant p-values were studied. The data analysis was performed using GraphPad Prism 8.2.0 software.

## 4.3 Results

### 4.3.1 Ovarian cancer- prognostic significance of *XAB2* transcripts in ovarian cancer

The prognostic significance of *XAB2* transcripts was evaluated in the KM plotter online database. The KM plotter (publicly available) database was generated by using gene expression datasets from 1287 ovarian cancer patients in The Cancer Genome Atlas (TCGA). To analyse the prognostic value of the selected gene, the patients were divided into groups and compared for progression-free survival and overall survival (Gyorffy B., 2012). The classification of gene expression analysis based on various groups was summarised in Table 4-1.

**Table 4-1:** Representation of gene expression analysis based on various classified group from KM plotter database.

| **Classification criteria:** | |
|---|---|
| **Gene** | XAB2 |
| **Split patients** | Median |
| **Number of patients with available clinical data** | n |
| **Treatment groups** | Debulking and chemotherapy. |

**The survival outcomes using KM plotter database.**

**A. Overall survival (OS), n= 1657**

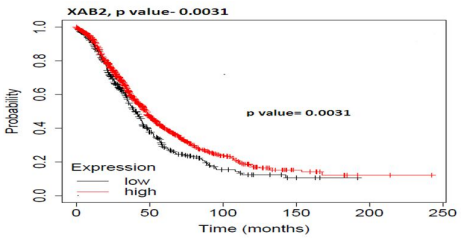


**B. Progression free survival (PFS), n= 1436**

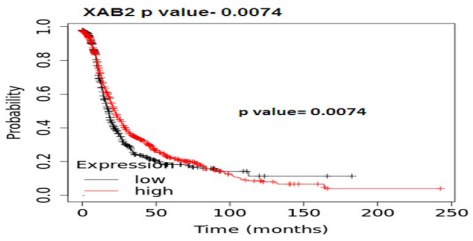


**C. Post-progression survival (PPS), n=782**

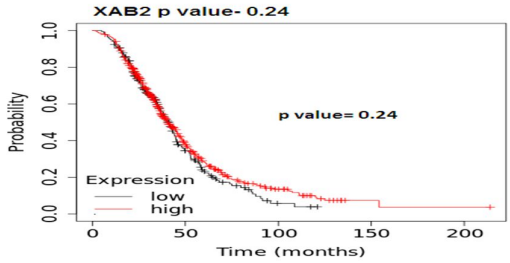


**Figure 4-1:** The survival outcomes using KM plotter (A) Overall survival (B) Progression free survival (C) Post-progression survival of ovarian cancer patients using KM plotter.

The survival curves of ovarian cancer patients were generated by Kaplan–Meier plotter (KM plotter) database for survival analysis. The prognostic significance of the selected gene XAB2 was studied and compared with survival outcomes (Figure 4-1).

Under KM plotter database, the significant p-values were obtained of XAB2 gene for survival outcomes in ovarian cancer including overall survival (OS), p=0.0031 (n=1657) and progression free survival (PFS), p=0.0074 (n=1436).

It was then proceeded to investigate the XAB2 protein expression in ovarian cancer cohort.

#### 4.3.1.1 Clinical Data

##### 4.3.1.1.1 The clinicopathological significance of XAB2 in ovarian cancer

Immunohistochemistry was used to detect XAB2 expression (nucleus) from patients in a well- characterised ovarian cancer cohort [N-525]. Not all cores within the TMA were included for IHC analysis due to missing cores or absence of tumour cells.

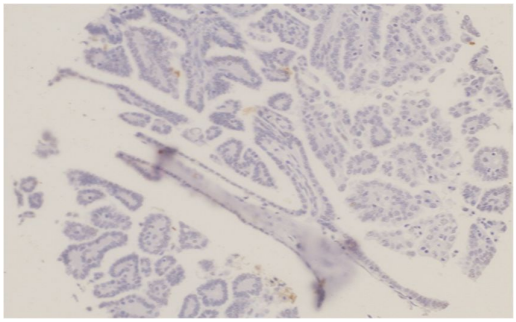

Negative XAB2 nuclear staining

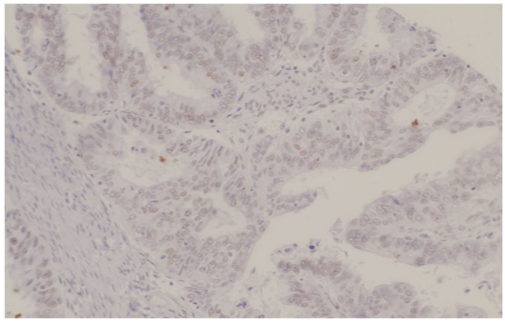

1:200 XAB2 nuclear staining

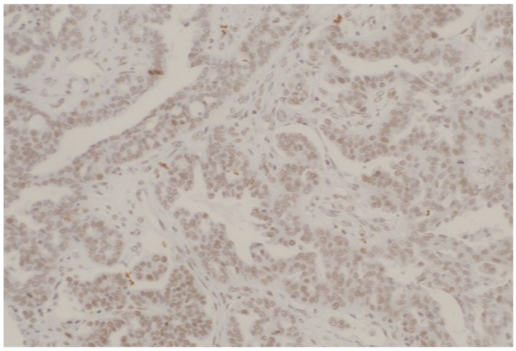

1:100 XAB2 nuclear staining

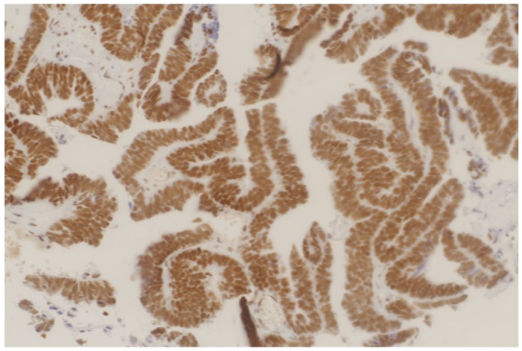

1:50 XAB2 nuclear staining (Positive-nucleus)

**Figure 4-2:** Representative photo micrographic images of XAB2 expression in ovarian cancers.

For optimization, the primary antibody XAB2 was diluted at different concentrations 1:50, 1:100 and 1:200. The clear nuclear localization of XAB2

was obtained at 1:50 (Figure 4-2). Furthermore, the ovarian tissue microarray (TMA) cohorts received were treated at this given optimization.

Ovarian cancer patient demographics was summarised in Table 4-2. Clinicopathological characteristics of ovarian cancer cohort were summarised in Table 4-3. The clinicopathological association of XAB2 in ovarian cancer was summarised in Table 4-4.

### Ovarian cancer patient demographics

**Table 4-2:** Ovarian cancer patient demographics.

| Characteristics | Number | Percentages |
|---|---|---|
| **Age at surgery** | | |
| <30 | 3 | 1.4% |
| 30-60 | 90 | 42.3% |
| >60 | 120 | 56.3% |
| **Pathological Type** | | |
| Serous adenocarcinoma | 129 | 60.6% |
| Mucinous adenocarcinoma | 24 | 11.3% |
| Endometrioid carcinoma | 25 | 11.7% |
| Clear cell carcinoma | 18 | 8.5% |
| Mixed | 9 | 4.2% |
| Other | 8 | 3.8% |
| **Tumour Grade** | | |
| Grade 1 | 27 | 14.6% |
| Grade 2 | 38 | 20.5% |
| Grade 3 | 120 | 64.9% |
| **FIGO Stage** | | |
| I | 81 | 39.1% |
| II | 34 | 16.4% |
| III | 86 | 41.5% |
| IV | 6 | 2.9% |
| **Surgical Optimal Debulking** | | |
| Optimally Debulked | 164 | 84.1% |
| Not Optimally Debulked | 31 | 15.9% |
| **Residual tumour** | | |
| None/Microscopic | 134 | 69.1% |
| <1cm | 26 | 13.4% |
| 1-2 cm | 9 | 4.6% |
| >2cm | 25 | 12.9% |

| | | |
|---|---|---|
| **Measurable Disease Before Chemotherapy** | | |
| Non | 137 | 71.4% |
| Measurable | 55 | 28.6% |
| **Chemotherapy Treatment** | | |
| NO | 20 | 10.6% |
| Adjuvant | 154 | 81.9% |
| Neoadjuvant | 14 | 7.4% |
| **Platinum Sensitivity** | | |
| Sensitive | 167 | 91.3% |
| Resistant | 16 | 8.7% |
| **BRCA2** | | |
| Low | 62 | 30.5% |
| High | 141 | 69.5% |
| **BRCA1** | | |
| Low | 114 | 57.6% |
| High | 84 | 42.4% |
| **Types of surgery** | | |
| Biopsy | 3 | 1.4% |
| Early debulking | 195 | 92.9% |
| Interval debulking | 10 | 4.8% |
| Delayed debulking | 2 | 1% |

**Table 4-3:** Clinicopathological characteristics of ovarian cancer cohort.

| **Clinicopathological Variables** | **Whole database (%)** |
|---|---|
| **Age at surgery (years)** | |
| <30 | 3 (1.4%) |
| 30-60 | 90 (42.3%) |
| >60 | 120 (56.3%) |
| **Pathology** | |
| Serous | 129 (60.6%) |
| Mucinous | 24 (11.3%) |
| Endometriod | 25 (11.7%) |
| Clear Cell | 18 (8.5%) |
| Other | 8 (3.8%) |
| Mixed | 9 (4.2%) |

| | |
|---|---|
| **Platinum sensitivity** | |
| Sensitive | 167 (91.3%) |
| Resistant | 16 (8.7%) |
| **Chemotherapy** | |
| No | 20 (10.6%) |
| Adjuvant | 154 (81.9%) |
| Neoadjuvant | 14 (7.4%) |
| **Residual tumour** | |
| None/Microscopic | 134 (69.1%) |
| <1 cm | 26 (13.4%) |
| 1-2 cm | 9 (4.6%) |
| >2 cm | 25 (12.9%) |
| **Histological Tumour Grade** | |
| 1 | 27 (14.6%) |
| 2 | 38 (20.5%) |
| 3 | 120 (64.9%) |
| **Relapse status** | |
| Progression-free | 114 (61%) |
| Relapsed | 73 (39%) |
| **Types of surgery** | |
| Biopsy | 3 (1.4%) |
| Early debulking | 195 (92.9%) |
| Interval debulking | 10 (4.8%) |
| Delayed debulking | 2 (1%) |
| **Survival status** | |
| Living | 76 (39.8%) |
| Dead | 115 (60.2%) |

**Table 4-4:** The clinicopathological features of XAB2 expression in ovarian cancer.

| Variables | Low expression | High expression | p-value |
|---|---|---|---|
| **Pathological type** | | | 0.031 |
| Serous adenocarcinoma | 52.7% | 69.3% | |
| Mucinous adenocarcinoma | 17.9% | 4.0% | |
| Endometrioid carcinoma | 11.6% | 11.9% | |
| Clear cell carcinoma | 8.9% | 7.9% | |
| Mixed | 5.4% | 3.0% | |
| **Tumour Grade** | | | 0.163 |
| Grade 1 | 19.6% | 9.7% | |
| Grade 2 | 19.6% | 21.5% | |
| Grade 3 | 60.9% | 68.8% | |
| **Surgical Optimal Debulking** | | | 0.547 |
| Optimally Debulked | 85.6% | 82.4% | |
| Not Optimally Debulked | 14.4% | 17.6% | |
| **Residual tumour** | | | 0.633 |
| None/Microscopic | 68.9% | 69.2% | |
| <1cm | 14.6% | 12.1% | |
| 1-2 cm | 2.9% | 6.6% | |
| >2cm | 13.6% | 12.1% | |

| | | | |
|---|---|---|---|
| **Measurable Disease Before Chemotherapy** | | | 0.569 |
| Non | 69.9% | 73.3% | |
| Measurable | 30.4% | 26.7% | |
| **Chemotherapy Treatment** | | | 0.252 |
| **NO** | 14.0% | 6.8% | |
| **Adjuvant** | 78% | 86.4% | |
| **Neoadjuvant** | 8% | 6.8% | |
| **Platinum Sensitivity** | | | 0.359 |
| **Sensitive** | 93.0% | 89.2% | |
| **Resistant** | 7% | 10.8% | |
| **BRCA1** | | | 0.00 |
| **Low BRCA1** | 79.2% | 35.1% | |
| **High BRCA1** | 20.8% | 64.9% | |
| **BRCA2** | | | 0.324 |
| **Low BRCA2** | 33.7% | 27.3% | |
| **High BRCA2** | 66.3% | 72.7% | |

**XAB2 expression influences patient survival in ovarian cancers**

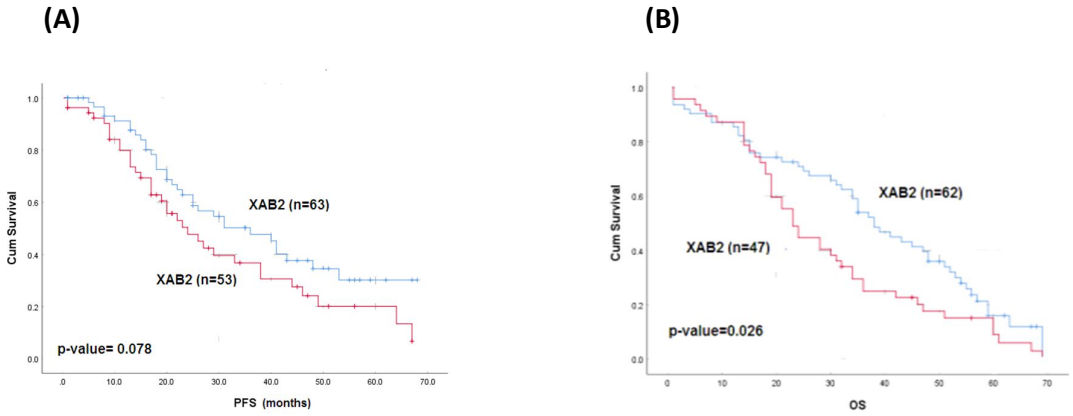


**Figure 4-3:** Kaplan Meier curve for ovarian cancer-specific survival (A) progression frees survival (PFS) (B) Overall survival (OS) in the whole cohort.

The Kaplan Meier curves were obtained using SPSS-21 software for ovarian cancer-specific survival. The blue curve represented low groups and red colour with high groups in KM curves. It illustrated the significance of XAB2 expression affecting the survival in ovarian cancers patients (Figure 4-3).

Under SPSS-21 software, Kaplan Meier curve and the significant p-value was obtained (p=0.026) of XAB2 gene for ovarian cancer overall survival (OS) (period 70 months).

**The KM survival curves using SPSS software.**

The Kaplan Meier curves for ovarian cancer in platinum sensitive and resistant patients were illustrated in Figure 4-4 and Figure 4-5 respectively.

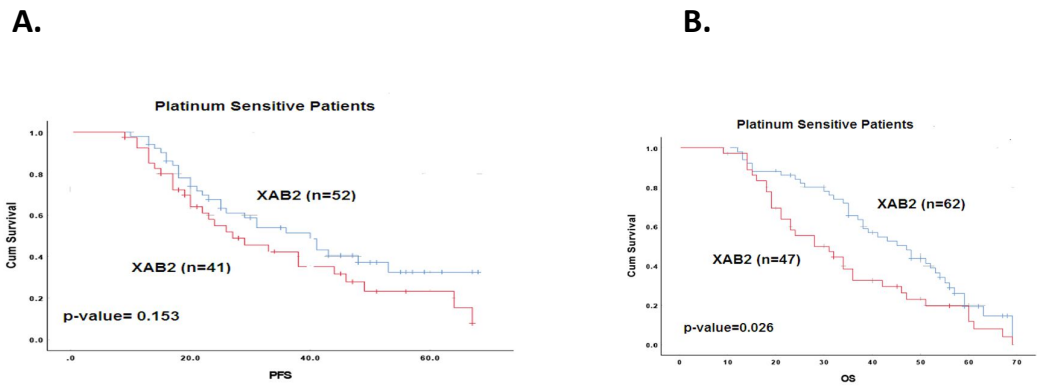


**Figure 4-4:** Kaplan Meier curve for ovarian cancer in platinum sensitive patients. For ovarian cancer (A) progression free survival (PFS) (B) ovarian cancer specific survival (OS) in platinum sensitive cohort

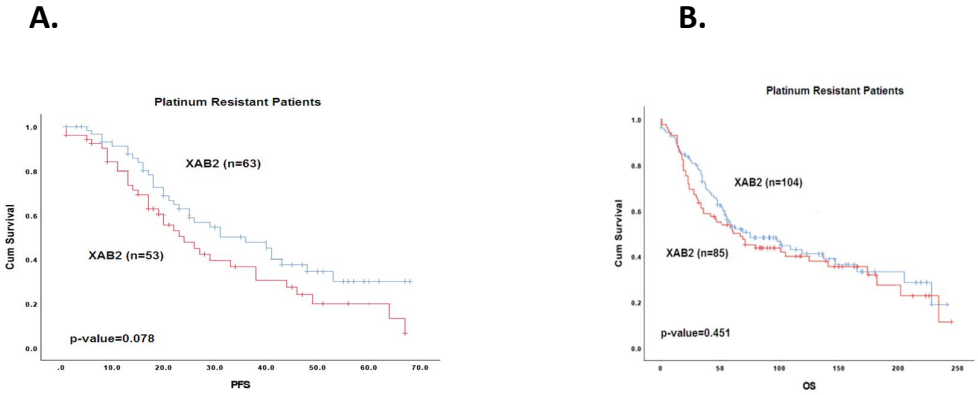


**Figure 4-5**: Kaplan Meier curve for ovarian cancer in platinum resistant patients. For ovarian cancer (A) progression frees survival (PFS) (B) ovarian cancer specific survival (OS) in platinum resistant patients.

XAB2 expression in a cohort of epithelial ovarian cancers was evaluated. The valid and suitable cases were selected for the analysis of XAB2 expression. The blue curve represented low groups and red colour with high groups in KM curves. The statistical study was presented by the pathologist group members. Tumour staging is mentioned according to the staging system for ovarian cancer of the International Federation of Obstetricians and Gynaecologists (FIGO). The ovarian cancer-specific survival (OCSS) is considered from the operation date until when any remaining survivors are censored. The progression-free survival is calculated from the date of the initial surgery to disease progression or from the date of the initial surgery to the last date known to be progression-free for those censored. The ovarian cancer patient demographics were summarised in Table 4-2.The clinicopathological characteristics of ovarian cancer cohort were summarised in Table 4-3.

The results studied the validation of XAB2 protein expression in ovarian cancers. The low nuclear XAB2 protein expression was correlated with ovarian cancer-specific survival for 70 months and the significant p-value was 0.026 (Figure 4-2). The low expression of XAB2 may show increased genomic instability in the cancer cells. In platinum-sensitive patients, low XAB2 expression was associated with significant ovarian cancer-specific survival (p value-0.026) (Figure 4-4). Therefore, XAB2 expression can be a predictor of patient outcome in ovarian cancer. The XAB2 protein was significantly overexpressed in serous adenocarcinoma (69.3%) while it was least noted in mucinous adenocarcinoma (4.0%). The clinicopathological features of XAB2 expression in ovarian cancer were summarised in Table 4-4.

### 4.3.2 Pre-clinical data

#### 4.3.2.1 XAB2 in ovarian cancer cell lines:

The protein level of XAB2 in a panel of human ovarian cancer cell lines was studied. The level of XAB2 protein was examined in ovarian cancer cell lines – PEO1, PEO4, A2780, A2780-cis, OVCR4 and SKOV3. The relative protein level was compared with band quantification (Figure 4-6).

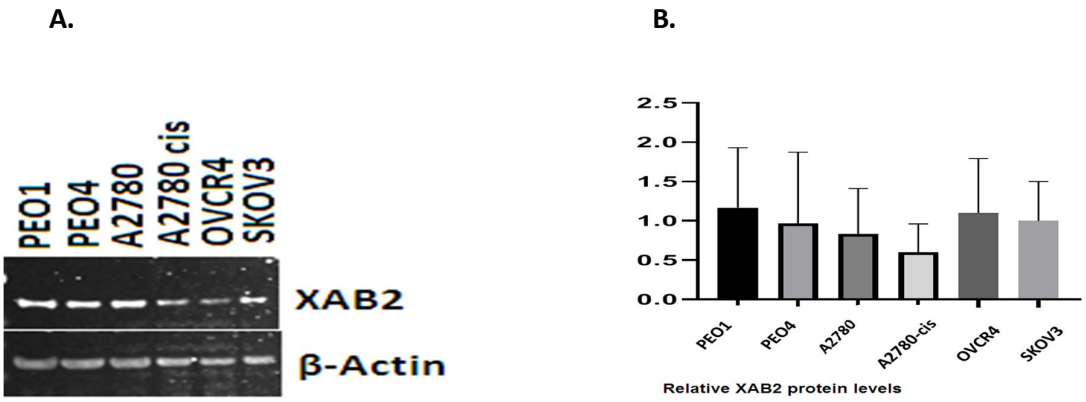


**Figure 4-6:** The western blot using ovarian cancer cell lines (A) Signal band intensity (protein expression) on the nitrocellulose membrane visualized under Licor Odyssey machine. (B) Relative XAB2 protein expression level in different ovarian cancer cell lines.

For optimization, the primary antibody XAB2 (rabbit) was checked at three different dilution factors 1:750, 1:1000 and 1:2000. The specific band for the given antibody was obtained at 1:2000. The molecular weight of the primary antibody was 100kDa. The internal loading control used for the western blot was β-actin (mouse) with a molecular weight 42kDa.

For each ovarian cancer cell line, the whole cell protein lysates were collected and samples were separated by electrophoresis on denaturing polyacrylamide. Blot was probed using specific XAB2 antibody with molecular weight 100kDa. As a loading control, β-actin antibody (42kDa) was used. The relative XAB2 expression in distinct ovarian cancer cell lines was calculated. The graph showed the XAB2 protein levels (ratio of protein/β -actin) quantitated using GraphPad Prism 8.2.0 software.

### 4.3.2.2 Pre and post cisplatin in ovarian cancer cell lines

The representation of nuclear and cytoplasmic expression in ovarian cancer cell lines was illustrated in Figure 4-7.

**A. PEO1**

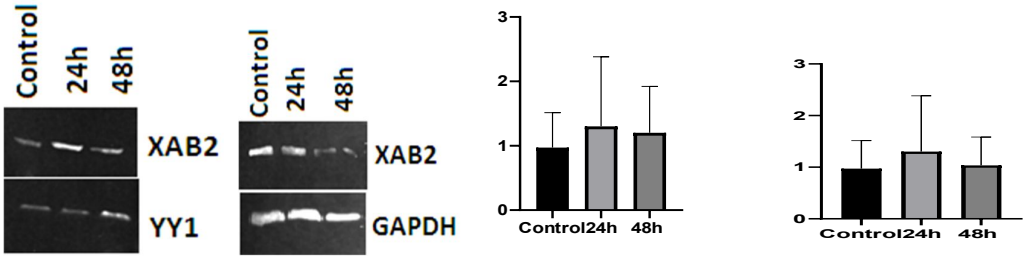


**B. PEO4**

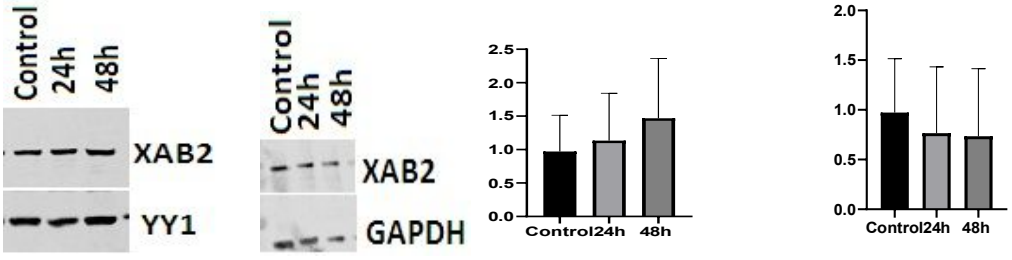


**Figure 4-7:** Nuclear and cytoplasmic expression in ovarian cancer cell lines.

(A) Western blot for XAB2 expression in nuclear and cytoplasmic extracts from PEO1 ovarian cancer cell line untreated and treated with cisplatin for 24 and 48 hours. Quantification of XAB2 protein expression by western blot (B) Western blot for XAB2 expression in nuclear and cytoplasmic extracts from PEO4 cell line untreated and treated with cisplatin for 24 and 48 hours Quantification of XAB2 protein expression by western blot. GAPDH was used as a loading control for cytoplasmic extracts and YY1 was used as the loading control for nuclear extracts.

The influence of XAB2 expression in the ovarian cancer cell line models PEO4 and PEO1 was investigated. These ovarian cancer cell lines showed XAB2 protein expression at the basal levels. The XAB2 expression fluctuated after cisplatin treatment in two cell lines. The protein expression was influenced variably upon platinum treatment in drug sensitive and resistant cell lines.

### 4.3.2.3 XAB2 siRNA in ovarian cancer cell lines.

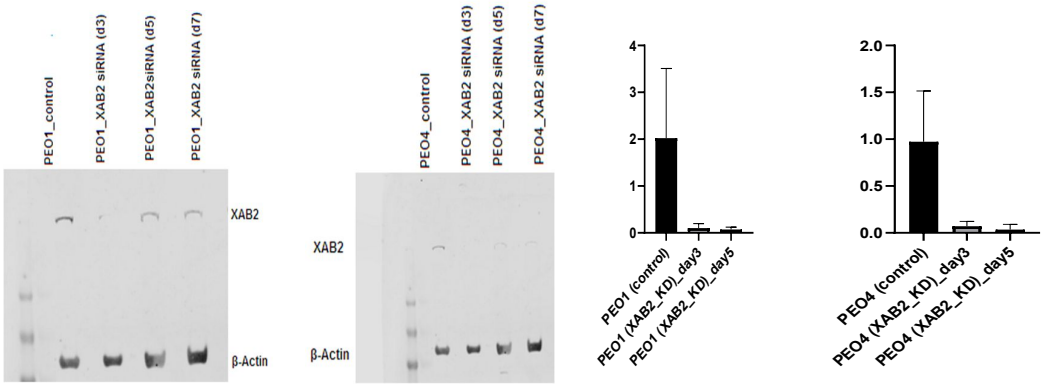


**Figure 4-8:** XAB2 siRNA in ovarian cancer cell lines.

The cells were plated overnight and the next day transfection with XAB2 siRNA was achieved using lipofectamine 3000 reagent (Invitrogen, UK) in opti-mem medium. The lysates were collected for a western blot on day 3, day 5 and day

7. The quantification of XAB2 protein levels was obtained relative to β-actin (loading control).

To explore further the implication of XAB2 deficiency in ovarian cancer, siRNA studies in ovarian cancer cell lines were conducted. PEO1 (cisplatin sensitive) and PEO4 (cisplatin-resistant) were used. The XAB2 siRNA achieved efficient knockdown on day 3 and day 5 in the tested cell lines (Figure 4-8).

### 4.3.2.4 Drug is toxic in XAB2 deficient ovarian cancer cell lines.

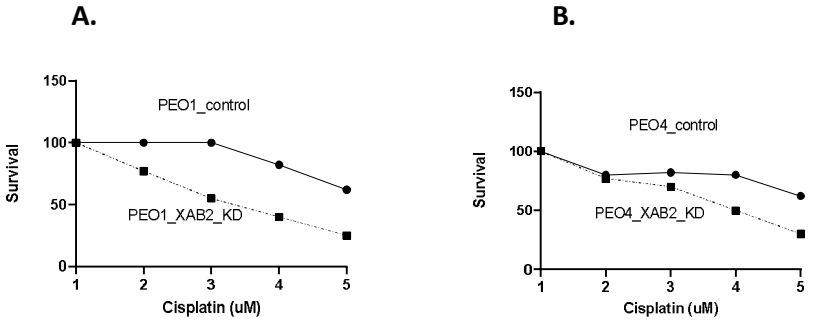


**Figure 4-9:** Clonogenic survival assay for cisplatin in ovarian cancer cell lines. The clonogenic survival curves for (A) PEO1 and PEO1_XAB2_KD (B) PEO4 and PEO4_XAB2_KD at different doses of cisplatin.

The cells were transfected with XAB2 siRNA for 24 hours. On day 2, the cells were trypsinized and re-plated in 6-well plates at 1000 cells/well cell density. The colonies were fixed, stained and counted.

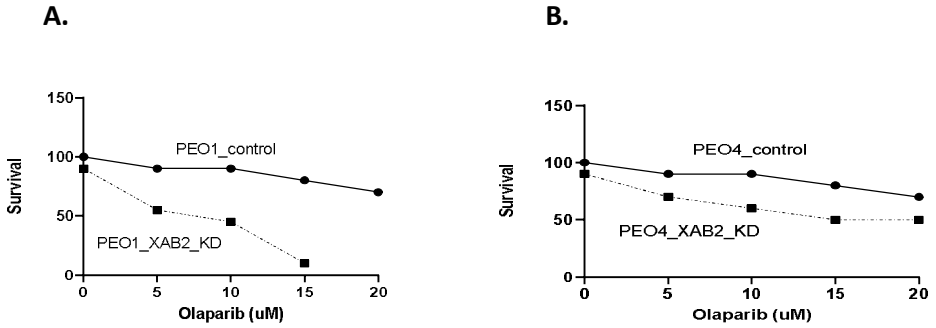


**Figure 4-10:** Clonogenic survival assay for olaparib in ovarian cancer cell lines. The clonogenic survival graphs for (A) PEO1 and PEO1_XAB2_KD (B) PEO4 and PEO4_XAB2_KD at different doses of olaparib.

The XAB2 knockdown (KD) was performed in ovarian cancer cell lines and the hypothesis was that cisplatin can induce toxicity in XAB2 deficient ovarian cells. Therefore, drug sensitivity in XAB2_KD PEO1 and PEO4 cells using a clonogenic survival assay was tested. It was observed that cytotoxicity in PEO1 (XAB2_KD) cells was high in comparison to XAB2-depleted PEO4 cells (Figure 4-9). This suggested more sensitivity to the drug in cisplatin-sensitive cells. It confirmed cisplatin sensitivity in XAB2 knockdown ovarian cancer cell lines.

Olaparib sensitivity in XAB2 deficient ovarian cancer cell lines was confirmed. The XAB2_KD PEO1 and PEO4 cells were olaparib sensitive (Figure 4-10). XAB2 expression was depleted with siRNA in both cell lines and olaparib cytotoxicity in PEO1, PEO4 control and XAB2 knockdown cells were tested by a clonogenic survival assay. The PEO1 (XAB2_KD) was more sensitive to olaparib than the control cells which emphasized the same results in other ovarian cancer drug-sensitive (XAB2_KD) cell lines.

The clonogenic cell survival assay was performed to test whether XAB2 deficient cells were drugs sensitive. The XAB2 knockdown and proficient cell lines were treated with increasing concentrations of cisplatin and olaparib

which were potent and selective drugs that affect DNA repair pathways. Clonogenic assay demonstrated that XAB2 deficient cells were more sensitive to drugs compared to XAB2 proficient cells.

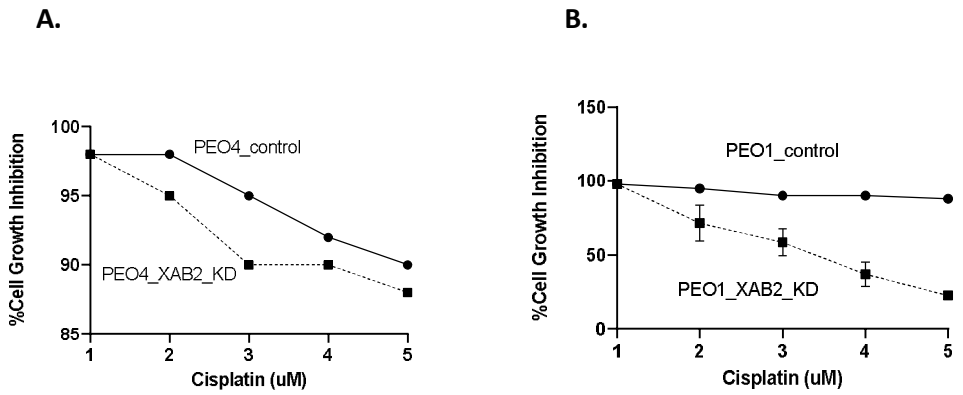


**Figure 4-11:** MTS cell growth inhibition assays of drug (A) PEO4 control cells compared to its XAB2 knockdown cells (B) PEO1 control cells compared to its XAB2 knockdown cells.

The cell lines with XAB2 deficiency exhibited reduced cell proliferation after treatment with cisplatin drug agent for 6 days compared to XAB2 proficient cell lines. Data were shown as the mean and SD values for each concentration from three independent experiments. For additional validation, the proliferation assay (MTS assay) was used to determine cell growth in response to cisplatin. As shown in Figure 4-11, XAB2 deficient PEO1 ovarian cancer cells were more sensitive to cisplatin than the control PEO1 cells. Similarly, sensitivity was demonstrated in XAB2 knockdown PEO4 cells compared to control cells.

As shown in clonogenic cell survival assay, XAB2 knockdown cells were more sensitive to drugs than XAB2 proficient cells. Similar sensitivity was also demonstrated by MTS cell growth inhibition assay of drugs in XAB2 knockdown

cells. Taken together, these data provided evidence that XAB2 deficient cells were sensitive to both drugs.

### 4.3.2.5 Cell cycle progression in XAB2 deficient cell lines

It is previously described that PARP1 has a role in cell cycle progression (Jelinic P, 2014). Therefore, cell cycle progression was evaluated following olaparib therapy (Figure 4-12).

PEO1, PEO4 control and its XAB2 _KD cells were seeded in 6-well plates overnight and treated with olaparib for 24 hours. Cells were stained with propidium iodide (PI) for analysing the phases of the cell cycle.

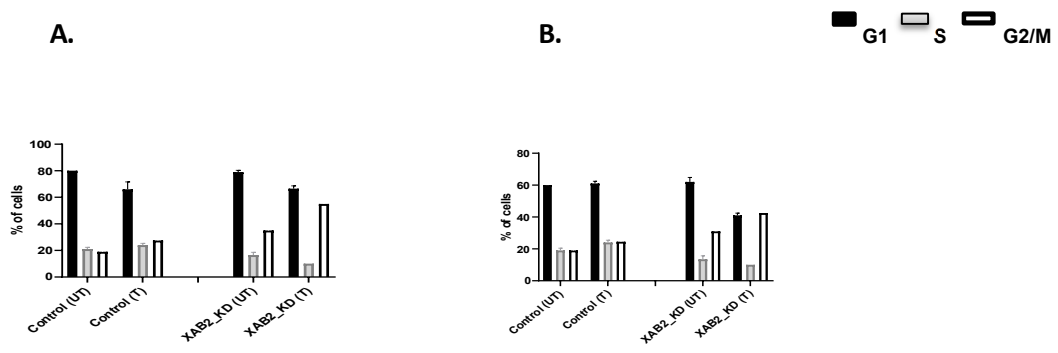


**Figure 4-12:** Functional studies of olaparib response in XAB2 knockdown cells. Cell cycle analysis by flow cytometry (A) PEO4 control cells and XAB2 knockdown cells (B) PEO1 control cells and XAB2 knockdown cells treated with 10μM olaparib for 24 hours.

The cells were transfected with XAB2 siRNA. The cells were treated with 10μM olaparib. The control cells were compared to its XAB2 knockdown (KD) cells.

The XAB2 proficient and XAB2 knockdown cells were treated with 10µM olaparib for 24 hours. The y-axis represented cell count and propidium iodides detected fluorescence was shown on the x-axis. The results for XAB2 proficient and XAB2 deficient cells following treatment with 10µM olaparib for 24 hours were shown in Figure 4-12. It demonstrated cell cycle arrest in olaparib treated XAB2 knockdown cells compared to untreated cells. The data was shown as the mean and standard deviation (SD) values for each concentration from three independent experiments. The graphs and statistical analysis were performed by using GraphPad Prism 8.2.0 software.

#### 4.3.2.6 Accumulation of the apoptotic cells upon drug treatment

To investigate the accumulation of apoptotic cells upon inhibition of PARP1 blockade in XAB2 deficient cells, Annexin-V and PI staining for the XAB2 proficient and deficient cell line treated with the olaparib was performed. The results showed an accumulation of early and late apoptotic cells in XAB2 deficient cell lines treated with the drug (Figure 4-13).

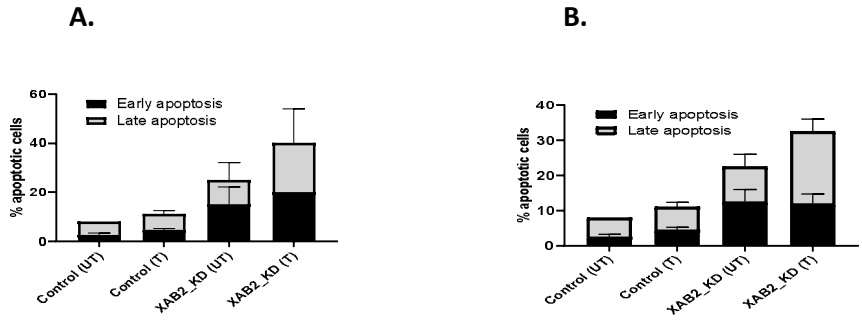


**Figure 4-13:** The percentage of apoptotic cells analysed by flow cytometry. Annexin V apoptosis graphs (A) PEO1 control and XAB2_KD cells (B) PEO4 control and XAB2_KD cells treated with olaparib (10µM) for 24 hours.

The cells were treated for 24 hours with 10μM olaparib then stained with Annexin V-FITC and propidium iodide (PI) for flow cytometric analysis.
Upon drug treatment, XAB2 deficient cells showed significant increase in apoptosis compared to XAB2 proficient cells.
The result for XAB2 proficient and XAB2 knockdown cells following treatment with 10μM olaparib for 24 hours was shown in Figure 4-13. Data were normalised against baseline apoptotic fraction (untreated cells) to determine the percentage increase in apoptosis. It demonstrated an increase in apoptosis under treated XAB2 knockdown cells compared to untreated cells.

## 4.4 Discussion

The significant clinical benefits of the PARP inhibitors for ovarian cancer treatment have been proved and it is an exciting new strategy among treatment options (Fong PC, 2010). However, patients eventually progress whilst on PARP inhibitor therapy. Identification of additional targets in ovarian cancer is a priority.

In the current study, the clinicopathological significance of XAB2 expression in a large cohort of ovarian cancers (n=525) was investigated. In this study, XAB2 expression was significantly correlated with serous type tumours (p value-0.031) and low XAB2 expression associated with poor survival.

The different stages of ovarian cancer are considered before treating the patients with chemotherapeutic agents. The frequently used chemotherapeutic agents are paclitaxel and docetaxel (taxane family) as well as cisplatin and carboplatin (platinum drugs) for the treatment of ovarian cancer (OC) (Chandra A., 2019). New major clinical trials continue to be launched in the ovarian cancer drug discovery sector (Gibson S.J, 2014).

The drug activity on the cells produced the platinum adducts and these were recognised and removed by the various DNA repair mechanisms. The mechanisms of the DNA repairing system have the potential to participate in polymorphisms, drug resistance, detailing gene mutation and deletion or duplication of genes therefore; these biomarkers can be considered for drug resistance development. The DNA repairing mechanisms that contribute to drug resistance are controlled by the new emerging combinations of drugs and it is a potential approach to overcome it. The cancer cells have vulnerabilities arising from DNA repair defects therefore; the DNA repair proteins are targeted directly in epithelial ovarian cancers (EOCs) (Damia G, 2019). This

concurred with the findings and suggested that platinum resistance could involve similar mechanisms. This may be an area of interesting future investigations.

It was shown in preclinical work that cisplatin and olaparib are sensitive in XAB2 deficient ovarian cell lines. This was more profound in platinum-sensitive PEO1 ovarian cells. The drugs reduced the cell's ability to form colonies in XAB2-depleted cells. The drug-treated XAB2 deficient cells were arrested in the G2/M phase and led to the accumulation of apoptotic cells.

In conclusion, the data presented that low XAB2 was associated with aggressive ovarian cancer. Pre-clinically, XAB2 deficient cells were sensitive to platinum and olaparib. The data suggested that XAB2 may be a promising biomarker in ovarian cancers.

# 5 FANCD2 in invasive breast cancer

## 5.1 Introduction

The cisplatin, mitomycin C (MMC) and diepoxybutane (DEB) are the DNA crosslinking agents and FA cells are particularly sensitive to these agents. During DNA replication or upon DNA damage, the Fanconi anaemia (FA) pathway is activated. Both FA and non-FA proteins participate in repairing the DNA damage. FA pathway is activated with monoubiquitination of FA Complementation Group D2 (FANCD2) which operates in cooperation with other proteins. In the signalling cascade of DNA damage repairing, the FA pathway plays an essential role. Many proteins are engaged in repairing DNA damage including breast cancer susceptibility proteins BRCA1/2, BRIP1 and PALB2 which are identified as four FA-gene products (FANCD1/J/N/S) taking part in the FA pathway.

Upon genotoxic stresses, FANCD2 and FANCI are monoubiquitinated. The DNA repairing systems including NER, TLS and Rad51-mediated HR are activated when the monoubiquitinated FANCI-FANCD2 complex is enrolled at the DNA damage sites. FANCD2 may also have roles during DNA replication elongation, termination step or during stalling of replication forks.

In response to the genotoxic stresses, the FA signalling pathway with its several significant proteins assist in maintaining genomic stability in the cells. In mammalian cells, the coordination of many signalling networks including FA pathway is required for repairing the cellular DNA damage crosslinks. Many research studies recognise the importance of FANCD2 in sensing DNA damage, DNA damage response (DDR) pathway, signal transduction and DNA repair. During DNA damage, it functions with other known repair proteins and some factors yet need to be identified. Phosphorylation of FANCD2 at Ser222 by ATM results in cell cycle arrest (Nepal M, 2017). To evaluate the possible role

of FANCD2, its expression is studied in sporadic and hereditary invasive breast cancer. In proliferating normal breast cells, FANCD2 interacts with BRCA1 and FANCD2 knockout mice develop breast tumours. The ionizing irradiation or mitomycin C induces a DNA damage response resulting in the activation of FANCD2 by mono-ubiquitination. This DDR signalling pathway also incorporates BRCA1 and BRCA2 (breast cancer susceptibility genes) called the FA-BRCA pathway. The proliferating cells express FANCD2 including premenopausal breast duct epithelium suggesting a role of FANCD2 during cell replication. The uncontrolled proliferation is a feature of cancer, a role of FANCD2 in breast carcinogenesis has been suggested. The FANCD2 expression is correlated with the proliferation factor Ki-67 in invasive cancer cells. It reflects the biological role of FANCD2 in the DNA repair of proliferating cells (Van der Groep P, 2007). The degradation of FANCD2 (celastrol treatment) sensitizes high-grade gliomas (HGGs) to carboplatin-mediated DNA damage hence proving the role of FANCD2 in preserving the genomic integrity in HGG cells. The expression of FA proteins in DDR may predict resistance to chemotherapy in cancers (Metselaar DS, 2019).

## 5.2 Results

### 5.2.1 Gene expression analysis using METABRIC database

#### 5.2.1.1 FA gene transcripts and breast cancer survival

Using the Molecular Taxonomy of Breast Cancer International Consortium (METABRIC) database, prognostic significance of FA repair genes were investigated (Figure 5-1). The numbers of breast cancer patients used for the analysis of genes were 1980 and the Beeswarm plot of gene expression was obtained. The Kaplan-Meier curves for overall survival (OS) and disease free survivals (DFS) of breast cancer were studied (Figure 5-2).

The Beeswarm plots of FANC genes expression based on clinicopathological characteristics were derived from Metabric database. These plots were used to identify the changes in distribution of data points across different categories. These plots were designed to present how the features in a dataset impact the overall output. The x-axis was represented by the number of that feature and accumulation of dots along each row displayed density. The y-axis showed the feature names in order of importance from top to bottom with the logarithmic scale. The value of the corresponding characteristic was represented by the colour (each point) on the graph. The red colour showed the high value and blue was meant for low value of a feature. Each point represented a row of data from the original dataset. In the beeswarm plot, the coloured dots indicated tumour.

It was a type of categorical scatter plot for visualizing the distribution of data points in a dataset. It had an application in exploring and analysing the relationship between two or more variables in a dataset. A dot represented each data point in a plot and the dots were arranged without overlapping manner.

Out of all fanconi anemia DNA repair genes (22) studied using the Metabric dataset, no significant results were observed for the following FA genes: FANCD1, FANCF, FANCJ, FANCN, FANCO, FANCP, FANCR, FANCS, FANCT, FANCU, FANCV and FANCW. The data for significant associations was discussed.

**FANCB**

**Age status: ≤40 vs 40-70 vs ≥70 yrs**

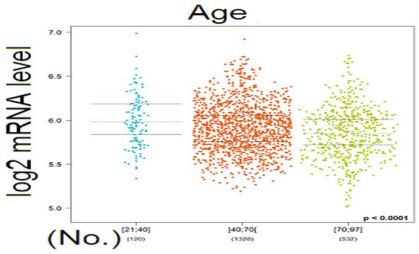


**p value <0.0001**

**Age status: ≤51 vs >51 yrs**

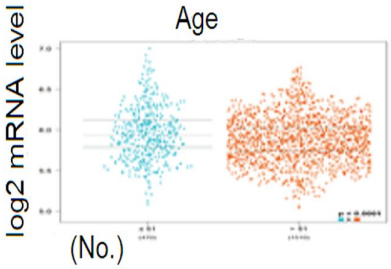


**p value <0.0001**

**Histological types**

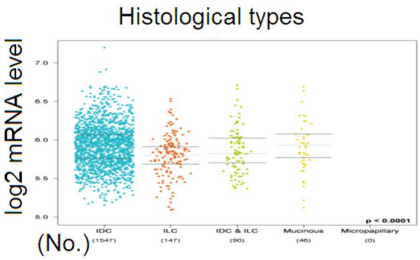


**p value < 0.0001**

**Nodal status**

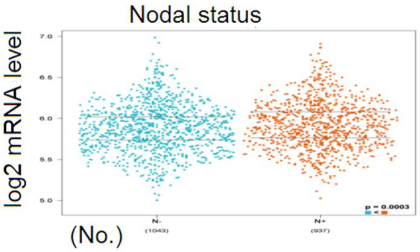


**p value = 0.0003**

**NPI**

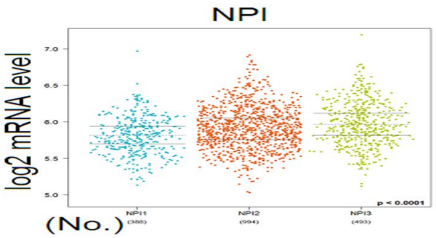


**p value < 0.0001**

**Oestrogen receptor status (ER)**

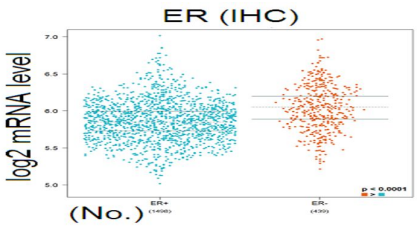


**p value < 0.0001**

**Progesterone receptor status (PR)**

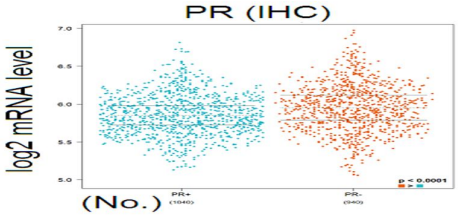


**p value < 0.0001**

**HER2 receptor status (HER2)**

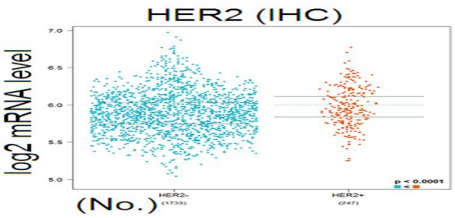


**p value < 0.0001**

**FANCC**

**Age status: ≤40 vs 40-70 vs ≥70 yrs**

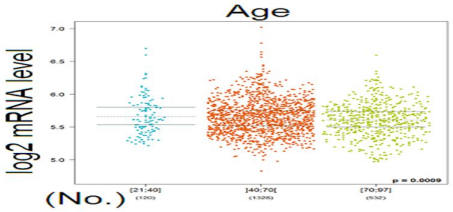


**p value = 0.0009**

**Age status: ≤51 vs >51 yrs**

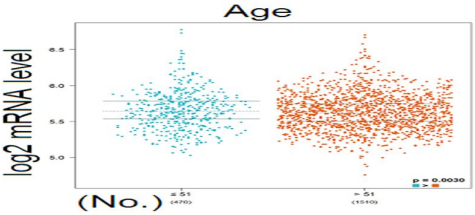


**p value = 0.0030**

**Histological types**

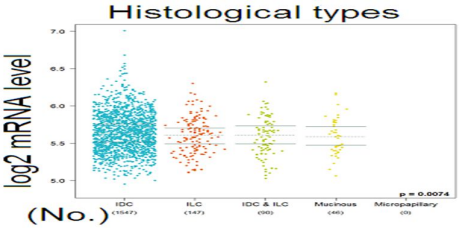


**p value =0.0074**

**Nodal status**

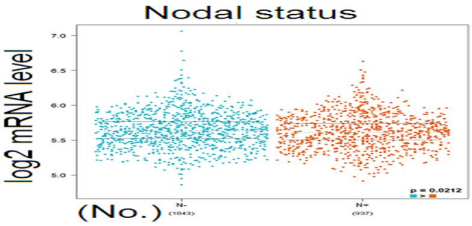


**p value =0.0212**

**NPI**

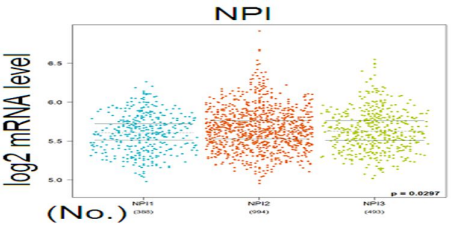


**p value = 0.0297**

**Oestrogen receptor status (ER)**

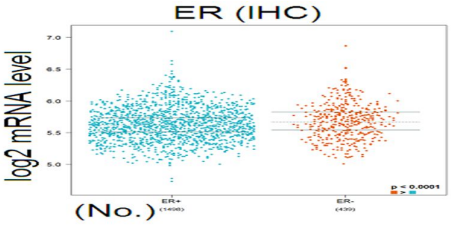


**p value < 0.0001**

**Progesterone receptor status (PR)**

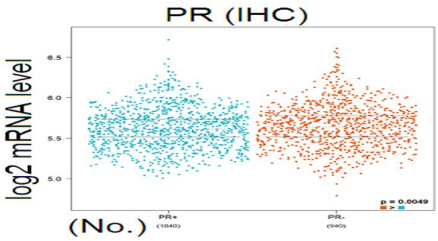


**p value = 0.0049**

**HER2 receptor status (HER2)**

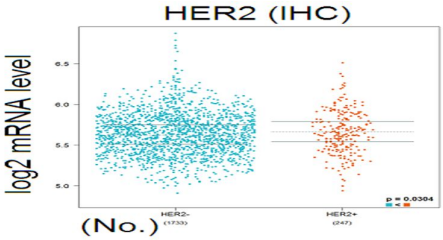


**p value = 0.0304**

**FANCD2**

**Age status: ≤40 vs 40-70 vs ≥70 yrs**

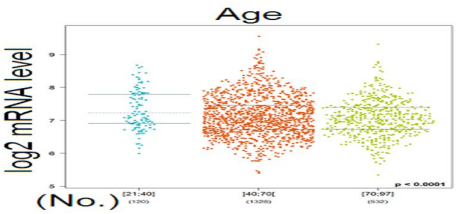


**p value < 0.0001**

**Age status: ≤51 vs >51 yrs**

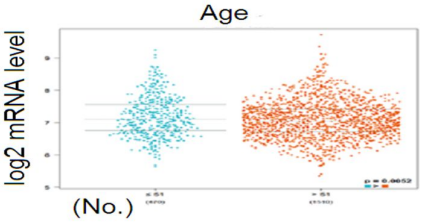


**p value = 0.0052**

**Histological types**

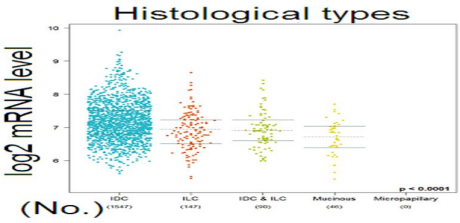


**p value < 0.0001**

**Nodal status**

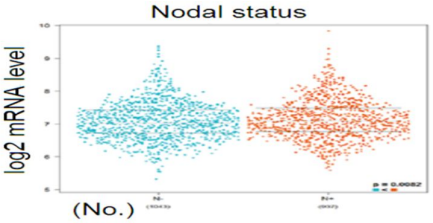


**p value = 0.0082**

**NPI**

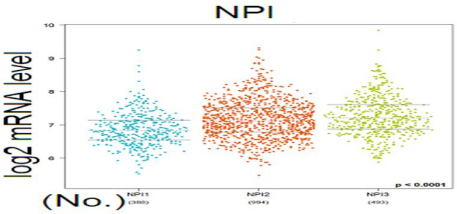


**p value < 0.0001**

**Oestrogen receptor status (ER)**

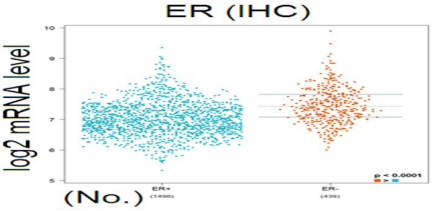


**p value < 0.0001**

**Progesterone receptor status (PR)**

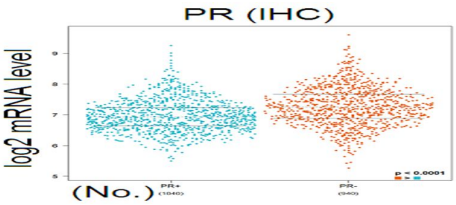


**p value < 0.0001**

**HER2 receptor status (HER2)**

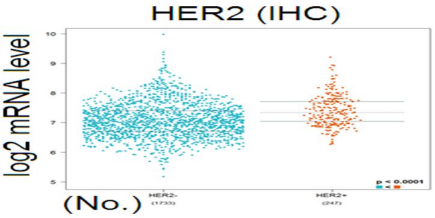


**p value < 0.0001**

**FANCE**

**Age status: ≤40 vs 40-70 vs ≥70 yrs**

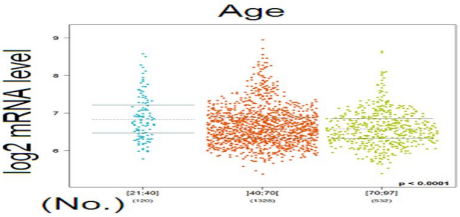


**p value < 0.0001**

**Age status: ≤51 vs >51 yrs**

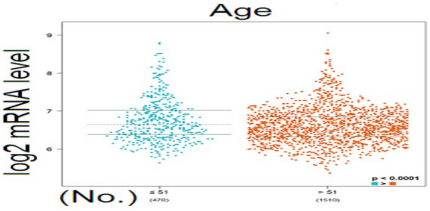


**p value < 0.0001**

**Histological types**

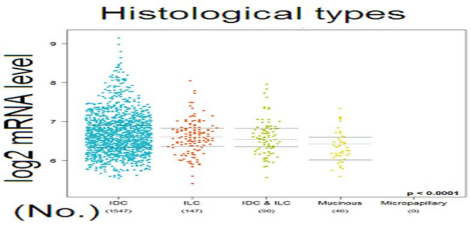


**p value < 0.0001**

**Nodal status**

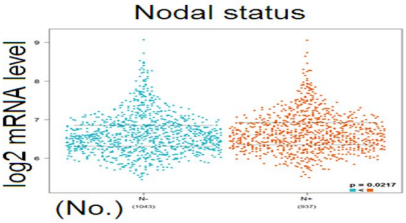


**p value = 0.0217**

**NPI**

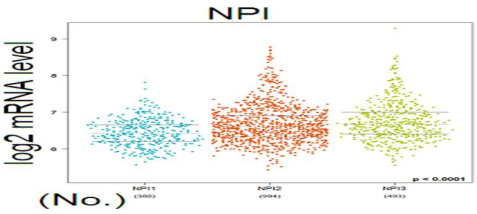


**p value < 0.0001**

**Oestrogen receptor status (ER)**

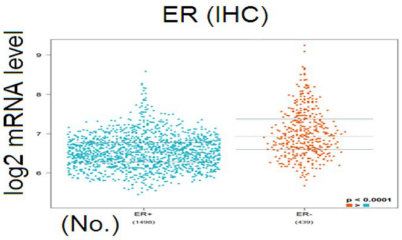


**p value < 0.0001**

**Progesterone receptor status (PR)**

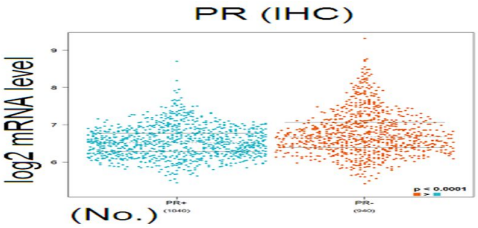


**p value < 0.0001**

**FANCG**

**Age status: ≤40 vs 40-70 vs ≥70 yrs**

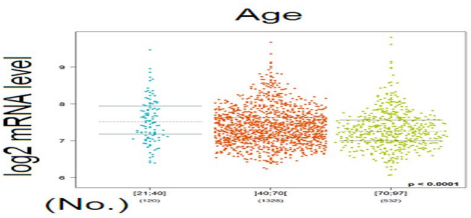


**p value < 0.0001**

**Age status: ≤51 vs >51 yrs**

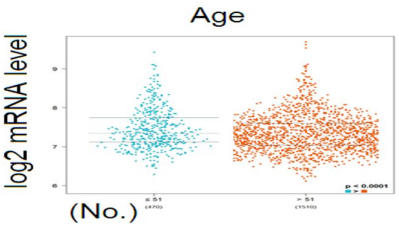


**p value < 0.0001**

**Histological types**

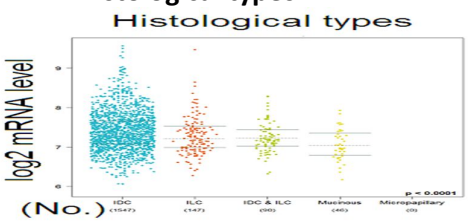


**p value < 0.0001**

**NPI**

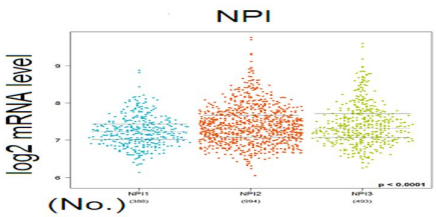


**p value < 0.0001**

**Oestrogen receptor status (ER)**

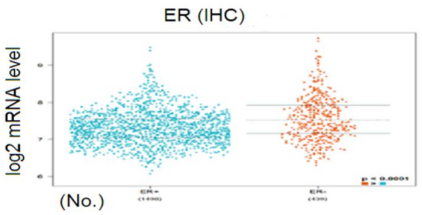


**p value < 0.0001**

**Progesterone receptor status (PR)**

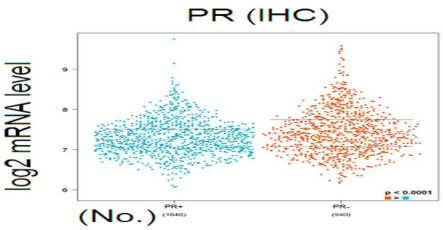


**p value < 0.0001**

**FANCI**

**Age status: ≤40 vs 40-70 vs ≥70 yrs**

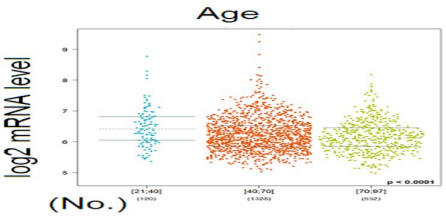


**p value < 0.0001**

**Age status: ≤51 vs >51 yrs**

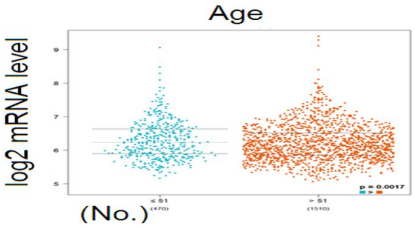


**p value = 0.0017**

**Histological types**

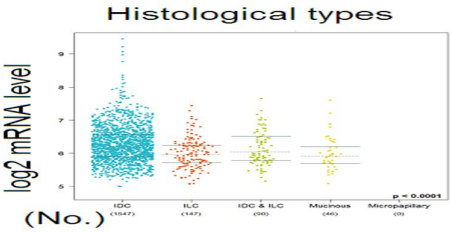


**p value < 0.0001**

**Nodal status**

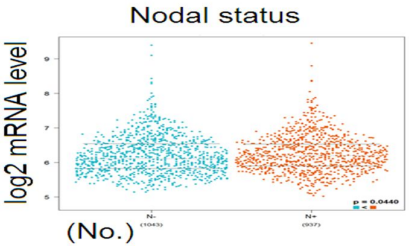


**p value = 0.0440**

**NPI**

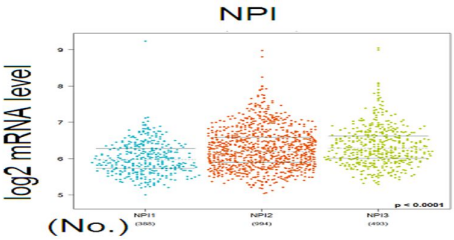


**p value < 0.0001**

**Oestrogen receptor status (ER)**

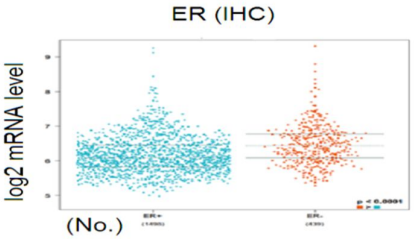


**p value < 0.0001**

**Progesterone receptor status (PR)**

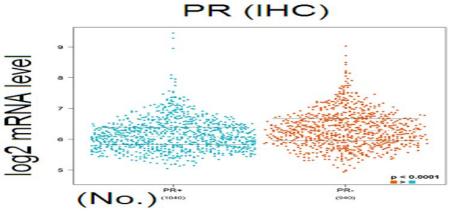


**p value < 0.0001**

**HER2 receptor status (HER2)**

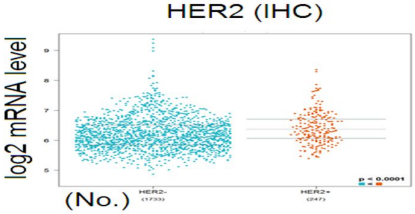


**p value < 0.0001**

**FANCL**

**Age status: ≤40 vs 40-70 vs ≥70 yrs**

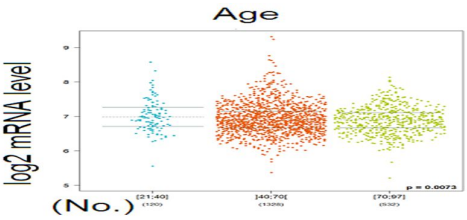


**p value = 0.0073**

**Age status: ≤51 vs >51 yrs**

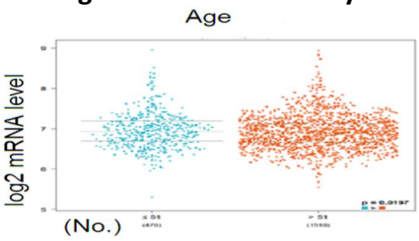


**p value = 0.0197**

**Histological types**

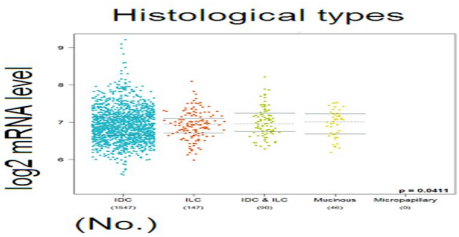


**p value = 0.0411**

**NPI**

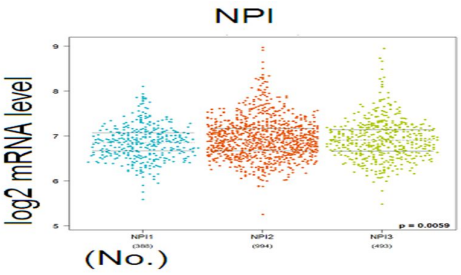


**p value = 0.0059**

**Oestrogen receptor status (ER)**

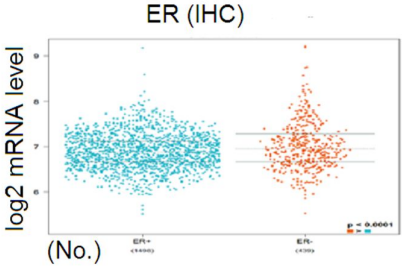


**p value < 0.0001**

**Progesterone receptor status (PR)**

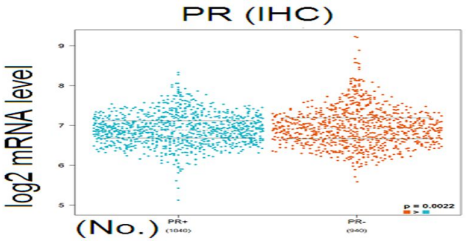


**p value = 0.0022**

**HER2 receptor status (HER2)**

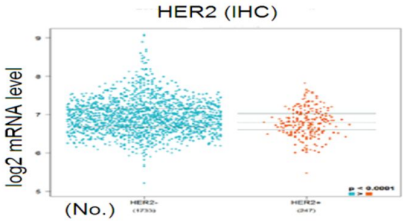


**p value < 0.0001**

**Figure 5-1:** FA genes for survival analysis in breast cancer patients using Metabric database.

The Molecular Taxonomy of Breast Cancer International Consortium (METABRIC) database was used to explore all the fanconi anaemia (FA) repair genes for survival curves and p-values. The Beeswarm plots of gene expression were generated for the analysis of DNA repair genes of breast cancer patients. These plots were used to examine the changes in gene expressions across different categories of clinicopathological parameters. This Metabric data studied the FANC genes expression based on clinicopathological characteristics.

### 5.2.1.2 Kaplan-Meier curves for overall survival (OS) of breast cancer patients using Metabric database

**FANCD2**

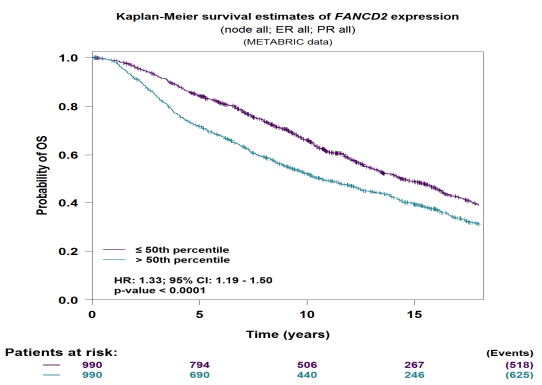


**p value < 0.0001**

**FANCE**

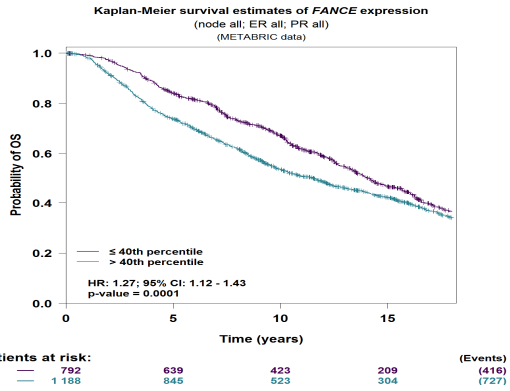


**p value = 0.0001**

**FANCI**

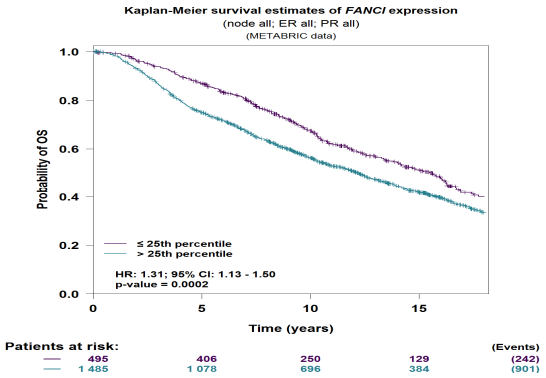


**p value = 0.0002**

**Figure 5-2:** Kaplan-Meier curves for OS of breast cancer patients using Metabric database.

For all the fanconi anaemia (FA) repair genes, the Kaplan-Meier (KM) curves including overall survival (OS) and disease free survivals (DFS) of breast cancer patients were generated by using METABRIC database. These KM curves were meant to evaluate the significant association between cancer patient survival and the expression of a gene set. This perspective recognised appropriate gene sets that were related with carcinoma condition.

Under Metabric database, Kaplan-Meier curves for overall survival (OS) and the significant p-values in breast cancer were obtained of different FA genes (period 15 years) including FANCD2 ($p < 0.0001$), FANCE ($p=0.0001$) and FANCI ($p=0.0002$).

### 5.2.1.3 Kaplan Meier plotter portal

Using Kaplan Meier plotter portal for breast cancer, all fanconi anemia DNA repair genes (22) were studied for overall (OS), progression free (PFS) and diseases free survival curves (DFS). A significant p value table was drawn for breast cancer. It was a tool that demonstrated the correlation between the

gene expression analysis and patient survival for the identification and functional depiction of prognostic markers in cancer cells. Single gene of FA pathway as input was typed in the dataset selection, a parameter survival type was chosen and Kaplan-Meier plots were obtained (Figure 5-3). The overall survival and distant metastasis free survival of breast cancer patients using KM plotter were summarised in Table 5-1. The FA genes significant in two different databases METABRIC and KM plotter were summarised in Table 5-2.

**Table 5-1**: Overall survival and distant metastasis free survival of breast cancer patients using KM plotter

| **Fanconi anemia genes** | **Overall survival (OS) p-value** | **Distant metastasis- free survival- DMFS) p-value** |
|---|---|---|
| FANCA | 0.0204 | 0.0004 |
| FANCB | 0.6207 | 0.4864 |
| FANCC | 0.7096 | 0.2763 |
| FANCD1 | 0.0117 | 0.0002 |
| FANCD2 | 0.7153 | 0.3149 |
| FANCE | 0.5323 | 0.1094 |
| FANCF | 0.0635 | 0.1021 |
| FANCG | 0.0046 | 0.0013 |
| FANCI | 1.7e-09 | 0.0001 |
| FANCJ | 0.6883 | 0.0473 |
| FANCL | 0.3689 | 0.0104 |
| FANCM | 0.3616 | 0.2316 |

## Overall survival

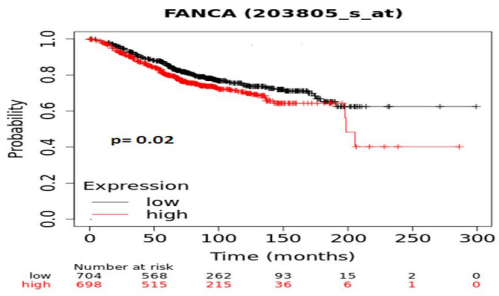


p value- 0.0204

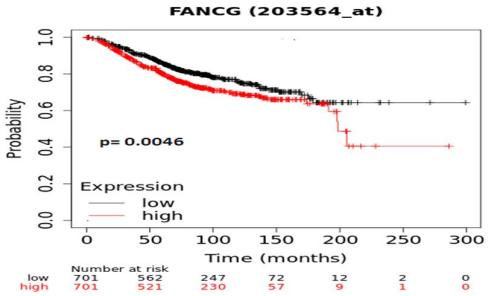


p value- 0.0046

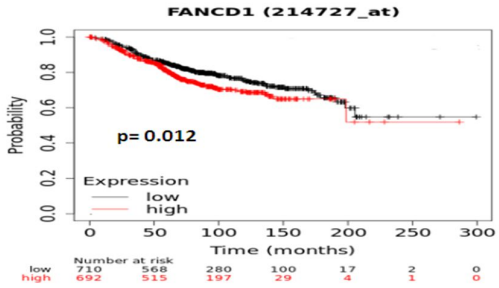


p value- 0.012

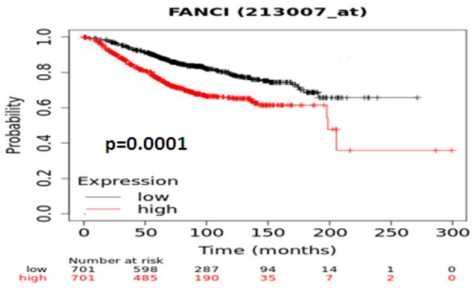


p value- 0.0001

## Distant metastasis free survival

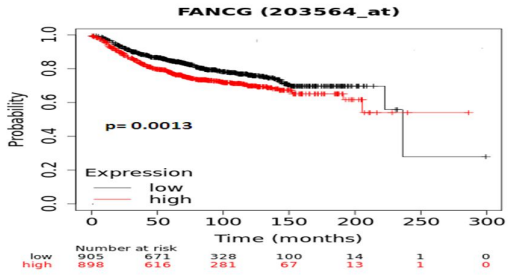


p value- 0.00041

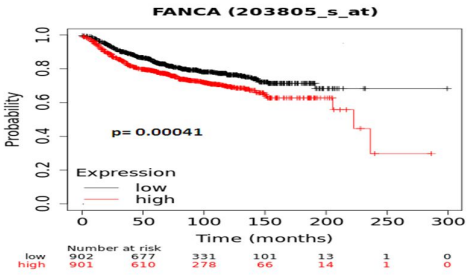


p value- 0.0013

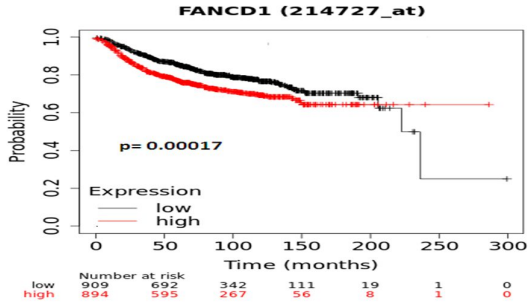


p value- 0.00017

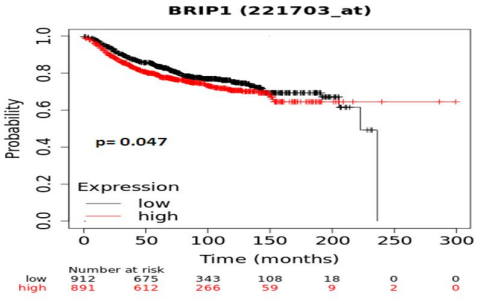


p value- 0.047 (FANCJ)

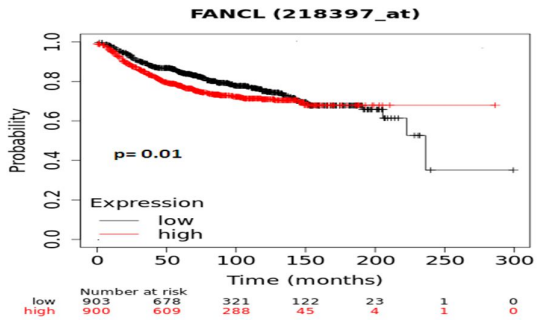


p value- 0.01

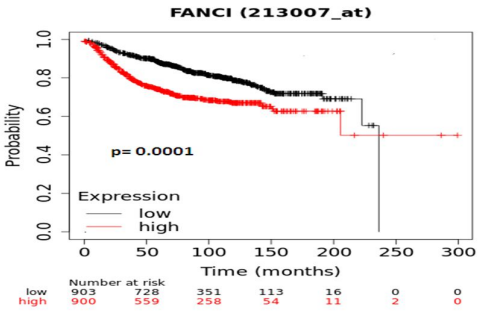


p value- 0.0001

## Disease Free survival or Recurrence free survival

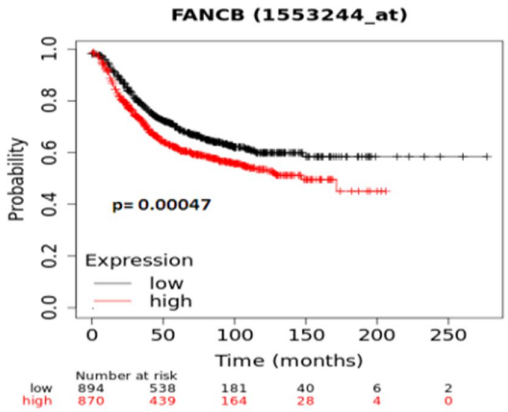


p value- 0.00047

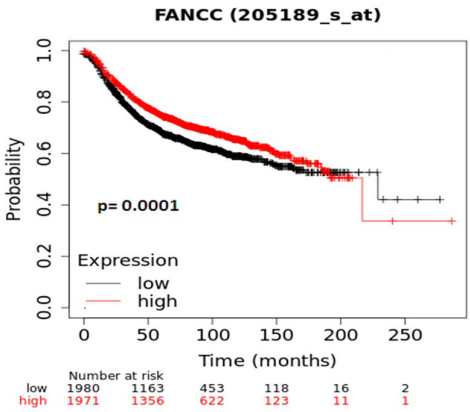


p value- 0.0001

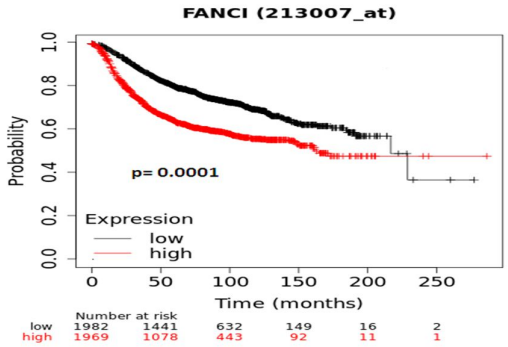


p value- 0.0001

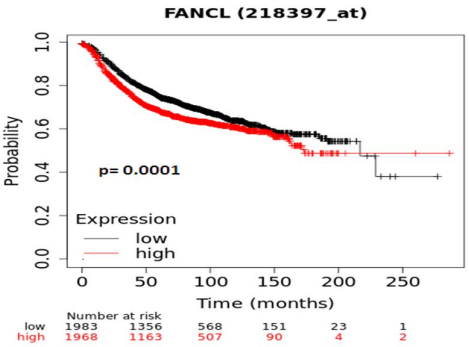


p value- 0.001

**Figure 5-3:** KM survival graphs using Kaplan Meier plotter database.

All FA genes were considered for overall (OS), progression free survival (PFS) and diseases free survival curves (DFS) of breast cancer patients by Kaplan Meier plotter portal. It was used to establish the link between the expression of DNA repair genes and breast cancer patient survival to spot the applicable prognostic markers in carcinomas.

Under KM plotter database, KM survival graphs and the significant p-values were obtained of different FA genes (period= 300 months) in breast cancer including overall survival (OS) for FANCA (p=0.02), FANCG (p=0.0046), FANCD1 (p=0.012) and FANCI (p= 0.0001).

For Distant metastasis free survival in breast cancer (period 300 months), FANCG (p=0.00041), FANCA (p=0.0013), FANCD1 (p=0.00017), FANCJ (p=0.047), FANCL (p=0.01) and FANCI (p=0.0001).

For Disease Free survival in breast cancer, FANCB (p=0.00047), FANCC (p=0.0001), FANCI (p=0.0001) and FANCL (p=0.001).

### Comparison between METABRIC dataset and KM plotter

**Table 5-2:** FA genes significant in METABRIC and KM plotter databases

| **Overall Survival (OS)** | **p value** | **Disease Free Survival (DFS)** | **p value** |
|---|---|---|---|
| **METABRIC** | | | |
| **FANCD2** | p<0.0001 | **FANCD2** | p= 0.0002 |
| **FANCE** | p=0.0001 | **FANCE** | p=0.0010 |

| | | | |
|---|---|---|---|
| **FANCI** | p<0.0001 | **FANCI** | p<0.0001 |
| **KM PLOTTER** | | | |
| **FANCA** | p= 0.0204 | **FANCB** | p= 0.0005 |
| **FANCG** | p= 0.0046 | **FANCG** | p=0.0001 |
| **FANCD1** | p= 0.0117 | **FANCC** | p=0.0001 |
| **FANCI** | p=0.0001 | **FANCI** | p=0.0001 |
| | | **FANCL** | p=0.0001 |

Under comparison between METABRIC and KM plotter databases, FA significant genes (METABRIC) for overall survival and disease free survival were FANCD2, FANCE and FANCI.

FA significant genes (KM plotter) for overall survival and disease free survival were FANCG and FANCI.

**5.3 Pre-clinical data:**

The FANCD2 protein expression in a panel of human breast cancer cell lines was studied. The protein level of FANCD2 was examined in various breast cancer cell lines – DCIS, MCF-7 and MDA-MB-231. The relative protein level was compared with band quantification (Figure 5-4).

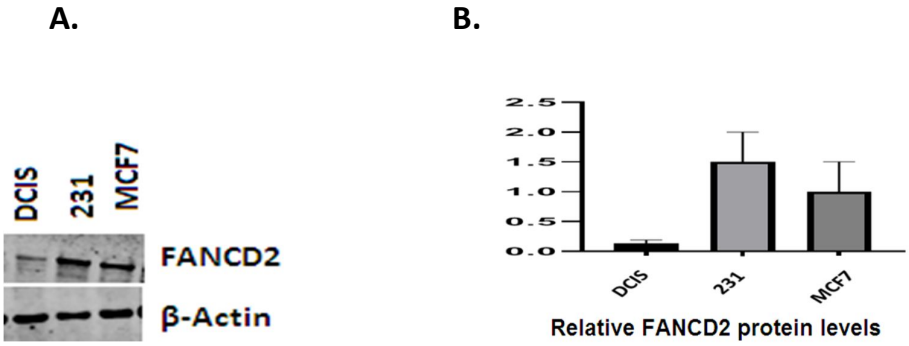


**Figure 5-4**: (A) Western blot shows FANCD2 protein expression in breast cancer cell lines (B) Relative FANCD2 protein expression level in different breast cancer cell lines. β-actin was used as a loading control.

For optimization, the primary antibody FANCD2 (rabbit-monoclonal) was checked at three different dilution factors 1:750, 1:1000 and 1:2000. The specific band for the given antibody was obtained at 1:2000. The molecular weight of FANCD2 antibody was 155kDa. The internal loading control used for the western blot was β-actin with molecular weight 42kDa. The level of FANCD2 protein was examined in different breast cancer cell lines – DCIS, MDA-MB-231 and MCF-7. The relative protein level was compared with band quantification.

Western blot analysis of FANCD2 protein levels was performed in human breast cancer cell lines. The FANCD2 protein expression was studied for detecting carcinomas characteristics. Representative results were shown. The

graph showed the quantification of FANCD2 protein levels using GraphPad Prism 8.2.0 software.

### 5.3.1 Pre and post cisplatin in breast cancer cell line.

Nuclear and cytoplasmic expressions of MCF-7 were illustrated in Figure 5-5.

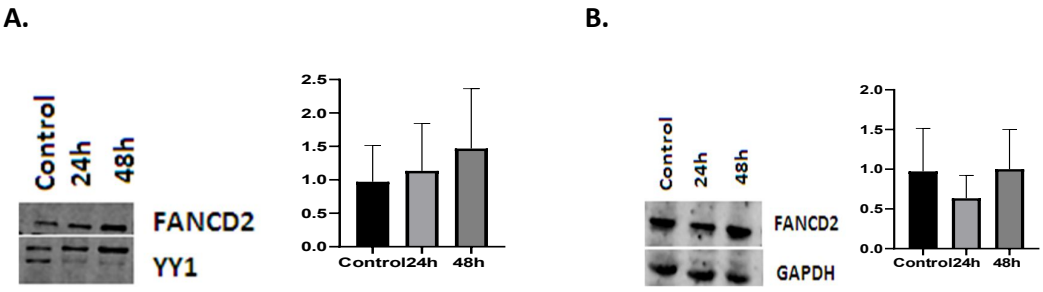


**Figure 5-5:** Nuclear and cytoplasmic expressions of MCF-7. (A) Western blot for FANCD2 expression in nuclear and cytoplasmic extracts from MCF-7 cells untreated and treated with cisplatin for 24 and 48 hours. (B) Quantification of FANCD2 protein expression by western blot. GAPDH was used as a loading control for cytoplasmic extracts and YY1 was used as the loading control for nuclear extracts.

The impact of FANCD2 protein expression was explored in breast cancer cell line MCF-7. The FANCD2 protein expression was observed at the basal levels under normal circumstances. After cisplatin treatment, FANCD2 expression was altered in breast cancer cell line after 48 hours drug treatment. Further studies are required to evaluate the role of FANCD2 in breast cancer cell lines.

### 5.3.1.1 FANCD2 siRNA in breast cancer cell line

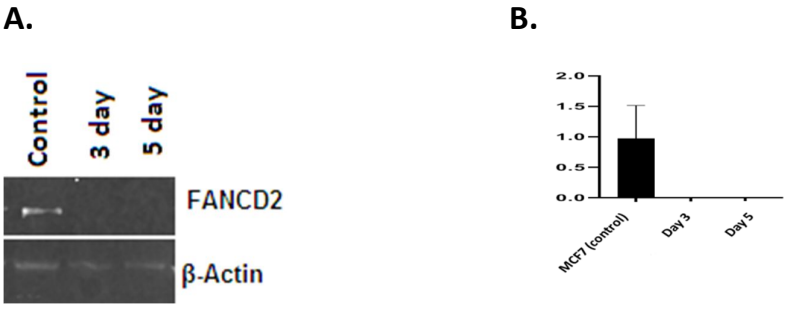


**Figure 5-6:** FANCD2 siRNA in breast cancer cell line (A) FANCD2 western blot (B) Quantification of FANCD2 protein levels relative to β-actin in MCF-7 transfected with FAND2 siRNA and negative scrambled control.

MCF-7_FANCD2_KD cells were collected at day 3 and day 5 to confirm the transfection efficiency. The quantification of FANCD2 protein levels relative to β -actin (loading control) was obtained (Figure 5-6).

### 5.3.1.2 Cisplatin and olaparib toxicity in FANCD2 deficient breast cancer cell line

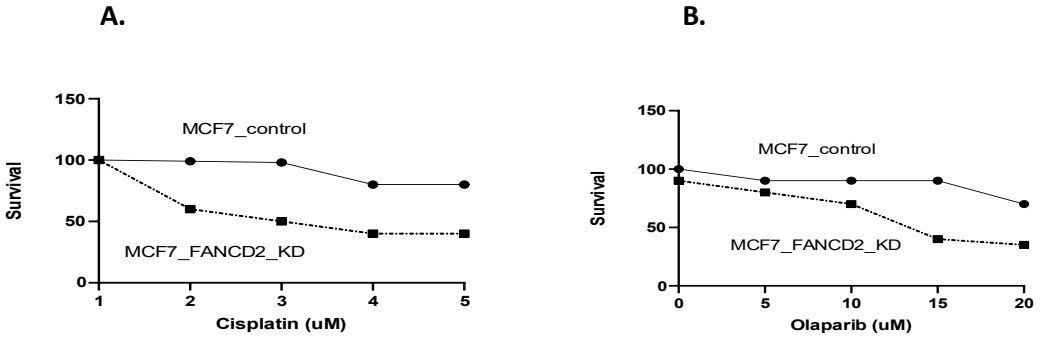


**Figure 5-7:** Cisplatin sensitivity in MCF-7 control and FAND2_KD cells. Clonogenic survival graphs (A) MCF-7 control and FANCD2 knock down cells treated at different doses of cisplatin (B) MCF-7 control and FANCD2_KD cells at different doses of olaparib.

The cells were transfected with FANCD2 siRNA or negative control in opti-mem low serum medium. Then cells were treated with cisplatin. The colonies were washed and stained.

The FANCD2 transient knockdown with siRNA was performed. The maximum FANCD2 inhibition on day 3 was achieved. Therefore, all experimental results were obtained on day 3. The FANCD2 knockdown MCF-7 cells were sensitized to cisplatin and clonogenic assay revealed higher number of cells killing in knockdown cells (Figure 5-7).

Olaparib sensitivity in the MCF-7 deficient breast cancer cell line was confirmed. FANCD2 with siRNA was depleted in a cell line and olaparib cytotoxicity in MCF-7 control and FANCD2 knockdown cells were tested by a clonogenic survival assay. MCF-7 (FANCD2_KD) was more sensitive to olaparib than the control cells.

**A.**

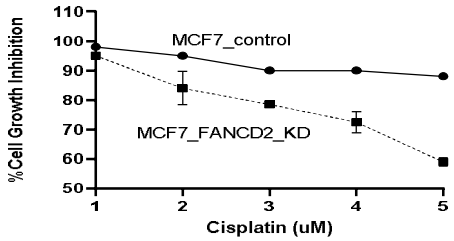


**Figure 5-8:** MTS cell growth inhibition assays of drug agent (A) MCF-7 control cells compared to FANCD2 gene knockdown MCF-7 cells.

The breast cancer cell line with FANCD2 deficiency exhibited low cell growth after treatment with cisplatin drug agent for 6 days compared to FANCD2 proficient cell lines. The data were shown as the mean and SD values for each concentration from three independent experiments.

For additional validation, the proliferation assay (MTS assay) was used to determine cell growth in response to cisplatin. As shown in the Figure 5-8, FANCD2 deficient MCF-7 breast cancer cells were more sensitive to cisplatin than the control cells.

### 5.3.1.3 Cell cycle progression in olaparib treated FANCD2 deficient cell line

MCF-7 control and its FANCD2 knockdown cells were seeded in 6-well plates overnight and treated with olaparib (10μM) for 24 hours. Then, cells were stained with propidium iodide for analysing DNA content. Observation depicted that olaparib treated FANCD2 knockdown cells were arrested in the G2/M phase.

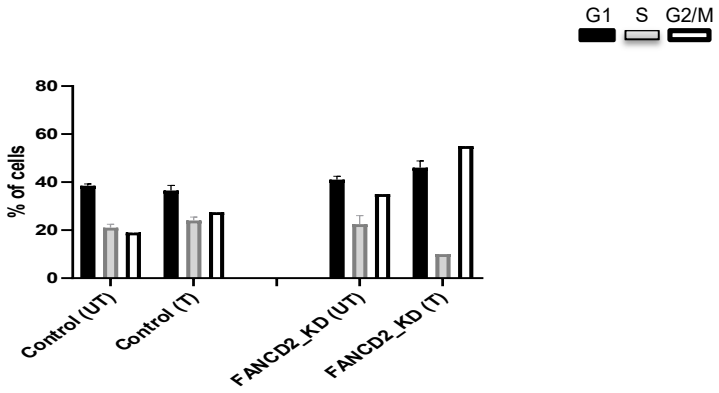


**Figure 5-9:** Functional studies of olaparib response in FANCD2 knockdown cells.

The MCF-7 control cells and FANCD2 knockdown cells were treated with 10μM olaparib for 24 hours. The cells were transfected with scrambled control or FANCD2 siRNA. On day 5, the cells were collected and stained. The flow cytometric cell cycle analysis was performed following olaparib for 24 hours. Control MCF-7 cells were compared to the treated FANCD2 knockdown cells. A

significant cell cycle arrest was observed in treated knockdown cells. In contrast, control MCF7 cells did not show the same result. The data were shown as the mean and SD values for each concentration from three independent experiments. The graphs were produced and statistical analysis performed using GraphPad Prism 8.2.0 software (Figure 5-9).

#### 5.3.1.4 Accumulation of the apoptotic cells upon drug treatment

The Annexin FITC-V/PI staining is used to quantify apoptosis. The adherent cancer cells were trypsin-digested and collected. The cells were resuspended in binding buffer, Annexin FITC-V and PI. The flow cytometric analysis depicts the percentage of apoptotic cells (Shi Y, 2014).

To investigate the accumulation of apoptotic cells upon inhibition of PARP1 activity in FANCD2 deficient cells, Annexin-V and PI staining was performed in the FANCD2 proficient and deficient cell line treated with olaparib. The results showed an accumulation of early and late apoptotic cells in FANCD2 deficient cell line treated with olaparib (Figure 5-10).

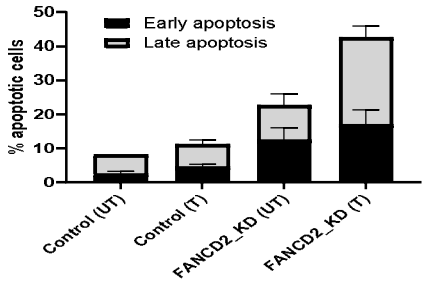


**Figure 5-10:** The percentage of apoptotic cells analysed by flow cytometry. Annexin V apoptosis assay in MCF-7 (control) and FANCD2_KD cells treated with olaparib (10μM) for 24 hours.

The apoptosis was detected by Annexin V-FITC flow cytometry after treating breast cancer cells with olaparib. The results were depicted for FANCD2 proficient and deficient cells following treatment with 10µM olaparib for 24 hours, data were normalised against baseline apoptotic fraction (untreated cells) to determine the percentage increase in apoptosis. Treatment with olaparib was associated with increase in apoptotic cells. Data were shown as the mean and SD values for each concentration from three independent experiments. Graphs were produced and statistical analysis performed using GraphPad Prism 8.2.0 software.

## 5.4 Discussion

The genomic stability in the cells is maintained by the DNA repairing systems that constitute several signalling pathways for eliminating DNA lesions. The emergence and progression of different groups of cancers including breast cancer are due to the DNA damage and non-functional components in DNA repair machinery (Majidinia M, 2017). The mechanisms of DNA repair protect the DNA from internal and external damaging factors hence the DNA integrity is maintained in the cells. The limitations or unaddressed DNA damage in repairing mechanisms result in the development of cancer for instance breast cancer (mutated BRCA1 and BRCA2). According to the recent research findings, the potential synergistic activity is suggested in the tumours retaining deficiency in one DNA repair pathway and the other active repair pathways could be inhibited for targeting tumour cell death. The homologous recombination (HR) deficient tumours can have synthetic lethality with drug inhibition of Poly ADP-ribose polymerase (PARP) enzyme, a fundamental element of the DNA repair pathway (Amir E, 2010).

The data presented here provides evidence that FANCD2 deficiency may be associated with poor prognosis in breast cancers. The HR pathway has two key proteins BRCA1 and BRCA2. A synthetic lethality approach can be attained in BRCA1 and BRCA2 mutated tumours as these can be targeted with PARP1 inhibitors (Wang Y, 2016). The functional BRCA1 and BRCA2 genes are required for repairing DNA damage which is generated after PARP1 inhibition (Farmer H, 2005). The olaparib drug is used for the treatment of advanced ovarian cancers (BRCA mutated) hence it opens a large therapeutic window for cancer treatment. The olaparib is also approved for the treatment of metastatic breast cancers (BRCA germline mutations). In current study, FANCD2 deficient

cells showed increased sensitivity of cisplatin and olaparib. Almost 25% breast cancers have non-functional FA pathway either due to FA gene mutation or silencing of FA genes (Gilmore E, 2019).These data provide preliminary evidence that FANCD2 deficient breast cancer may be suitable for a SL application using PARP inhibitors. However, detailed pre-clinical studies in additional cell line and in vivo model are required to validate the initial observation.

Targeting FANCD2 deficient tumours with DNA damage inhibitors provided a new therapeutic potential for breast cancers. The data suggested that DNA damage inhibitor in FANCD2 deficient breast cancers is an attractive therapeutic approach for personalized breast cancer treatment. The active DNA repair pathways are vulnerable to therapies and some DNA repair mechanisms can be dysfunctional in cancer cells which leave cells dependent on other remaining active pathways. Several genes participate in a complex mechanism of the Fanconi Anemia (FA) pathway and this pathway works in coordination with HR, NER and translesion synthesis for re-organising DNA replication after DNA damages (Gilmore E, 2019).

The research studies analysis (2017) demonstrates that the FANCD2 gene has the potential of breast cancer susceptibility due to FANCD2 gene mutation hence this FA gene is associated with hereditary breast carcinoma. The FA pathway allows favourable targets for breast cancer therapy; the defects in FA mechanisms cause non-effective DNA repair, tumorigenesis and genomic instability in the cells. The biological processes including DNA replication, recombination, DNA repair and chromatin remodelling demand PARPs activity. The stalled replication forks and DSBs exist in cells after SSB lesions caused by defective or inhibited PARP-1. To compensate for the loss of PARP1 activity,

cells that retain functional HR pathways are capable of repairing DSBs. Although defects in the HR system for instance in breast cancer (mutated BRCA1/BRCA2), DNA damages cannot be repaired resulting in tumour-specific cell death. This outcome is simplified by synthetic lethality interactions where one of the two genes can keep a cell viable whereas the simultaneous loss of two genes causes cell death. Breast, ovarian and other cancer (BRCA1 and BRCA2 deficient) patients are treated with PARPi effectively (Fang CB, 2020).

# 6 FANCD2 and FANCA in ovarian cancers

## 6.1 Introduction

The FA Complementation Group D2 (FANCD2) plays an important role in the HR pathway. Platinum chemotherapy produces inter-strand cross links that require FANCD2 for repair. The non-functional genes in the FA pathway may cause homologous recombination deficiency (HRD). Moreover, G2 and M phases of the cell cycle, the cell tubular system (polymerization and stabilization of β-tubulin unit) is impaired by the taxanes compound which can activate spindle assembly checkpoint (SAC). The cells develop resistance to antimitotic agents with a prolonged cell-cycle arrest which may result in apoptosis or mitotic exit by sliding into the G1 cell cycle phase. Recent research studies on cell lines demonstrate that SAC is regulated by FA genes. FANCD2 may be involved in the protection of stalled replication forks. BRCA1 and BRCA2 also interact with FANCD2 (Moes-Sosnowska J, 2019).

Ovarian cancer is often diagnosed at late stages because the early stages of this cancer characterised by a lack of specific clinical symptoms. After a diagnosis of ovarian cancer, the first treatment option is the surgical cytoreduction of the tumour followed by platinum-based chemotherapy arrangements. Currently, 47% is the survival rate for ovarian cancer for 5 years and almost 25% of patients develop platinum resistance within six months of therapy.

For repairing inter-strand crosslinks (ICLs) lesions, the functional HR pathway is essential and it is mediated by BRCA genes and Fanconi anaemia (FA) genes. FANCD2 requires nuclear localization to perform DNA repair function. The N-terminal (first 58 amino acids) domain of FANCD2 is required for nuclear localization before FANCD2 monoubiquitination (Joshi S, 2020).

The biallelic mutations in FA genes cause Fanconi anaemia (FA). Fanconi anaemia (FA) causing congenital defects, bone marrow failure and cancer predisposition. The FA genes encode DNA repair proteins in the FA pathway for maintaining the genomic integrity in cells. These FA-repairing proteins are crucial for inter-strand crosslink repair and collaborate with homologous recombination (HR) and non-homologous end joining mechanisms (Del Valle J, 2020).

Approximately 65% of FA cases have defects in the FA Complementation Group A (FANCA) gene. In response to DNA damage, FANCA and other FA gene complex compartments are required for FANCD2 ubiquitination. The process of FANCD2 ubiquitination is selected to the nuclear foci of RAD51 and BRCA1 (DNA repair proteins). This protein complex interacts with FANCD1 (FA protein), cancer (breast and ovarian) susceptibility gene, BRCA2. The alterations in FA genes are related to the development of breast and ovarian carcinoma (Thompson E, 2005). Moreover, TCGA and GTEx databases have been used for studying the differential gene expression of all FA genes considering both tumour and normal cells, the results show the overexpression of many FA genes in various cancer types. Therefore, it is observed that elevated expression of the FA gene and the potential of repairing damaged DNA are valuable for reducing DNA lesions and chromosomal abnormalities that cause high proliferation in cancer cells. According to computational studies, many genes of the FA mechanism are considered genes of interest and display the potential for synthetic lethality application (Liu W, 2020). In the current study, FANCD2 and FANCA are investigated in ovarian cancer cells.

Drug resistance is acquired following platinum drug treatment hence the research studies have demonstrated multiple mechanisms of resistance. The

DNA platinum adducts are recognised and eliminated by several DNA repair mechanisms. The potential biomarkers for drug resistance in cancer cells are explained by gene mutations and polymorphisms in DNA repair pathways. To improve the outcome of cancer patients and find ways to control drug resistance, it is vital to interpret the different mechanisms of drug resistance accurately along with the development of suitable models. The DNA damage response (DDR) is activated after DNA damage leading to the interruption of DNA synthesis, cell cycle and DNA repair pathways. These pathways are key components of DDR and competent in managing genomic integrity in the cells (Damia G, 2019).

## 6.2 Results

### 6.2.1 Fanconi anemia gene expression analysis using Kaplan–Meier plotter (KM plotter) database for survival analysis.

Using Kaplan Meier plotter portal for ovarian cancer, all Fanconi anemia DNA repair genes (22) were studied for overall (OS) and progression free survival (PFS). A p- value significant table was drawn for ovarian cancer. The Kaplan Meier plotter was a useful tool for evaluating the correlation between the genes expression (mRNA) and patient survival in different tumour types including ovarian carcinoma. The number of ovarian cancer patients used for the analysis of genes was 1435 and the survival curves were generated. The overall survival and progression free survival of ovarian cancer patients using KM plotter were summarised in Table 6-1.

**Table 6-1:** Overall survival and progression free survival of ovarian cancer patients using KM plotter

| Fanconi anemia genes | Overall survival (OS) p-value | Progression free survival (PFS) p-value |
|---|---|---|
| FANCA | 0.2371 | 0.0209 |
| FANCB | 0.1622 | 0.1443 |
| FANCC | 0.0288 | 0.0075 |
| FANCD1 | 0.0264 | 0.0152 |
| FANCD2 | 0.0034 | 0.0001 |
| FANCE | 0.0428 | 0.0304 |
| FANCF | 0.0216 | 0.0542 |
| FANCG | 0.0051 | 0.0061 |

| | | |
|---|---|---|
| FANCI | 0.0997 | 0.3547 |
| FANCJ | 0.0267 | 0.0001 |
| FANCL | 0.0629 | 0.0001 |
| FANCM | 0.124 | 0.167 |
| FANCN | 0.0571 | 0.1887 |

### 6.2.1.1 Ovarian cancer survival curves using KM plotter database

The ovarian cancer survival curves were studied by using KM plotter database (Figure 6-1).

**Overall survival**

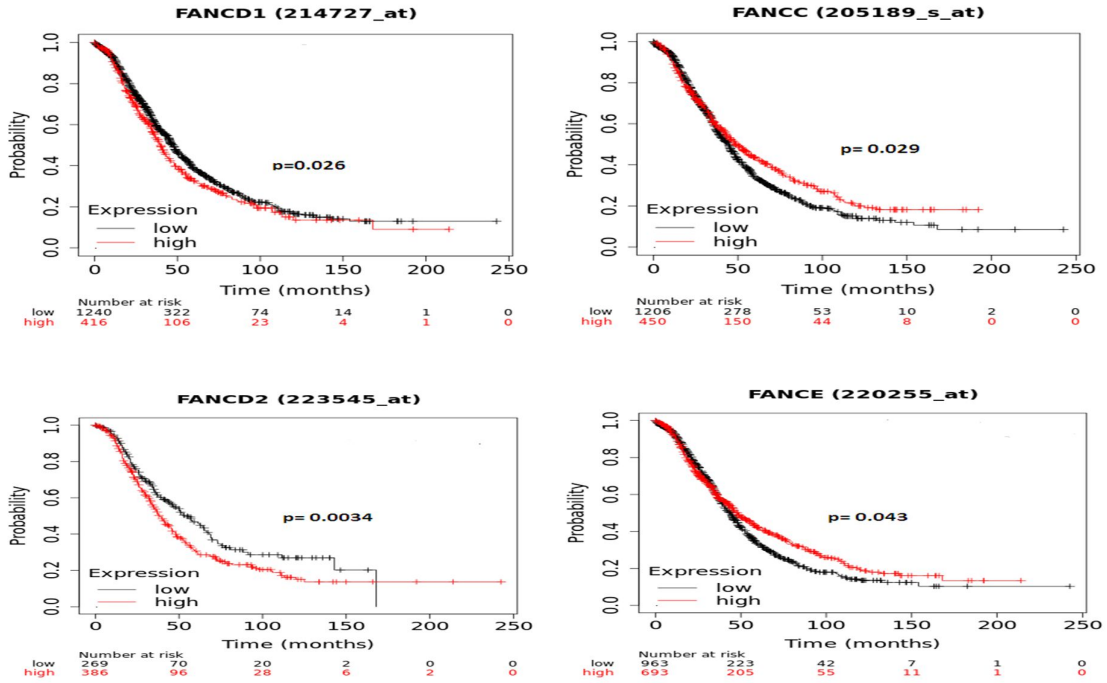

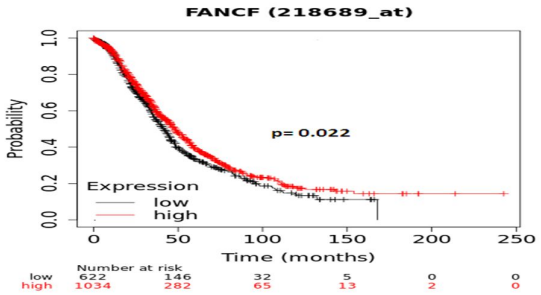


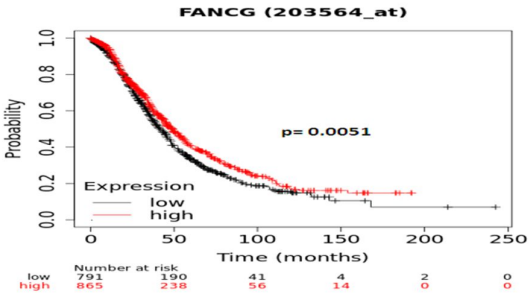


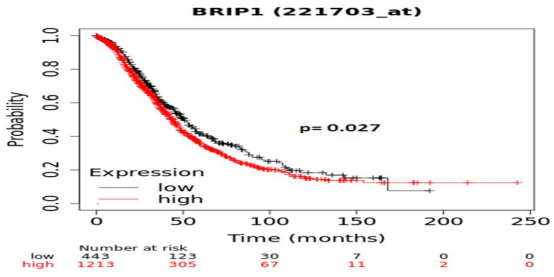


## Progression Free Survival (PFS)

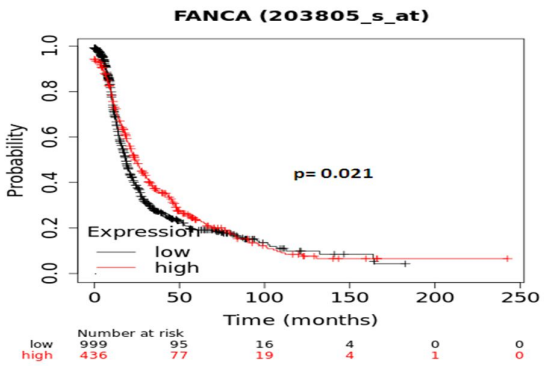


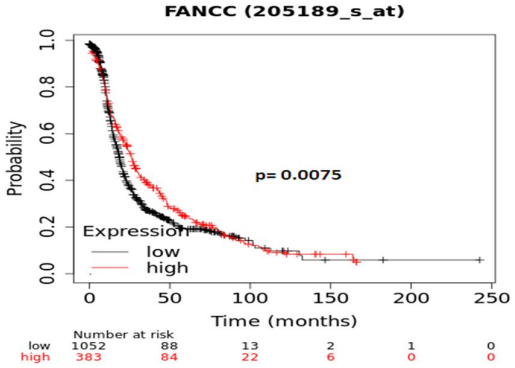


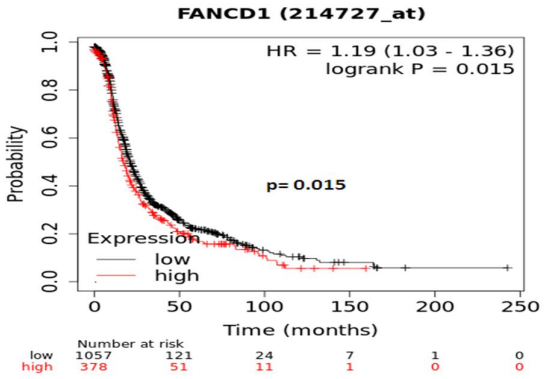


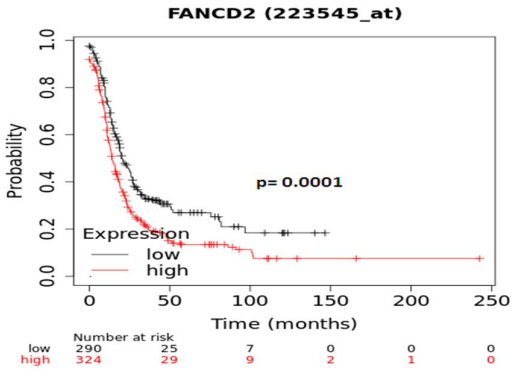

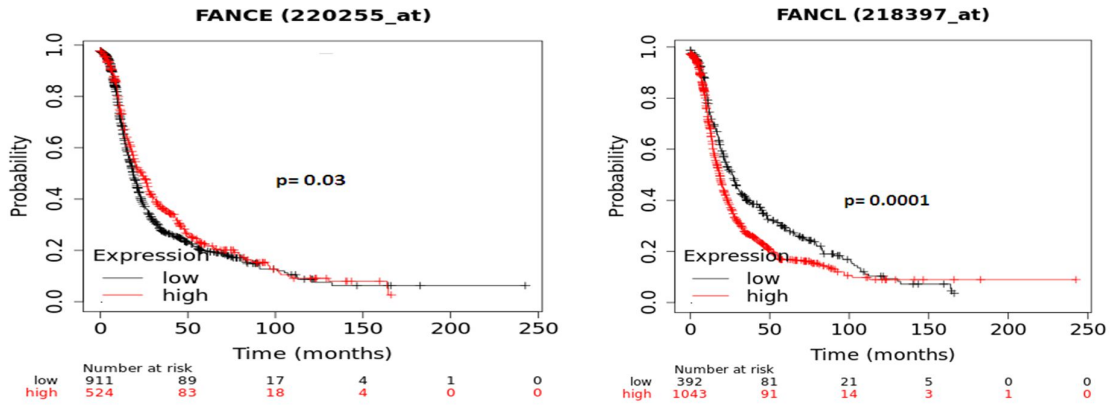


**Figure 6-1:** Ovarian cancer survival curves using KM plotter database.

The ovarian cancer patient survival analysis was associated with the expression of fanconi anemia genes and the survival curves were studied using Kaplan–Meier plotter (KM plotter) database. The survival curves of overall survival (OS) and progression free survival (PFS) of ovarian cancer patients were generated by Kaplan Meier plotter portal.

Under KM plotter database, the significant p-values were obtained of various FA genes for overall survival in ovarian cancer including FANCD1 (p=0.026), FANCC (p=0.029), FANCD2 (p=0.0034), FANCE (p=0.043), FANCF (p=0.022), FANCG (p=0.0051) and BRIP1 (p=0.027).

For progression free survival (PFS) in ovarian cancer, FANCA (p=0.021), FANCC (p=0.0075), FANCD1 (p=0.015), FANCD2 (p=0.0001), FANCE (p=0.03) and FANCL (p=0.0001).

### 6.3 Pre-clinical Data

#### 6.3.1 FANCD2 expression in ovarian cancer cell lines

**A.** **B.**

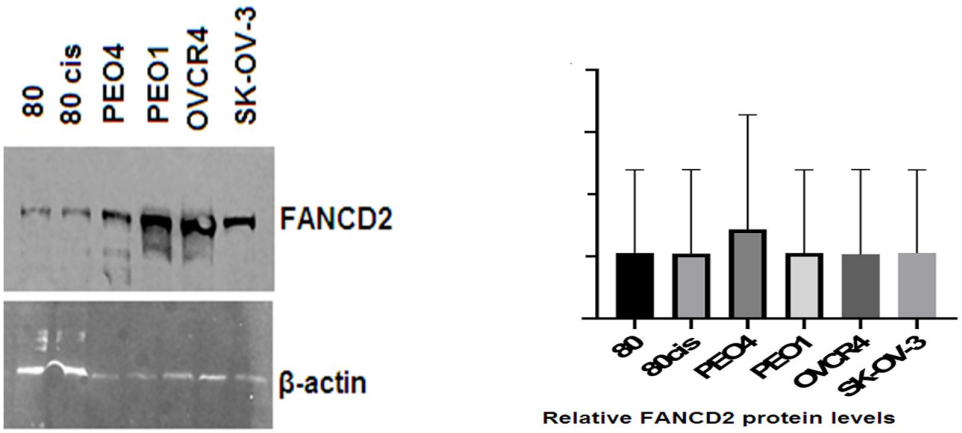


**Figure 6-2:** FANCD2 protein expression in ovarian cancer cell lines (A) Western blot showing FANCD2 protein expression in ovarian cell lines (B) Relative FANCD2 protein expression level in different ovarian cancer cell lines. β-actin was used as a loading control.

For optimization, the primary antibody FANCD2 (rabbit) was checked at three different dilution factors 1:750, 1:1000 and 1:2000. The specific band for the given antibody was obtained at 1:2000. The molecular weight of the primary antibody was 155kDa. The internal loading control used for the western blot was β-actin (mouse) with molecular weight 42kDa. The western blot analysis was performed for FANCD2 protein expression. The level of FANCD2 protein was examined in various ovarian cancer cell lines- PEO1, PEO4, A2780, A2780cis, SK-OV-3 and OVCR-4. The relative FANCD2 protein levels (ratio of protein/ β-actin) were compared with band quantification using GraphPad Prism 8.2.0 software (Figure 6-2).

### 6.3.1.1 Pre and post cisplatin in ovarian cancer cell lines

**A. PEO4**

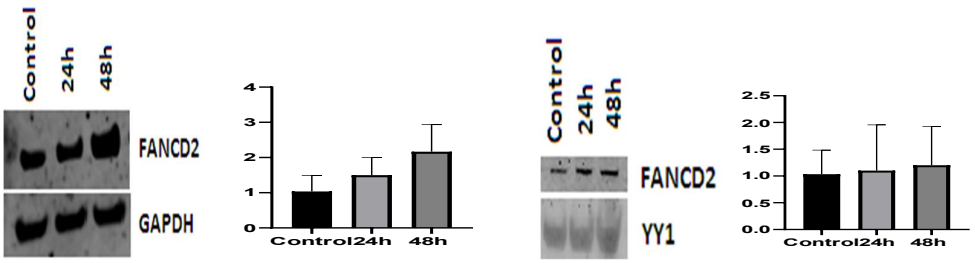


**B. PEO1**

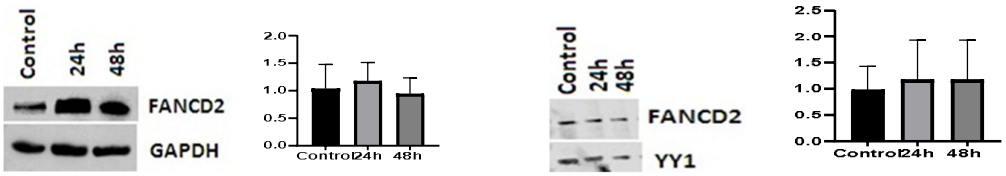


**Figure 6-3:** Pre and post cisplatin in ovarian cancer cell lines.

To investigate the influences of FANCD2 expression in the ovarian cancer cell lines, PEO4 and PEO1 cell line models were used. At the basal levels, ovarian cancer cell lines showed FANCD2 protein expression. Interestingly, the induction of FANCD2 expression was observed in cisplatin treated cell lines after 48 hours cisplatin treatment (Figure 6-3). The results indicated that FANCD2 expression can be induced upon platinum treatment.

In cisplatin-resistant ovarian cancer cell lines, the molecular pathways and the associated mechanisms after cisplatin exposure need to be examined in details. The kinetics of gene expression variations can be studied in both cisplatin-sensitive and resistant cell lines. The FANCD2 protein expression was affected after cisplatin treatment at different intervals of time. Further research studies can be conducted to explore the effects of platinum treatment in these malignant cells.

### 6.3.1.2 FANCD2 siRNA knock-down in PEO1and PEO4 cell lines

**A. PEO1**

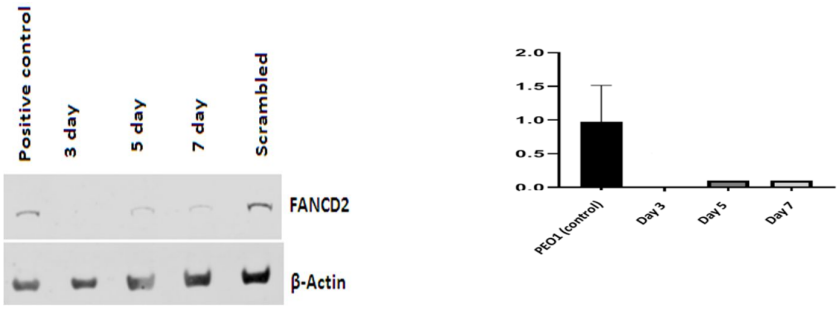


**B. PEO4**

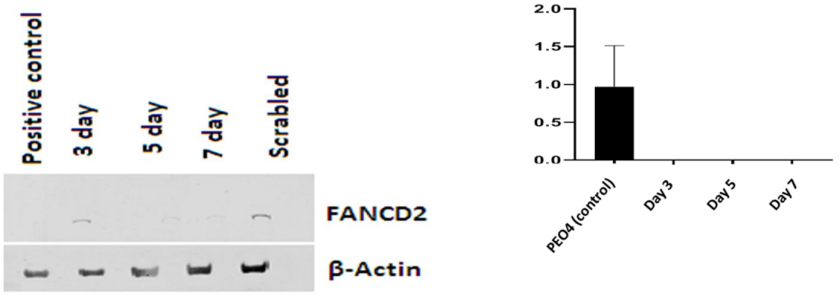


**Figure 6-4:** FANCD2 siRNA knock-down (A) FANCD2 siRNA western blot and quantification of FANCD2 protein levels relative to β-actin in PEO1 ovarian cancer cell line, transfected with negative scrambled control and FANCD2 siRNA. PEO1_FANCD2_KD cells were lysed at day 3, day 5 and day 7 to confirm transfection efficiency. (B) FANCD2 siRNA western blot and quantification of FANCD2 protein levels relative to β-actin in PEO4, transfected with negative scrambled control and FANCD2 siRNA. Knock down cells were lysed at day 3, day 5 and day 7 to confirm transfection efficiency.

The FANCD2 mRNA was targeted for its degradation by inducing sequence-specific gene silencing. The knockdown or specific inhibition of FANCD2 gene in cultured ovarian cancer cell lines was performed. The cell lysates were collected for a western blot on day 3, day 5 and day 7. The quantification of

FANCD2 protein levels relative to β -actin (loading control) was obtained (Figure 6-4).

### 6.3.1.3 Cisplatin and olaparib are toxic in FANCD2 deficient ovarian cancer cell lines

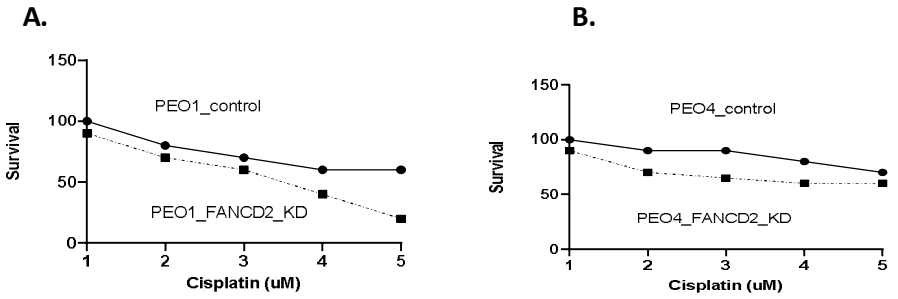


**Figure 6-5:** Cisplatin sensitivity in control along with FANCD2_KD cells of PEO1 and PEO4 ovarian cancer cell lines (A) Clonogenic survival assay showing cisplatin sensitivity in PEO1 control and PEO1_FANCD2_KD cells. (B) Clonogenic survival assay for PEO4 control and PEO4_FANCD2_KD cells at different doses of cisplatin.

Ovarian cancer cell lines were transfected with FANCD2 siRNA or negative control. Then cells were treated with the indicated doses of cisplatin. Colonies were washed and stained.

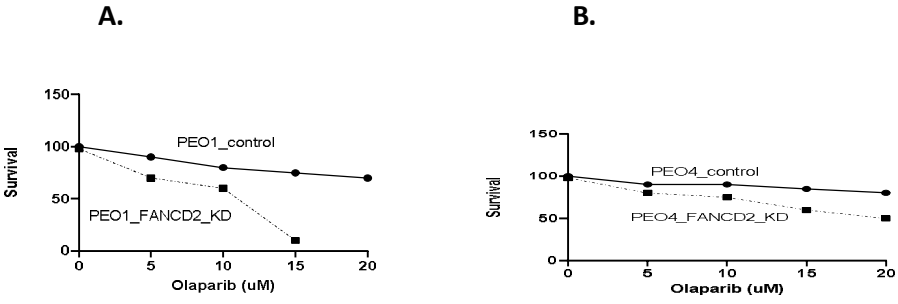


**Figure 6-6:** Clonogenic survival assay for olaparib in ovarian cancer cell lines. (A) Clonogenic survival graph of olaparib sensitivity in PEO1 and

PEO1_FANCD2_KD cells (B) Clonogenic survival graph for PEO4 and PEO4_FANCD2_KD cells at different doses of olaparib.

A cell survival curve defines a correlation between the amount of the agent and the number of cells that have the potential to proliferate. These graphs are meant to explore the effects of chemotherapy agents along with its potential applications in the clinic. One of the major applications of the survival curves is to check the proliferative capacity of distinct cells in the tissue culture system using ovarian cancer cell lines (Munshi A, 2005).

As FANCD2 knock-down was performed in ovarian cancer cell lines, it was speculated that cisplatin can induce toxicity in FANCD2 deficient ovarian cells. Therefore, drug sensitivity was tested in FANCD2_KD PEO1 and PEO4 cells in a clonogenic survival assay. Increased cytotoxicity in PEO1 (FANCD2_KD) cells was observed in comparison to FANCD2-depleted PEO4 cells (Figure 6-5). This suggested more sensitivity to the drug in cisplatin-sensitive cells. Cisplatin sensitivity in PEO1 and PEO4 control cells was confirmed. As previously published PEO1 cells were more sensitive to cisplatin than PEO4 cells (Roberts D., 2005).

Olaparib sensitivity was confirmed in FANCD2 deficient ovarian cancer cell lines. PEO1 cells were drug sensitive in comparison to PEO4 cells. FANCD2 was depleted by using siRNA in both ovarian cancer cell lines PEO1 and PEO4. Olaparib cytotoxicity in control and FANCD2 knockdown cells was tested by a clonogenic survival assay (Figure 6-6). PEO1 (FANCD2_KD) was more sensitive to olaparib than the control cells which emphasized the same results in other ovarian cancer drug sensitive cell lines.

The clonogenic survival assays of cisplatin and olaparib were studied. The ovarian cancer cell lines with reduced FANCD2 expression exhibited low colony

forming ability after treatment with drugs for 14 days compared to FANCD2 proficient cell lines. Clonogenic data were shown as the mean and SD values for each concentration from three independent experiments.
FANCD2 knockdown ovarian cancer cell lines along with control cells were treated with increasing concentration of drugs. Clonogenic survival assay results were shown in figures.

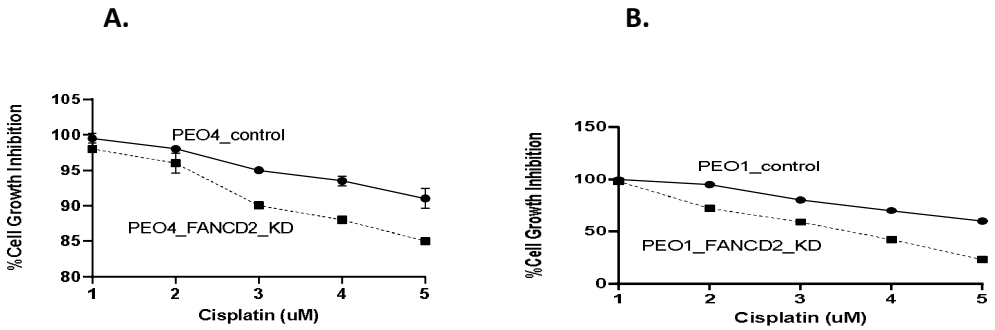


**Figure 6-7:** MTS cell growth inhibition assays of drug. (A) PEO4 control cells compared to FANCD2 knockdown PEO4 cells. (B) PEO1 control cells compared to FANCD2 knockdown PEO1 cells.

FANCD2 deficient cells were more sensitive to drug than the control cells. Cell lines with depleted FANCD2 expression exhibited low cell growth after treatment with cisplatin drug for 6 days compared to FANCD2 proficient cell lines. Data were shown as the mean and SD values for each concentration from three independent experiments.

For additional validation, the proliferation assay (MTS assay) was used to determine cell growth in response to cisplatin. As shown in the Figure 6-7, FANCD2 deficient PEO1 ovarian cancer cells were more sensitive to cisplatin than the control PEO1 cells. Similar sensitivity was demonstrated in FANCD2 knockdown PEO4 cells compared to control cells.

### 6.3.1.4 Cell cycle progression in FANCD2 deficient cell line upon olaparib treatment

Olaparib drug has been approved as personalized therapy for patients with BRCA1/2-mutated advanced ovarian cancer. PARPi modulates the AKT activation and downstream molecules causing apoptosis. In PARPi-treated cells, activated caspase-3 protein and low expression of phospho-AKT and Bcl2 proteins are observed. The molecular mechanisms of PARPi can influence the cell cycle process. Cell cycle progression is driven by the cellular regulations of certain proteins like cyclin D1 expression, p21 cell cycle regulator, cdc25C, cdc2 and cyclin B1 levels (Camero S, 2019).

Therefore, the effect of olaparib treatment on cell cycle progression was investigated. Control cells along with FANCD2 knockdown cells of PEO1 and PEO4 were treated with olaparib (10μM) for 24 hours. Then, cells were stained with propidium iodide (PI) for analysing DNA content. Observation depicted that olaparib treated FANCD2 knockdown cells were arrested in the G2/M phase (Figure 6-8).

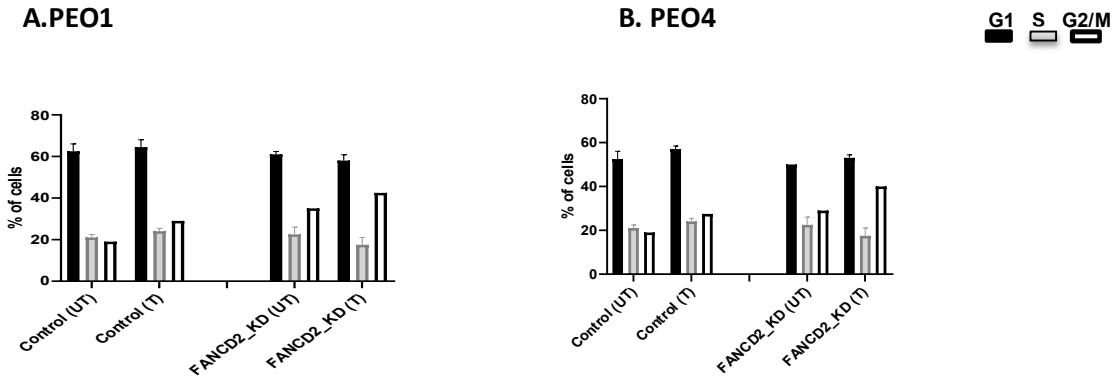


**Figure 6-8:** Functional studies of olaparib response in FANCD2 knockdown cells.

Cell cycle analysis performed using flow cytometry in (A) PEO1 control and FANCD2 knockdown cells (B) PEO4 control and FANCD2 knockdown cells.

The cells were treated with 10μM olaparib for 24 hours. Cells were transfected with scrambled control or FANCD2 siRNA. On day 5, the cells were collected and stained. The control cells were compared to its FANCD2_ KD cells.

Results for FANCD2 proficient and deficient ovarian cancer cells following olaparib treatment were shown in Figure 6-8. The data demonstrated cell cycle arrest in olaparib treated FANCD2 knockdown cells compared to untreated cells. Data were shown as the mean and SD values for each concentration from three independent experiments. The graphs were produced and statistical analysis performed using GraphPad prism 8.2.0 software.

#### 6.3.1.5 Accumulation of apoptotic cells upon olaparib treatment

For anticancer therapy, targeting the apoptotic pathways for cell death is a promising approach. In cancer, the expressions of apoptotic proteins may influence apoptosis. New anticancer therapies are studied that involve the activation of apoptotic pathways (Pfeffer CM, 2018).
DNA repairing single-strand breaks (SSBs) require the enzymatic activity of Poly (ADP-ribose) polymerases (PARPs). PARP inhibitors (PARPi) increase the accumulation of SSBs and DNA double-strand breaks (DSBs) which results in DNA replication stress and genomic instability.
The olaparib (PARPi) has been studied in combination with other drugs previously for the treatment of ovarian cancer. It confirms that olaparib and drug combination treatment suppressed cell proliferation and increased cell apoptosis in ovarian cancer cells. Olaparib promotes DNA damage-mediated cell apoptosis (Tang S, 2022).

To investigate the accumulation of apoptotic cells upon inhibition of PARP1 activity in FANCD2 deficient cells, Annexin-V and PI staining was performed for the FANCD2 proficient and deficient cell lines treated with the drug. The results showed an accumulation of early and late apoptotic cells in FANCD2 deficient cell lines treated with drug (Figure 6-9).

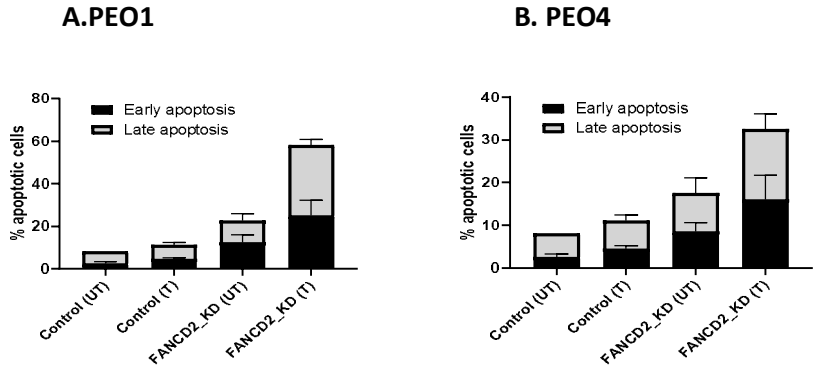


**Figure 6-9:** The percentage of apoptotic cells analysed by flow cytometry. Annexin V apoptosis assay (A) PEO1 (control) and FANCD2_KD cells (B) PEO4 (control) and FANCD2_KD cells treated with olaparib (10μM) for 24 hours.

The percentage of apoptotic cells was detected by Annexin V-FITC flow cytometry after treatment with olaparib. Following evaluation of cell growth inhibition in FANCD2 deficient cells, Annexin V was used in conjunction with a propidium iodide (PI) to identify the apoptotic cells. The apoptosis process could be the cause of low survival observed in FANCD2 knockdown cells in the clonogenic survival assay. Cells were treated for 24 hours with 10μM olaparib. The increase in apoptotic cells was evident after 24 hours in FANCD2 deficient cells treated with olaparib compared to control cells.

Results for FANCD2 proficient and deficient ovarian cancer cells following treatment with olaparib (10μM) for 24 hours were shown in Figure 6-9, data

were normalised against baseline apoptotic fraction (untreated cells) to determine the percentage increase in apoptosis. Data were shown as the mean and SD values for each concentration from three independent experiments. The graphs were produced and statistical analysis performed using GraphPad Prism 8.2.0 software.

## 6.4 Results

### 6.4.1 Pre-clinical data for FANCA

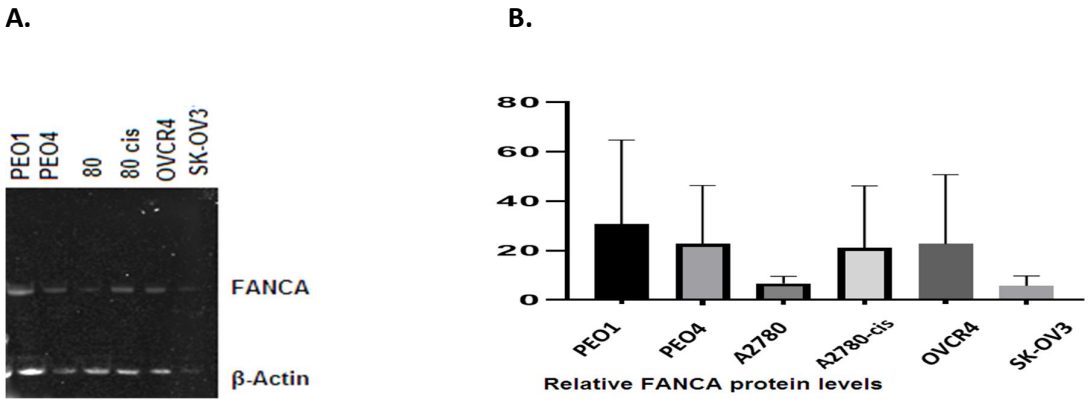


**Figure 6-10:** FANCA protein expression in ovarian cancer cell lines (A) Western blot shows FANCA protein expression in PEO1, PEO4, A2780, A2780-cis, OVCAR-4 and SK-OV3 (B) Relative FANCA protein expression level in different ovarian cancer cell lines. β-actin was used as a loading control.

For optimization, the primary antibody FANCA (rabbit-monoclonal) was checked at three different dilution factors 1:750, 1:1000 and 1:2000. The specific band for the given antibody was obtained at 1:1000. The molecular weight of the primary antibody was 161kDa. The internal loading control used for the western blot was β -actin with molecular weight 42kDa. The level of FANCA protein was examined in the ovarian cancer cell lines – PEO1, PEO4, A2780, A2780-cis, OVCAR-4 and SK-OV3. The relative protein level was compared with band quantification (Figure 6-10).

The protein expression of FANCA was determined in ovarian cancer cell lines by western blotting. Whole cell protein lysates were collected for each cell line and samples were separated by electrophoresis. Quantification of protein expression (ratio of protein/β-actin) was shown in Figure 6-10.

### 6.4.1.1 Pre and post cisplatin in ovarian cancer cell lines

**A. PEO4**

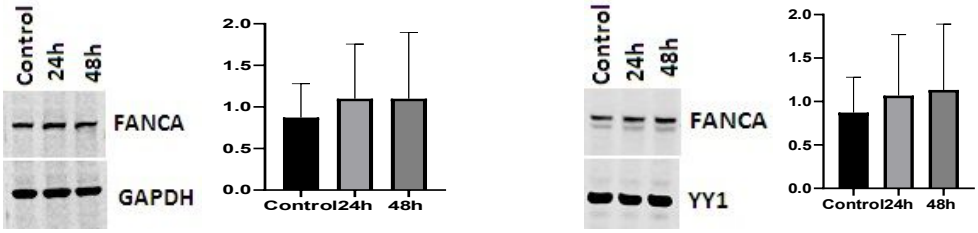


**B. PEO1**

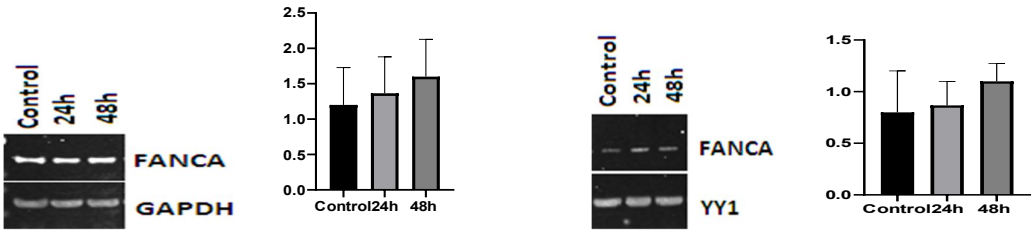


**Figure 6-11:** Pre and post cisplatin in ovarian cancer cell lines.

Ovarian cancer cell lines PEO4 and PEO1 were used to investigate the influence of FANCA expression. At the basal levels, ovarian cancer cell lines showed FANCA protein expression. Interestingly, upon cisplatin treatment induction of FANCA protein expression in cisplatin-treated cell lines was found after 48 hours of treatment (Figure- 6-11). The results indicated that FANCA expression can be induced upon platinum treatment.

In cisplatin-resistant ovarian cancer cell lines, increased interstrand cross-link repair (ICL repair) in response to platinum chemotherapy has been observed. In a recent study, it has been indicated that in chemoresistant cell lines, the cancer cells with FA pathway deficiency have ability to remove methylated modification from promoter sites of FA genes and acquire reversal mutations to re-establish DNA repair pathway function and promote cell survival (Taylor SJ, 2020).

### 6.4.1.2 FANCA siRNA in ovarian cancer cell lines

**PEO1**

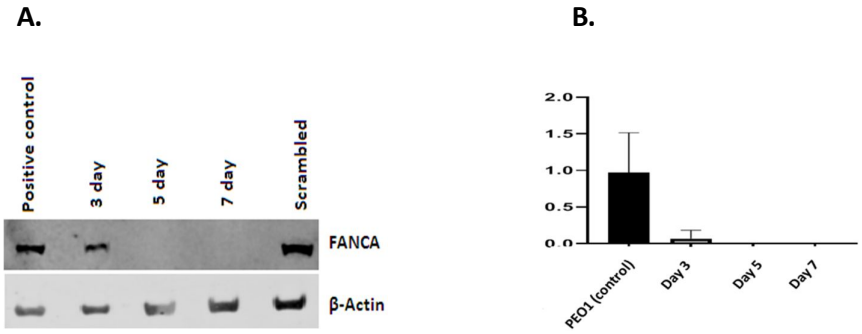


**Figure 6-12**: FANCA siRNA knockdown (A) FANCA siRNA western blot (B) Quantification of FANCA protein levels relative to β-actin in PEO1 cell line transfected with negative scrambled control and FANCA siRNA. PEO1_FANCA_KD cells were lysed at day 3, day 5 and day 7 to confirm transfection efficiency.

**PEO4**

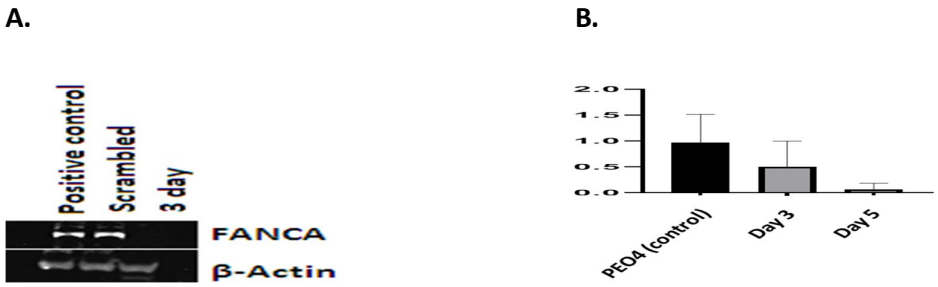


**Figure 6-13:** FANCA siRNA in ovarian cancer cell line (A) FANCA siRNA western blot (B) Quantification of FANCA protein levels relative to β-actin in PEO4 cell line transfected with negative scrambled control and FANCA siRNA.

The cells were transfected with FANCA siRNA. The FANCA protein levels relative to β-Actin (loading control) were quantified in the PEO4 ovarian cancer cell line. To explore further the implication of FANCA deficiency in ovarian cancer, siRNA studies in ovarian cancer cell lines were conducted (Figure 6-12).

The PEO1 (cisplatin sensitive) and PEO4 (cisplatin-resistant) cell lines were used (Figure 6-13). The efficient FANCA siRNA knockdown was achieved on day 3 and day 5 in the tested cell lines.

### 6.4.1.3 Cisplatin and olaparib are toxic in FANCA deficient ovarian cancer cell lines

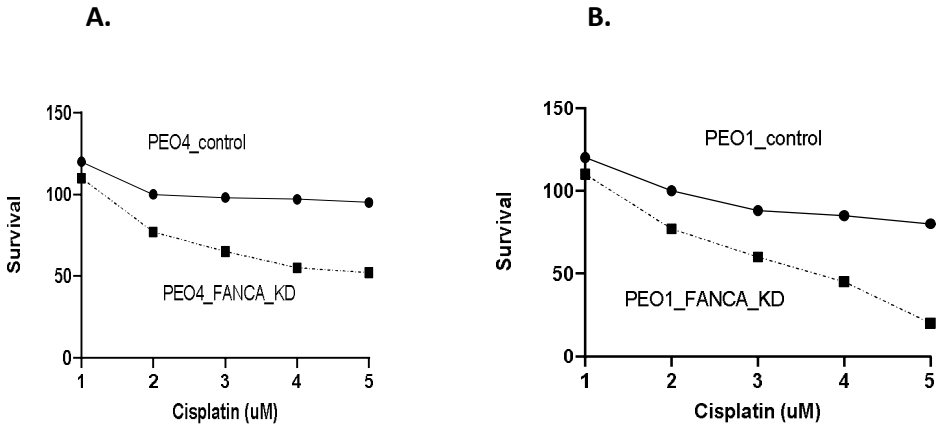


**Figure 6-14:** Clonogenic survival assay for cisplatin in ovarian cancer cell lines. Clonogenic survival assay (A) PEO4 control and PEO4_FANCA_KD cells (B) PEO1 control and PEO1_FANCA_KD cells at different doses of cisplatin.

The cells were transfected with FANCA siRNA for 24hrs. On day 2, cells were re-plated at 1000 cells/well cell density. The colonies were fixed, stained and counted.

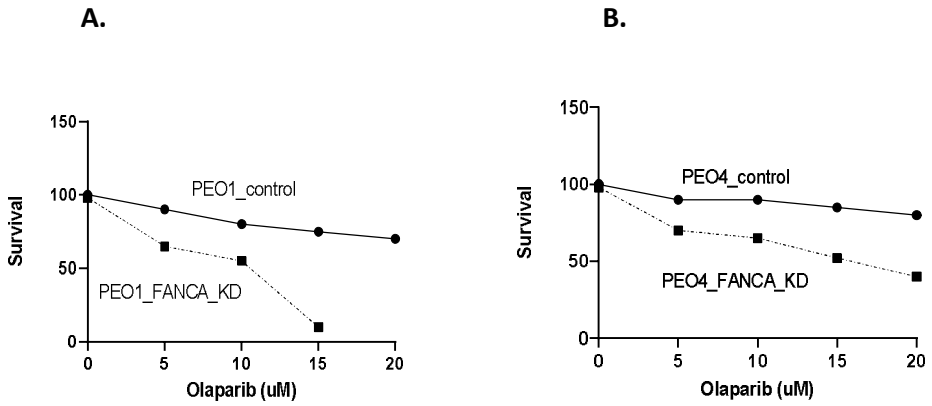


**Figure 6-15:** Clonogenic survival assay for olaparib in ovarian cancer cell lines. Clonogenic survival graphs (A) PEO1 control and PEO1_FANCA_KD cells (B) PEO4 and PEO4_FANCA_KD cells treated at different doses of olaparib.

The olaparib sensitivity was tested in PEO1 and PEO4 ovarian cancer cell lines and its successive FANCA gene knockdown cells. A cell survival curve defines a correlation between the amount of the agent and the number of cells that have the potential to reproduce. These graphs are meant to explore the effects of chemotherapy agents along with its potential applications in the clinic. One of the major applications of the survival curves is to check the reproductive capacity of distinct cells in tissue culture system using ovarian cancer cell lines (Munshi A, 2005).

As FANCA knock-down was performed in ovarian cancer cell lines, a hypothesis was tested that cisplatin can induce toxicity in FANCA deficient ovarian cells. Therefore, drug sensitivity was investigated in control, FANCA_KD PEO1 and PEO4 cells in a clonogenic survival assay. Increased cytotoxicity in PEO1 (FANCA_KD) cells was observed in comparison to FANCA-depleted PEO4 cells (Figure 6-14). As previously published PEO1 cells were more sensitive to cisplatin than PEO4 cells (Roberts D., 2005).

Clonogenic survival assay was performed to test whether FANCA deficient cells were sensitive to cisplatin and olaparib. FANCA knockdown ovarian cancer cells along with control cells were treated with increasing concentrations of drugs. The clonogenic survival assay result demonstrated that FANCA knockdown cells were more sensitive to cisplatin and olaparib compared to control cells (Figure 6-15).

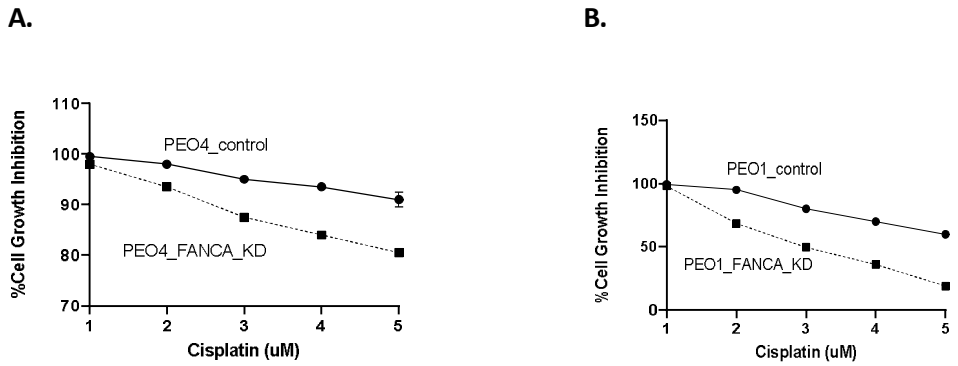


**Figure 6-16:** MTS cell growth inhibition assay of inhibitor (A) PEO4 control cells compared to FANCA knockdown (KD) PEO4 cells (B) PEO1 control cells are compared to FANCA knockdown (KD) PEO1 cells.

The data were shown as the mean and SD values for each concentration from three independent experiments. The cell lines with FANCA deficiency exhibited low cell growth after treatment with cisplatin drug for 6 days compared to FANCA proficient cell lines. For additional validation, the proliferation assay (MTS assay) was used to determine cell growth in response to cisplatin. As shown in the Figure 6-16, FANCA deficient PEO1 ovarian cancer cells were more sensitive to cisplatin than the control PEO1 cells. Similarly, the cell sensitivity was demonstrated in FANCA knockdown (KD) PEO4 cells compared to its control cells.

FANCA knockdown ovarian cancer cells were more sensitive to drug than control cells. FANCA deficient cells exhibited low cell growth after exposure to drug compared to FANCA proficient ovarian cancer cell lines.
As clonogenic cell survival assay showed FANCA knockdown cells were more sensitive to drug than control cells. Similar sensitivity was also demonstrated in FANCA knockdown cells compared to control cells in MTS assay results. Taken together, the data showed that FANCA deficient cells were sensitive to drug.

### 6.4.1.4 Olaparib affects cell cycle progression in FANCA deficient cell line

PEO1 and PEO4 control cells along with FANCA knockdown cells were treated with olaparib (10μM) for 24 hours. Then, the cells were stained with propidium iodide for analysing the DNA content. Observation depicted that olaparib treated FANCA knockdown cells were arrested in the G2/M phase.

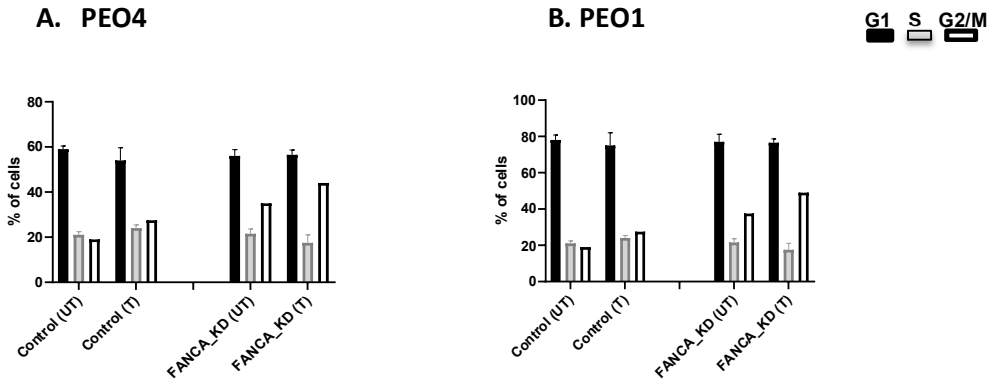


**Figure 6-17:** Functional studies of olaparib response in FANCA knockdown cells. Cell cycle analysis by flow cytometry (A) PEO4 control and FANCA knockdown cells (B) PEO1 control and FANCA knockdown cells treated with 10μM olaparib for 24 hours.

The cells were transfected with scrambled control and FANCA siRNA. The cells were treated with 10μM olaparib. On day 5, the cells were collected and stained.

Flow cytometric cell cycle analysis following olaparib treatment was performed. FANCA knockdown treated cells were compared to its respective control cells. Cells treated with 10μM olaparib showed cell cycle arrest in treated FANCA deficient cells compared to untreated cells. Data were shown as the mean and SD values for each concentration from three independent experiments. The graphs were produced and statistical analysis performed using GraphPad Prism 8.2.0 software (Figure 6-17).

### 6.4.1.5 Accumulation of the apoptotic cells upon olaparib treatment

To investigate the accumulation of apoptotic cells upon inhibition of PARP1 activity in FANCA deficient cells, Annexin-V and PI staining was performed for the FANCA proficient and deficient cell lines treated with the drug. The results showed an accumulation of early and late apoptotic cells in FANCA deficient cell lines treated with drug (Figure- 6-18).

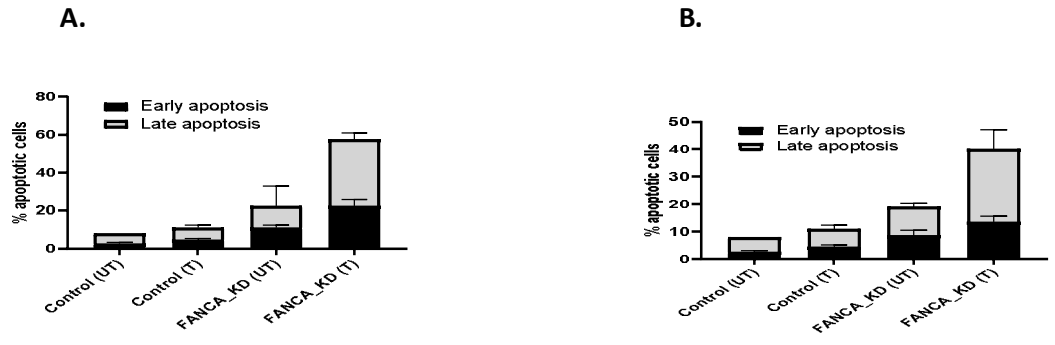


**Figure 6-18:** The percentage of apoptotic cells analysed in (A) PEO1 and (B)

PEO4 by flow cytometry. Annexin V apoptosis assay in PEO1 and PEO4 cells (control) and FANCA_KD treated with olaparib (10μM) for 24 hours.

Apoptosis was detected by Annexin V-FITC flow cytometry in response to olaparib. Treatment with olaparib was associated with increase in apoptotic cells. Data were normalised against baseline apoptotic fraction to determine the percentage increase in apoptosis. FANCA knockdown ovarian cancer cells were compared to its respective control cells. Data were shown as the mean and SD values for each concentration from three experiments. Graphs were produced and statistical analysis performed using GraphPad Prism 8.2.0 software.

## 6.5 Discussion

FANCD2 has a role during homologous recombination (HR) pathway (Moes-Sosnowska J, 2019). In the current study, FANCD2 expression was first analysed at the mRNA level. It was observed that high FAND2 transcript was associated with poor survival outcomes suggesting a role as predictive or prognostic factor. According to previous research studies on colorectal cancer the overexpression of FANCD2 is connected with poor prognosis in cancer patients (Joshi S, 2020). In the ovarian cancer cell lines, the upregulation of FANCD2 expression was more in cisplatin-resistant cells (PEO4) than in PEO1 control cells. The cisplatin treatment induced FANCD2 expression at mRNA levels and protein levels. The nuclear and cytoplasmic extraction showed induction of FANCD2 expression in the ovarian cancer cell lines treated with cisplatin after 24 hours and 48 hours of treatment. The data from this study and previous studies suggested that FANCD2 had a role in the platinum response.

The first line of therapy for ovarian cancer treatment is platinum based (Van Zyl B, 2018). The tumour resistance and recurrence of a disease is a considerable challenge in ovarian cancer due to the origin of an intrinsic and extrinsic resistance mechanism in cancer cells. The platinum DNA adducts (intra-strand cross-links) are produced with cisplatin target therapy. As a result, nucleotide excision repair pathway (NER) is activated following the DNA lesion 1, 2-d (GpG) formed by cisplatin (Iwatsuki M,, 2009). The DNA adducts and interstrand cross-links (ICLs) are also created by the platinum compounds. Therefore, HR and FA pathways are involved in the repair of platinum induced DNA damage (Moes-Sosnowska J, 2019).

This study revealed that FANCD2 depletion by siRNA sensitized ovarian cancer cells increased sensitivity to cisplatin and olaparib. The data suggested the role of FANCD2 in cisplatin resistance mechanisms. The olaparib was toxic in

FANCD2 deficient cells compared to control cells. The nuclear and cytoplasmic localization of FANCD2 may influence survival outcomes in ovarian cancer patients. FANCD2 is involved in the oestrogen-mediated signalling, innate immune system, amyloid fibre formation and cellular response to heat stress. In a recent study, the genetic deletion of FANCD2 in mouse hematopoietic stem progenitor cells (HSPCs) results in increased reactive oxygen species (ROSs) and mitochondrial respiration is enhanced. It has been reported that flaws in the cellular function of mitochondria result in oncogenesis. This data illustrate the importance of FANCD2 cytoplasmic activity in regulating the anti-tumour properties (Joshi S, 2020).

In conclusion, the study showed that FANCD2 has predictive and prognostic significance in ovarian cancer. FANCD2 deficient ovarian cancer cells may be suitable for synthetic lethality using PARP inhibitors.

In current study, the sensitivity to olaparib was observed in FANCA deficient ovarian cancer cell lines. This was more profound in platinum-sensitive PEO1 ovarian cells. The treated FANCA deficient cells were arrested in the G2/M cell cycle phase and the apoptotic cells were accumulated.

Among FA genes, the FANCA gene is frequently mutated in patients causing fanconi anaemia, an autosomal recessive inherited disease. It emerges with homozygous genetic mutation in fanconi complementary group genes (FANCA-FANCU). As per the recent analytical studies, the interconnection between modifications in FA pathways and carcinogenesis is established. Along with breast and ovarian cancers, the FANCA mutations are also reported to be associated with other cancers for instance colorectal cancer, gastric cancer and prostate cancer (Xia Q, 2020).

The cancer cells carrying defects in one DNA repair pathway rely on alternative pathways for survival. In this particular case, the tumour cells with defective

HR pathways (mutated BRCA1 and BRCA2) rely on an alternative end-joining pathway and base excision repair (PARP1 dependent) pathway. Therefore, the HR-deficient tumour cells response to cytotoxic PARP inhibitors (Cai MY, 2020).

# 7 FANCA in invasive breast cancer

## 7.1 Introduction

The mutations in anticancer genes convert the normal cells into malignant cells consequently the survival of cancer cells depend on other genes. To develop advanced drug-based treatments against cancer, suitable proteins are targeted in cells. The knowledge on tumour-cell genomes is extracted with the advanced technologies in cancer biology for instance the sequence of protein-coding regions and whole genome sequencing. The cell-based cancer models are accessible for studying gene-expression profiles; these show the potential of identifying mutations in oncogenes and tumour suppressor genes for targeting vulnerabilities in cancer cells.

The loss-of-function genetic mutations encode non-functional proteins resulting in human cancers. The mutations in tumour-suppressor genes cause cancers in human cells. Therefore, the non-functional proteins are not directly targeted with drugs because the genetic mutations result in the absence of a protein. However, a principle of synthetic lethality works in cancer cells with loss-of-function mutations that leave the cancer cells dependent on other specific genes for its survival. Synthetic lethality is an association between two genes A and B in which the loss of either gene can be tolerated by cells however, the loss of both genes results in tumour cell death. Synthetic lethality is a new therapeutic approach and incorporates the mutated tumour-suppressor genes (BRCA1/BRCA2) with PARP inhibition in cancer treatment. The clinical trials on BRCA gene mutations display approval of PARP inhibitors; the ovarian, breast and prostate cancers often have mutations in BRCA1 and BRCA2 genes hence it is an essential condition for treating cancer with PARP inhibitors (Feng FY, 2019).

The cellular vulnerabilities of cancer cells are targeted by various drugs in order to identify other therapeutic agents. The drugs affect tumour cell phenotypes caused by high DNA damage load resulting in metabolic, replicative and proteotoxic stress. Therefore, the agents are considered potential therapies that are capable of sensitizing cancer cells to these stresses (De Raedt T, 2011).

The cells are susceptible to breast cancer that retains the FA gene mutations in the FA pathway including FA Complementation Group A (FANCA) gene mutation. Additionally, a severe form of FA disease is caused by the homozygous mutations in the BRCA2 gene. Similarly, the breast and ovarian cancer syndromes are exhibited in heterozygous BRCA1 mutated cells and the FA disease is developed due to biallelic loss of BRCA1 genes. The breast cancer susceptibility genes that participate in the FA pathway are PALB2/FANCN and BRIP1/FANCJ. The non-functional FA pathway develops defective DNA repair, genomic instability and imparts favourable targets for breast cancer therapy. The human genome is targeted by DNA damaging agents; these are capable of producing inter-strand crosslinks, single-strand breaks and double-strand breaks. The homologous (HR) and non-homologous end joining (NHEJ) pathways assist in restoring double-strand breaks (DSBs). The nucleotide excision repair (NER), mismatch repair (MMR) and base excision repair (BER) pathways are involved in restoring single-strand breaks (SSBs) of DNA. The activity of poly ADP-ribose polymerases (PARPs) enzyme in the BER pathway aids in single-strand breaks (SSBs) repairing that recruits other DNA repair proteins at the DNA damaged site. DNA replication, DNA repairs, chromatin remodelling and recombination processes involve the activity of PARPs enzyme. The PARP-1 inhibition causes defective single-strand breaks repair (SSBR) resulting in the accumulation of DSBs and stalled replication forks. The functional HR pathway repairs the DSBs intending to compensate for the loss

of PARP1 activity. However, breast cancer cells with defective HR pathways (mutated BRCA1/2) are incapable to repair DNA damages leading to tumour-specific cell death. This is interpreted by synthetic lethality concept where the defective two genes result in a lethal phenotype and the inactivity of either gene causes the cell to remain viable. Specifically, the cells die with the simultaneous loss of the BRCA1/2 gene (HR pathway) and PARP-1 while cells displaying a defect in either of these have the ability to survive. The effective treatment options for breast, ovarian or other cancers with germline mutations in BRCA1/BRCA2 are PARP inhibitors (PARPi). The first FDA-approved PARPi is the olaparib for the treatment of breast cancer patients with BRCA deficiency.

Apart from synthetic lethality conditions, the cells carrying defects in several FA genes, particularly those working in the HR mechanism show hypersensitivity to chemotherapeutic agents. The cisplatin or carboplatin agents cause sensitivity in cells carrying pathogenic BRCA1/2 mutations including triple-negative breast cancer cells. On this account, the non-operating FA pathway in a cell can act as a cancer biomarker in predicting response to chemotherapeutic agents. The extensive study of FA biochemical mechanisms can be used to spot new biomarkers and produce the potent therapeutic targets (Fang CB, 2020).

## 7.2 RESULTS

### 7.2.1 FANCA gene analysis using METABRIC database

FANCA gene was studied for survival graphs and p-values using Metabric dataset (Figure 7-1).

**Age status: ≤40 vs 40-70 vs ≥70 yrs**

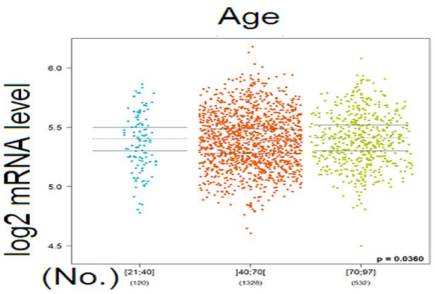


**p value = 0.0360**

**Age status: ≤51 vs >51 yrs**

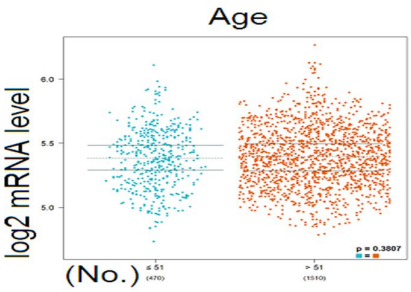


**p value = 0.3807**

**Nottingham Prognostic Index status (NPI)**

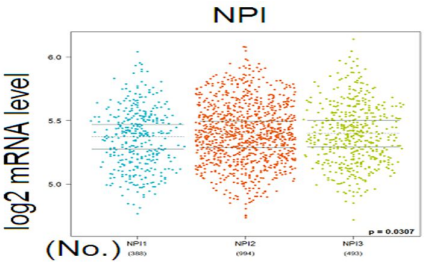


**p value = 0.0307**

**Oestrogen receptor status (ER)**

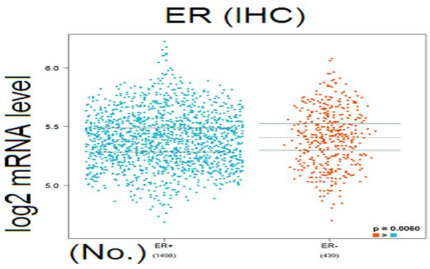


**p value = 0.0060**

**Histological types**

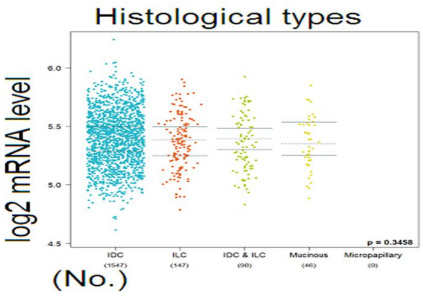


**p value = 0.345**

**Nodal status**

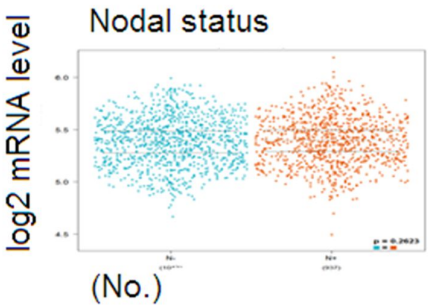


**p value = 0.2623**

**Progesterone receptor status (PR)**

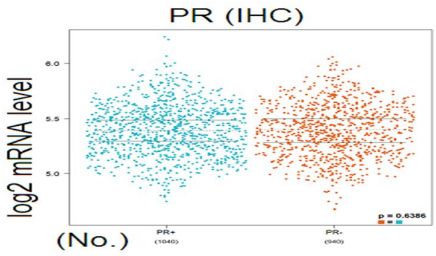


**p value = 0.6386**

**HER2 receptor status (HER2)**

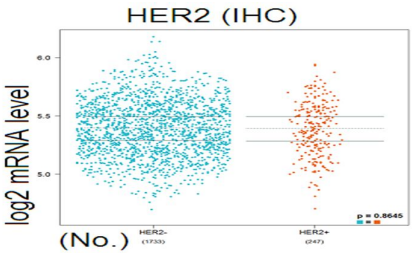


**p value = 0.8645**

**Figure 7-1:** FANCA gene analysis using METABRIC database.

The METABRIC (Molecular Taxonomy of Breast Cancer International Consortium) database was used to study one of the Fanconi anaemia (FA) repair genes FANCA for survival curves and p-values. The Beeswarm plots of gene expression were concluded for FANCA gene analysis. These plots were used to investigate the changes in gene expressions across different categories of clinicopathological parameters.

Under METABRIC database, the significant p-values were obtained of FANCA gene for clinicopathological parameters including age status ≤40 (p= 0.0360), Nottingham Prognostic Index status (NPI) (p= 0.0307) and oestrogen receptor status (ER) (p= 0.0060).

Using KM plotter database for survival analysis in breast cancer, FANCA gene was studied for overall survival (OS) and distant metastasis free survival (Figure 7-2).

**Overall survival** **Distant metastasis free survival**

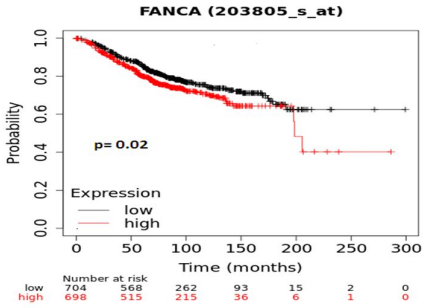


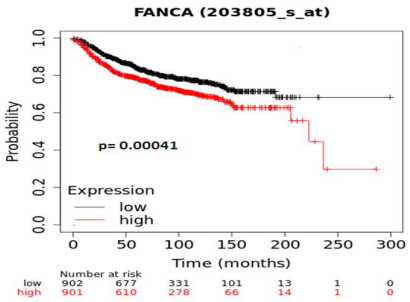


**p value- 0.0204** **p value- 0.0013**

**Figure 7-2**: Survival graphs using Kaplan Meier plotter database.

FANCA gene was considered for overall survival (OS) and distant metastasis free survival in cancer patients by Kaplan Meier plotter portal. It was used to establish the link between the FANCA gene expression and cancer patient survival to locate the applicable prognostic markers in carcinomas. FANCA gene of FA pathway was identified in the dataset selection, a parameter survival type was chosen and Kaplan-Meier plots were generated.

Under KM plotter database, the significant p-values were obtained of FANCA gene for survival curves in breast cancer including overall survival (OS) (p=0.0204) and distant metastasis free survival (p=0.0013).

**Pre-clinical data:**

The level of FANCA protein was examined in different breast cancer cell lines – DCIS, MCF-7 and MDA-MB-231. The relative protein level was compared with band quantification.

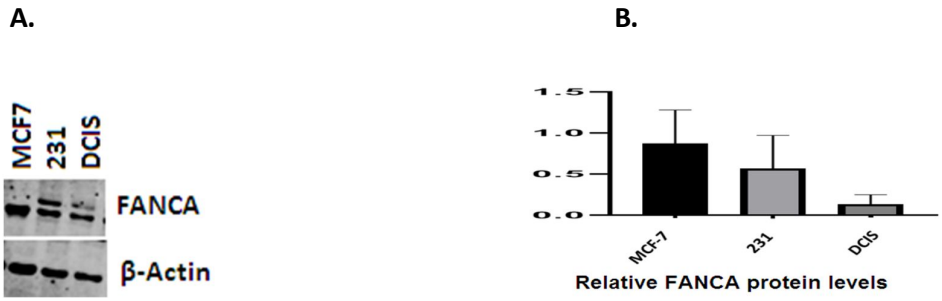


**Figure 7-3**: (A) Western blot showing FANCA protein expression in breast cancer cell lines (B) Relative FANCA protein expression level to β-actin. Values plotted were means ± SD of the fold-change (ratio of protein/β-actin).

The whole cell protein lysates were collected for each cell line and samples were separated by electrophoresis. The blot was probed using a specific FANCA antibody with a predicted molecular weight 161kDa. The loading control used was β-actin (42kDa).

For optimization, the primary antibody FANCA (rabbit-monoclonal) was checked at three different dilution factors 1:750, 1:1000 and 1:2000. Several dilutions were checked for optimal antibody concentration. The specific band for the given antibody was obtained at 1:1000. The FANCA protein expression was checked in various breast cancer cell lines – MCF-7, MDA-MB-231 and DCIS. The relative protein level was compared with band quantification using GraphPad Prism 8.2.0 software (Figure 7-3).

### 7.2.1.1 Pre and post cisplatin in breast cancer cell line

Nuclear and cytoplasmic expressions of MCF-7 were illustrated in Figure 7-4.

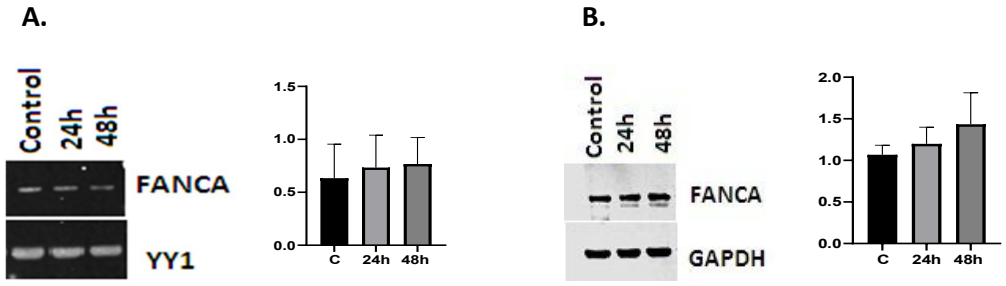


**Figure 7-4:** Nuclear and cytoplasmic expressions of MCF-7. (A) Western blot for FANCA expression in nuclear and cytoplasmic extracts from MCF-7 cells untreated and treated with cisplatin at 24 and 48 hours (B) Quantification of FANCA protein expression by western blot. GAPDH was used as a loading control for cytoplasmic extracts and YY1 was used as the loading control for nuclear extracts.

The influence of FANCA expression in the breast cancer cell line MCF-7 was investigated. The result of FANCA expression in malignant cells varied after the cisplatin treatment at different intervals of time. The kinetics of gene expression changed when cancer cells were exposed to platinum compounds at definite period of time. The molecular mechanisms of specific genes alter and produce transcriptional responses following cisplatin treatment. The mechanism of cisplatin-resistant cancer cells and platinum associated biological pathways can be characterised further in research areas.

### 7.2.1.2 FANCA siRNA in breast cancer cell line

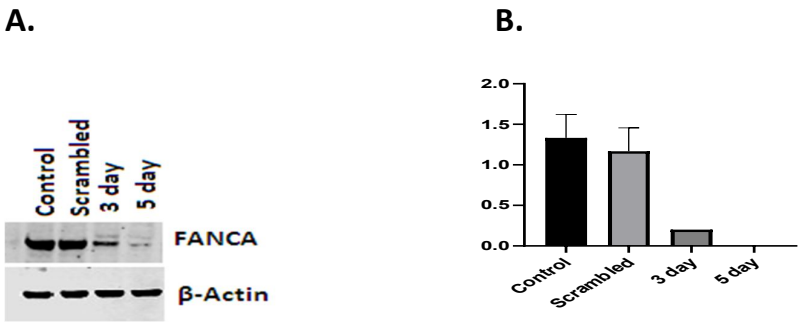


**Figure 7-5:** FANCA siRNA in breast cancer cell line (A) FANCA western blot (B) Quantification of FANCA protein levels relative to β-actin in MCF-7 transfected with FANCA siRNA and negative scrambled control. MCF-7_FANCA_KD cells were lysed at day 3 and day 5 to confirm transfection efficiency.

The cells were transfected with FANCA siRNA. The lysates were collected for a western blot on day 3 and day 5. The quantification of FANCA protein levels relative to β -actin (loading control) was measured (Figure 7-5). Graph and statistical analysis were obtained by GraphPad Prism 8.2.0 software.

### 7.2.1.3 Cisplatin and olaparib are toxic in FANCA deficient breast cancer cell line

**Clonogenic survival assay**

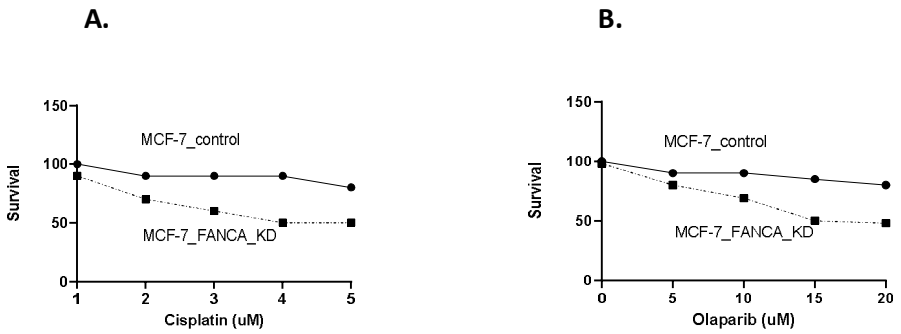


**Figure 7-6:** Clonogenic survival graphs (A) Cisplatin sensitivity in MCF-7 control and FANCA_KD cells (B) Olaparib sensitivity in MCF-7 control and FANCA_KD cells.

The clonogenic survival assay showed cisplatin and olaparib sensitivity in the MCF-7 breast cancer cell line. MCF-7 control and FANCA knockdown cells were treated at different doses of cisplatin and olaparib. The cells were transfected with FANCA siRNA or negative. Cells were treated with the indicated doses of drugs.

The cell line with FANCA deficiency exhibited low colony-forming ability after treatment with drugs for 14 days compared to FANCA proficient cell line. The clonogenic data were shown as the mean and standard deviation (SD) values for each concentration from three independent experiments. In general, increasing concentrations of drugs reduced the colony forming ability in FANCA deficient cells compared to the FANCA proficient cells. This clonogenic assay result demonstrated that FANCA knockdown cells were more sensitive to drugs than control cells.

FANCA transient knockdown with siRNA was performed and achieved maximum FANCA inhibition on day 5 (Figure 7-5). Therefore, day 5 was chosen to read all siRNA experimental results. FANCA knockdown sensitized MCF-7 cells to drugs and increased cell killing as shown in the clonogenic assay (Figure 7-6).

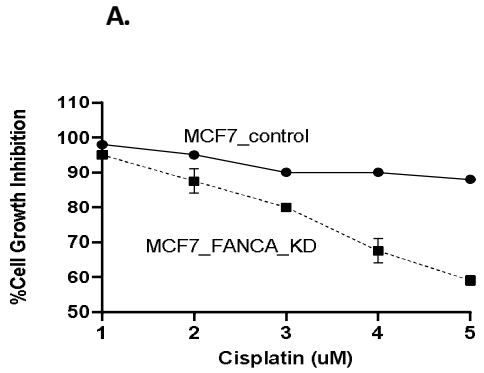


**Figure 7-7:** MTS cell growth inhibition graph of drug (A) MCF-7 control cells compared to FANCA gene knockdown cells. Data were shown as the mean and SD values for each concentration from three independent experiments.

MTS cell growth assay was performed using cisplatin. The cancer cells showed growth inhibition in response to cisplatin. It demonstrated that FANCA knockdown cells were more sensitive to cisplatin than the control cells. Breast cancer cell line with reduced FANCA expression exhibited low cell growth after treatment with cisplatin for 6 days compared to FANCA proficient cell line (Figure 7-7). Functional studies of drug response were then carried out to investigate the effect of drug in FANCA deficient cells.

### 7.2.1.5 Drug affects cell cycle progression in FANCA deficient cell line

The tumour genomic instability is established with continuous cell division. Cell cycle checkpoints are responsible to regulate cell cycle and maintain genomic

balance during cell division. DNA damage checkpoints and DNA replication stress checkpoints play significant role in cell cycle control. DNA repair is facilitated with cell cycle arrest after activated DNA damage checkpoints (ATM-CHK2-p53) capable of monitoring genetic errors.

Poly (ADP-ribose) polymerase inhibitors (PARPi) work in participation with synthetic lethality mechanisms that involve genetic mutation in DNA repair pathways. Current studies suggest combination therapies like PARPs and cell cycle checkpoints synergistically act to produce DNA errors and cell cycle arrest (Li S, 2022). Therefore, the effect of olaparib treatment on cell cycle progression was investigated. MCF-7 control and its FANCA knockdown cells were treated with olaparib (10μM) for 24 hours. Observation depicted that olaparib treated FANCA knockdown cells were arrested in the G2/M phase.

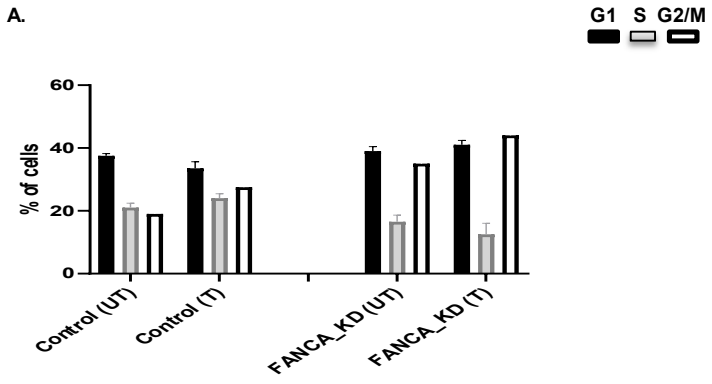


**Figure 7-8**: Functional studies of olaparib response in FANCA knockdown cells.

The cell cycle analysis was performed by flow cytometry. MCF-7 control cells and FANCA knockdown cells were treated with 10μM olaparib for 24 hours. The cells were transfected with scrambled control or FANCA siRNA. On day 5, the cells were collected and stained. MCF-7 control cells were compared to its FANCA knockdown (KD) cells.

Cell cycle analysis by propidium iodide flow cytometry after treatment with olaparib was studied. Results for FANCA proficient and deficient cells following treatment with olaparib for 24 hours demonstrated cell cycle arrest in treated FANCA knockdown cells compared to untreated breast cancer cells. Data were shown as the mean and SD values for each concentration from three independent experiments. The graphs were produced and statistical analysis performed using GraphPad Prism 8.2.0 software (Figure 7-8).

#### 7.2.1.4 Accumulation of apoptotic cells upon cisplatin and olaparib treatment

The tumour-selective cell death is a crucial therapeutic goal in cancer. The mechanisms of cell death are studied to establish the efficacy of cancer treatments. Tumours show the expression of apoptotic modulators related with sensitivity to cancer therapies. The loss of p53 protein or other effector molecules affect therapeutic cell death pathway. The biological functions of p53 include cell cycle and apoptosis regulation under cellular stress condition. The cytotoxic anticancer drugs have potential to induce apoptosis in cancer cells (Sellers WR, 1999). To investigate the accumulation of apoptotic cells upon inhibition of PARP1 activity in FANCA deficient cells, Annexin-V and PI staining was performed for the FANCA proficient and deficient cells treated with the drug. The results showed an accumulation of early and late apoptotic cells in FANCA deficient cell line treated with the drug (Figure 7-9).

**A.**

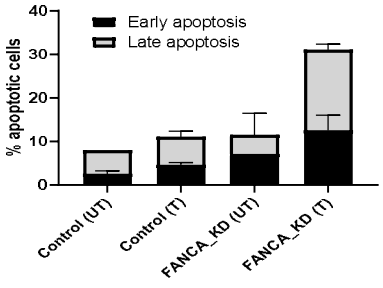


**Figure 7-9:** The percentage of apoptotic cells analysed by flow cytometry. Annexin V apoptosis assay in MCF-7 (control) and FANCA_KD cells treated with olaparib (10μM) for 24 hours.

Cells were treated with olaparib for 24 hours then stained with Annexin V-FITC and propidium iodide (PI) for flow cytometric analysis.
Results showed rise in apoptosis process in treated FANCA knockdown cells compared to untreated breast cancer cells. Treatment with olaparib was associated with increase in apoptotic cells. Data were normalised against baseline apoptotic fraction to determine the percentage increase in apoptosis. Data were shown as the mean and SD values for each concentration from three experiments. Graphs were produced and statistical analysis performed using GraphPad Prism 8.2.0 software.

## 7.3 Discussion

The biallelic mutations in one of 22 Fanconi anaemia (FA) genes cause a recessive hereditary disorder called Fanconi anaemia disease. The DNA crosslinking agents sensitize the FA cells leading to the accumulation of chromosomal aberrations and suggesting its key role in the FA/BRCA pathway of interstrand cross link (ICL) repair. Approximately 64% of all FA mutations, FANCA is the most commonly affected component of the FA core complex. The FA pathway carrying FANCD2 monoubiquitination, the FANCA participates in double strand breaks (DSBs) repair and interstrand cross-link (ICL) repairing mechanisms (Benitez A, 2018).

The FA cells are characterised by hematopoietic stem progenitor cell death due to high genomic instability and FA-related malignancies with unregulated cell proliferation. To eliminate the damaging effects of DNA ICLs, the FA proteins function with several other coordinating DNA repair proteins. In the tumour-suppressor network, the FA pathway participates to maintain genomic integrity by the regulation of cytokinesis, diminishing replication stress and stabilizing replication forks. The monoallelic germline mutations in FA genes like BRCA1 and BRCA2 enhance cancer susceptibility sporadically in the general population however, homozygous germline mutations in 22 FANC genes result in FA disorder (Niraj J, 2019).

In this study, screening of cisplatin and olaparib sensitivity in FANCA deficient and proficient breast cancer cell line was performed and a consistent sensitivity in the FANCA deficient breast cancer cell line was observed in MTS and clonogenic survival assays. The accumulation of apoptotic cells after 24 hours of olaparib treatment in FANCA deficient cells revealed the selective olaparib toxicity in the FANCA deficiency background. The olaparib treatment

induced cell cycle arrest which appeared to be influenced by p53 genetic background. The accumulation of double strand break (DSB) reflects that the SSB lesions generated by PARP inhibition fail to be repaired and convert to more serious DSB DNA damage lesions. In this study, investigation on MCF-7 breast cancer cell line confirmed that FANCA deficiency was essential for PARP1 inhibitor sensitivity and synthetic lethality. Thus, finding other targets that would achieve synthetic lethality with PARP inhibitors could be a novel approach.

Almost 5-10% of ICL DNA adducts display toxic effects in response to platinum-based chemotherapeutics that produce intrastrand and interstrand crosslinks. This causes high deformity in the helix structure of DNA, interfering with the functions of main biological processes for instance DNA replication and gene expression. Due to the interconnections among the DNA repair pathways and coordinated several repair proteins, a synthetic lethality approach with the FA pathway is considered for designing targeted therapies. The defective DNA repair pathways in the tumour cells are explored and it provides possibilities of inducing selective cell death whereas normal cells with functional repairing pathways are unaffected. The prominent illustration of the synthetic lethality approach is PARP inhibitors specifically with BRCA1/2 deficient cells carrying defective homologous recombination (HR) and interstrand cross link (ICL) pathways. The FA pathway promotes the HR mechanism for synthetic lethality therapies and FA proteins participate in various DNA repair pathways along with HR and ICL which widens the therapeutic opportunities. The single strand annealing process in DSB repair requires a key factor of the FA pathway called FANCA. Therefore, extensive study of this pathway could show many applications for synthetic lethality approaches to maximize therapeutic potential. The loss of function mutations in BRCA1/2 shows synthetic lethality

with PARP inhibition, the activity of PARP in the base-excision repair (BER) pathway is prevented resulting in unattended single and double-strand DNA breaks. The defective HR pathway is inadequate to repair these DNA damages leading to chromosomal instability and apoptosis (Taylor SJ, 2020).

# 8 General discussion & future directions

The DNA damage response (DDR) has a role around the biological network of DNA replication, cell cycle and DNA repair pathways. The synchronized efforts of these cellular processes assist in maintaining the genomic stability which is essential for cell survival. New therapeutic opportunities such as synthetic lethality display the therapeutic benefit of PARP blockade in BRCA deficient breast and ovarian cancer (Minchom A, 2018). It is accepted that the synthetic lethality approach has the ability to selectively kill cancer cells. The tumours carrying BRCA1/2 mutations including ovarian cancer, prostate cancer, pancreatic cancer and breast cancer can be treated with PARP inhibitors. Emerging data and research also suggest that additional synthetic lethality approaches are feasible in cancer therapeutics (Topatana W, 2020). Chemotherapy such as platinum compounds can induce intra strand and inter strand cross links. Inter strand cross links can active FA pathway. The first-line chemotherapy for the treatment of cancer patients is platinum-based agents under interstrand crosslinking (ICL) factors. The ICL factors trigger the DNA damage response (DDR) in malignant cells. Mitotic catastrophe or apoptosis are the consequences of high DNA damage load where the malignant cells lose the ability to divide. Patients with advanced malignancies receive therapeutic benefits from PARP inhibitors, these therapies target DNA damage response (DDR) mechanisms that cause DNA damage and the platinum-based agents induce replication stress in tumour cells. The research studies demonstrate that using platinum-based agents with PARP inhibitors is a good strategy for treating ovarian cancer patients carrying BRCAness conditions with loss-of-function mutations (BRCA1/BRCA2). According to research results, the combination therapies involving platinum-based agents and DDR-targeting therapies with advanced mechanism-based studies should be examined for cancer treatment (Basourakos SP, 2017).

The main aim of current study was to evaluate biomarker significance of FA pathway in breast and ovarian cancer. In addition, it was aimed to identify additional new synthetic lethality targets. In breast cohort, it was shown that XPA Binding Protein 2 (XAB2) expression was associated poor prognosis. The clinical data also showed that in invasive breast cancer cohort, low nuclear expression of XAB2 was significantly associated with number of characteristics: high mitotic count (p value-0.001), high tumour grade (p value-0.008), moderate NPI (p value-0.010), HER2- tumour (p value-0.025), tumour type-NST (p value- 0.038), low tumour stage (p value-0.037), radiotherapy local (p value-0.021) and no significance with ER, PR status. Therefore, low XAB2 expression had clinicopathological associations with aggressive forms of breast cancer. This suggested that targeting XAB2 deficient tumours could have promising clinical potential. The cisplatin and olaparib treatment was associated with selective cytotoxicity in XAB2 deficient breast cancer cells.
In ovarian cancer, XAB2 expression was significantly correlated with serous type tumour (p value-0.031). In ovarian cohort, XAB2 expression predicted the outcome of platinum-sensitive patients with significant overall survival (p value-0.026) at 70 months. The cisplatin and olaparib treatment was associated with selective cytotoxicity in XAB2 deficient ovarian cancer cells. The drug toxicity was associated with cell cycle arrest, double-strand break accumulation and apoptosis. The data suggested a new synthetic lethality interaction between PARP inhibitor and XAB2 in the ovarian cancer model.

In the current study, data also suggested that XAB2 expression in ovarian cancers could be an alternative predictive biomarker for PARPi response. FA Complementation Group D2 (FANCD2) and FA Complementation Group A (FANCA) expression in breast and ovarian cancer were also investigated. The

DNA interstrand crosslink (ICL) damages are recognised by the FA pathway which activates DNA repair pathways. It is established that the susceptibility to breast and ovarian cancer is high with mutations in the FA pathway. In this study, a correlation between FANCD2 deficiency and poor prognosis of breast cancers was shown. Current study also included the screening of olaparib sensitivity in FANCD2 deficient and proficient breast cancer cell lines. A consistent sensitivity in FANCD2 deficient breast cancer cells was observed. Moreover, FANCD2 expression also influenced clinical outcome in ovarian cancer. FANCD2 depletion by siRNA sensitized ovarian cancer cells to cisplatin and olaparib. The cisplatin-treated FANCD2 depleted cells accumulated cell cycle arrest and increased apoptosis. This suggested the role of FANCD2 in cisplatin resistance mechanisms and the possibility of overcoming it by FANCD2 inhibition.

The activation of the fanconi anaemia (FA) pathway is essential for HR-mediated DNA damage repairing in a cell. The homologous recombination deficiency (HRD) is induced by genetic defects in the FA pathway, this condition is necessary for cell sensitivity to PARP inhibitors and DNA damaging agents. The PARP inhibitors and other chemotherapeutic agents may provide a tool for improving cancer patient's survival by the inhibition of FANCD2 expression and it depicts the potential of these agents to sensitize cancer cells (Moes-Sosnowska J, 2019). The poly (ADP-ribose) polymerase (PARP) protein has a role in the base excision repair (BER) system fixing DNA single-strand breaks and double-strand breaks (DSB) by alternative non-homologous end-joining (NHEJ). The clinical development of combination strategies includes DNA damaging agents integrated with DDR inhibitors. To maximise the benefits and potential of several DDR inhibitors available in preclinical and

clinical settings, the mechanisms of action of these agents were studied and considered attentively (Brown JS, 2017).

The most commonly affected complementation group in the FA pathway is FANCA (~64%) due to genetic mutations. In this study, increased sensitivity to cisplatin and olaparib in FANCA deficient cells compared to proficient cells was observed. This data suggests an alternative synthetic lethality approach. In FANCD2 deficient cells, a similar pattern of increased sensitivity to cisplatin and olaparib was observed. Taken together current data suggests that FA pathway could be a promising alternative target for synthetic lethality. The mutations in DNA repair genes and resistance or sensitivity to platinum compounds have been shown related in preclinical evidences (Damia G, 2019).

With the emergence of functional implications of genomic and transcriptomic variability studies, targeted or precision medicine in cancer biology develops fast. The upcoming approaches to stratifying patients according to their genetic alterations are still ongoing rather than by their tumour origin (Minchom A, 2018). The balance between genomic instability and DNA damage responses in cancer cells represents an innovative strategy to combat the tumour burden. Several pieces of evidence have suggested that the drugs inducing synthetic lethality have offered the eminent therapeutic window for clinical success based on the DNA damage repair system (Gavande NS, 2016). The Fanconi anaemia (FA) pathway plays a major role in the DNA repair system. The anomalous behaviour of this pathway has contributed for acquiring chemoresistance against a wide variety of cancers. This becomes an alluring choice of agents as it can be exploited for their inhibition and targeting properties to enhance the efficacy of chemotherapy (Taylor SJ, 2020).

A limitation to current study as the following:

1) Immunohistochemical study included retrospective cohorts. Therefore, prospective clinical study would be required to confirm whether XAB2, FANCD2 and FANCA have prognostic or predictive significance in breast and ovarian cancer.

2) The transcript studies were in unrelated clinical cohorts. Future studies should include IHC and transcriptomic analyses in the same cohort for validation.

3) The cancer cell line-based studies were limited to a few cell lines only. Expansion to additional cancer cell lines will be required for further validation. In addition, stable knockout cell lines of XAB2, FANCD2 and FANCA will be required for additional confirmation.

4) Only one PARP inhibitor (olaparib) was tested in the current study. Whether other PARP inhibitors used in the clinic such as niraparib, talazoparib and rucaparib will have selective toxicity in XAB2 deficient, FANCD2 deficient or FANCA deficient cells remain to be established.

Future studies should explore the limitations described above. Moreover, whether combinatorial strategies such as combining PARP inhibitor with other emerging DNA repair inhibitors (ATM, ATR, and Wee1) will have clinical potential on FA deficient cell lines will need to be investigated.

The strength of current study is that the clinicopathological significance of XAB2, FANCD2 and FANCA in large clinical datasets is explored. Although the studies are preliminary, these provide proof of principle that target beyond BRCA; particularly FA pathway may be suitable synthetic lethality targets.

# 9 References

Abbotts R, Thompson N, Madhusudan S. (2014) 'DNA repair in cancer: emerging targets for personalized therapy.' *Cancer management and research*; 6:77-92. doi:10.2147/CMAR.S50497.

Alberts B. (2003) 'DNA replication and recombination.' *Nature.*; 421(6921):431-5. doi: 10.1038/nature01407.

Amir E, Bostjan Seruga, Rosario Serrano et al., (2010) 'Targeting DNA repair in breast cancer: A clinical and translational update' *Cancer Treatment Reviews*; 36, 557-565. doi:0.1016/j.ctrv.2010.03.006.

Basourakos SP, Li L, Aparicio AM et al., (2017) 'Combination platinum-based and DNA damage response-targeting cancer therapy: Evolution and future directions.' *Current Medicinal Chemistry*; 24(15), 1586-1606. doi:10.2174/0929867323 666161214114948.

Benitez A, Anna Palovcak & Yanbin Zhang (2018) 'FANCA promotes DNA Double-Strand Break Repair by Catalyzing Single-Strand Annealing and Strand Exchange.' *Molecular cell*; 71(4). doi: 10.1016/j.molcel.2018.06.030.

Benjamini Y, Yekutieli D, Edwards D (2005) 'False Discovery Rate-Adjusted Multiple Confidence Intervals for Selected Parameters.' *Journal of the American Statistical Association*; 100.71-81. doi: 10.1198/016214504000001907.

Blanpain C, Mohrin M, Sotiropoulou PA et al., (2011) 'DNA-damage response in tissue-specific and cancer stem cells.' *Cell Stem Cell;* 8(1):16-29. doi:10.1016/j. stem.2010.12.012.

Boiteux S, Jinks-Robertson S. (2013) 'DNA repair mechanisms and the bypass of DNA damage in Saccharomyces cerevisiae.' *Genetics*; 193(4):1025-1064. doi: 1 0.1534/genetics.112.145219.

Brown JS, O'Carrigan B, Jackson SP et al., (2017). 'Targeting DNA Repair in Cancer: Beyond PARP Inhibitors.' *Cancer Discovery*; 7(1), 20-37. doi: 10.1158 /2159-8290.CD-16-0860.

Cai MY, Dunn CE, Chen W et al., (2020) 'Cooperation of the ATM and Fanconi Anemia/BRCA Pathways in Double-Strand Break End Resection.' *Cell reports*; 30(7), 2402–2415.e5. doi:10.1016/j.celrep.2020.01.052.

Camero S, Ceccarelli S, De Felice et al. (2019) 'PARP inhibitors affect growth, survival and radiation susceptibility of human alveolar and embryonal rhabdomyosarcoma cell lines.' *J Cancer Res Clin Oncol;* 145, 137–152. doi:10.1 007/s00432-018-2774-6.

Cerrato A, Francesco Morra, Angela Celetti (2016) 'Use of poly ADP-ribose polymerase [PARP] inhibitors in cancer cells bearing DDR defects: The rationale for their inclusion in the clinic.' *Journal of Experimental & Clinical Cancer Research*; 35 (1). doi:10.1186/s13046-016-0456-2.

Chandra A, Pius C, Nabeel M et al., (2019) ‘Ovarian cancer: Current status and strategies for improving therapeutic outcomes.’ *Cancer Med*.; 8(16):7018-7031. doi:10.1002/cam4.2560.

Chatterjee N, Walker GC. (2017) ‘Mechanisms of DNA damage, repair and mutagenesis.’ *Environmental and molecular mutagenesis*; 58(5):235-263. doi:10.1002/em.22087.

Damia G & Broggini M. (2019) ‘Platinum Resistance in Ovarian Cancer: Role of DNA Repair.’ *Cancers*; 11(1),119. doi:10.3390/cancers11010119.

De Raedt T, Walton Z, Yecies JL et al., (2011) ‘Exploiting cancer cell vulnerabilities to develop a combination therapy for ras-driven tumors.’ *Cancer cell*; 20(3), 400–413. doi:10.1016/j.ccr.2011.08.014.

Del Valle J, Rofes P, Moreno-Cabrera JM et al., (2020) ‘Exploring the Role of Mutations in Fanconi Anemia Genes in Hereditary Cancer Patients.’ *Cancers*; 12(4), 829. doi:10.3390/cancers12040829.

Deng N, Zhou H, Fan H et al., (2017) ‘Single nucleotide polymorphisms and cancer susceptibility.’ *Oncotarge*t; 8(66):110635-110649. doi:10.18632/oncotarget.22372.

Dorr JR, Yu Y, Milanovic M, et al., (2013) ‘Synthetic lethal metabolic targeting of cellular senescence in cancer therapy.’ *Nature;* 501(7467). doi:10.1038/nature12437.

Douglas-Jones AG, Morgan JM, Appleton MAC et al., (2000) 'Consistency in the observation of features used to classify duct carcinoma in situ (DCIS) of the breast.' *Journal of Clinical Pathology*. doi:10.1136/jcp.53.8.596.

Facchetti G, Zampieri M, Altafini C. (2012) 'Predicting and characterizing selective multiple drug treatments for metabolic diseases and cancer.' *BMC Systems Biology*; 6:115. doi:10.1186/1752-0509-6-115.

Fang CB, Wu HT, Zhang ML et al., (2020) 'Fanconi Anemia Pathway: Mechanisms of Breast Cancer Predisposition Development and Potential Therapeutic Targets.' *Frontiers in cell and developmental biology*; 8, 160. doi:10.3389/fcell.2020.00160.

Farmer H, McCabe N, Lord CJ et al., (2005) 'Targeting the DNA repair defect in BRCA mutant cells as a therapeutic strategy.' *Nature*; 434, 917–921. doi:10.10 38/nature03445.

Feng FY & Luke A. Gilbert (2019) 'Lethal clues to cancer-cell vulnerability.' *Nature;* 568, 463-464. doi:10.1038/d41586-019-01086-w.

Feng Y, Spezia M, Huang S et al., (2018) 'Breast cancer development and progression: Risk factors, cancer stem cells, signaling pathways, genomics, and molecular pathogenesis.' *Genes Dis*; 5(2):77-106. doi:10.1016/j.gendis.05.001.

Fong PC, Yap TA, Boss DS et al., (2010) 'Poly (ADP)-ribose polymerase inhibition: frequent durable responses in BRCA carrier ovarian cancer

correlating with platinum-free interval.' *Journal of clinical oncology*; 28(15), 2512-2519. doi:10.1200/JCO.2009.26.9589.

Formenti SC, Demaria S. (2008) 'Local control by radiotherapy: is that all there is?' *Breast Cancer Res; 10(6):215*. doi:10.1186/bcr2160.

Fuss JO, Cooper PK (2006) 'DNA repair: dynamic defenders against cancer and aging.' *PLoS Biology*; (6):e203. doi:10.1371/journal.phio.0040203.

Gavande NS, VanderVere-Carozza PS, Hinshaw HD et al., (2016) 'DNA repair targeted therapy: The past or future of cancer treatment?' Pharmacology & therapeutics; 160, 65–83. doi:10.1016/j.pharmthera.2016.02.003.

Gadad SS, Camacho CV, Malladi V et al., (2021) 'Poly (ADP-ribose) polymerase-1 regulates oestrogen-dependent gene expression in oestrogen receptor α-positive breast cancer cells.' *Mol Cancer Res;* 19 (10): 1688–1698. doi:10.1158/1541-7786.MCR-21-0103.

Gaitskell K, Green J, Pirie K. (2018) 'Histological subtypes of ovarian cancer associated with parity and breastfeeding in the prospective Million Women Study.' *International journal of cancer*; 142(2):281-289. doi:10.1002/ijc.31063.

Gaitskell K, Martinek I, Bryant A et al., (2011). 'Angiogenesis inhibitors for the treatment of ovarian cancer.' *The Cochrane database of systematic reviews*; (9), CD007930. doi:10.1002/14651858.

Gibson S.J, Tewari K.S, Monk B.J et al. (2014) ‘Updates on drug discovery in ovarian cancer.’ *Gynecologic Oncology Research and Practice*; 1, 3. doi:10.118 6/2053-6844-1-3.

Giglia-Mari G, Zotter A, Vermeulen W. (2011) ‘DNA damage response.’ *Cold Spring Harb Perspect Biol*.; 3(1):a000745. doi:10.1101/cshperspect.a000745.

Gilmore E, Mccabe, Nuala & Kennedy et al., (2019) ‘DNA Repair Deficiency in Breast Cancer: Opportunities for Immunotherapy.’ *Journal of Oncology*; 1-14. doi:10.1155/2019/4325105.

Green AR, Caracappa D, Benhasouna AA et al., (2015) ‘Biological and clinical significance of PARP1 protein expression in breast cancer.’ *Breast cancer research and treatment*; 149(2), 353–362. doi:10.1007/s10549-014-3230-1.

Green AR, Mohammed A. Aleskandarany, Reem Ali et al., (2017) ‘Clinical Impact of Tumor DNA Repair Expression and T-cell Infiltration in Breast Cancers.’ *Cancer Immunol Res*. doi:10.1158/2326-6066.

Green AR, Powe DG, Rakha EA et al., (2013) ‘Identification of key clinical phenotypes of breast cancer using a reduced panel of protein biomarkers’ *Br J Cancer*; 109(7):1886-94. doi:10.1038/bjc.2013.528.

Gupta D, Lis C.G. (2009) ‘Role of CA125 in predicting ovarian cancer survival - a review of the epidemiological literature.’ *Journal of Ovarian Research;* 2, 13. doi:10.1186/1757-2215-2-13.

Gyorffy B, Lanczky A & Szallasi Z (2012) 'Implementing an online tool for genome-wide validation of survival-associated biomarkers in ovarian-cancer using microarray data from 1287 patients.' *Endocrine-Related Cancer*; 19(2), 197-208. doi:10.1530/ERC-11-0329.

Han T, Tong J, Wang M et al., (2022) 'Olaparib Induces RPL5/RPL11-Dependent p53 Activation via Nucleolar Stress.' *Front Oncol.*; 12:821366. doi:10.3389/ fonc.2022.821366.

Hanahan D & Weinberg RA (2011) 'Hallmarks of Cancer: The Next Generation.' *Cell;* 144. 646-74. doi:10.1016/j.cell.2011.02.013.

Helleday T. (2011) 'The underlying mechanism for the PARP and BRCA synthetic lethality: clearing up the misunderstandings.' *Mol Oncol.*; 5(4):387-93. doi:10.1016/j.molonc.2011.07.001.

Hiller K., Metallo C.M. (2013) 'Profiling metabolic networks to study cancer metabolism.' *Current Opinion in Biotechnology;* 24(1): 60-68. doi:10.1016/j. copbio.2012.11.001.

Hosoya N & Miyagawa K (2014) 'Targeting DNA damage response in cancer therapy.*'* *Cancer science*; 105(4):370-88. doi:10.1111/cas.12366.

Hou S, Li Na, Zhang Q et al. (2016) 'XAB2 functions in mitotic cell cycle progression via transcriptional regulation of CENPE.' *Cell Death and Disease*; 7. e2409. doi:10.1038/cddis.2016.313.

Huang R & Zhou PK. (2021) ‘DNA damage repair: historical perspectives, mechanistic pathways and clinical translation for targeted cancer therapy.’ *Signal transduction and targeted therapy*; 6(1):254. doi:10.1038/s41392-021-00648-7.

Iwatsuki M, Mimori K, Yokobori T et al., (2009) ‘A platinum agent resistance gene, POLB, is a prognostic indicator in colorectal cancer.’ *Journal of Surgical Oncology*; 100,261 - 266. doi:10.1002/jso.21275.

Janysek DC, Kim J, Duijf PHG et al., (2021) ‘Clinical use and mechanisms of resistance for PARP inhibitors in homologous recombination-deficient cancers.’ *Transl Oncol.*; 14(3):101012. doi:10.1016/j.tranon.2021.101012.

Jelinic P & Levine DA (2014) ‘New insights into PARP inhibitors' effect on cell cycle and homology-directed DNA damage repair.’ *Molecular Cancer Therapeutics*; 13.6, 1645-1654. doi:10.1158/1535-7163.MCT-13-0906.

Jelovac D, Deborah K. Armstrong (2011) ‘Recent progress in the diagnosis and treatment of ovarian cancer’ *CA: A Cancer Journal for Clinicians*. doi:10.33 22/caac.20113.

Jiang X, Li X, Li W et al., (2019) ‘PARP inhibitors in ovarian cancer: Sensitivity prediction and resistance mechanisms.’ *Journal of cellular and molecular medicine*; 23(4), 2303–2313. doi:10.1111/jcmm.14133.

Joshi S, Campbell S, Lim JY et al., (2020) 'Subcellular localization of FANCD2 is associated with survival in ovarian carcinoma.' *Oncotarget*; 11(8), 775–783. doi:10.18632/oncotarget.27437.

Jurkovicova D, Neophytou CM, Gasparovic AC et al., (2022) 'DNA Damage Response in Cancer Therapy and Resistance: Challenges and Opportunities.' *Int J Mol Sci.*; 23(23):14672. doi:10.3390/ijms232314672.

Ju SH, Lee SE, Kang YE et al., (2022) 'Development of Metabolic Synthetic Lethality and Its Implications for Thyroid Cancer.' *Endocrinol Metab; 37(1):53-61*. doi:10.3803/EnM.2022.1402.

Keung MY, Wu Y, Badar F et al., (2020) 'Response of Breast Cancer Cells to PARP Inhibitors Is Independent of BRCA Status.' *Journal of Clinical Medicine*; 9(4):940. doi:10.3390/jcm9040940.

Koh J, Kim MJ (2019) 'Introduction of a New Staging System of Breast Cancer for Radiologists: An Emphasis on the Prognostic Stage.' *Korean journal of radiology*; 1: 69-82. doi:10.3348/kjr.2018.0231.

Kononen J., Bubendorf L., Kallionimeni A. (1998) 'Tissue microarrays for high-throughput molecular profiling of tumor specimens.' *Nature Medicine*; 4, 844–847. doi:10.1038/nm0798-844.

Konstantinopoulos PA, Spentzos D, Karlan BY et al., (2010) 'Gene expression profile of BRCAness that correlates with responsiveness to chemotherapy and with outcome in patients with epithelial ovarian cancer.' *Journal of clinical*

*oncology: official journal of the American Society of Clinical Oncology*; 28(22), 3555–3561. doi:10.1200/JCO.2009.27.5719.

Kuraoka I, Ito S, Wada T et al., (2008) 'Isolation of XAB2 complex involved in pre-mRNA splicing, transcription and transcription-coupled repair.' *Journal of Biological Chemistry;* 283(2):940-50. doi:10.1074/jbc.M706647200.

Kurman RJ, Shih IeM. (2016) 'The Dualistic Model of Ovarian Carcinogenesis: Revisited, Revised and Expanded.' *The American journal of pathology*; 186(4): 733-747. doi:10.1016/j.ajpath.2015.11.011.

Lachaud C, Moreno A, Marchesi F et al., (2016) 'Ubiquitinated Fancd2 recruits Fan1 to stalled replication forks to prevent genome instability.' *Science*; 351 (6275):846-849. doi:10.1126/science.aad5634.

Lagerwerf S, Vrouwe MG, Overmeer RM et al., (2011) 'DNA damage response and transcription.' *DNA Repair (Amst).*; 10(7):743-50. doi: 10.1016/j.dnarep. 2011.04.024.

Le Meur N, Gentleman R. (2008) 'Modeling synthetic lethality.' *Genome Biology*; 9(9):R135. doi:10.1186/gb-2008-9-9-r135.

Li H, Liu ZY, Wu N et al., (2020) 'PARP inhibitor resistance: the underlying mechanisms and clinical implications.' *Mol Cancer*. 20; 19(1):107. doi:10.11 86/s12943-020-01227-0.

Li L, Tan W, Deans AJ. (2020) 'Structural insight into FANCI-FANCD2 monoubiquitination.' *Essays in biochemistry*; 64(5):807-817. doi:10.1042/EBC20200001.

Li S, Topatana W, Juengpanich S et al., (2020) 'Development of synthetic lethality in cancer: molecular and cellular classification.*' Sig Transduct Target Ther; 5, 24.* doi:10.1038/s41392-020-00358-6.

Li S, Wang L, Wang Y et al. (2022) 'The synthetic lethality of targeting cell cycle checkpoints and PARPs in cancer treatment.' *J Hematol Oncol;* 15, 147. doi:10.1186/s13045-022-01360-x.

Liu W, Palovcak A, Li F et al., (2020) 'Fanconi anemia pathway as a prospective target for cancer intervention.' *Cell & Bioscience*; 10, 39. doi:10.1186/s13578-020-00401-7.

Liu Y, Pan B, Qu W et al., (2021) 'Systematic analysis of the expression and prognosis relevance of FBXO family reveals the significance of FBXO1 in human breast cancer.' *Cancer Cell International*; 21(1):130. doi:10.1186/s12935-021-01833-y.

Ljungman.M, David P Lane (2004) 'Transcription — guarding the genome by sensing DNA damage.*' Nature Reviews Cancer;* 4, 727–737. doi:10.1038/nrc1435.

Lukasiewicz S, Czeczelewski M, Forma A et al., (2021) 'Breast Cancer-Epidemiology, Risk Factors, Classification, Prognostic Markers and Current

Treatment Strategies-An Updated Review' *Cancers (Basel)*; 13(17):4287.doi:10.3390/cancers13174287.

Luvero D, Milani A, Ledermann JA. (2014) 'Treatment options in recurrent ovarian cancer: latest evidence and clinical potential.' *Therapeutic advances in medical oncology;* 6(5):229-239. doi:10.1177/1758834014544121.

Majidinia M, Yousefi, Bahman (2017) 'DNA repair and damage pathways in breast cancer development and therapy.*'* *DNA Repair*; 54, 22-29. doi:10.1016/j.dnarep.03.009.

Marteijn JA, Hannes Lans, Wim Vermeulen et al., (2014) 'Understanding nucleotide excision repair and its roles in cancer and ageing.*'* *Nature Reviews Molecular Cell Biology;* 15(7):465-81. doi:10.1038/nrm3822.

McLornan DP, A List and GJ Mufti (2014) 'Applying synthetic lethality for the selective targeting of cancer.' *New England Journal of Medicine*; 371(18):1725-35. doi:10.1056/NEJMra1407390.

McShane LM, Altman DG, Sauerbrei W et al., (2005) 'Reporting recommendations for tumour marker prognostic studies (REMARK).' *British journal of cancer*; 93(4), 387–391. doi:10.1038/sj.bjc.6602678.

Menon G, Alkabban FM et al., (2024) 'Breast Cancer.' *Treasure Island (FL): StatPearls Publishing*; NBK482286. PMID: 29493913.

Metselaar DS, Meel MH, Benedict B et al (2019) 'Celastrol-induced degradation of FANCD2 sensitizes pediatric high-grade gliomas to the DNA-crosslinking agent carboplatin.' *EBioMedicine*; 50, 81–92. doi:10.1016/j.ebiom.10.062.

Mikolaskova B, Jurcik M, Cipakova I et al., (2018). 'Maintenance of genome stability: the unifying role of interconnections between the DNA damage response and RNA-processing pathways.' *Current Genetics*; 64(5):971-983. doi:10.1007/s00294-018-0819-7.

Milanowska K, Krwawicz J, Papaj G et al. (2011) 'REPAIRtoire--a database of DNA repair pathways.' *Nucleic acids research*; 39(Database issue):D788-D792. doi:10.1093/nar/gkq1087.

Minchin S, Lodge J.(2019) 'Understanding biochemistry: structure and function of nucleic acids.' *Essays Biochem.*; 63(4):433-456. doi:10.1042/EBC20180038.

Minchom A, Aversa C, Lopez J. (2018) 'Dancing with the DNA damage response: next-generation anti-cancer therapeutic strategies.' *Therapeutic advances in medical oncology;* 10, 1758835918786658. doi:10.1177/1758835918786658.

Mittal D, Biswas L, Verma AK (2021) 'Redox resetting of cisplatin-resistant ovarian cancer cells by cisplatin-encapsulated nanostructured lipid carriers' *Epub,* 16(12):979-995. doi:10.2217/nnm-2020-0400.

Moes-Sosnowska J, Rzepecka IK, Chodzynska J et al., (2019) 'Clinical importance of FANCD2, BRIP1, BRCA1, BRCA2 and FANCF expression in ovarian

carcinomas.' *Cancer biology & therapy*; 20(6), 843–854. doi:10.1080/15384047.2019.1579955.

Momenimovahed Z, Tiznobaik A, Taheri S et al., (2019) 'Ovarian cancer in the world: epidemiology and risk factors.' *Int J Womens Health*; 11:287-299. doi:10.2147/IJWH.S197604.

Muggerud AA, Michael Hallett, Hilde Johnsen et al., (2010) 'Molecular diversity in ductal carcinoma in situ (DCIS) and early invasive breast cancer.' *Molecular Oncology*. doi:10.1016/j.molonc.2010.06.007.

Munshi A, Marvette Hobbs, Raymond E Meyn (2005) 'Clonogenic Cell Survival Assay.' *Methods in molecular medicine;* 110, 21-8. doi:10.1385/1-59259-869-2:021.

Murphy CG, Conleth & Dickler, Maura. (2010). 'Exploring the Concept of Synthetic Lethality to Improve Therapeutic Options for Patients with Breast Cancer.' *Current Breast Cancer Reports*; 2.1-3. doi:10.1007/s12609-010-0001-9.

Musella A, Bardhi E, Marchetti C et al., (2018) 'Rucaparib: An emerging parp inhibitor for treatment of recurrent ovarian cancer.' *Cancer Treatment Reviews;* 66, 7-14. doi:10.1016/j.ctrv.2018.03.004.

Nakatsu Y, Asahina H, Citterio et al., (2000) 'XAB2, a novel tetratricopeptide repeat protein involved in transcription-coupled DNA repair and transcription.' *Journal of Biological Chemistry*; 275(45):34931-7. doi:10.1074/jbc.M004936200.

Nepal M, Che R, Ma C et al., (2017) ‘FANCD2 and DNA Damage.’ *International journal of molecular sciences*; 18(8), 1804. doi:10.3390/ijms18081804.

Nijman SM. (2011) ‘Synthetic lethality: general principles, utility and detection using genetic screens in human cells.’ *FEBS Letters*; 585(1):1-6. doi:10.1016/j. febslet.2010.11.024.

Niraj J, Farkkila A, D'Andrea AD (2019) ‘The Fanconi Anemia Pathway in Cancer.’ *Annual review of cancer biology*; 3:457-478. doi:10.1146/annurev-cancerbio-030617-050422.

Nowsheen S, Yang ES (2012) ‘The intersection between DNA damage response and cell death pathways.’ *Experimental oncology*; 34(3):243-54. PMID: 23070009.

Orrantia-Borunda E, Anchondo-Nunez P, Acuna-Aguilar LE et al., (2022) ‘Subtypes of Breast Cancer.’ *Breast Cancer. Brisbane (AU): Exon Publications*. doi:10.36255/exon-publications-breast-cancer-subtypes.

Perou CM, Sorlie T, Eisen MB et al., (2000) ‘Molecular portraits of human breast tumours.’ *Nature*; 406(6797):747-52. doi:10.1038/35021093.

Petrucelli N, Daly MB, Pal T et al., (2023) ‘BRCA1 and BRCA2 Associated Hereditary Breast and Ovarian Cancer.’ *Adam MP, Feldman J, Mirzaa GM, et al., editors. GeneReviews* ; NBK1247. PMID: 20301425**.**

Pfeffer CM, Singh ATK. (2018) ‘Apoptosis: A Target for Anticancer Therapy.’ *Int J Mol Sci*. 2;19(2):448. doi:10.3390/ijms19020448.

Pinder SE (2010) ‘Ductal carcinoma in situ (DCIS): pathological features, differential diagnosis, prognostic factors and specimen evaluation.’ *Modern Pathology*. doi:10.1038/modpathol.2010.40.

Pinder SE, Duggan C, Ellis IO et al., (2010) ‘A new pathological system for grading DCIS with improved prediction of local recurrence: results from the UKCCCR/ANZ DCIS trial.’ *Br J Cancer*. doi:10.1038/sj.bjc.6605718.

Pozarowski P & Darzynkiewicz Z. (2004) ‘Analysis of Cell Cycle by Flow Cytometry Methods.’ *Methods in molecular biology (Clifton, N.J.);* 281, 301-11. doi:10.1385/1-59259-811-0:301.

Reid BM, Permuth JB, Sellers TA. (2017) ‘Epidemiology of ovarian cancer: a review.’ *Cancer biology& medicine. Chinese Anti-Cancer Association*; 14(1):9-32. doi:10.20892/j.issn.2095-3941.2016.0084.

Riccardi C, Nicoletti I. (2006) ‘Analysis of apoptosis by propidium iodide staining and flow cytometry.’*Nature protocols*; 1.1458-61. doi:10.1038/nprot.238.

Ricci F, Affatato R, Carrassa L et al., (2018) ‘Recent Insights into Mucinous Ovarian Carcinoma.*’ International journal of molecular sciences*; 19(6):1569. doi:10.3390/ijms19061569.

Ring A, Nguyen-Strauli BD, Wicki A et al., (2023) ‘Biology, vulnerabilities and clinical applications of circulating tumour cells.’ *Nat Rev Cancer;* 23, 95–111. doi:10.1038/s41568-022-00536-4.

Riss TL, Moravec RA, Niles AL et al., (2016) 'Cell Viability Assays' *Bethesda (MD): Eli Lilly & Company and the National Center for Advancing Translational Sciences;* NBK144065. PMID: 23805433.

Roberts D., Schick J., Conway S. et al., (2005) 'Identification of genes associated with platinum drug sensitivity and resistance in human ovarian cancer cells.' *British journal of cancer*; 92, 1149–1158. doi:10.1038/sj.bjc.6602447.

Sadeghi M, Enferadi M, Shirazi A. (2010) 'External and internal radiation therapy: Past and future directions.' *Journal of Cancer Research and Therapeutics; 6(3):p 239-248*. doi:10.4103/0973-1482.73324.

Saldivar JS, Wu X, Follen M et al., (2007). 'Nucleotide excision repair pathway review I: Implications in ovarian cancer and platinum sensitivity.' *Gynecologic oncology*; 107. S56-71. doi:10.1016/j.ygyno.2007.07.043.

Scharer OD. (2013) 'Nucleotide excision repair in eukaryotes.' *Cold Spring Harbor perspectives in biology*; 5(10):a012609. doi:10.1101/cshperspect. a012609.

Sellers WR, Fisher DE. (1999) 'Apoptosis and cancer drug targeting.' *J Clin Invest*.; 104(12):1655-61. doi:10.1172/JCI9053.

Shi Y, Zhou F, Jiang F et al., (2014) 'PARP inhibitor reduces proliferation and increases apoptosis in breast cancer cells'. *Chin J Cancer*; 26(2):142-7. doi: 10.3978/j.issn.1000-9604.2014.02.13.

Shimamura A, Rocio Montes de Oca, John L. Svenson et al., (2002) 'A novel diagnostic screen for defects in the Fanconi anemia pathway.' *Blood*; 4971. doi:10.1182.

Shiroma Y, Takahashi RU, Yamamoto Y et al., (2020) 'Targeting DNA binding proteins for cancer therapy.' *Cancer Sci.; 111(4):1058-1064*. doi:10.1111/cas. 14355.

Sugasawa K. (2016) 'Molecular mechanisms of DNA damage recognition for mammalian nucleotide excision repair.' *DNA Repair (Amst)*; 44:110-117. doi: 10.1016/j.dnarep.2016.05.015.

Sun YS, Zhao Z, Yang ZN et al., (2017) 'Risk Factors and Preventions of Breast Cancer.' *Int J Biol Sci*. doi:10.7150/ijbs.21635.

Tang S, Shen Y, Wei X et al. (2022) 'Olaparib synergizes with arsenic trioxide by promoting apoptosis and ferroptosis in platinum-resistant ovarian cancer.' *Cell Death Dis;* 13, 826. doi:10.1038/s41419-022-05257-y.

Tasaki E, Mitaka Y, Nozaki T et al., (2018) 'High expression of the breast cancer susceptibility gene BRCA1 in long-lived termite kings.' *Aging (Albany NY)*; 10(10):2668-2683. doi:10.18632/aging.101578.

Taylor SJ, Arends MJ, Langdon SP (2020) 'Inhibitors of the Fanconi anaemia pathway as potential antitumour agents for ovarian cancer.' *Exploration of Targeted Anti-tumor Therapy*; 1,26-52. doi:10.37349/etat.00003.

Teicher BA, Linehan WM, Helman LJ. (2012) 'Targeting cancer metabolism.' *Clinical cancer research: an official journal of the American Association for Cancer Research*; 18(20):5537-5545. doi:10.1158/1078-0432.CCR-12-2587.

Thompson E, Dragovic RL, Stephenson SA et al., (2005) 'A novel duplication polymorphism in the FANCA promoter and its association with breast and ovarian cancer.' *BMC Cancer*; 5, 43. doi:10.1186/1471-2407-5-43.

Tiek D, Cheng SY. (2021) 'DNA damage and metabolic mechanisms of cancer drug resistance.' Cancer Drug Resist.; 5(2):368-379. doi:10.20517/cdr.2021. 148.

Topatana W, Juengpanich S, Li Set al., (2020) 'Advances in synthetic lethality for cancer therapy: cellular mechanism and clinical translation.' *Journal of Hematology & Oncology*; 13,118. doi:10.1186/s13045-020-00956-5.

Travis RC, Key TJ. (2003) 'Oestrogen exposure and breast cancer risk.' *Breast Cancer Res*; 5(5):239-47. doi:10.1186/bcr628.

Tsuiko O, Jatsenko T, Parameswaran Grace LKet al., (2018) 'A speculative outlook on embryonic aneuploidy: Can molecular pathways be involved?' *Developmental Biology*. doi:10.1016/j.ydbio.2018.01.014.

Van der Groep P, Hoelzel M, Buerger H et al., (2008) 'Loss of expression of FANCD2 protein in sporadic and hereditary breast cancer.' *Breast cancer research and treatment;* 107(1), 41-7. doi:10.1007/s10549-007-9534-7.

Van Zyl B, Tang D, Bowden NA. (2018) 'Biomarkers of platinum resistance in ovarian cancer: what can we use to improve treatment.' *Endocrine-Related Cancer;* 25(5),R303-R318. doi:10.1530/ERC-17-0336.

Vander Heiden MG, DeBerardinis RJ. (2017) 'Understanding the Intersections between Metabolism and Cancer Biology.' *Cell; 168(4):657-669*. doi:10.1016/ j.cell.2016.12.039.

Wang Y, Bernhardy AJ, Cruz C et al., (2016) 'The BRCA1-Δ11q alternative splice isoform bypasses germline mutations and promotes therapeutic resistance to PARP inhibition and cisplatin.' *Cancer Research*; 76(9):2778-90. doi:10.1158/ 0008-5472.CAN-16-0186.

Wang Y, Krais JJ, Bernhardy AJ et al., (2016) 'RING domain-deficient BRCA1 promotes PARP inhibitor and platinum resistance.' *The Journal of clinical investigation*; 126(8), 3145–3157. doi:10.1172/JCI87033.

Wang Y, Wiltshire T, Senft J et al., (2006). 'Fanconi anemia D2 protein confers chemoresistance in response to the anticancer agent, irofulven.' *Molecular cancer therapeutics*; 5:3153-61. doi:10.1158/1535-7163.

Watanabe T, Yamaguchi T, Tsunoda H et al., (2017) 'Ultrasound Image Classification of Ductal Carcinoma In Situ (DCIS) of the Breast: Analysis of 705 DCIS Lesions' *Ultrasound in Medicine & Biology*. doi:10.1016/j.ultrasmedbio. 2017.01.008.

Wood RD, Mitchell M, Sgouros J et al., (2001) 'Human DNA repair genes.' *Environmental and Molecular Mutagenesis*; 37(3):241-83. doi:10.1002/em. 1033.

Xia Q, Zhao LY, Yan YD et al., (2020) 'A Multiple Primary Malignancy Patient With FANCA Gene Mutation: A Case Report and Literature Review.' *Frontiers in oncology*; 10, 1199. doi:10.3389/fonc.2020.01199.

Yersal O, Barutca S (2014) 'Biological subtypes of breast cancer: Prognostic and therapeutic implications'. *World J Clin Oncol*.; 5(3):412-424. doi:10.5306/wjco. v5.i3.412.

Zecchini V., Frezza C. (2017) 'Metabolic synthetic lethality in cancer therapy.' *Biochim Biophys Acta Bioenerg; 1858(8):723-731*. doi:10.1016/j.bbabi.12.003.

Zhou BB, Elledge SJ. (2000) 'The DNA damage response: putting checkpoints in perspective.' *Nature;* 408, 433–439. doi:10.1038/35044005.

Zimmer AS, Gillard M, Lipkowitz S et al. (2018) 'Update on PARP Inhibitors in Breast Cancer.' *Current treatment options in oncology*; 19, 5 21. doi:10.1007/ s11864-018-0540-2.